



THE UNIVERSITY OF QUEENSLAND
A U S T R A L I A

**Resolving the role of zooplankton in the marine ecosystem
with functional size spectra**

Ryan Fintan Heneghan
B.Sc. (Hons.), University of Queensland, 2014

*A thesis submitted for the degree of Doctor of Philosophy at
The University of Queensland in 2018
School of Mathematics and Physics*

Abstract

Zooplankton are the linchpin of the marine ecosystem, serving as the main energy pathway from primary producers to higher trophic level organisms, such as fish. Despite their critical role, zooplankton are typically oversimplified or ignored altogether in current marine ecosystem models, and we have limited understanding of how variation in the zooplankton affects energy transfer from phytoplankton to fish. An alternative to resolving the enormous taxonomic diversity of the zooplankton is to focus on functional traits, such as body size, feeding strategy and body composition, since these are the factors that determine an organism's fitness in any given environment, and their role in the marine food web. Body size is the master trait, however zooplankton exhibit vast diversity in other important functional traits, such as predator-prey mass ratio (PPMR) and body composition. Energy transfer through the marine food web depends on these traits, so to better understand the role of zooplankton in marine ecosystems, any realistic representation of the zooplankton must incorporate this diversity. In this thesis, I use recent developments in size-spectrum modelling, coupled with the extensive literature on zooplankton physiology and size-based feeding characteristics, to explore the structure of the zooplankton community across the global ocean, and their role in mediating energy from phytoplankton to fish.

We begin by reviewing the development of size-spectrum modelling, particularly focusing on the last 10 years and the recent innovations in size-spectrum modelling. In particular, we review the development of functional size-spectrum modelling, which allows size-spectrum models to resolve multiple groups by their functional traits, and how this has been used for various higher trophic level groups, especially fish. The focus on fish means that the unique dynamics of the plankton have been overlooked in these models. We use the functional size-spectrum framework to demonstrate how changes in the size-based feeding behaviour of the zooplankton community affects the productivity of higher trophic levels, and their resilience to fishing pressure: the higher the PPMR of the zooplankton community, the more productive and resilient the fish community. However, higher zooplankton PPMR also increases the temporal variability of the zooplankton and fish communities.

The most common modelling assumption with respect to the zooplankton community is that its composition does not change across environmental gradients. However, there is strong evidence that the composition of the zooplankton community is not static, but varies across the global ocean, and this will have implications for how energy moves from phytoplankton to fish. We explore the role of functional traits in structuring the zooplankton community

across the global ocean. We develop a functional size-spectrum model of the marine ecosystem, which resolves the body size ranges, size-based feeding characteristics and carbon content of nine of the most abundant zooplankton groups (heterotrophic flagellates and ciliates, larvaceans, omnivorous and carnivorous copepods, chaetognaths, euphausiids, salps and jellyfish). Zooplankton community composition emerges from the model across global environmental gradients, based on the functional traits of the nine groups. Across the global ocean, the emergent distributions and composition of the zooplankton community broadly agreed with empirical observation and theory. Heterotrophic flagellates and ciliates, salps, larvaceans, carnivorous copepods and chaetognaths were a larger component of zooplankton biomass in oligotrophic waters, omnivorous copepods were prevalent everywhere, and euphausiids and jellyfish dominated the zooplankton in eutrophic waters.

Traditionally, eutrophic systems are hypothesised to be more efficient at transferring energy from phytoplankton to fish, compared to oligotrophic systems. We use the zooplankton-resolved functional size-spectrum model to test this hypothesis, and assess the role of zooplankton composition in mediating transfer efficiency from phytoplankton to fish. Changes in the composition of the zooplankton lead to eutrophic waters supporting three times more fish biomass per unit phytoplankton, compared to oligotrophic waters. However, we also found that salps and larvaceans – despite their low carbon content – were critical in oligotrophic waters, providing a direct energy pathway from the small pico-phytoplankton which dominates in oligotrophic regions, to planktivorous fish. Without salps and larvaceans, total fish biomass was up to 50% lower in oligotrophic waters, and 17% lower across the global ocean.

The work presented here demonstrates the power of the functional traits to explain global patterns in the zooplankton community. We explore the role of the zooplankton in the change in transfer efficiency from oligotrophic to eutrophic waters, and demonstrate how salps and larvaceans are a critical trophic link between primary producers and fish in oligotrophic waters. The zooplankton-resolved size spectrum model developed here is a step forward in trait-based modelling, and our understanding of the role of zooplankton in the marine ecosystem.

Declaration by author

This thesis is composed of my original work, and contains no material previously published or written by another person except where due reference has been made in the text. I have clearly stated the contribution by others to jointly-authored works that I have included in my thesis.

I have clearly stated the contribution of others to my thesis as a whole, including statistical assistance, survey design, data analysis, significant technical procedures, professional editorial advice, financial support and any other original research work used or reported in my thesis. The content of my thesis is the result of work I have carried out since the commencement of my higher degree by research candidature and does not include a substantial part of work that has been submitted to qualify for the award of any other degree or diploma in any university or other tertiary institution. I have clearly stated which parts of my thesis, if any, have been submitted to qualify for another award.

I acknowledge that an electronic copy of my thesis must be lodged with the University Library and, subject to the policy and procedures of The University of Queensland, the thesis be made available for research and study in accordance with the Copyright Act 1968 unless a period of embargo has been approved by the Dean of the Graduate School.

I acknowledge that copyright of all material contained in my thesis resides with the copyright holder(s) of that material. Where appropriate I have obtained copyright permission from the copyright holder to reproduce material in this thesis and have sought permission from co-authors for any jointly authored works included in the thesis.

Publications during candidature

Blanchard, J. L., **Heneghan, R. F.**, Everett, J. D., Trebilco, R., and Richardson, A. J. (2017). From Bacteria to Whales: Using Functional Size Spectra to Model Marine Ecosystems. *Trends in Ecology and Evolution* 32, 174–186.

Everett, J. D., Baird, M. E., Buchanan, P., Bulman, C., Davies, C., Downie, R., Griffiths, C., **Heneghan, R.**, et al. (2017). Modelling What We Sample and Sampling What We Model: Challenges for Zooplankton Model Assessment. *Frontiers in Marine Science* 4, 1–19.

Heneghan, R. F., Everett, J. D., Blanchard, J. L., and Richardson, A. J. (2016). Zooplankton Are Not Fish: Improving Zooplankton Realism in Size-Spectrum Models Mediates Energy Transfer in Food Webs. *Frontiers in Marine Science* 3, 1–15.

Publications included in this thesis

Blanchard, J. L., **Heneghan, R. F.**, Everett, J. D., Trebilco, R., and Richardson, A. J. (2017). From Bacteria to Whales: Using Functional Size Spectra to Model Marine Ecosystems. *Trends in Ecology and Evolution* 32, 174–186.

- incorporated as Chapter 2

RFH undertook the literature review, and wrote the first draft of the manuscript and figures. Before submission for publication, a review similar to **RFH**'s was published, by an independent research group. **RFH** requested that JLB – who has expertise in size-spectrum modelling – take the role of lead author, to broaden the message and change the structure of the review, before attempting publication again. JLB agreed, and recrafted the review by taking the lead in writing subsequent drafts and figures, with input from **RFH** and AJR, JEE, RT.

Contributor	Statement of contribution
Ryan F. Heneghan (Candidate)	Conception and design (35%) Analysis and interpretation (50%) Drafting and production (30%)
Julia L. Blanchard	Conception and design (35%) Analysis and interpretation (30%) Drafting and production (45%)
Anthony J. Richardson	Conception and design (20%) Analysis and interpretation (10 %) Drafting and production (15%)
Jason E. Everett	Conception and design (5%) Analysis and interpretation (5%) Drafting and production (5%)
Rowan Trebilco	Conception and design (5%) Analysis and interpretation (5%) Drafting and production (5%)

Heneghan, R. F., Everett, J. D., Blanchard, J. L., and Richardson, A. J. (2016). Zooplankton Are Not Fish: Improving Zooplankton Realism in Size-Spectrum Models Mediates Energy Transfer in Food Webs. *Front. Mar. Sci.* 3, 1–15.

- incorporated as Chapter 3

All authors were involved in conceiving the original idea for this study. JLB provided code from past size-spectrum modelling studies. **RFH** undertook the literature review, constructed the model, conducted the analysis, and wrote the manuscript, with input from AJR, JLB, and JEE.

Contributor	Statement of contribution
Ryan F. Heneghan (Candidate)	Conception and design (50%) Analysis and interpretation (80%) Drafting and production (80%)
Anthony J. Richardson	Conception and design (25%) Analysis and interpretation (10%) Drafting and production (10%)
Julia L. Blanchard	Conception and design (15%) Analysis and interpretation (5%) Drafting and production (5%)
Jason E. Everett	Conception and design (10%) Analysis and interpretation (5%) Drafting and production (5%)

Contributions by others to the thesis

No contributions by others.

Statement of parts of the thesis submitted to qualify for the award of another degree

None.

Research Involving Human or Animal Subjects

No animal or human subjects were involved in this research.

Acknowledgements

I would like to first thank my primary supervisor, Anthony Richardson for his guidance over the past three and a half years. I can learn all the math and biology I want, but if I do not know what questions to ask, I am not a good scientist. Anthony, you have modelled to me what it looks like to ask good questions, in fact you never stop! At the same time, you have always treated me with respect. You have championed me in my successes, and used my mistakes to teach me. Thank you for modelling what it looks like to be a good scientist and a good teacher. To my secondary supervisor Julia Blanchard, thank you for your enthusiasm and generosity. The times working in Hobart with you were some of the best weeks of my PhD, and your enthusiasm for science is contagious. I appreciate the time you made for me, especially in these final months, and I am glad that we are going to keep working closely. I am also thankful to the University of Queensland's School of Mathematics and Physics, who have provided me with the resources and administrative support to complete this PhD. As part of this thesis, I collaborated with Jason Everett and Iain Suthers from UNSW and Claire Davies from CSIRO. Jason, thanks for helping me tease apart the results from my model, I am excited about how we are going to push this work forward. Iain, thank you for your advice on Chapter 3, and your unapologetic passion for plankton. Claire, I am indebted to you for lending me your expertise in copepod biology - you pulled together information for me about copepod diets in a day that would have taken me weeks.

My special thanks to my parents, who have patiently given me unconditional support during the highs and lows of the past three and a half years. I would also especially like to thank my mother-in law, Anne-Marie, who having gone through the PhD process was always able to give me a sympathetic ear, but at the same time good perspective on how fortunate I am. I am grateful to my sister Tara, I always enjoy our weekly phone calls, your weirdness and love of the absurd has brought needed relief in many stressful times. I would also like to thank my friends, who have seen less of me, particularly in the past few months, for keeping me sane.

I am not able to fully express my gratitude for my wife, Marie. I love that we could do our PhDs together. You are meticulous, thoughtful and considerate all the time, and I love you so much.

Finally, to my Lord Jesus, I pray that this work would be acceptable in your sight.

Financial support

This research was supported by an Australian Government Research Training Program Scholarship (formerly, Australian Postgraduate Award).

Keywords

zooplankton, marine ecosystem modelling, functional size spectrum, ecosystem efficiency, fish

Australian and New Zealand Standard Research Classifications (ANZSRC)

ANZSRC Code: 050102, Ecosystem Function, 50%

ANZSRC Code: 060205, Marine and Estuarine Ecology, 25%

ANZSRC Code: 050101, Ecological Impacts of Climate Change, 25%

Fields of Research (FoR) Classification

FoR Code: 0501, Ecological Applications, 40%

FoR Code: 0602, Ecology 40%

FoR Code: 0102, Applied Mathematics, 20%

Table of Contents

Chapter 1 Introduction	1
1.1 Understanding ecosystem dynamics with mathematical models.....	2
1.2 The role of zooplankton in the marine ecosystem.....	2
1.3 Using functional size spectra to model marine ecosystems	5
1.4 Zooplankton are not fish	7
1.5 Functional traits give rise to zooplankton community composition	8
1.6 Zooplankton composition across the global ocean mediates transfer efficiency from phytoplankton to fish.....	9
Chapter 2 From Bacteria to Whales: Using Functional Size Spectra to Model Marine Ecosystems	10
2.1 Abstract.....	10
2.2 Size matters for individuals to ecosystems	11
2.3 How to model the community size-spectrum?.....	12
2.3.1 Static models	12
2.3.2 Individual-based models	13
2.3.3 SSMs	14
2.3.4 Discrete size class models	15
2.3.5 Trait-based SSMs: including other functional traits	15
2.4 Limitations of SSMs.....	18
2.5 Beyond bacteria to whales: future research directions for size-based ecosystem models	20
2.5.1 Beyond one size fits all: unifying models through functional traits.....	20
2.5.2 Beyond slopes: testing predictions with observed size spectra	23
2.5.3 Beyond fixed traits: extinctions, invasions, and evolution	25
2.5.4 Beyond fishing and warming: multiple stressors and their interactions	26
2.6 Concluding remarks	26
Chapter 3 Zooplankton are not fish: improving zooplankton realism in size-spectrum models mediates energy transfer in food webs	28
3.1 Abstract.....	28
3.2 Introduction	29
3.3 Methods	32
3.3.1 The model.....	32

3.3.2 Community characteristics	38
3.3.3 Numerical implementation	40
3.3.4 Zooplankton are not fish	41
3.3.5 Sensitivity analysis.....	41
3.3.6 Mediating primary production and fishing	41
3.4 Results	42
3.4.1 Zooplankton are not fish	42
3.4.2 Sensitivity analysis.....	45
3.4.3 Mediating primary production and fishing	47
3.5 Discussion	50
3.6 Supplementary Information	54
 Chapter 4 Global patterns in zooplankton community composition: functional traits matter 55	
4.1 Abstract.....	55
4.2 Introduction	56
4.3 Methods	61
4.3.1 Overview of the size-spectrum model.....	61
4.3.2 Parameterising the static phytoplankton abundance spectrum	63
4.3.3 Incorporating functional traits.....	65
4.3.4 Testing the size-spectrum model	70
4.3.5 Numerical implementation	74
4.4 Results	76
4.4.1 Size-spectrum model predictions.....	76
4.4.2 Size-spectrum model assessment.....	81
4.5 Discussion	84
4.6 Supplementary Information	88
4.6.1 Empirical abundance distributions (GAMs).....	89
 Chapter 5 Zooplankton composition across oligotrophic and eutrophic waters mediates transfer efficiency from phytoplankton to fish 100	
5.1 Abstract.....	100
5.2 Introduction	101
5.3 Methods	105
5.3.1 The zooplankton-resolved functional size-spectrum model	105
5.3.2 Diets and trophic levels.....	109

5.3.3 Ecosystem efficiency	109
5.4 Results	110
5.4.1 The emergent plankton community	110
5.4.2 Who is eating phytoplankton?.....	111
5.4.3 Emergent diets and trophic levels.....	112
5.4.4 The emergent food web in oligotrophic versus eutrophic waters.....	115
5.4.5 The role of salps and larvaceans as an energy pathway from phytoplankton to fish	117
5.5 Discussion	119
5.6 Supplementary Information	124
Chapter 6 Concluding Discussion	128
6.1 Integrating zooplankton using functional traits	129
6.2 Higher trophic levels are sensitive to zooplankton feeding behaviour	130
6.3 Functional traits explain global patterns in zooplankton community composition.....	131
6.4 Implications for higher trophic levels	132
6.5 Limitations of approach	136
6.6 Final remarks	139
References	141
Appendix 1 Numerical Implementation of Second Order McKendrick-von Foerster Equation	164

List of Figures

Chapter 2

Figure 2.1 How to Model the Size-spectrum? Taxonomy of the different types of approaches that have been used to model the community size-spectrum. An expanded reference list for each model type can be found at https://doi.org/10.1016/j.tree.2016.12.003 . Abbreviations: IBM, individual- based model; SSM, size-spectrum model.	13
Figure 2.2 Functional Size-spectrum: An Illustration Applied to a Conceptual Marine Ecosystem from Bacteria to Whales. (a) Stylised size-structured ecosystem model emphasising different processes across the size-spectrum. Larger circles are used to illustrate relative changes in size within functional groups. Black arrows illustrate the presence of feeding within and across groups but do not show the full extent of the many feeding links present in size-spectrum models. Thick colored arrows represent growth in size. (b) Hypothetical emergent size spectra for the same types of functional groups shown in a) but here represented via life history traits depicted by differences in offspring and adult asymptotic sizes (Andersen <i>et al.</i> , 2016b).	19

Chapter 3

Figure 3.1 Conceptual illustration of the phytoplankton-zooplankton-fish system. The background (phytoplankton) spectrum is held constant, the dynamic zooplankton and fish community spectrums are governed by equation 1 and the equations in Table 3.2.	33
Figure 3.2 \log_{10} PPMR for the range of quantitative feeding modes from carnivores to herbivores (Wirtz 2012). The solid lines indicate realised \log_{10} PPMR for different feeding modes, across the size range of the zooplankton community.	37
Figure 3.3 The zooplankton and fish community size-spectra when various parameters are updated a-e) one at a time and f) all together. The dashed lines in each plot represent the zooplankton and fish communities in the base model parameterisation, and the solid lines denotes the average abundance of the fish and zooplankton communities over 10 years in the modified model. The shaded areas show the regions of the travelling wave solutions over 10 years if the steady state is unstable.	43
Figure 3.4 a, b, c) The total fish community biomass (g m^{-3}) and d, e, f) the fish to zooplankton biomass ratio (F:Z) for different values of zooplankton feeding mode (m) , feeding kernel width (σ_Z) and assimilation efficiency (Kz). In each plot, the other feeding parameters not specified are held constant at m = 0, σ_Z = 0.75 and Kz = 0.7. The dashed	

line in d, e, f) indicates the F:Z in the base model, where the zooplankton community are parameterised as fish.	45
Figure 3.5 The fish community biomass coefficient of variation (CV) against zooplankton a) feeding mode (m), b) feeding kernel width (σ_Z) and c) assimilation efficiency (K_Z), and the stability regions of d) m against σ_Z , e) σ_Z against K_Z and f) m against K_Z . In d, e, f) the dashed lines indicate the transect over which the CV in the plot above is taken. In each plot, the other feeding parameters not specified are held constant at $m = 0$, $\sigma_Z = 0.75$ and $K_Z = 0.7$	47
Figure 3.6 The zooplankton and fish community size-spectra when the zooplankton community is defined by the feeding characteristics of a single functional group (Fuchs and Franks 2010; Wirtz 2012). Here, m denotes the feeding mode of the zooplankton and σ_Z the width of the feeding kernel. The solid lines denotes the average abundance slope of the zooplankton and fish communities over 10 years. The shaded areas show the regions of the travelling wave solutions over 10 years if the steady state is unstable.	49
Figure 3.7 Relative fish biomass against (a) total phytoplankton abundance ($\text{g}^{-1}\text{m}^{-3}$) and (b) fishing mortality (yr^{-1}) for fish communities supported by a zooplankton community with the feeding characteristics of different functional groups. The relative fish biomass is calculated from the total fish biomass divided by the total fish biomass at a) the lowest phytoplankton abundance (0.1 mg m^{-3} chlorophyll a) and b) no fishing mortality (0 yr^{-1}).	49

Chapter 4

Figure 4.1 Change in phytoplankton community size structure across eutrophic (high chlorophyll) and oligotrophic (low chlorophyll systems).....	60
Figure 4.2 Conceptual illustration of the functional size-spectrum model.	61
Figure 4.3 Global maps of the phytoplankton community. Proportion of phytoplankton that is a) picoplankton ($< 2\mu\text{m}$ ESD), b) nanoplankton ($2\mu\text{m}-20\mu\text{m}$ ESD), c) microplankton ($> 20\mu\text{m}$ ESD), and d) the slope distribution of the phytoplankton abundance spectrum.	64
Figure 4.4 Overview of the size ranges of the model's functional groups (solid boxes), and their prey size ranges (dashed boxes).....	68
Figure 4.5 Data locations for a) Larvaceans, b) Omnivorous Copepods, c) Carnivorous Copepods, d) Chaetognaths, e) Euphausiids, f) Salps and g) Jellyfish. Number of	

datapoints after aggregating samples by functional group and sample given in parentheses	73
Figure 4.6 Annual average wet weight biomass from the size-spectrum model (g m^{-3}) for a) Heterotrophic Flagellates, b) Heterotrophic Flagellates, c) Larvaceans, d) Omnivorous Copepods, e) Carnivorous Copepods, f) Chaetognaths, g) Euphausiids, h) Salps and i) Jellyfish.....	77
Figure 4.7 Plots of wet weight biomass g m^{-3} against chlorophyll a for a) Heterotrophic Flagellates, b) Heterotrophic Ciliates, c) Larvaceans, d) Omnivorous Copepods, e) Carnivorous Copepods, f) Chaetognaths, g) Euphausiids, h) Salps and i) Jellyfish....	78
Figure 4.8 Relative biomass (wet weight composition) of the micro-plankton community, from the size-spectrum model. Proportion of total wet weight from a) Phytoplankton, b) Heterotrophic Flagellates, c) Heterotrophic Ciliates.	79
Figure 4.9 Relative biomass (wet weight composition) of the macro zooplankton community (excluding flagellates and ciliates), from the size-spectrum model. Proportion of total zooplankton wet weight (excluding flagellates and ciliates) from a) Larvaceans, b) Omnivorous Copepods, c) Carnivorous Copepods, d) Chaetognaths, e) Euphausiids, f) Salps and g) Jellyfish.	80
Figure 4.10 Assessing emergent abundance distributions from the size-spectrum model. The empirical abundance distributions from the generalised additive models (GAMs) (left column, $\log_{10}(\# \text{ m}^{-3})$), the emergent zooplankton distributions from the size-spectrum model (centre column, $\log_{10}(\# \text{ m}^{-3})$), and Pearson's correlation plots between the two a) Larvaceans, b) Omnivorous Copepods, c) Carnivorous Copepods and d) Chaetognaths.	82
Figure 4.10 (continued) Assessing emergent abundance distributions from the size-spectrum model. The empirical abundance distributions from the generalised additive models (GAMs) (left column, $\log_{10}(\# \text{ m}^{-3})$), the emergent zooplankton distributions from the size-spectrum model (centre column, $\log_{10}(\# \text{ m}^{-3})$), and Pearson's correlation plots between the two a) Euphausiids, b) Salps and c) Jellyfish.....	80
Figure S 4.1 Annual average a) sea surface temperature (SST) and b) $\log_{10}(\text{Chlorophyll a mg m}^{-3})$, aggregated to 5 degree latitude by 5 degree longitude grid squares. These fields are used as environmental inputs to drive the size-spectrum model. For both SST and $\log_{10}(\text{Chlorophyll a mg m}^{-3})$, we obtained the annual average for each grid square by averaging over the monthly climatologies obtained from MODIS-Aqua, standardised for the number of months in which satellite observations were taken.	88

Figure S 4.2 Best model fit for larvaceans: a) Fitted interaction surface between sea surface temperature (SST) and day of year, standardised to the northern hemisphere, and partial residuals from the main effect of b) $\log_{10}(\text{Chlorophyll a})$, c) Depth and d) the Gear and Mesh factor levels. For b, c and d) the main effect for each predictor is given by the blue line, with the 95% confidence intervals given by the shaded areas.....	93
Figure S 4.3 Best model fit for omnivorous copepods: a) Fitted interaction surface between sea surface temperature (SST) and day of year, standardised to the northern hemisphere, and partial residuals from the main effect of b) $\log_{10}(\text{Chlorophyll a})$, c) Depth and d) the Gear and Mesh factor levels. For b, c and d) the main effect for each predictor is given by the blue line, with the 95% confidence intervals given by the shaded areas.....	94
Figure S 4.4 Best model fit for carnivorous copepods: a) Fitted interaction surface between sea surface temperature (SST) and day of year, standardised to the northern hemisphere, and partial residuals from the main effect of b) $\log_{10}(\text{Chlorophyll a})$, c) Depth and d) the Gear and Mesh factor levels. For b, c and d) the main effect for each predictor is given by the blue line, with the 95% confidence intervals given by the shaded areas.....	95
Figure S 4.5 Best model fit for chaetognaths: a) Fitted interaction surface between sea surface temperature (SST) and day of year, standardised to the northern hemisphere, and partial residuals from the main effect of b) $\log_{10}(\text{Chlorophyll a})$, c) Depth and d) the Gear and Mesh factor levels. For b, c and d) the main effect for each predictor is given by the blue line, with the 95% confidence intervals given by the shaded areas.....	96
Figure S 4.6 Best model fit for euphausiids: a) Fitted interaction surface between sea surface temperature (SST) and day of year, standardised to the northern hemisphere, and partial residuals from the main effect of b) $\log_{10}(\text{Chlorophyll a})$, c) Depth and d) the Gear and Mesh factor levels. For b, c and d) the main effect for each predictor is given by the blue line, with the 95% confidence intervals given by the shaded areas.....	97
Figure S 4.7 Best model fit for salps: a) Fitted interaction surface between sea surface temperature (SST) and day of year, standardised to the northern hemisphere, and partial residuals from the main effect of b) $\log_{10}(\text{Chlorophyll a})$, c) Depth and d) the Gear and Mesh factor levels. For b, c and d) the main effect for each predictor is given by the blue line, with the 95% confidence intervals given by the shaded areas.....	98
Figure S 4.8 Best model fit for jellyfish: a) Fitted interaction surface between sea surface temperature (SST) and day of year, standardised to the northern hemisphere, and partial residuals from the main effect of b) $\log_{10}(\text{Chlorophyll a})$, c) Depth and d) the	

Gear and Mesh factor levels. For b, c and d) the main effect for each predictor is given by the blue line, with the 95% confidence intervals given by the shaded areas. 99

Chapter 5

Figure 5.1 Hypothesised food chains in a) oligotrophic versus b) eutrophic systems. Width of arrows shows the magnitude of energy transfer between steps in the food chain. 105

Figure 5.2 Plots of the proportion of the total biomass of a) phytoplankton, comprising pico ($<2\text{ }\mu\text{m}$), nano (2-20 μm) and micro ($>20\text{ }\mu\text{m}$) size classes), heterotrophic flagellates and ciliates, and b) zooplankton, comprising omnivorous copepods, carnivorous copepods, larvaceans, chaetognaths, jellyfish, salps and euphausiids. To clarify the trend with chlorophyll a, over temperature, we used a spline smoother with 5 degrees of freedom..... 111

Figure 5.3 Proportion of total phytoplankton consumed by various zooplankton groups, versus chlorophyll a. To clarify the trend with chlorophyll a, over temperature, we used a spline smoother with 5 degrees of freedom..... 112

Figure 5.4 Diet composition and resulting trophic levels across chlorophyll a for heterotrophic flagellates (a, b), heterotrophic ciliates, (c, d), larvaceans (e, f), omnivorous copepods (g, h), euphausiids (i, j), salps (k, l), carnivorous copepods (m, n), chaetognaths (o, p), jellyfish (q, r) and planktivorous fish (s, t). To highlight the trend with chlorophyll a, rather than temperature, we used a spline smoother with 5 degrees of freedom. 113

Figure 5.5 The average emergent community composition and food web for oligotrophic (a, c) and eutrophic (b, d) waters. The food web diagrams (c, d) show the flow of biomass from predation between the different groups, with the width of the arrows proportional to the biomass flow (g yr^{-1})..... 116

Figure 5.6 Fish-Phytoplankton Biomass Ratio against chlorophyll a. 117

Figure 5.7 Proportion of ingested wet weight by planktivorous fish that is carbon, against chlorophyll a..... 118

Figure 5.8 Ratio of total fish biomass when zooplankton community includes salps and larvaceans, over total fish biomass when salps and larvaceans are removed from the model, against chlorophyll a. The red line shows where the ratio is 1, the green dashed line is the global average ratio. 118

Figure S 5.1 Annual average a) sea surface temperature (SST) and b) $\log_{10}(\text{Chlorophyll a mg m}^{-3})$, aggregated to 5 degree latitude by 5 degree longitude grid squares. These fields are used as environmental inputs to drive the size-spectrum model. For both SST and $\log_{10}(\text{Chlorophyll a mg m}^{-3})$, we obtained the annual average for each grid square

by averaging over the monthly climatologies obtained from MODIS-Aqua, standardised for the number of months in which satellite observations were taken.	127
--	-----

List of Tables

Chapter 3

Table 3.1 Table of parameter values for the phytoplankton-zooplankton-fish dynamic size-spectrum model.	34
Table 3.2 Model equations with their units. An equation number is given that is used in the main text.	38
Table 3.3 Fish community biomass (FB), fish to zooplankton biomass ratio (F:Z), fish community production to biomass ratio (P:B) and throughput (TP) relative to the base model (r), and the variation in fish community biomass (coefficient of variation: CV) when the zooplankton community feeding parameters are updated one at a time, and all together. The system has a stable steady state when $\lambda_{\max} < 0$, and an unstable, oscillating steady state when $\lambda_{\max} > 0$	44
Table 3.4 Fish community biomass (FB), fish to zooplankton biomass ratio (F:Z), fish community production to biomass ratio (P:B) and throughput (TP), and the variation in fish community biomass (coefficient of variation: CV) when the zooplankton community is defined by the feeding characteristics of different functional groups. The system has a stable steady state when $\lambda_{\max} < 0$, and an unstable, oscillating steady state when $\lambda_{\max} > 0$	48

Chapter 4

Table 4.1 Model equations with their units and in-text reference numbers.	65
Table 4.2 Parameter values for the nine zooplankton and three fish groups.	69
Table 4.3 Model parameter values.	70
Table S 4.1 Pearson correlation coefficient between environmental predictor variables used for empirical abundance GAMs of larvaceans, omnivorous copepods, carnivorous copepods, chaetognaths, salps, krill and jellyfish.	89
Table S 4.2 Summary of final GAMs for the seven zooplankton functional groups, with Akaike information criterion (AIC) and deviance explained.	90
Table S 4.3 Skill of empirical GAMs with different predictor combinations. Model skill given in terms of Akaike Information Criterion (AIC) and deviance explained. Best models for each group are highlighted in yellow.	90

Chapter 5

Table S 5.1 Model equations with their units.....	124
Table S 5.2 Parameter values for the nine zooplankton and three fish groups.....	125
Table S 5.3 Other model parameter values.	126

List of Boxes

Chapter 2

Box 2.1 How can ecological data inform SSMs?.....	16
Box 2.2 How are size-spectrum models being used?	21
Box 2.3 Predicting ecosystem structure and function in an era of rapid change: managing uncertainty	24

List of abbreviations

COPEPOD: Coastal and Ocean Plankton Ecology, Production, and Observation Database
CV: Coefficient of Variation
DVM: Diel Vertical Migration
ESD: Equivalent Spherical Diameter
FB: Fish Biomass
FPBR: Fish-Phytoplankton Biomass Ratio
F:Z: Fish-Zooplankton Biomass Ratio
GAM: Generalised Additive Model
GM: Gear-Mesh Factor
IMOS: Integrated Marine Observing System
MODIS: Moderate Resolution Imaging Spectroradiometer
MvF-D: McKendrick-von Foerster with Diffusion Equation
P:B: Production-Biomass Ratio
PPMR: Predator-Prey Mass Ratio
rFB: relative Fish Biomass
rF:Z: relative Fish-Zooplankton Biomass Ratio
rP:B: relative Production-Biomass Ratio
SSM: Size-Spectrum Model
SST: Sea Surface Temperature
TP: Throughput

Chapter 1

Introduction

1.1 Understanding ecosystem dynamics with mathematical models

Human are placing large and growing demands on marine ecosystems. Annual per capita supply from wild fisheries and aquaculture has more than tripled in the past 50 years to over 150 million tonnes per year, and will continue to increase with an additional 2 billion people by mid-century (UN DESA, 2015; FAO, 2016). At the same time, atmospheric carbon dioxide levels have increased by 40% since the Industrial Revolution, with significant further increases all but certain over the next 100 years (IPCC, 2014). These pressures manifest at different levels of biological organisation in the marine ecosystem, from individuals to ecosystems, and will have serious consequences for ecosystem services and human society (Cheung *et al.*, 2009; Brierly *et al.*, 2009; Hoegh-Guldberg and Bruno, 2010; Doney *et al.*, 2012; Barange *et al.*, 2014).

Improving our understanding of the functioning of marine ecosystems is necessary to better predict and manage how they will respond to human and environmental impacts. To that end, mathematical models of marine ecosystems have been constructed to assess how ecosystems respond to external pressures and to help support ecosystem-based management (Plagányi, 2007). Typically, models of lower trophic levels (e.g., phytoplankton) and higher trophic levels (e.g., fish) have been developed separately, however there is a growing recognition of the importance of representing the whole ecosystem in one framework (Rose *et al.*, 2009; Travers *et al.*, 2009; Fulton, 2010; Blanchard *et al.*, 2017). Combining the dynamics of the plankton and higher trophic levels in one modelling framework makes it possible to assess the bottom up effects of the environment on lower trophic levels, together with the top down impacts of fishing (Travers *et al.*, 2007; Brown *et al.*, 2010). Moreover, the productivity of higher trophic level organisms such as fish ultimately depends on phytoplankton production at the base of the marine food web (Ryther, 1969; Pauly and Christensen, 1995; Chassot *et al.*, 2010; Stock *et al.*, 2017).

1.2 The role of zooplankton in the marine ecosystem

The relationship between phytoplankton and higher trophic levels is not straightforward, as zooplankton is the main energy pathway from phytoplankton to fish (Carlotti and Poggiale, 2010; Mitra and Davis, 2010; Everett *et al.*, 2017). Zooplankton are any animals that float in the water and cannot progress against currents. All marine phyla are represented in the zooplankton, either permanently as holoplankton (e.g., copepods) or temporarily as meroplankton (e.g., fish larvae). Zooplankton exhibit an enormous diversity of traits, for example the body size range of zooplankton ranges over 15 orders of magnitude from

heterotrophic flagellates (10 pg; Hansen *et al.*, 1997) to jellyfish (> 1 kg; Acuña *et al.*, 2011; Levinton, 2013). Zooplankton are also critical in the transfer of energy between pelagic and benthic systems (Lassalle *et al.*, 2013), and for carbon export from surface waters to the deep ocean (Steinberg and Landry, 2017).

Energy transfer through food webs is dependent upon the relative size of predator and prey (Silvert and Platt, 1978; Jennings and Mackinson 2003; Law *et al.*, 2009), known as the predator-prey mass ratio (PPMR). Everything else being equal, the larger the average PPMR in a marine food chain, the more efficiently energy is shunted from lower to higher trophic levels, because there are fewer trophic steps separating small and large organisms (Brown *et al.*, 2004). Zooplankton vary hugely in their PPMR, a consequence of their enormous phylogenetic diversity and thus vastly different feeding strategies. Wirtz (2012) shows PPMRs of zooplankton vary by 7 orders of magnitude – from active ambush carnivory for carnivorous copepods (PPMR ~ 10) to passive suspension grazing of salps (PPMR ~ 100 million). By comparison, fish PPMRs span 1 order of magnitude, from 100 to 1000 (Andersen and Ursin, 1977; Kerr and Dickie, 2001; Barnes *et al.*, 2010). The type of zooplankton present – with vastly different PPMRs – is likely to be critical for understanding energy transfer through food webs.

The most common assumption with respect to zooplankton in marine ecosystem modelling is that the zooplankton community does not change across space or time (Everett *et al.*, 2017). However, the composition of the zooplankton is not constant, with different groups dominating from oligotrophic (low primary productivity) to eutrophic (high primary productivity) regions (Barton *et al.*, 2013). Variation in the zooplankton affects how efficiently energy moves through the marine food web, with implications for ecosystem resilience and productivity (Friedland *et al.*, 2012; Jennings and Collingridge, 2015; Heneghan *et al.*, 2016; Dam and Baumman, 2017).

Changes in the size structure of the phytoplankton drive changes in the zooplankton, which in turn affects how energy moves from phytoplankton to fish (Sommer and Stibor, 2002; Stibor *et al.*, 2004). This is because different PPMRs mean that zooplankton do not all feed from the same prey size range. Therefore, depending on the size structure of the phytoplankton, certain zooplankton groups will have more prey than others in different regions. Traditionally, food chains in eutrophic systems are hypothesised to be more efficient than oligotrophic food chains (Ryther, 1969; Lalli and Parsons, 1995; Boyce *et al.*, 2015). This is because in oligotrophic waters, phytoplankton have a smaller median size and are

dominated by picoplankton < 2 µm (Agawin *et al.*, 2000; Brewin *et al.*, 2010; Barnes *et al.*, 2011). In contrast, phytoplankton communities in eutrophic waters have a larger median size and are dominated by larger nano (2 µm – 20 µm) and microplankton (>20 µm). Most of the phytoplankton in oligotrophic systems is too small to be directly accessed by large herbivores like copepods and euphausiids, which are prey for planktivorous fish (Stibor *et al.*, 2004). Instead, in oligotrophic systems these large crustaceans feed on flagellates and ciliates (protists) which feed on the picoplankton and fall within these groups' prey size ranges. This adds an additional trophic step to the food chain, leading to less available energy for fish. In contrast, in eutrophic systems large crustaceans can directly access the larger phytoplankton for food, cutting out the extra protist step. Moreover, carbon is the major structural component of zooplankton (Kiørboe, 2013; McConville *et al.*, 2017), and the carbon content of different zooplankton groups affects their relative fitness and how efficiently they mediate energy from phytoplankton to higher trophic levels (Acuña *et al.*, 2011; Kiørboe, 2011; Kiørboe and Hirst, 2014). Groups with a low carbon content such as salps and jellyfish, are a less nutritious food source for predators, compared to more carbon dense zooplankton such as copepods and euphausiids. It follows that environmental conditions which favour more gelatinous zooplankton will lead to less efficient energy transfer from phytoplankton to fish.

In current marine ecosystem models, the dynamics of the zooplankton are typically poorly resolved or ignored (Mitra *et al.*, 2014). Many existing global ecosystem models use highly idealised representations of zooplankton, typically one or two amorphous boxes that transfer biomass from phytoplankton to fish (Everett *et al.*, 2017). The assumption implicit in current ecosystem models not resolving the zooplankton is that the dynamics of this group does not affect ecosystem function. However, recent studies have shown that the productivity and structure of higher trophic levels is highly sensitive to the parameterisation of lower trophic levels. For example, Fuchs and Franks (2010) found that zooplankton with high PPMRs that ate a narrow size range of prey gave rise to a flatter plankton abundance size spectra (relatively more large organisms), in comparison to zooplankton with small PPMRs and a larger feeding kernel, which led to a steeper plankton size spectra. Moving beyond the plankton, Jennings and Collingridge (2015) demonstrated that the productivity and total biomass of the global fish community was highly sensitive to how energy moved through the lower planktonic trophic levels – from phytoplankton to zooplankton. Moreover, Irigoien *et al.*, (2014) suggested global fish biomass could be an order of magnitude higher than previously thought and that this could be due to a poor understanding of transfer efficiency

in the zooplankton. It follows that current model formulations that do not resolve the zooplankton are neglecting a critical component of the ecosystem.

In this thesis, we use recent developments in size-spectrum modelling, with the extensive literature exploring zooplankton functional traits, to better resolve zooplankton dynamics in the global ocean. We focus on resolving the size-based feeding traits of the zooplankton in a functional size-spectrum ecosystem model, and assessing the role of zooplankton in mediating energy from phytoplankton to fish across the global ocean. We explore the idea that functional traits such as body size, feeding behaviour and carbon content could structure their communities across global environmental productivity gradients, and how this regulates the movement of energy from phytoplankton to fish from oligotrophic to eutrophic waters.

1.3 Using functional size spectra to model marine ecosystems

As marine ecosystems are strongly size-structured, with the general pattern from bacteria to whales being that big things eat small, body size has been described as the “master trait” (Andersen et al., 2016a). Body size also sets the pace of life for individual organisms, dictating physiological processes such as metabolism, movement, ingestion and respiration (Peters, 1983; West et al., 1997; Gillooly et al., 2002; Brown et al., 2004; Kiørboe, 2011). Over the past decade, size-based ecosystem models have been developed that focus on how individual body size, rather than species identity, govern feeding interactions and biological rates and give rise to the emergent distributions of biomass, abundance and productivity in the marine ecosystem (Follows et al., 2007; Ward et al., 2012; Jennings and Collingridge, 2015; Andersen et al., 2016b).

The field of size-based ecosystem modelling is rooted in over 50 years of empirical observations of the scaling of abundance with body size, beginning with Sheldon (Sheldon et al., 1972). The abundance of individual organisms of size w , $N(w)$, scales with body mass according to a power law relationship $N(w) = aw^b$. When expressed on a log-log scale, this power-law relationship is known as the size-spectrum, where a is the intercept, and b is the slope. Sheldon observed that the relationship between body size and abundance of plankton had a consistent slope of -1, meaning that the biomass of plankton was equal across logarithmic body mass intervals. Sheldon and his colleagues hypothesised that this remarkable consistency would hold from “bacteria to whales”. Since then, this relationship between abundance and body size has been shown to hold across marine ecosystems, with slopes of around -1 reported in the open ocean (Rodriguez et al., 2001; San Martin et al.,

2006; Moreno-Ostos et al., 2015), benthic (Hua et al., 2013; Kelly-Gerreyen et al., 2014), coastal (Macpherson et al., 2002; Zhou et al., 2009) and freshwater (Heath, 1995; Boukal, 2014) ecosystems, and has led to the development of size-spectrum models to explore the mechanisms that give rise to this consistency.

The field of size-spectrum modelling has grown quickly over the past five decades, with a diverse range of models emerging that focus on how the size-based processes of predation, growth and mortality of individual organisms give rise to community size spectra in the marine environment. These models span body sizes from phytoplankton (Baird and Suthers, 2007; Banas et al., 2011) to large fish and whales (Dueri et al., 2014; Harfoot et al., 2014), and have been used to assess ecosystem impacts of fishing (Law et al., 2012; Blanchard et al., 2014; Andersen et al., 2015), climate change (Blanchard et al., 2012; Barange et al., 2014; Lefort et al., 2015), biodiversity (Purves et al., 2013; Reuman et al., 2014; Fung et al., 2015) and habitat loss (Rogers et al., 2014).

A limitation of a strict size spectrum approach is that often different species or functional groups have different traits. For example, planktivorous fish and piscivorous fish could be the same size but eat very different food of very different size. However, recent theoretical developments in size-spectrum modelling allow models to resolve unique size-based processes for various functional groups, which is critical to representing the vast diversity of size-scaling across different components of the marine ecosystem (Andersen et al., 2016a). This approach thus retains the generality and strength of a size-based framework but allows the inclusion of functional groups where they could be ecologically or economically important.

In Chapter 2 of this thesis, we review progress and trends in size-spectrum modelling, particularly focusing on the past 10 years, 50 years after the pioneering work of Sheldon and Parsons, (1967). We explore how Sheldon's vision of modelling the marine ecosystem from bacteria to whales has been developed and built upon, and what more needs to be done to realise his idea of representing the whole ecosystem using the size-spectrum framework. Size-based ecosystem models face the same challenge as other modelling frameworks, of integrating lower and higher trophic level processes. Despite the versatility of the size-spectrum framework for modelling different functional groups, representing the zooplankton (and other taxa beyond fish) remains an open problem. We propose the development of "functional size-spectrum" models to address this imbalance. Functional size-spectrum models unify functional traits with traditional size-spectrum models, allowing

different components of the marine ecosystem to be resolved within the same modelling framework.

1.4 Zooplankton are not fish

The focus of size-spectrum models has been on higher trophic levels, primarily resolving different functional groups and species of fish by their functional traits (Andersen *et al.*, 2016b; Guiet *et al.*, 2016a). These models have focused on assessing impacts of fishing (Benoît and Rochet, 2004; Andersen and Pedersen, 2010; Blanchard *et al.*, 2014; Jacobsen *et al.*, 2014; Law *et al.*, 2016) and climate change (Blanchard *et al.*, 2012; Woodworth-Jefcoats *et al.*, 2013; Dueri *et al.*, 2014). The focus on fish means that the dynamics of the plankton have been neglected in model formulations, and realistic coupling of lower and higher trophic level processes has been identified as a key source of uncertainty in these fish-focused models (Jennings and Collingridge, 2015). In current size-spectrum models, the minimum size of the dynamic consumer spectrum extends into the mesozooplankton, and smaller zooplankton and phytoplankton are typically represented in three ways. First, as a static resource spectrum for small fish (Maury *et al.*, 2007; Blanchard *et al.*, 2009, 211, 2012; Law *et al.*, 2009; Guiet *et al.*, 2016b). Second, as externally forced input variables from satellite estimates or other lower trophic level models, with no predation feedback from larger size classes (Woodworth-Jefcoats *et al.*, 2013; Lefort *et al.*, 2015; Le Mézo *et al.*, 2016). Third, as a semi-chemostat system with a fixed carrying capacity, and predation feedback from higher trophic levels (Hartvig *et al.*, 2011; Blanchard *et al.*, 2014; Scott *et al.*, 2014; Zhang *et al.*, 2015, 2016). These current representations essentially lump phytoplankton and zooplankton together as a resource for small fish, and represent larger mesozooplankton as small fish.

In size-spectrum models, size-based feeding behaviour is broadly defined by five key parameters (Woodward *et al.*, 2005; Andersen *et al.*, 2016b): 1) predator-prey mass ratio (PPMR), 2) the coefficient and 3) exponent for how the prey search rate of an individual scales with body size, 4) the breadth of prey sizes around the preferred PPMR and 5) the proportion of ingested prey that is converted to new predator biomass – the assimilation efficiency. Modelling and empirical studies have demonstrated that varying these parameters for fish have a large effect on food web dynamics (Law *et al.*, 2009; Datta *et al.*, 2011; Plank and Law, 2011; Zhang *et al.*, 2013). Feeding behaviour in the zooplankton scales differently with body size, compared to fish. For example, zooplankton PPMRs vary over 7 orders of magnitude, from carnivorous copepods ~ 10 , to salps $\sim 10^8$ (Wirtz, 2012),

whereas the PPMR of fish only varies over 1 order of magnitude, from 100 – 1000 (Andersen and Ursin, 1977; Kerr and Dickie, 2001; Barnes *et al.*, 2010). The sensitivity of size spectra to how fish feeding behaviour are represented suggests that the first step toward resolving zooplankton in functional size-spectrum models is to include an accurate representation of their unique feeding characteristics.

In Chapter 3 of this thesis, we explore how the unique size-dependent feeding characteristics of different zooplankton functional groups affects the productivity, stability and resilience of fish to changes in primary production and fishing pressure. To do this, we built a functional size-spectrum model which resolves the unique feeding traits of several different zooplankton groups, and a base model that represents the zooplankton as small fish. We explore how varying 1) how search rate scales with body size, 2) PPMR, 3) the breadth of prey size ranges around the PPMR and 4) assimilation efficiency in the zooplankton influences total fish biomass and productivity, the stability of the marine ecosystem, and how efficiently energy moves from phytoplankton to fish. We then consider how the PPMR and breadth of prey size ranges of 5 zooplankton functional groups (salps, herbivorous copepods, chaetognaths, flagellates and carnivorous copepods) affects the biomass of the fish community, and how resilient the fish are to fishing pressure. Our results from Chapter 3 demonstrate that zooplankton cannot be lumped with phytoplankton as a resource, or represented as small fish. The unique feeding characteristics of the zooplankton have significant implications for the productivity and resilience of higher trophic levels and the stability of the entire marine ecosystem.

1.5 Functional traits give rise to zooplankton community composition

In Chapter 4, we explore the role of zooplankton functional traits in structuring the zooplankton community across the global ocean. We extend the functional size-spectrum model concepts developed in Chapters 2 and 3 to model nine major zooplankton functional groups (heterotrophic flagellates and ciliates, larvaceans, omnivorous and carnivorous copepods, chaetognaths, euphausiids, salps and jellyfish) with each group defined by its body size range, carbon content and size-based feeding characteristics.

The model breaks the marine ecosystem into three communities: phytoplankton, zooplankton and fish, with the zooplankton community emerging across environmental gradients based on changes in the size structure of the phytoplankton, and the size based feeding characteristics of the nine functional groups. There has been no global analysis of how zooplankton communities change along environmental gradients, so in order to test

how well the emergent distributions of the zooplankton functional groups agreed with empirical distributions, we constructed maps of the abundance distributions of the 7 largest zooplankton groups in the model (everything except heterotrophic flagellates and ciliates). To do this, we used the extensive sample data from the COPEPOD (O'Brien, 2005; <https://www.st.nmfs.noaa.gov/copepod/>) and IMOS (<http://imos.org.au/>) databases to construct generalised additive models that map the relationship between sampled abundances and environmental variables. The emergent patterns of abundance from the model broadly agreed with empirical distributions, and we identified clear shifts in the composition of the emergent zooplankton community across the global ocean. The model we develop in Chapter 4 demonstrates the powerful roles body size, size-based feeding behaviour and carbon content have in structuring the zooplankton community across the global environmental gradients.

1.6 Zooplankton composition across the global ocean mediates transfer efficiency from phytoplankton to fish

Zooplankton community composition is not static, but varies across environmental gradients. In Chapter 5, we use the zooplankton-resolved functional size-spectrum model developed in Chapter 4 to explore how changes in the zooplankton affects how energy moves from phytoplankton to fish, across oligotrophic and eutrophic waters. To do this, we evaluated the change in diets and trophic levels of the nine zooplankton functional groups, and planktivorous fish, and how this leads to a change in the ratio of fish to phytoplankton biomass from oligotrophic to eutrophic waters.

Phytoplankton in oligotrophic waters is dominated by picoplankton, which cannot be directly consumed by omnivorous copepods and euphausiids, which are prey for planktivorous fish. However, salps and larvaceans have very large PPMRs ($\sim 10^8$), and they cover the same body size range as omnivorous copepods and euphausiids, which is why they have been hypothesised to be an important energy pathway from pico-phytoplankton to planktivorous fish in oligotrophic waters (Dieble and Lee, 1992; Bone, 1997; Jaspers et al., 2009). In Chapter 4, we use the zooplankton-resolved functional size spectrum model to evaluate the hypothesised role of salps and larvaceans in oligotrophic waters.

Finally, we conclude in Chapter 6 with a synthesis of the key findings of the thesis, the limitations of the functional size-spectrum model we have constructed, and highlight promising directions for future research.

Chapter 2

From Bacteria to Whales: Using Functional Size Spectra to Model Marine Ecosystems

2.1 Abstract

Size-based ecosystem modelling is emerging as a powerful way to assess ecosystem-level impacts of human - and environment-driven changes from individual-level processes. These models have evolved as mechanistic explanations for observed regular patterns of abundance across the marine size-spectrum hypothesised to hold from bacteria to whales. Fifty years since the first size-spectrum measurements, we ask how far have we come? Although recent modelling studies capture an impressive range of sizes, complexity, and real-world applications, ecosystem coverage is still only partial. We describe how this can be overcome by unifying functional traits with size spectra (which we call functional size spectra) and highlight the key knowledge gaps that need to be filled to model ecosystems from bacteria to whales.

2.2 Size matters for individuals to ecosystems

Ecosystems are under pressure from human activities and environmental change. These changes in marine systems manifest at different levels of biological organisation, from individuals to ecosystems, with consequences for a range of services to society. Models are needed to understand and predict how ecosystems are changing in response to these pressures and to help ecosystem-based management promote recovery and prevent further degradation.

Body size has been described as the ‘master trait’, setting the pace of life by dictating processes such as metabolism, respiration, development, movement, and constraining the role of an individual in its food web (Elton, 1927; Kleiber, 1932; Andersen *et al.*, 2016a). Species-based food web models traditionally represent species as nodes either irrespective of their body size or using an average population-level body size to determine food web interactions (Brose *et al.*, 2016). However, over the past decade there has been rapid development of size-based ecosystem models that focus on how individual size governs feeding interactions and biological rates, originally ignoring species identity. This powerful approach gives rise to emergent distributions of biomass, abundance, and production of organisms and is now being applied in a wide range of environments, most notably in the global ocean (Ward *et al.*, 2012; Watson *et al.*, 2014; Jennings and Collingridge, 2015; Lefort *et al.*, 2015). Although primarily developed for aquatic communities and ecosystems, this perspective has also influenced recent developments to model all life on Earth (Purves, 2013; Harfoot *et al.*, 2014).

The field of size-based ecosystem modelling is rooted in 50 years of the empirical size-spectrum. The size-spectrum is the size distribution of all individuals in a community or ecosystem according to numerical abundance or biomass. It stems from observations of equal biomass of plankton in logarithmic body mass bins (which equates to declining abundance of individuals with body size), famously hypothesised by Sheldon and colleagues to hold ‘from bacteria to whales’ (Sheldon *et al.*, 1972). The general approach traces even further back, to Elton’s ‘pyramids of numbers’ in the 1920s (Elton, 1927; Trebilco *et al.*, 2013). Since Sheldon’s hypothesis, observed size spectra have shown a remarkable regularity in shape and slope across a range of ecosystems (Sprules and Barth, 2015) and communities, including those from the open ocean (Rodríguez *et al.*, 2001; San Martin *et al.*, 2006), sea bottom (Hua *et al.*, 2013; Kelly-Gerreyen *et al.*, 2014), coasts (Macpherson *et al.*, 2002), freshwater (Sprules *et al.*, 1991), and even land (Reumann *et al.*, 2008; Mulder,

2010). Sheldon's call for a solid theoretical foundation to explain this regularity prompted the development of mathematical models and size-spectrum theory (Sprules *et al.*, 2015; Andersen *et al.*, 2016b).

Fifty years on from Sheldon's first empirical spectra, and 90 years since Elton set the stage for size spectra with the introduction of ecological pyramids, we revisit Sheldon's vision and ask how far have we come? Can we now robustly model the size-spectrum from bacteria to whales? We begin by explaining the different types of size-based models, how they scale individual processes to predict ecosystem properties, and how they are being applied across the size-spectrum to answer real-world problems. We find that the vision to span sizes of bacteria to whales has largely been realised, but that total ecosystem coverage is not yet complete. To model the entire ecosystem under human exploitation and environmental change, we argue that we must unify size spectra with other functional traits to advance size-based ecosystem models. We discuss four future research priorities to help achieve this.

2.3 How to model the community size-spectrum?

Over the past five decades, a diverse range of models has emerged that focuses on how individual-level size-based processes give rise to community size spectra, primarily in the marine environment (Figure 2.1). Here, we provide a road map for these different approaches, with a focus on models developed over the past decade.

2.3.1 Static models

The simplest models to predict the size-spectrum are based on assumptions about the mean ratio of predator to prey sizes and the metabolic scaling of consumption and/or turnover rates with body size. The first of these focused on broad predator and prey groupings or trophic levels and assumed an average size for each group to infer a community predator: prey mass ratio (PPMR) (Sheldon *et al.*, 1977; Kerr, 1974). More recently, stable isotope analysis has been used to derive trophic level–body size relationships across individuals within size classes to improve estimates of mean PPMRs and predict the scaling of abundance and biomass with body mass (Jennings and Mackinson, 2003; Trebilco *et al.*, 2013). These models, typically predict biomass size-spectrum slopes of 0 or steeper (and 1 or steeper for the abundance spectrum). Using primary production as inputs, these simple macroecological models can be used to estimate marine consumer biomass and productivity in the global ocean in the absence of fishing (Jennings *et al.*, 2008; Jennings and

Collingridge, 2015). They have also been used to assess the contribution of fish to the marine inorganic carbon cycle (Jennings and Wilson, 2009; Wilson *et al.*, 2009). Because they do not have explicit mortality terms, assessing the impacts of fishing involves snapshot comparisons between predicted unexploited and observed exploited size spectra (Jennings and Blanchard, 2004).

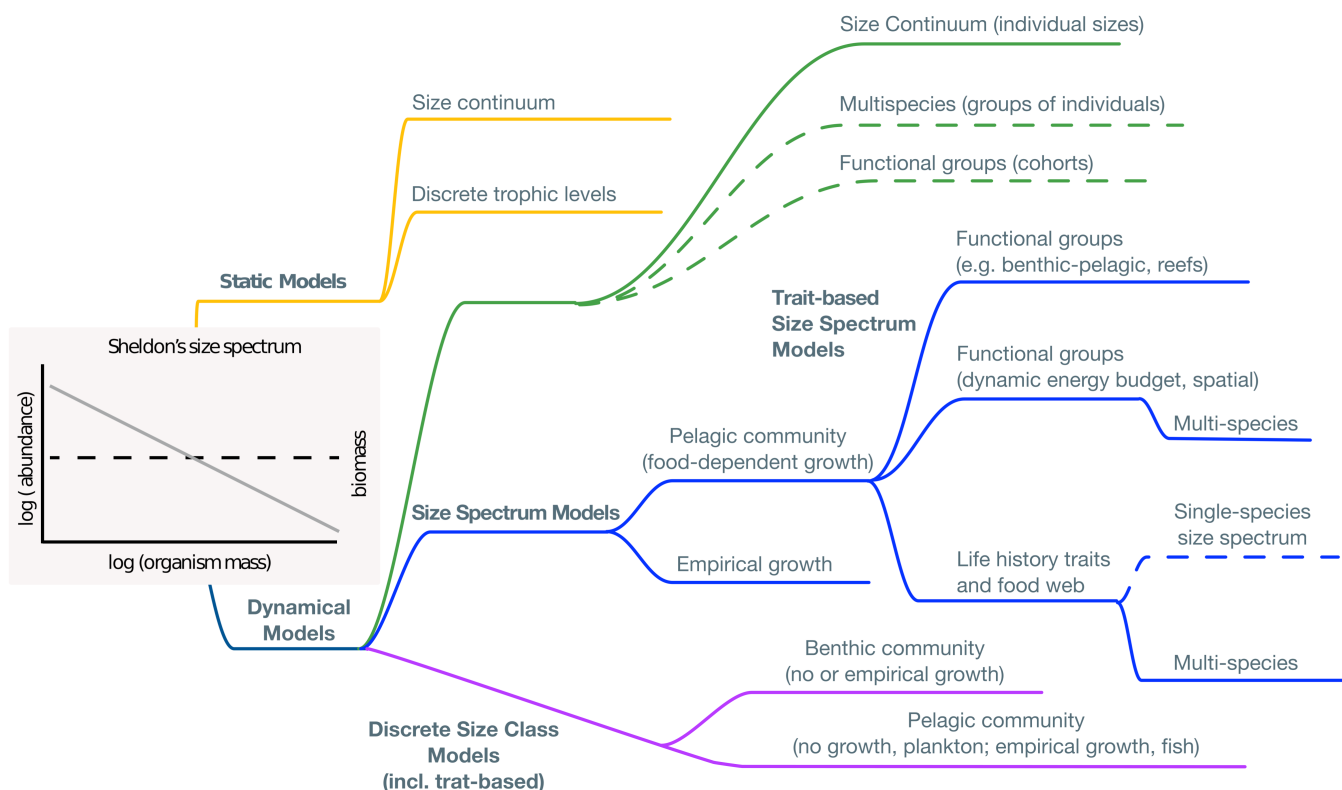


Figure 2.1 How to Model the Size-spectrum? Taxonomy of the different types of approaches that have been used to model the community size-spectrum. An expanded reference list for each model type can be found at <https://doi.org/10.1016/j.tree.2016.12.003>. Abbreviations: IBM, individual- based model; SSM, size-spectrum model.

2.3.2 Individual-based models

In reality, the size-spectrum is an emergent property of many individual-level processes: feeding, growing, dying, reproducing, and moving in space and time. These processes are stochastic and can be represented through the use of individual-based models (IBMs), which describe a set of rules and events that affect individuals. IBMs focusing on the processes of size-based predation driving growth and death have been used to model the community size-spectrum and produce emergent size spectra that are broadly consistent with the Sheldon expectation of an abundance size-spectrum slope of 1 when taken as an average

across many stochastic realisations (Shin and Cury, 2004; Harfoot *et al.*, 2014). More detailed IBMs have introduced greater complexity through representation of species-specific or functional traits and, to accommodate this, use cohorts or groups of individuals as agents to predict emergent size spectra (Shin and Cury, 2004; Harfoot *et al.*, 2014). A powerful use of IBMs formulated with stochastic size-based processes has been to derive simpler size-spectrum models (SSMs) that capture the processes of an average individual based purely on size and to assess how well these capture the mean across many stochastic realisations (Law *et al.*, 2009; Datta *et al.*, 2010).

2.3.3 SSMs

SSMs are dynamic deterministic models that explicitly predict changes in the size-spectrum through time, starting with size-based, individual-level mechanistic processes (see Andersen *et al.*, 2016b and Guiet *et al.*, 2016a for reviews). At the core of this modelling approach is the McKendrick von Foerster (MF) partial differential equation that is modified to represent a distribution of sizes rather than ages. The first dynamic size-spectrum models represented open-water (pelagic) systems, focusing on how gains through growth and losses through respiration or predation propagated along the size-spectrum through time (Silvert and Platt, 1978; Zhou and Huntley, 1997). SSMs proliferated following a pivotal study that resolved the food-dependent growth and mortality component, provided an analytic solution to the size-spectrum slope, as well as demonstrating how it changed with fishing (Benoît and Rochet, 2004). SSMs track the changing abundance of individuals at size through time as a function of fluxes due to growth and mortality with a renewal term at smallest sizes that represents the birth rate of new offspring. Feeding rates are a consequence of size-dependent prey availability, encounter rates, and ontogenetic changes in the preferred prey size and range (Box 1.1). Prey size selection is specified from the distribution of the preferred PPMR. SSMs have been extended to include more detailed processes such as energy allocation to reproduction, spatial processes, and seasonality (Maury *et al.*, 2007; Maury 2010; Castle *et al.*, 2011; Datta and Blanchard, 2016). In the absence of any fishing, SSMs produce abundance size-spectrum slopes close to 1, conforming to Sheldon's conjecture of near equal biomass across logarithmically binned body mass classes. In contrast to the static scaling models, predicted size spectra from SSMs on a log-log plot can exhibit nonlinear patterns such as truncation at the largest body masses and time-varying oscillations that propagate through the size-spectrum (travelling waves; Law *et al.*, 2009; Plank and Law, 2012).

2.3.4 Discrete size class models

SSMs focus on size-dependent predation as the key process linking growth, death, and reproduction. However, processes other than predation, such as nutrient uptake and intake rates of filter feeders can be modelled as size dependent processes. For instance, nutrient uptake scales with cell size for phytoplankton (Moloney and Field, 1989), and this has been used to model nutrient and light fixation and thus photosynthesis by unicellular phytoplankton (Irwin *et al.*, 2006). These models usually include discrete size classes where changes in abundance through time are from birth and death processes and where individuals do not grow in size (similar to a species-based allometric food web model) (Baird and Suthers, 2007; Banas, 2011; Ward *et al.*, 2012). For organisms that do grow in size (e.g., fish and benthic invertebrates), discrete size class models often use empirical growth relationships (Duplisea *et al.*, 2002; Pope *et al.*, 2006 Thorpe *et al.*, 2015), based on the assumption that growth is not strongly food dependent; contrary to the assumptions of most (but not all, e.g., Zhou and Huntley, 1997; Carozza *et al.*, 2016) SSMs where both growth and predation are linked to size-based feeding.

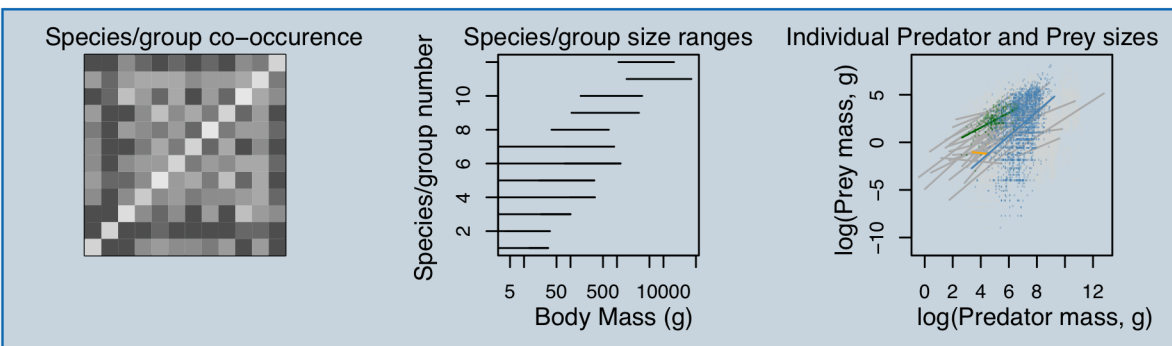
2.3.5 Trait-based SSMs: including other functional traits

Perhaps the biggest leap in the development of SSMs has involved blurring the distinction with species-based food web models. Trait-based SSMs resolve species-specific traits through asymptotic maximum size and size at maturation, and allow species-specific interactions (Hartvig *et al.*, 2011; Maury and Poggiale, 2013; Scott *et al.*, 2014). Even with this added layer of complexity, these models predict an overall community size-spectrum that is consistent with simpler models, but also provide a size-spectrum for each species (Box 1.1). This advance makes SSMs similar to physiologically structured population models but capable of resolving the complexity of food web models through the use of traits (Brose *et al.*, 2016; Maury and Poggiale, 2013; Hartvig *et al.*, 2011; De Roos and Persson, 2013). Increasing trait diversity in the SSMs has the effect of stabilising complex ecological communities (Hartvig and Andersen, 2013; Zhang *et al.*, 2013; Zhang *et al.*, 2014). Multispecies extensions of the trait-based model have enabled real-world ecosystem applications in combination with extensive species-specific trait data for parameterisation (Blanchard *et al.*, 2014; Spence *et al.*, 2015; Zhang *et al.*, 2015; Houle *et al.*, 2016) (Box 1.1). Although trait-based models have so far focused on fish communities they also include a background resource size-spectrum, which implicitly represents the plankton community

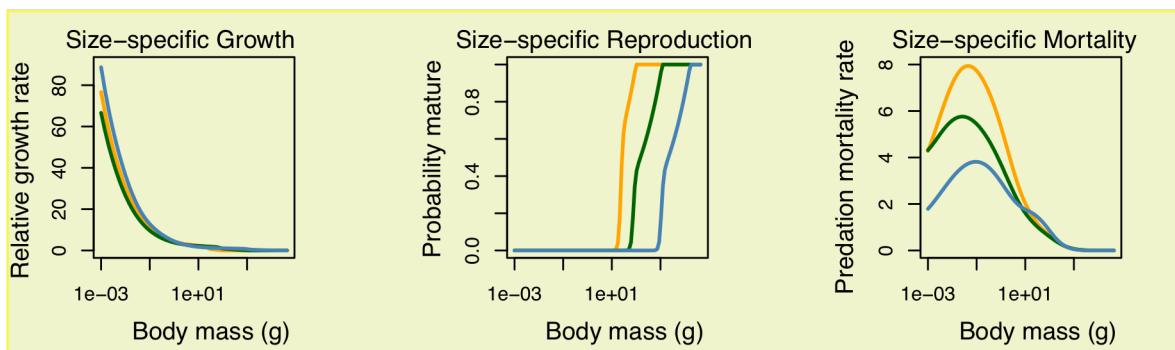
Box 2.1 How can ecological data inform SSMs?

SSMs scale individual-level processes up to ecosystem structure and dynamics. Here, we illustrate in three steps how species and size-specific data can be used to develop a multispecies or functional size-spectrum models (Figure I).

Step 1: Empirical patterns and parameters



Step 2: Predicted individual-level processes



Step 3: Emergent population, community and ecosystem-level properties

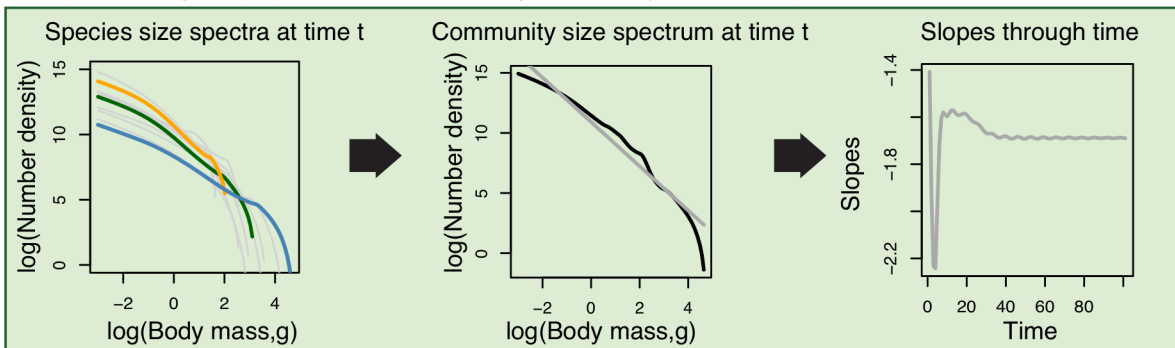


Figure I: Example showing three steps for building a size-spectrum model that involve linking empirical patterns (Step 1) to individual (Step 2) and population and community level predictions (Step 3).

Step 1. First, species-specific and individual-level data that can be used to parameterise SSMs include: spatial or habitat co-occurrences of species; groups or size classes (example data from Scott *et al.*, 2014 and Blanchard *et al.*, 2014); information on offspring, adult and asymptotic sizes (example data from Andersen *et al.*, 2016a); and individual-level PPMRs (data from Barnes *et al.*, 2008). Three contrasting species, embedded within the community size-spectrum, are shown in orange, green, and blue.

Step 2. Once parameterised, an SSM can be set up using an initial size-spectrum at the first time step (Scott *et al.*, 2014). At each time step, species- and size-specific rates of feeding and energy allocation into maturation are calculated. These are then used to predict individual food- dependent, size-specific growth, mortality, and reproductive rates. Growth and mortality rates determine the fluxes of abundance in and out of each size, and new offspring enter the size-spectrum of each species at its smallest size.

Step 3. Because the growth, mortality, and reproduction depend on the abundance of predators and prey in each time step, the predicted changes in abundance at size through time are solved numerically by looping through time steps until an equilibrium is reached. The numerical density (N) at body mass (w) for each group or species is summed across all groups to give the normalised size-spectrum. These are outputted at each time step along with predicted changes in size-specific growth, reproduction, and mortality rates. Changes in the size-spectrum slopes can be calculated by fitting, at each time step, a straight line through the predicted size-spectrum if plotted on a log–log plot or alternatively by fitting a power law if estimating exponents. Predicted changes in individual level (Step 2) and population and community level (Step 3) properties can then be confronted with empirical data for comparison or repeating the above process in conjunction with a statistical procedure to formally estimate parameters and their uncertainty (Box 1.3).

as a series of discrete size classes that do not grow in body size (Hartvig *et al.*, 2011) and thus are partial representations of ecosystems.

Despite the ubiquity of size-based processes in pelagic ecosystems, not all processes and communities are size based. SSMs have moved beyond pure pelagic communities and towards greater ecosystem coverage by representing different communities and functional groups; some of which are not size structured (Blanchard *et al.*, 2009; 2011). The benthic community receives much of its energy flow directly from detritus fall (sinking rates are size based) from the pelagic ecosystem, but once there, the widely flexible scavengers can feed

on both pelagic and benthic components. However, intake rates of filter feeders and scavengers still scale with body size. The latter can still be modelled with SSMs, but by relaxing the prey size selection assumption where individuals of different sizes compete for a shared unstructured resource (Blanchard *et al.*, 2009). For example, on coral reefs, large herbivorous fishes compete in a size-based manner for non-size based resources such as macroalgae (Rogers *et al.*, 2014). Dynamic size spectra of organisms that share energy in this way tend to have shallower and more variable size spectra than those that follow ‘big eat small’ rules. The use of functional groups can help to resolve size-dependent spatial movement and habitat use embedded in SSMs (Maury, 2010; Castle *et al.*, 2011; Watson *et al.*, 2014). For example, (Maury, 2010) breaks the pelagic ecosystem into epipelagic, mesopelagic, and migratory communities, and includes both vertical and horizontal movement of individuals, which affects their vulnerability to predation. Habitat structural complexity and size-dependent hiding is an important feature that affects prey vulnerability on coral reefs and influences emergent predictions of size spectra that are consistent with observations across a gradient of habitat complexity (Rogers *et al.*, 2014).

2.4 Limitations of SSMs

Despite the utility of SSMs, they have several limitations, some of which are inherent, and others are challenging and slowly being overcome. First, SSMs are not always well suited to address questions relating to single-species population dynamics, especially where food is unlimited and where predation mortality is less important – two key processes in SSMs.

Many population dynamic models are applied to well-studied species, where parameter values for key processes and life stages are relatively well known, making SSMs unnecessary (although see (Andersen and Beyer, 2015) for their utility in data-poor cases). Second, when ontogenetic variation in body size is small (e.g., in seabirds - Webb *et al.*, 2011) simpler unstructured, stage-structured, or allometric models (that use a mean body size) are likely to be more appropriate than SSMs (De Roos *et al.*, 2008; Brose *et al.*, 2016). Third, SSMs have generally been applied at regional and larger spatial (Woodworth-Jefcoats *et al.*, 2013; Blanchard *et al.*, 2014; Jacobsen *et al.*, 2016) scales, and might not be as appropriate at finer scales (Guillet *et al.*, 2016a). Many management-related questions need to be addressed on a local scale where the community dynamics might be well understood in terms of species and habitat interactions (Ling *et al.*, 2014), and the size-dependent nature of these interactions are nuances rather than key drivers of the dynamics. Having said this, recent work has shown that output from a functional group SSM applied on coral

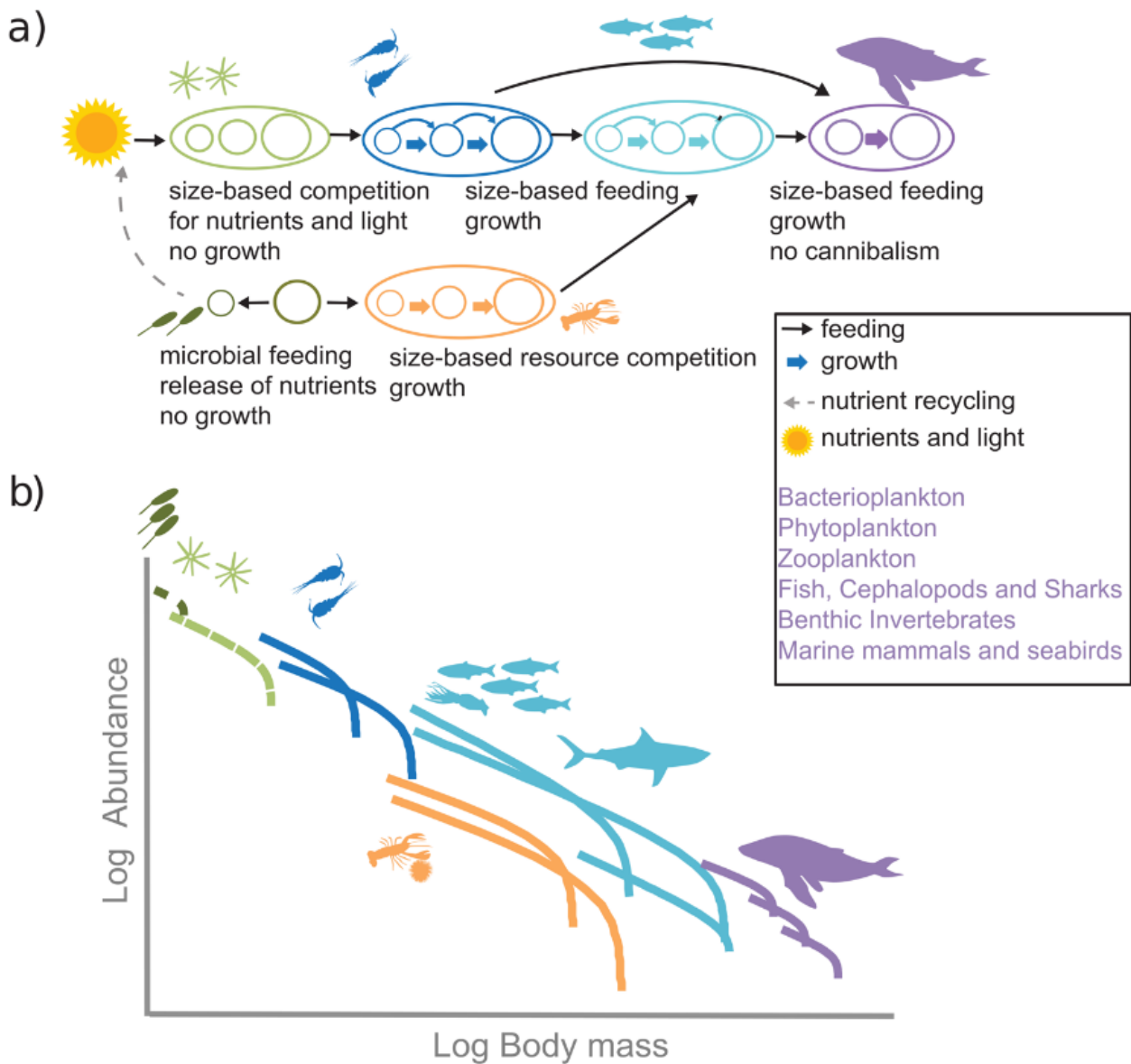


Figure 2.2 Functional Size-spectrum: An Illustration Applied to a Conceptual Marine Ecosystem from Bacteria to Whales. (a) Stylised size-structured ecosystem model emphasising different processes across the size-spectrum. Larger circles are used to illustrate relative changes in size within functional groups. Black arrows illustrate the presence of feeding within and across groups but do not show the full extent of the many feeding links present in size-spectrum models. Thick colored arrows represent growth in size. (b) Hypothetical emergent size spectra for the same types of functional groups shown in a) but here represented via life history traits depicted by differences in offspring and adult asymptotic sizes (Andersen *et al.*, 2016b).

reefs, where species-based food web descriptions were lacking, compared well with data at local scales (Rogers *et al.*, 2014). The appropriate spatial scale for applying SSMs is still an open question and requires more detailed cross- scale tests of theory to resolve. Last, SSMs have focused on taxonomic subsets of the size-spectrum (e.g., plankton and fish communities; Box 1.2) and therefore have only achieved partial ecosystem coverage so far. However, by bringing together different strands of size- based modelling this issue can be addressed. The functional size-spectrum framework shown in Figure 2.2 builds upon the trait-based approach by combining alternative model structures (including non-size based ones) and could form the basis of size-based ecosystem models that resolve the dynamics of important microbial, plankton and nekton functional groups, all the way up to marine mammals and seabirds. We expand on this and other research opportunities below.

2.5 Beyond bacteria to whales: future research directions for size-based ecosystem models

Despite SSMs not having been fully developed all the way from bacteria to whales, in many respects, the recent achievements of size-based models extend beyond Sheldon 's initial vision for describing the size-spectrum (Box 1.2). SSMs are being used to examine: spatial distributions of abundance (Lefort *et al.*, 2015), species interactions (Blanchard *et al.*, 2014), diversity-stability links (Zhang *et al.*, 2013), eco-evolutionary processes (Zhang *et al.*, 2015), and consequences of human-induced and environmental change (Jacobsen *et al.*, 2014; 2016; Blanchard *et al.*, 2012). Here, we highlight four promising research innovations that will help us realise the full potential and wider generality of this approach for modelling whole ecosystems.

2.5.1 Beyond one size fits all: unifying models through functional traits

The simple rule of size-based prey selection has proven useful for understanding the structure and dynamics of communities but one size-based rule will not universally fit all organisms with life-history, morphology, habitat, and behavioral traits all affecting realised food web interactions (Boukal, 2014). For example, marine mammals illustrate how technological innovations enable different size-based strategies to maximise energy intake. Baleen plates and the ability to forage over large spatial scales (also dependent on large body size) allow baleen whales to feed down food chains and exploit highly productive but patchy plankton and nekton. Similarly, echolocation enables beaked whales to extend their prey detection range and forage selectively on larger, energetically richer, but more sparsely

distributed prey compared to seals of similar body sizes that are constrained to forage on smaller but more predictably distributed prey (Naito *et al.*, 2013). Differences in size-based rules also apply to species of zooplankton (Henschke *et al.*, 2016), fish, sharks (Barnes *et al.*, 2010), and seabirds (Webb *et al.*, 2011).

These differences are not exceptions, but rather demonstrate that one size does not necessarily fit all. Most organisms have a distribution of prey size preference bounded by a minimum and maximum size (Elton, 1927). In SSMs, as long as the size preference is known, then the feeding function can be adapted for different types of feeding (Canales *et al.*, 2015; Houle *et al.*, 2016). This is powerful; it means that a size-spectrum framework becomes more generalisable through greater flexibility in these functional traits. Even organisms such as parasites can be represented as they follow a ‘reverse size rule’ that

Box 2.2 How are size-spectrum models being used?

A synthesis of 75 papers published on since 2010 (<https://doi.org/10.1016/j.tree.2016.12.003>) illustrates that the different types of size-based models (Figure I b, c) collectively cover a size range of >20 orders of magnitude (Figure I a). However, there are no models that span this entire range. Only 13 of the 75 papers explicitly capture the dynamics of more than one functional group. Furthermore, none of the 75 papers resolve the size classes dominated by bacteria and none explicitly capture the dynamics of marine mammals or seabirds.

Fish and fisheries studies dominate both in terms of focal taxa and the characteristic size range (Figure I a) covered by dynamic models, even though there are more plankton empirical studies (Figure I b, see <https://doi.org/10.1016/j.tree.2016.12.003> for references). Of these studies, 44 studies have used SSMs and 37 of these have used them to investigate the ecosystem consequences of fishing intensity and selectivity, marine protected areas, climate change, patterns of biodiversity, and structural habitat loss (Figure I c, see <https://doi.org/10.1016/j.tree.2016.12.003> for references). These recent studies include real-ecosystem applications spanning from the global ocean (Lefort *et al.*, 2015) to local coral reefs (Rogers *et al.*, 2014). Fishing applications are most numerous among these. Reductions in the empirical slopes of fish community size spectra have been attributed to the removal of large-bodied individuals (and release of their smaller prey) through fishing (Blanchard *et al.*, 2005). These features of exploited marine ecosystems have led to some of the key developments of dynamic SSMs to provide a theoretical framework for the use of size-based indicators to monitor the

means they feed on larger organisms but still have a minimum and maximum size for hosts (Warren *et al.*, 2010).

ecosystem effects of fishing (Andersen *et al.*, 2015b). From a conservation and management viewpoint, a key advantage of the size-based approach is that predictions can be compared to modelled unexploited size spectra under changing environmental conditions, rather than relying solely on historical baselines that may not be relevant under current or future environmental conditions (Jennings and Blanchard, 2004). The application of SSMs in this context can also include analysis of how several changing input variables – including primary production, temperature, and fishing mortality rates – affect predicted changes in abundance, biomass, production, slopes, or other outputs.

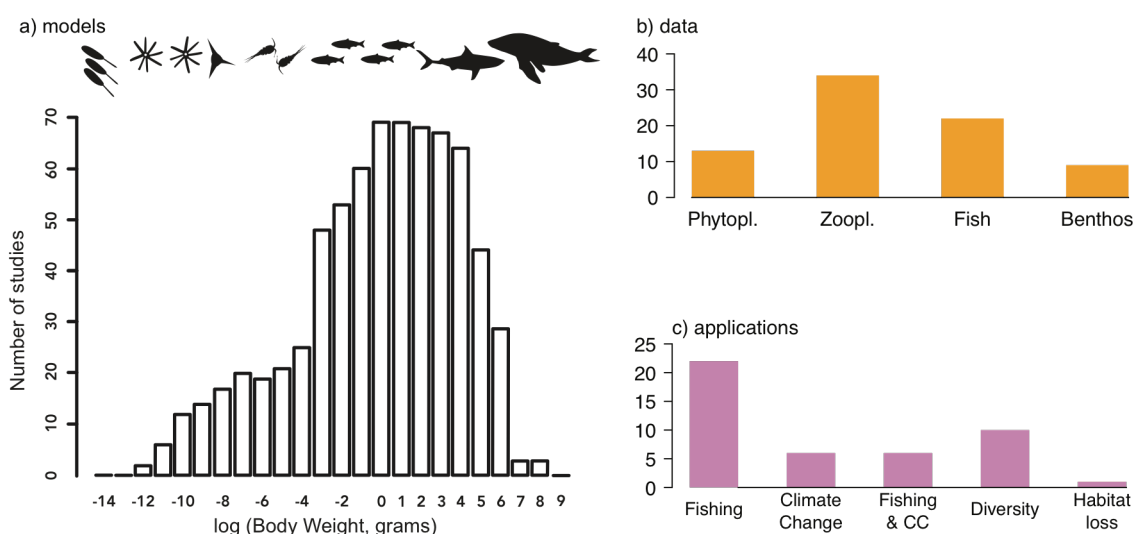


Figure I: Synthesis of SSM Size-spectrum Studies Published in the Last 5 Years (references and keyword search terms are available at <https://doi.org/10.1016/j.tree.2016.12.003>). (a) Number of modelling studies that explicitly represent size classes spanning bacteria to whales. (b) Number of empirical size-spectrum papers published for different focal communities. (c) Number of different types of size-based ecosystem model applications. Abbreviations: CC; climate change; Phytopl.; phytoplankton; Zoopl.; zooplankton.

Currently, there is limited cross-fertilisation between plankton-focused and higher trophic level size-based models, but realistic coupling to plankton is recognised as a key uncertainty in higher trophic level models (Jennings and Collingridge, 2015). For these higher trophic level models, plankton dynamics are usually assumed to be: (i) static (Benoît and Rochet,

2004); (ii) modelled as a discrete size classes (without fluxes of growth through the size-spectrum) (Andersen and Pedersen, 2010); or (iii) externally forced (Blanchard *et al.*, 2012; Barange *et al.*, 2014; Lefort *et al.*, 2015). Externally forced plankton inputs are often derived from satellite estimates (Jennings and Collingridge, 2015) or coarsely size-structured Earth systems or regional biogeochemical models (Carozza *et al.*, 2016), rather than being explicitly linked to phytoplankton and zooplankton size-spectrum dynamics (Fuchs and Franks, 2010) or emerging plankton trait-based models (Andersen *et al.*, 2015a). To improve ecosystem coverage and feedbacks, there is much scope for better integration of dynamic SSMs already in use in different parts of the size-spectrum.

Formulating ecosystem models as functional size spectra overcomes some of the limitations of purely size- or species-based approaches and also has other advantages. First, most components are likely to have some features that are size dependent. For example, although seabirds and seals do not have large variation in individual sizes they still exert strong prey size selectivity on fish communities (Houle *et al.*, 2016), and have search and intake rates that scale with body size. Second, size- and trait-based parameterisation of food webs can help to constrain parameters and reduce uncertainty in complex models (Box 1.3). A functional size-spectrum approach also has the potential to be expanded to some terrestrial food webs, where interest in individual body size distributions has increased in recent years (Reumann *et al.*, 2008; Turnbull *et al.*, 2014), and where the manner in which individual-level processes scale up to ecosystems is beginning to be explored (Harfoot *et al.*, 2014).

2.5.2 Beyond slopes: testing predictions with observed size spectra

Clearly, SSMs have come a long way, but do we actually have the data to assess whether or not they can predict abundance and biomass all the way from bacteria to whales in an integrated fashion? While empirical size spectra studies are numerous (for reviews, see Turnbull *et al.*, 2014 and Sprules and Barth, 2015), a key limitation of SSMs is that model skill assessment is difficult across the entire ecosystem. This is because technology has limited data collection to taxonomically defined communities or habitats due to the challenges of a huge variety of sampling platforms to observe bacteria and plankton (bottle samples, small nets, and optical counters), fish (trawls and acoustics), mammals (visual or acoustics), reefs (visual census), and benthos (grabs and cores). It is clear that we need better integration of whole ecosystem data and models, from accurate representation of underlying individual processes to more detailed tests of their predictions.

While there is consistency in the prediction of steady state size-spectrum slopes across several models, both modelled and observed size spectra can exhibit nonlinear patterns. Different hypotheses have been proposed to explain lumpy (nonlinear) patterns in size spectra, including habitat complexity (Nash *et al.*, 2013; Rogers *et al.*, 2014), omnivory (Chang *et al.*, 2014), smaller PPMR, and narrower range of prey sizes (Plank and Law, 2012), and dynamic seasonal or longer-term cycles (Canales *et al.*, 2015; Datta and Blanchard, 2016). Dynamic oscillations (travelling waves) have been shown to arise due to changes in parameters (such as PPMR) or through perturbations such as size-selective fishing (Blanchard *et al.*, 2011; Jacobsen *et al.*, 2014; Law *et al.*, 2014) or bottom-up disturbances (Blanchard *et al.*, 2011; Datta *et al.*, 2011) that affect the stability of size-spectrum. Temporal variation around a time-averaged size-spectrum can have important consequences for ecosystem services, such as fisheries stability. In contrast, individuals hiding in size-structured refugia, such as coral reef crevices (Rogers *et al.*, 2014), produce lumpy size spectra that are beneficial for survival rather than evidence of oscillations or instability. Empirical examples show lumpy zooplankton size spectra in productive coastal eddies result in older and larger larval fish due to increased food availability and hence survival (Mullaney and Suthers, 2013). Under different environmental conditions, it is likely that there are multiple causes of nonlinear patterns and variability in the size spectra that emerge at different time and space scales, but these have yet to be tested in a systematic and inclusive way.

Box 2.3 Predicting ecosystem structure and function in an era of rapid change: managing uncertainty

Data are needed to parameterise and test size-spectrum models to apply them to real ecosystems and assess how accurate their predictions of ecosystem structure and function are (Box 1.1). Because size-spectrum models are computationally inexpensive relative to more complex ecosystem models, there could be scope for the development of SSMS as real-time observational models. Predictions from models could be combined with data collected at different scales or organisational levels ranging from individual growth rates, tagging data, species or community biomass and abundance or large fisheries catches (Blanchard *et al.*, 2012; Dueri and Maury, 2013; Blanchard *et al.*, 2014). More research on the level of complexity needed to accurately capture ecosystem function and dynamics without inflating uncertainty is needed.

Models have been confronted by data in different ways: qualitative comparisons with size-spectrum slopes from the relevant part of the size-spectrum and more quantitative

assessment of models by calibrating and fitting them to data. Calibrating the model with earlier observations and then assessing model skill by comparing time-series of predictions with later observations is an approach that is being used for size-spectrum models (Blanchard *et al.*, 2014; Spence *et al.*, 2015; Zhang *et al.*, 2015).

Uncertainty also comes from our imperfect knowledge about what drives the structure of ecosystems. This is especially critical in ecosystem models, where different models make different assumptions and prioritise species identity over size (or vice versa) in how individuals interact. Model inter-comparisons (Jacobsen *et al.*, 2015; Woodworth-Jefcoats, 2015) enable these approaches to be considered in a wider context and such broad-scale uncertainties are being tackled through their use as part of ecosystem model ensembles. Tools to formally integrate data and assess parameter uncertainty are beginning to be used in conjunction with size-spectrum models and data. One advantage of the Bayesian framework is that it can account for the effects of parameter and observational uncertainty on model outputs, by presenting these outputs probabilistically. This allows a more informed assessment of the uncertainty and associated risk of using modelled outcomes for management decisions and for identification of which sources of uncertainty matter the most (Zhang *et al.*, 2014; Spence *et al.*, 2015; Thorpe *et al.*, 2015). The latter is particularly useful for prioritising data needs.

2.5.3 Beyond fixed traits: extinctions, invasions, and evolution

A fundamental area of ecological research involves understanding how the loss of a species affects biodiversity throughout the food web (Brose *et al.*, 2016). Although early SSMs ignored species identity and were viewed as too simple to represent biodiversity, recent work suggests that SSMs could hold considerable promise in biodiversity research. In addition to representing functional diversity (species, traits, and functional groups), SSMs have been extended to explain patterns in size-based diversity (diversity size-spectrum; Reuman *et al.*, 2014). From these models, empirically observed macroecological patterns such as species richness versus body mass emerge. Whether or not this theory holds across different types of ecosystems warrants investigation.

Coexistence and persistence of different species and functional groups is affected by how density dependence and competition are incorporated into models (Andersen *et al.*, 2017). Changes in phenotypic and genotypic plasticity also affect coexistence, and have recently

been incorporated into SSMs examining species invasions, community assembly, and adaptive dynamics (Zhang *et al.*, 2015). Given the large redistribution of species under climate change, advances that enable species composition and traits to change and evolve provide a framework for exploring the emergence and evolution of novel communities and trait distributions.

2.5.4 Beyond fishing and warming: multiple stressors and their interactions

A key strength of applied SSMs has been the ability to test joint and marginal effects of fishing and climate change on the size-spectrum. In terms of fishing, until recently, human–natural ecosystem interactions have involved simplified representations of fishing as an impact by including a size and gear and/or species-dependent mortality term. The role of economic and behavioral drivers such as the technological development of fisheries, affecting the efficiency to catch fish, is beginning to be tackled through more detailed consideration of the two-way feedbacks between humans and size-structured ecosystems (Carozza *et al.*, 2016; Plank *et al.*, 2016).

Two of the biggest missing stressors in the context of climate and environmental change include effects of acidification and disease outbreaks. Given the expected incidence of acidification and disease outbreaks under global warming, we need a better understanding of how these stressors operate at the individual level before incorporating them in SSMs. Incorporating a wider range of stressors into the size-spectrum modelling framework could enable initial assessments of cumulative ecosystem impacts to be made, as well as better integration with empirical size-spectrum studies where stressors such as temperature, nutrients, pollution, and pH have been studied across gradients in natural and controlled experimental aquatic ecosystems (Schwinghamer, 1988; Yvon-Durocher, 2011). Development of theory in this area could focus on understanding physiological mechanisms controlling size-dependence of performance and stress responses and, in the case of disease, susceptibility and immunity. A first step could be to combine modelled experimental and observational systems to test hypotheses of multiple stressors.

2.6 Concluding remarks

Size-based community and ecosystem models are being applied to a wide range of ecosystems to investigate structure and function, biogeochemical cycles, as well as the impacts of climate change, habitat loss, and fishing but there are still Outstanding Questions. Nevertheless, Sheldon's vision of considering the marine pelagic ecosystem from bacteria

to whales has motivated 50 years of both empirical and modelling work on size spectra. His vision has largely been realised, and expanded; we have SSMs that go from sizes of phytoplankton to whales, and even include benthic systems. However, other key components of marine ecosystems have either not yet been tackled or are only superficially treated. The roles of bacteria and viruses in the microbial loop, which lead to nutrient recycling and enhance trophic efficiency in the food web, has yet to be integrated into SSMs. Furthermore, diseases and parasites, which are increasingly recognised as important components of marine systems (Wilson *et al.*, 2002), have not yet been tackled. Finally, the largest animals, the baleen whales, which feed on much smaller animals than themselves, have only been implicitly represented in SSMs so far (but, see Harfoot *et al.*, 2014).

By using functional size spectra and trait-based approaches, we have the tools needed to model whole ecosystems. Although early models ignored species identity, SSMs can now capture species traits and functional groups, suggesting that further development and unification of approaches across the size-spectrum is likely to result in a wider range of ecosystem and biodiversity applications in the near future. By showing the diverse applications and emerging approaches that allow us to tackle the entire ecosystem, we hope this review stimulates wider consideration of size-spectrum models in ecology.

Chapter 3

Zooplankton are not fish: improving zooplankton realism in size-spectrum models mediates energy transfer in food webs

3.1 Abstract

The evidence for an equal distribution of biomass from bacteria to whales has led to development of size-spectrum models that represent the dynamics of the marine ecosystem using size rather than species identity. Recent advances have improved the realism of the fish component of the size-spectrum, but these often assume that small fish feed on an aggregated plankton size-spectrum, without any explicit representation of zooplankton dynamics. In these models, small zooplankton are grouped with phytoplankton as a resource for larval fish, and large zooplankton are parameterised as small fish. Here we investigate the impact of resolving zooplankton and their feeding traits in a dynamic size-spectrum model. First, we compare a base model, where zooplankton are parameterised as smaller fish, to a model that includes zooplankton-specific feeding parameters. Second, we evaluate how the parameterisation of zooplankton feeding characteristics, specifically the predator-prey mass ratio (PPMR), assimilation efficiency and feeding kernel width, affects the productivity and stability of the fish community. Finally, we compare how feeding characteristics of different zooplankton functional groups mediate increases in primary production and fishing pressure. Incorporating zooplankton-specific feeding parameters increased productivity of the fish community, but also changed the dynamics of the entire system from a stable to an oscillating steady-state. The inclusion of zooplankton feeding characteristics mediated a trade-off between the productivity and resilience of the fish community, and its stability. Fish communities with increased productivity and lower stability were supported by zooplankton with a larger PPMR and a narrower feeding kernel – specialised herbivores. In contrast, fish communities that were stable had lower productivity, and were supported by zooplankton with a lower PPMR and a wider feeding kernel – generalist carnivores. Herbivorous zooplankton communities were more efficient at mediating increases in primary production, and supported fish communities more resilient to fishing. Our results illustrate that zooplankton are not just a static food source for larger

organisms, nor can they be resolved as very small fish. The unique feeding characteristics of zooplankton have enormous implications for the dynamics of marine ecosystems, and their representation is of critical importance in size-spectrum models, and end-to-end ecosystem models more broadly.

3.2 Introduction

In the 50 years since Sheldon *et al.* (1967) first hypothesised an equal concentration of biomass from bacteria to whales, a range of size-spectrum models have been developed to explain this remarkable consistency (Andersen *et al.*, 2016b; Guiet *et al.*, 2016a). Size-spectrum models represent the entire marine community as a size distribution, and traditionally do not resolve species identity. Their simplicity and parsimonious parameterisation makes it possible for them to be used to investigate human impacts at the community level, including fishing (e.g., Andersen and Pedersen, 2010; Law *et al.*, 2014; Jacobsen *et al.*, 2014), climate change (e.g., Blanchard *et al.*, 2012; Woodworth-Jefcoats *et al.*, 2013; Barange *et al.*, 2014; Dueri *et al.*, 2014) and habitat loss (Rogers *et al.*, 2014). The focus of these models has been on higher trophic levels – primarily fish and fishing – and in recent years there has been considerable effort in improving their parameterisation (Andersen *et al.*, 2016b; Guiet *et al.*, 2016a). For example, recent theoretical developments now allow size-spectrum models to resolve different functional groups and even species by their traits, and this has been implemented for various fish (e.g., Blanchard *et al.*, 2014; Dueri *et al.*, 2014; Zhang *et al.*, 2015). The focus on fish has meant that the dynamics of the plankton-dominated lower trophic levels has been neglected in model formulations. Zooplankton, as the main consumers of phytoplankton and prey of small fish are the chief intermediaries between primary production and higher trophic levels, and thus play a critical role in marine food web dynamics (Carlotti and Poggiale, 2010; Mitra and Davis, 2010).

In current dynamic size-spectrum models, the minimum size of the dynamic consumer spectrum extends to mesozooplankton. For smaller zooplankton, there are three common representations. First, phytoplankton and small zooplankton are represented as a fixed resource spectrum (with a varying intercept and a slope held at -1), and are considered only as a food source for the smallest fish size classes (Maury *et al.*, 2007; Law *et al.*, 2009; Blanchard *et al.*, 2009, 2011, 2012; Datta *et al.*, 2010; Guiet *et al.*, 2016b). Second, the phytoplankton and small zooplankton spectrum is determined by an external nutrient-phytoplankton-zooplankton (NPZ) model, with no predation feedback from the larger dynamic size classes (Woodworth-Jefcoats *et al.*, 2013; Lefort *et al.*, 2015; Le Mézo *et al.*, 2016). Third, phytoplankton and small zooplankton are modelled as a semi-chemostat

system, with a fixed carrying capacity and predation feedback from higher trophic levels (Hartvig *et al.*, 2011; Blanchard *et al.*, 2014; Scott *et al.*, 2014; Zhang *et al.*, 2015, 2016). The latter approach is the only one in which the size-spectrum of fish dynamically interacts with phytoplankton and small zooplankton. These current representations essentially group smaller zooplankton and phytoplankton together as food for the smallest dynamic size classes, and larger zooplankton as small fish.

Assuming zooplankton have the same dynamics as phytoplankton or small fish is not only incorrect, but could have considerable effects on energy transfer in food webs. Zooplankton have feeding characteristics distinctly different from fish. For instance, the average predator-prey mass ratio (in grams of wet weight) for fish is typically around 100 (Jennings *et al.*, 2001) but for zooplankton it is >1,000 (Kiørboe, 2008; Wirtz, 2012). Additionally, zooplankton exhibit vast phylogenetic biodiversity, with at least eight phyla commonly present (crustaceans, chordates, chaetognaths, molluscs, cnidarians, echinoderms, ctenophores and annelids), each with considerable differences in their feeding ecology, from passive suspension grazing of the water column to active ambushing and carnivory (Kiørboe, 2011). Further complicating their feeding, various species of jellyfish, copepods, and microzooplankton can switch between suspension and ambush feeding modes, and this is reflected in different optimal prey sizes realised by the same species (Landry, 1981; Goldman and Dennett, 1990; Saiz and Kiørboe, 1995).

Size-based predation is the key driver of dynamics in size-based ecosystems (Jennings *et al.*, 2001; Woodward *et al.*, 2005; Andersen *et al.*, 2016a) and is broadly defined by five key parameters: 1) preferred predator-prey mass ratio (PPMR); 2) search rate coefficient; 3) body-size exponent, which determines how the search rate scales with body-size; 4) assimilation efficiency; and 5) the width of the feeding kernel (the diet breadth around the preferred PPMR), and modelling studies of the size-spectra of fish have shown that these parameters have a large effect on food web dynamics (Law *et al.*, 2009; Datta *et al.*, 2011; Zhang *et al.*, 2013). For instance, a wider feeding kernel and lower PPMR dampens travelling waves through the fish community size-spectrum (Blanchard, 2008; Law *et al.*, 2009; Zhang *et al.*, 2013). Further, there is evidence that higher assimilation efficiency has a similar effect on the steady state of the size-spectrum (Datta *et al.*, 2011). The sensitivity of ecosystem dynamics to parameterisation of fish feeding characteristics strongly suggests that zooplankton feeding characteristics could be important to energy transfer through the food web. Therefore, the first step towards including zooplankton in end-to-end size-spectrum models is to include an accurate representation of their feeding characteristics.

The extensive experimental work elucidating zooplankton feeding characteristics has formed the basis of several recent syntheses of size-based feeding (Kiørboe, 2011; Wirtz, 2012, 2014; Fuchs and Franks, 2010) and provides an opportunity for improving zooplankton parameterisation in size-spectrum models. Wirtz (2012) used the data collected by Hansen et al. (1994) and Fuchs and Franks (2010) to develop a mechanistic model that links zooplankton PPMR with their feeding characteristics. In another paper, Wirtz (2014) derived an ideal feeding kernel width for zooplankton from simple biomechanical laws, which agrees well with empirical data. Fuchs and Franks (2010) synthesised data from previous studies to investigate the relationship between zooplankton PPMR and the width of the feeding kernel. They found that the feeding kernel width decreased with decreasing PPMR, suggesting increasing selectivity amongst individuals who prey on individuals closer to their own size. Kiørboe (2011) found that the size-specific zooplankton search rate is independent of body size across seven different functional groups.

Here, we evaluate how the size-dependent feeding characteristics of zooplankton affect the dynamics of higher trophic levels in size-structured pelagic ecosystems. We extract feeding characteristics from a range of syntheses of size-based feeding (Kiørboe, 2011, 2013; Wirtz, 2012, 2014; Fuchs and Franks, 2010) and implement them in a dynamic size-spectrum model framework (Datta et al., 2010; Andersen et al., 2016b; Guiet et al., 2016a). To our knowledge this is the first dynamic size-spectra model to resolve predation-based growth and mortality of zooplankton. The model has three components – a static phytoplankton resource spectrum and two dynamic spectra representing a general zooplankton and fish community, respectively. In our model, biomass flows from smaller to larger size classes as a consequence of larger organisms consuming smaller organisms, and growth at one size is balanced by mortality in smaller size classes. We separate our findings in three parts. In Section 3.4.1 *Zooplankton are not fish*, we provide a size-spectrum model using the best parameter estimates from the literature, and establish the individual effect each of the five key zooplankton feeding parameters has on the community size-spectrum, by comparing against a base model where zooplankton are parameterised as just another fish community. In Section 3.4.2 *Sensitivity analysis*, we assess how varying the feeding characteristics of the zooplankton community impact the stability and productivity of the fish community size-spectrum. Finally in Section 3.4.3 *Mediating primary production and fishing*, we evaluate how the feeding characteristics of different zooplankton functional groups – salps, chaetognaths, herbivorous copepods, flagellates and carnivorous copepods – mediate effects of variation in phytoplankton abundance and increased fishing mortality on the fish

community size-spectrum. The purpose of this study is not to give a quantitative evaluation of zooplankton or fish abundance, rather we wish to illustrate how incorporating zooplankton-specific feeding characteristics could affect the dynamics of size-structured ecosystems. Our ultimate aim is to investigate how zooplankton feeding characteristics influence energy transfer from phytoplankton and fish, and thus move toward a more realistic and consistent parameterisation for the zooplankton component of size-spectrum models.

3.3 Methods

3.3.1 The model

We developed a size-spectrum model that consists of a size-spectrum comprised of three communities: phytoplankton, zooplankton and fish (Figure 3.1; Tables 3.1 and 3.2). The phytoplankton component covers the smallest size classes $[w_p, w_z]$ and is held constant as a background resource spectrum for zooplankton. Size-dependent processes of growth and mortality drive the zooplankton and fish components. These two components are delineated by different size ranges and feeding characteristics. The zooplankton community covers the size range between phytoplankton and fish $[w_z, \bar{W}_z]$, and the fish community covers the largest size classes $[w_f, \bar{W}_f]$, although some of the smallest fish size classes extend into the zooplankton range (from $w_f = 0.1$ gram to $\bar{W}_z = 1$ gram). Fish community size classes that extend into the zooplankton range represent larvae and very small fish that are smaller than the largest zooplankton. Predation is size-dependent, with big things eating smaller ones, so depending on their size, zooplankton can feed on phytoplankton, smaller zooplankton and the smallest fish size classes. Similarly, fish feed on zooplankton and smaller fish.

The temporal dynamics of the zooplankton and fish communities are governed by separate McKendrick-von Foerster equations with second-order diffusion terms (Datta *et al.*, 2010),

$$\frac{\delta}{\delta t} N_i(w, t) = -\frac{\delta}{\delta w} (g_i(w, t)N_i(w, t)) - \mu_i(w, t)N_i(w, t) + \frac{1}{2} \frac{\partial^2}{\partial w^2} (f_i(w, t)N_i(w, t)). \quad (1)$$

The density of individuals in community i (where i is either zooplankton or fish) per unit mass per unit volume ($\text{g}^{-1}\text{m}^{-3}$) is denoted by $N_i(w, t)$. Growth, mortality and diffusion rates of individuals of group i at size w and time t , are denoted by $g_i(w, t)$, $\mu_i(w, t)$ and $f_i(w, t)$, respectively. In this context, the diffusion term allows the model to incorporate demographic variation in the growth rates of each community. That is, within each community two individuals of the same weight eating the same food will not grow by the same amount (Datta

et al., 2010). This not only increases model realism, but the stability of the system steady state, over the traditional first-order McKendrick-von Foerster equation (Datta *et al.*, 2011).

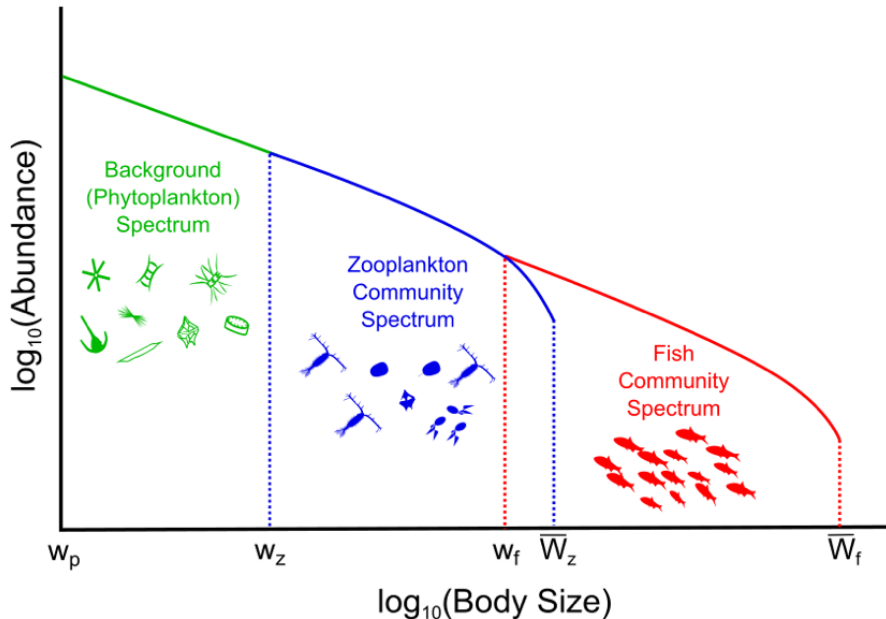


Figure 3.1 Conceptual illustration of the phytoplankton-zooplankton-fish system. The background (phytoplankton) spectrum is held constant, the dynamic zooplankton and fish community spectra are governed by equation 1 and the equations in Table 3.2.

Phytoplankton dynamics in the background resource spectrum are not explicitly modelled, with the density of individuals held constant through time:

$$N_P(w, t) = aw^b. \quad (\text{E11})$$

Equations are also found in Table 3.2. We use an exponent of -1 for the background spectrum, implying equal biomass over logarithmically equal body-mass intervals in keeping with past dynamic size-spectrum models (Benoît *et al.*, 2004; Law *et al.*, 2009; Blanchard *et al.*, 2012; Law *et al.*, 2014). The coefficient a for the background spectrum (E11) was calculated using the empirical equation from Barnes *et al.* (2011) and annual median chlorophyll a concentrations for different ocean basins between 2005-2010 (Rosseaux and Gregg, 2014). Unless specified otherwise, we use the global median chlorophyll a value (0.16 mg m^{-3}) to give a value of 0.017 for a .

From the predator's perspective, total consumption depends on the total biomass of suitable prey. For an individual of size w at time t from community i , this is determined by the predator's search rate:

$$V_i(w) = \gamma_i w^{\alpha_i}, \quad (\text{E5})$$

and the density of suitable prey:

$$D_i(w, t) = \int_{w_p}^w \phi_i(w, w') \sum_j N_j(w', t) w' dw'. \quad (\text{E6})$$

Table 3.1 Table of parameter values for the phytoplankton-zooplankton-fish dynamic size-spectrum model.

Symbol	Definition	Value	Unit	Source
	Body mass ranges for:			
1. w_p, w_z	1. Phytoplankton	$1.10^{-15}, 10^{-5}$	g	-
2. w_z, \bar{W}_z	2. Zooplankton	$2.10^{-5}, 10^0$		1
3. w_f, \bar{W}_f	3. Fish	$3.10^{-3}, 10^6$		2, 3, 4
β_F	PPMR for fish	100	-	5
	Quantitative feeding mode for			
m	1. Salps & Doliolids	1. -2.68	-	6
	2. Herbivorous copepods	2. -0.48		
	3. Chaetognaths	3. -0.20		
	4. General community	4. 0.00		
	5. Flagellates	5. 0.53		
	6. Carnivorous copepods	6. 1.50		
σ	Feeding kernel width for zooplankton and fish	$\sigma_Z = 0.75$ $\sigma_F = 1$	-	7 2, 3, 4
α	Exponent of search rate for zooplankton and fish	$\alpha_Z = 1.01$ $\alpha_F = 0.80$	-	8 9
γ	Coefficient of search rate for zooplankton and fish	$\gamma_Z = 875$ $\gamma_F = 640$	$g^{-\alpha} m^{-3} \text{ yr}^{-1}$	8 9
K	Assimilation efficiency for zooplankton and fish	$K_Z = 0.7$ $K_F = 0.6$	-	See text 5
B_0	Coefficient for background mortality	0.04	$g^{-c} \text{ yr}^{-1}$	2, 4
c	Exponent for background mortality	-0.25	-	2, 4, 11
S_0	Coefficient for senescence mortality	0.2	$g^{-s} \text{ yr}^{-1}$	2, 4, 10
s	Exponent for senescence mortality	1.2	-	2, 4, 10
w_S	Body size at which senescence mortality begins for zooplankton and fish	$w_{S_Z} = 10^{-2}$ $w_{S_F} = 10^4$	g	- -
a	Coefficient for background size-spectrum	0.017	$g^{-1-b} m^{-3}$	12, 13
b	Exponent for background size-spectrum	-1	-	2, 3, 4

Sources: 1. Zhou et al., (2010), 2. Blanchard et al., (2009), 3. Benoît et al., (2004), 4. Blanchard et al., (2011), 5. Andersen et al., (2015), 6. Wirtz, (2012), 7. Wirtz, (2014), 8. Kiørboe, (2011), 9. Press, (1983), 10. Hall et al., (2006), 11. Brown et al., (2004), 12. Barnes et al., (2011), 13. Rousseaux and Gregg, 2015.

The growth rate of an individual of size w at time t is fuelled by consumption of prey from smaller size classes:

$$g_i(w_i, t) = K_i V_i(w) D_i(w, t), \quad (\text{E7})$$

where K_i is the assimilation efficiency of community i . Kiørboe (2011) found that the search rate (E5) for zooplankton, across a wide range of taxa is largely independent of organism size ($\alpha_Z = 1.01$). This stands in contrast to the scaling for fish ($\alpha_F = 0.8$; Peters, 1983) that implies the specific search-rate per unit mass declines with increasing body size. Further, the search rate coefficient is higher for zooplankton $\gamma_Z = 875 \text{ g}^{-\alpha_Z} \text{ m}^3 \text{ year}^{-1}$ (Kiørboe, 2011), compared to fish $\gamma_F = 640 \text{ g}^{-\alpha_F} \text{ m}^3 \text{ year}^{-1}$ (Peters, 1983). The probability that a predator of size w will consume an individual of size w' is given by the log-normal function (E4), where β_i and σ_i are community i 's PPMR and feeding kernel width.

In previous size-spectrum models the PPMR is held constant across the entire size range of the community (Andersen *et al.*, 2016b). For zooplankton, the wide variation in observed PPMR across phyla suggests a constant value across all zooplankton size classes is inappropriate (Wirtz, 2012). We have thus used the mechanistic formulation from Wirtz (2012) who argues that for zooplankton, PPMR will increase non-linearly as predator size increases, due to the non-isometric scaling of feeding-related apparatus with body size (Figure 3.2):

$$\beta_Z(w) = \left(\exp \left(0.02 \ln \left(\frac{D_w}{D_0} \right)^2 - m + 1.832 \right) \right)^3, \quad (\text{E2})$$

where D_w is the predator equivalent spherical diameter (ESD) in μm :

$$D_w = 2 \sqrt[3]{3w \times \frac{10^{12}}{4\pi}}. \quad (\text{E1})$$

The mechanistic model from Wirtz (2012) also allows the range of feeding modes across different zooplankton functional groups to be quantitatively incorporated. The feeding mode of the zooplankton community is denoted by m , and ranges from -3 to 2. A larger, positive m -value (say $m = 2$) suggests a more raptorial, carnivorous feeding strategy with a lower PPMR (Figure 3.2). Alternatively, a negative m -value (say $m = -3$) implies a more passive, herbivorous feeding strategy. For the fish community, we set $\beta_F = 100$ (Andersen *et al.*, 2016b).

A wider feeding kernel means an individual feeds over a wider range of size classes, implying a more generalist feeding strategy. Wirtz (2014) obtained a general feeding kernel width for zooplankton of $0.75 \log_{10}$ grams body-size from simple biomechanical laws, and found this value agreed well with measured values from different species.

Fuchs and Franks derived an empirical equation that links zooplankton PPMR β_z with the feeding kernel width:

$$\sigma_z = 0.05 \log_{10}(\beta_z) + 0.33 \quad (\text{E3})$$

This equation suggests a positive relationship between the width of the feeding kernel and the PPMR. In other words, more active, carnivorous groups ($m > 0$), have a narrower, more selective prey size range compared to passive, filter feeding groups ($m < 0$) that have a wider, more generalist prey size range. For the fish community, we set $\sigma_F = 1$ (Andersen *et al.*, 2016b).

For individuals in community i , a fraction K_i of consumed biomass, the assimilation efficiency, is assimilated into new biomass. Observational and experimental work across different zooplankton functional groups show that assimilation efficiency of ingested food into new biomass ranges from 0.3 – 0.9 (Landry *et al.*, 1984; Kiørboe, 2008; Montagnes and Fenton, 2012; Abe *et al.*, 2013). Assimilation efficiency of copepods (Landry *et al.* 1984), dinoflagellates and larval fish (Kiørboe 2008) depends on whether they were acclimated to or prey available had a significant effect on zooplankton assimilation efficiency – higher environments have a higher assimilation efficiency compared to those from high food environments. Similarly, the density and type density and higher carbon content of prey gave In previous models, assimilation efficiency for zooplankton is usually held constant at 0.70 (e.g., Zhou *et al.*, 2006; Fuchs and Franks, 2010; Ward *et al.*, 2012, 2014). Unless specified otherwise, we keep $K_Z = 0.7$ to follow previous size-based plankton-focused models (Baird & Suthers, 2007; Zhou *et al.*, 2006; Stock *et al.*, 2008; Fuchs and Franks, 2010; Banas *et al.*, 2011). For the fish community, we set $K_F = 0.6$, as this is a common values given in previous dynamic size-spectrum models (Andersen *et al.*, 2016b).

From the prey's perspective, the total predation pressure from all larger size classes gives the predation mortality rate:

$$\mu_p(w, t) = \sum_j \mathbb{I}_{\{w < \bar{W}_j\}} \int_w^{\bar{W}_j} \phi_j(w', w) V_j(w') N_j(w', t) dw'. \quad (\text{E8})$$

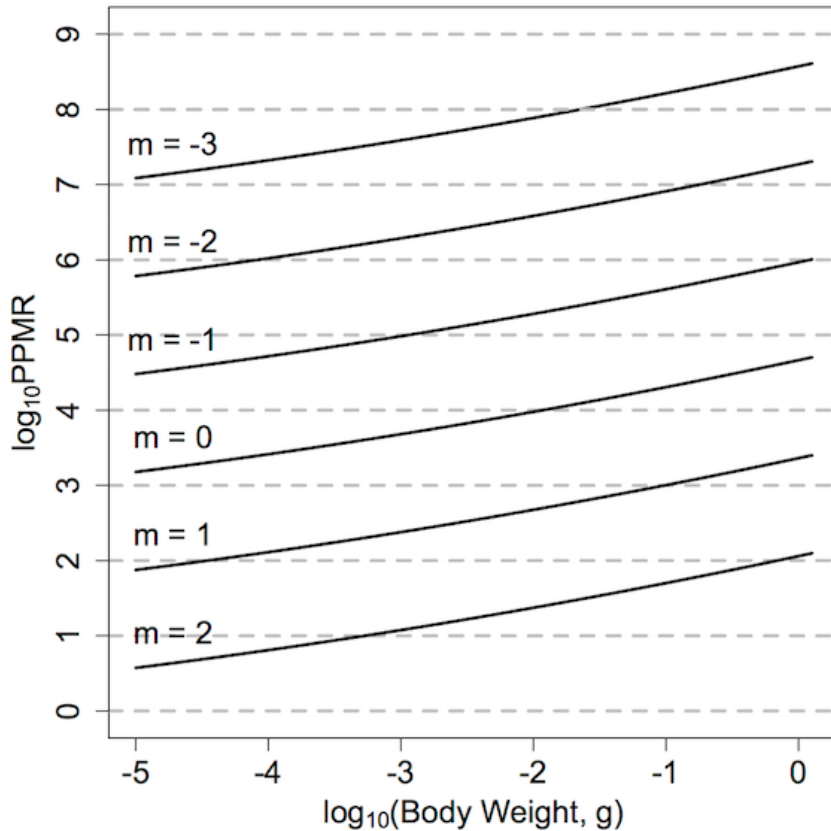


Figure 3.2 $\log_{10}\text{PPMR}$ for the range of quantitative feeding modes from carnivores to herbivores (Wirtz 2012). The solid lines indicate realised $\log_{10}\text{PPMR}$ for different feeding modes, across the size range of the zooplankton community.

To account for other sources of mortality (e.g., disease), we include a U-shaped intrinsic mortality term:

$$\mu_{0_i}(w, t) = B_0 w^c + S_{0_i} w^s, \quad (\text{E9})$$

that covers non-predation sources of mortality such as disease and senescence (Brown *et al.*, 2004; Hall *et al.*, 2006; Blanchard *et al.*, 2009, 2011). Since individuals grow through time, the background mortality term describes rapidly decreasing background mortality in the early stages of life, a constant mortality for middle-age individuals, and an increasing mortality with senescence. The increase in senescence mortality with body size acts as a closure term for the largest size classes, by preventing a buildup of very large individuals (Andersen *et al.*, 2016b).

Table 3.2 Model equations with their units. An equation number is given that is used in the main text.

Description	Equation	Units	Equation Number
Zooplankton Characteristics:			
Zooplankton size in ESD	$D_w = 2\sqrt[3]{3w \times 10^{12} / 4\pi}$	μm	E1
PPMR	$\beta_z(w) = (\exp(0.02 \ln(D_w/D_0)^2 - m + 1.832))^3$	-	E2
Feeding kernel width	$\sigma_z = 0.05 \log_{10}(\beta_z) + 0.33$	-	E3
Consumption and Growth:			
Size selection	$\phi_i(w, w') = \exp[-(ln(\beta_i(w)w'/w))^2 / 2\sigma_i^2] / (\sigma_i \sqrt{2\pi})$	-	E4
Search rate	$V_i(w) = \gamma_i w^{\alpha_i}$	$\text{m}^3 \text{yr}^{-1}$	E5
Density of suitable prey	$D_i(w, t) = \int_{w_p}^w \phi_i(w, w') \sum_j N_j(w', t) w' dw'$	g m^{-3}	E6
Growth rate	$g_i(w_i, t) = K_i V_i(w) D_i(w, t)$	g yr^{-1}	E7
Mortality:			
Predation	$\mu_p(w, t) = \sum_j \mathbb{I}_{\{w < \bar{w}_j\}} \int_w^{\bar{w}_j} \phi_j(w', w) V_j(w') N_j(w', t) dw'$	yr^{-1}	E8
Intrinsic mortality	$\mu_{0i}(w, t) = B_0 w^c + S_{0i} w^s$	yr^{-1}	E9
Total Mortality	$\mu_i(w, t) = \mu_p(w, t) + \mu_{0i}(w, t)$	yr^{-1}	E10
Other equations:			
Background (Phytoplankton) Spectrum	$N_P(w, t) = aw^b$	$\text{g}^{-1} \text{m}^{-3}$	E11
Zooplankton boundary condition	$N_Z(w_z) = aw_z^b$	$\text{g}^{-1} \text{m}^{-3}$	E12
Fish boundary condition	$N_F(w_F, t) = N_Z(w_F, t)$	$\text{g}^{-1} \text{m}^{-3}$	E13
Diffusion term	$f_i(w, t) = \gamma_i w^{\alpha_i} \sum_j K_{ij}^2 \int_{w_p}^w (w')^2 \phi_i(w, w') N_j(w', t) dw'$	$\text{g}^2 \text{yr}^{-1}$	E14
Community <i>i</i> characteristics:			
Total biomass	$B_i(t) = \int_{w_i}^{\bar{w}_i} w N_i(w, t) dw$	g m^{-3}	E15
Total throughput	$T_i(t) = \int_{w_i}^{\bar{w}_i} w V_i(w) D_i(w, t) N_i(w, t) dw$	$\text{g m}^{-3} \text{yr}^{-1}$	E16
Production-Biomass Ratio	$PB_i(t) = \int_{w_i}^{\bar{w}_i} w \mu_i(w, t) N_i(w, t) dw / \int_{w_i}^{\bar{w}_i} w N_i(w, t) dw$	yr^{-1}	E17
Fish-Zooplankton Biomass Ratio	$FZ(t) = B_F(t) / B_Z(t)$	-	E18

3.3.2 Community characteristics

To evaluate effects of feeding characteristics of the zooplankton community on the fish community, we calculated several community-level measures. The total biomass of community *i* was obtained by integrating the abundance in all size classes:

$$B_i(t) = \int_{w_i}^{\bar{w}_i} w N_i(w, t) dw. \quad (\text{E15})$$

Similar to Blanchard et al. (2011), we defined the total throughput of community i as the total consumption rate:

$$T_i(t) = \int_{w_i}^{\bar{w}_i} w V_i(w) D_i(w, t) N_i(w, t) dw. \quad (\text{E16})$$

The production to biomass ratio of a community i - where production was defined as the total flux out of the community from all sources of mortality (Brown et al., 2004) - was used to evaluate the total energy flux through a community:

$$PB_i(t) = \left(\int_{w_i}^{\bar{w}_i} w \mu_i(w, t) N_i(w, t) dw \right) / \left(\int_{w_i}^{\bar{w}_i} w N_i(w, t) dw \right). \quad (\text{E17})$$

Total throughput is a measure of how energy moves internally through the system from predation processes, whereas the production to biomass ratio is an indicator of how much new biomass is produced to replace biomass lost to mortality, per unit of existing biomass.

To evaluate the transfer efficiency from zooplankton to the fish community, we calculate the ratio of total fish biomass to total zooplankton biomass:

$$FZ(t) = B_F(t)/B_Z(t) \quad (\text{E18})$$

This is similar to the approach taken in previous studies evaluating the transfer efficiency of phytoplankton to zooplankton (Havens and Beaver, 2012; Friedland et al., 2012).

We use two measures to evaluate the stability and total variability of the system. First, the nature of the system steady state was determined using the Newton-Raphson multidimensional root-finding method (Press et al., 2007). For each configuration of zooplankton feeding characteristics in Results sections 3.4.1, 3.4.2 and 3.4.3, the abundance of the zooplankton and fish communities was taken after 20 years. The stability of this abundance was determined by the maximum real part (λ_{\max}) of the eigenvalues of the Jacobian matrix calculated with the Newton-Raphson method. If $\lambda_{\max} < 0$, the entire system will settle into a stable equilibrium over time where the abundance in each size-class does not fluctuate. The more negative λ_{\max} is, the faster the system will recover from local perturbations to the steady state. Alternatively, if $\lambda_{\max} > 0$, over time the system will settle into a repeating, periodic travelling wave of abundance from smaller to larger size-classes. In this case, the more positive λ_{\max} is, the faster the travelling wave moves through the size classes. Second, we measured the total variability of the system by calculating the coefficient of variation (CV) of the time-series of biomass over the last 10 years of the simulation. The Newton-Raphson stability analysis and the CV work together; the first will

identify if the steady state is stable or oscillating, and the CV gives a measure of the magnitude of these oscillations through time.

3.3.3 Numerical implementation

Dynamics of the zooplankton and fish communities are modelled with Equation 1, which we solve numerically using a second-order semi-implicit upwind finite difference scheme (see Appendix 1; Press *et al.*, 2007). We present the results in \log_{10} space for ease of interpretation, mathematical convenience and comparison with previous work. For the numerical implementation we discretize the dynamic size range $[10^{-5}, 10^6]$ into equal 0.1 \log_{10} size intervals (on a \log_{10} gram scale), and use a daily-time step for the time interval. We chose these values to discretize the time and weight ranges to ensure convergence in our numerical implementation without requiring unnecessary computational effort, in keeping with past studies (Press *et al.*, 2007; Zhang *et al.*, 2013; Plank *et al.*, 2012; Law *et al.*, 2014). For simplicity we are not explicitly modelling reproduction, thus the abundances of the smallest size classes in the zooplankton and fish communities are held constant. This implies that we are assuming constant recruitment for zooplankton and fish (Law *et al.*, 2009; Blanchard *et al.*, 2012). The assumption of constant recruitment permits a clearer evaluation of how the feeding characteristics of the zooplankton affect the dynamics of a fish community, in keeping with previous community size-spectrum models (e.g., Benoît *et al.*, 2004; Maury *et al.*, 2007; Law *et al.*, 2009; Zhang *et al.*, 2013). For the zooplankton community, the density of individuals in the smallest size class is determined from the continuation of the phytoplankton size-spectrum: $N_Z(w_z) = aw_z^{-b}$ (E12), and the density of the smallest size class in the fish community is held equal to the equivalent zooplankton size class:

$$N_F(w_F, t) = N_Z(w_F, t). \quad (\text{E13})$$

We ran each simulation for a 20-year period. In each simulation, our initial condition starts the zooplankton and fish community spectra as a continuation of the resource spectrum (E11). If the solution was stable ($\lambda_{\max} < 0$), there would initially be some oscillations around the steady state that would diminish over time. For a stable solution, the closer λ_{\max} was to zero the greater the initial variance and the longer it took for the system to stabilise. When the solution was a travelling wave ($\lambda_{\max} > 0$), the variance of the system and magnitude of the oscillations would increase over time until the steady state was achieved. In this situation, the closer λ_{\max} was to zero, the longer the system took to find the unstable steady

state. In all simulations the system achieved steady state within the first 5 years, therefore we discarded the first 10 years as a burn-in period.

3.3.4 Zooplankton are not fish

To establish the individual effect each of the five zooplankton feeding parameters has on the fish community, we begin with a base model where zooplankton are parameterised as another general fish community. From the base model, we build up to a model where the zooplankton community feeding characteristics are parameterised to represent a general, mixed zooplankton community. To do this, we use $m = 0$ to represent the average PPMR of a zooplankton community characterised equally by herbivorous and carnivorous feeding behavior, and set $\sigma_z = 0.75$, $K_z = 0.7$, $\gamma_z = 875 \text{ g}^{-\alpha_z} \text{ m}^{-3} \text{ year}^{-1}$ and $\alpha_z = 1.01$ to reflect the average feeding characteristics of zooplankton across multiple functional groups.

We change each zooplankton feeding parameter one at a time, then all together, and evaluate their individual relative impact on fish community measures against the base model, by calculating the change in the measure against the base model. For example, the relative fish biomass (rFB) for a new parameterisation of the zooplankton community is obtained by dividing the fish biomass from the new model by the fish biomass from the base model.

3.3.5 Sensitivity analysis

In this section, we assess how variation in the feeding characteristics of the zooplankton community affects the productivity and stability of the fish community. We focus on zooplankton feeding mode (m), feeding kernel width (σ_z) and assimilation efficiency (K_z), since these parameters vary across different zooplankton functional groups and environmental conditions. We vary m between -3 - 2, σ_z between 0.4 – 2.2 and K_z between 0.3 – 0.9.

3.3.6 Mediating primary production and fishing

In our final section, we assess how the feeding characteristics of different zooplankton functional groups affect the productivity and stability of the fish community, and mediate increased primary production and fishing pressure, by evaluating the effect of these changes on the average total biomass of the fish community. We use the m -values from Wirtz (2012) for five different zooplankton functional groups (salps, chaetognaths, herbivorous copepods, flagellates and carnivorous copepods) and a general zooplankton community (Table 1). The

width of the feeding kernel for each of the six groups was determined with Fuchs and Franks' (2010) empirical equation (E3), which links the average zooplankton community PPMR with the feeding kernel width. For all groups, we hold the search rate and assimilation efficiency constant (see Table 1).

We used chlorophyll a concentrations from 2 ocean basins – the North Central Pacific (0.06 mg m⁻³) and the North Atlantic (high concentration, 0.28 mg m⁻³) – to give a range of coefficient values (intercept of the spectrum; a) between 0.010 and 0.024, which corresponds to a total phytoplankton abundance in the background resource spectrum of between 0.23 and 0.55 g⁻¹m⁻³. To include fishing pressure, we incorporate an additive fishing mortality term with a value between 0-2 yr⁻¹, for all individuals in the fish community > 200 g.

3.4 Results

3.4.1 Zooplankton are not fish

The base model (denoted as the dashed line in each of the sub-plots in Figure 3.3 was a stable spectrum (λ_{\max} of -0.58), with the dynamic zooplankton and fish communities essentially a continuation of the static background spectrum in the base model.

Individually changing the zooplankton assimilation efficiency K_Z from 0.6 and 0.7 (Figure 3.3 a) increased the total throughput and production to biomass ratio of the fish community, in comparison to the base model (Table 3.3), and increased resilience of the entire system to local perturbations, with $\lambda_{\max} = -0.71$. Increasing the zooplankton community search rate coefficient (γ_Z) from 640 to 875 (g^{-α_Z} m⁻³ yr⁻¹) (Figure 3.3 b), had a negligible effect on the total biomass or productivity of the fish community, compared to the base model (Table 3.3), however it did increase the stability of the system, with $\lambda_{\max} = -0.76$. Changing the search rate exponent for the zooplankton community ($α_Z$; Figure 3.3 c) from 0.82 to 1.01 reduced the total fish biomass by almost 70%, and reduced the relative production to biomass ratio (45% decrease) and relative total throughput (87% decrease), against the base model. Updating $γ_Z$ decreased the resilience of the system, with $\lambda_{\max} = -0.04$, however the steady state remained a stable spectrum.

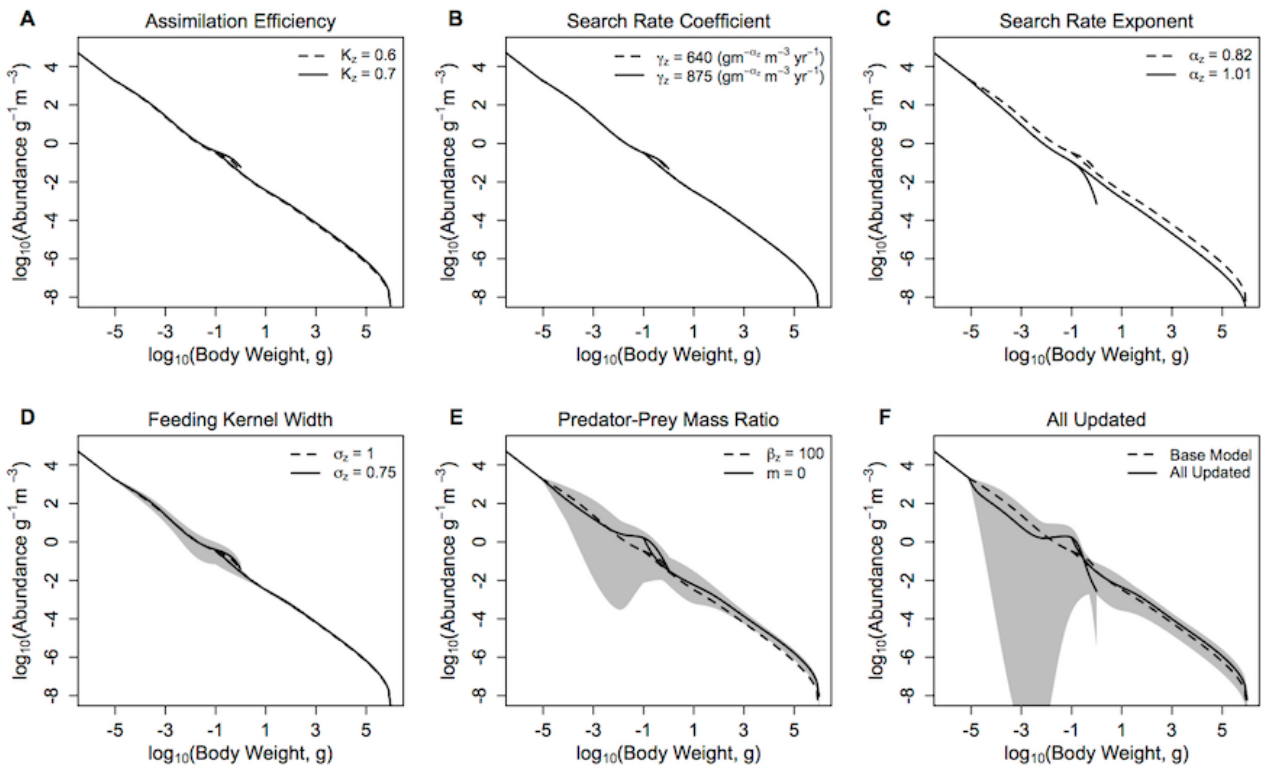


Figure 3.3 The zooplankton and fish community size-spectra when various parameters are updated a-e) one at a time and f) all together. The dashed lines in each plot represent the zooplankton and fish communities in the base model parameterisation, and the solid lines denotes the average abundance of the fish and zooplankton communities over 10 years in the modified model. The shaded areas show the regions of the travelling wave solutions over 10 years if the steady state is unstable.

Individually reducing the zooplankton feeding kernel (σ_z ; Figure 3.3d) from 1 to 0.75, and changing the PPMR (Figure 3.3e) of the zooplankton component increased the total biomass, throughput and production to biomass ratio of the fish community, in comparison to the base model (Table 3.3). Changing the PPMR of the zooplankton gave the most significant increase in relative production to biomass (75% increase) and relative total throughput (335% increase) of the fish community. Only changing the zooplankton PPMR affected the relative fish to zooplankton biomass significantly, with a 22% increase against the base model. Changing the feeding kernel width and the PPMR for the zooplankton community changed the steady state from a stable spectrum to an oscillating system. Between the two parameters, changing PPMR gave the fastest oscillations, with $\lambda_{\max} = 0.65$ compared to $\lambda_{\max} = 0.24$ for σ_z . Further, the magnitude of the oscillations was larger when the zooplankton community PPMR was updated (CV = 0.28), compared to σ_z (CV = 0.07) (Table 3.3, Figure 3.3 d, e).

Table 3.3 Fish community biomass (FB), fish to zooplankton biomass ratio (F:Z), fish community production to biomass ratio (P:B) and throughput (TP) relative to the base model (r), and the variation in fish community biomass (coefficient of variation: CV) when the zooplankton community feeding parameters are updated one at a time, and all together. The system has a stable steady state when $\lambda_{\max} < 0$, and an unstable, oscillating steady state when $\lambda_{\max} > 0$.

	rFB	rF:Z	rP:B (Fish)	rTP (Fish)	CV (Fish)	λ_{\max}
Base Model	1.00	1.00	1.00	1.00	0.00	-0.58
$K_Z = 0.7$	1.17	1.00	1.11	1.35	0.00	-0.71
$\gamma_Z = 875$	0.99	0.96	1.00	0.99	0.00	-0.76
$\alpha_Z = 1.01$	0.34	0.96	0.55	0.13	0.00	-0.04
$\sigma_Z = 0.75$	1.06	0.95	1.04	1.13	0.07	0.24
$m = 0$	2.27	1.22	1.75	4.35	0.28	0.65
All changed	1.69	1.44	1.42	2.40	0.62	0.47

When all parameters were changed for the zooplankton community (Figure 3.3 f) there were significant increases against the base model in total fish biomass (69%), the fish to zooplankton biomass ratio (44%), and the fish community production to biomass ratio and total throughput (44% and 140% respectively). Except for the relative fish to zooplankton biomass ratio, the increase in the total fish biomass and productivity measures were lower when all the parameters were updated, compared to just updating the zooplankton PPMR. (Table 3.3). The overall system was not stable ($\lambda_{\max} = 0.47$), and the magnitude of the oscillations through the system were higher than any seen in a system with a single parameter updated, with $CV = 0.62$. However, oscillations were slower compared to the system where only zooplankton PPMR was updated.

3.4.2 Sensitivity analysis

The total biomass of the fish community increases exponentially as m decreases (Figure 3.4 a). From $m = 2 - -3$ (corresponding to an average zooplankton community PPMR range of 1 – 7.5), total fish biomass increases over 3 orders of magnitude (0.3 g m^{-3} for $m = 2$ to 620 g m^{-3} for $m = -3$). The exponential increase in fish biomass and productivity measures with respect to zooplankton PPMR starts at around $m = -0.5$, which corresponds to an average zooplankton community PPMR of 4.5. Similarly, a smaller feeding kernel width (σ_z) – indicating a predator that feeds on a narrower size range of prey – results in an almost exponential increase in total fish community biomass (Figure 3.4 b). From $\sigma_z = 0.4$ to 1.1,

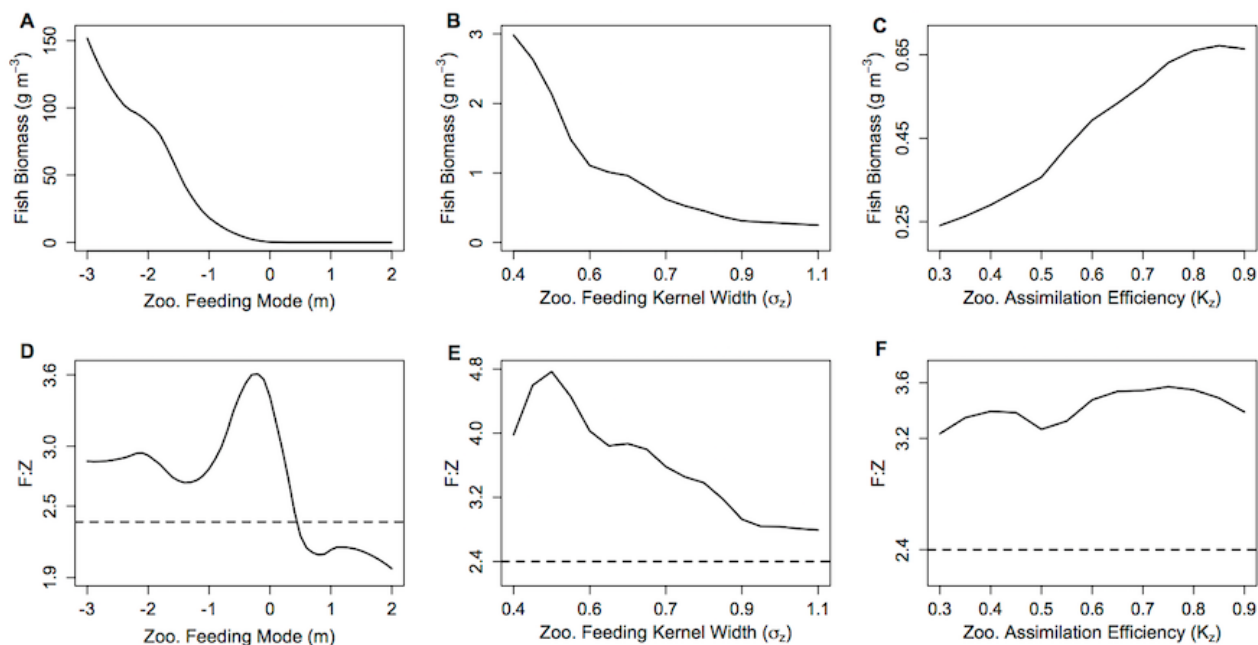


Figure 3.4 a, b, c) The total fish community biomass (g m^{-3}) and d, e, f) the fish to zooplankton biomass ratio (F:Z) for different values of zooplankton feeding mode (m), feeding kernel width (σ_z) and assimilation efficiency (K_z). In each plot, the other feeding parameters not specified are held constant at $m = 0$, $\sigma_z = 0.75$ and $K_z = 0.7$. The dashed line in d, e, f) indicates the F:Z in the base model, where the zooplankton community are parameterised as fish.

total fish biomass increases from 0.25 g m^{-3} to 2.9 g m^{-3} . There is a roughly linear, positive relationship between total fish biomass and the assimilation efficiency K_z of the zooplankton community (Figure 3.4 c). As K_z increases from 0.3 to 0.9, total fish biomass increases from 0.20 g m^{-3} to 0.65 g m^{-3} . Similar patterns can be seen in the relationship between zooplankton PPMR, feeding kernel width and assimilation efficiency and the fish community productivity measures (Supplementary Information Figure S 3.1).

The fish to zooplankton biomass ratio peaks at around $m = 0$ (3.60), and stays around 2.9 for $m < -1$, and decreases for $m > 0.5$ to settle around 2.1 (Figure 3.4 d). For σ_z , the fish to zooplankton biomass ratio peaks at $\sigma_z = 0.5$ around 4.8, before uniformly declining as σ_z increases (Figure 3.4 e). There is minimal change in fish to zooplankton biomass ratio with increasing K_z , which suggests zooplankton biomass and fish biomass increase at the same rate (Figure 3.4 f). Except for $m > 0.5$, the fish to zooplankton biomass ratio was higher than the base model (dashed line in Figures 3.4 d, e, f) across the ranges of m , σ_z and K_z . With $\sigma_z = 0.75$, the CV is zero for m -values above 1 (Figure 3.5 a) which corresponds to a stable steady state region (Figure 3.5 d). The CV increases as m decreases from 0.5 to -0.5, which implies increasing variability in total fish biomass as the zooplankton community shifts from carnivorous to herbivorous feeding behavior. The CV stabilises between 1 and 1.5 for $m < 0$. This suggests that even though the total fish community biomass is still exponentially increasing as m becomes more negative, the relative variation in fish biomass through time does not increase. There is a negative relationship between increasing σ_z and CV, indicating increasing stability with a wider feeding kernel (Figure 3.5 b). A similar pattern is observed in Figure 5 d; the range of m -values that enable a stable system is larger, as σ_z increases. The CV of the fish community varies across the range of K_z values but within a much smaller range than the other two parameters (Figure 3.5 c). Increasing K_z slightly increases the minimum σ_z , and decreases the minimum m required for a stable steady state (Figures 3.5 e, f).

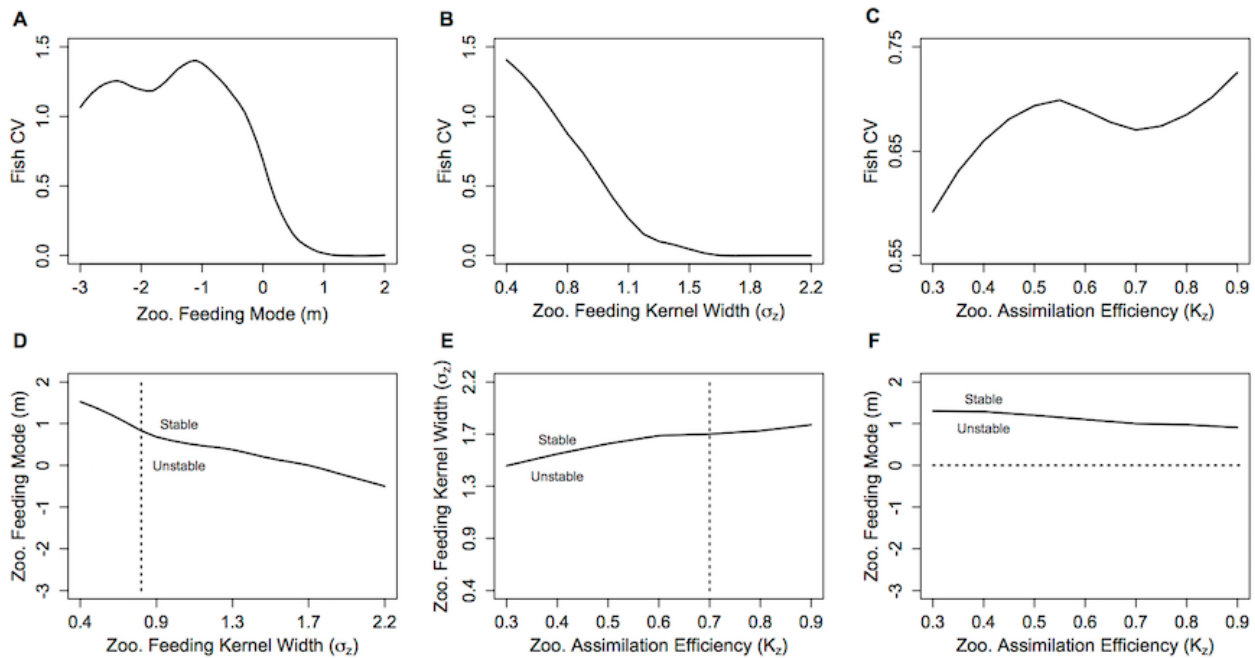


Figure 3.5 The fish community biomass coefficient of variation (CV) against zooplankton a) feeding mode (m), b) feeding kernel width (σ_z) and c) assimilation efficiency (K_z), and the stability regions of d) m against σ_z , e) σ_z against K_z and f) m against K_z . In d, e, f) the dashed lines indicate the transect over which the CV in the plot above is taken. In each plot, the other feeding parameters not specified are held constant at $m = 0$, $\sigma_z = 0.75$ and $K_z = 0.7$.

3.4.3 Mediating primary production and fishing

Our results suggest a trade-off between the stability of the overall system and the total average fish productivity and biomass for most zooplankton groups (Figure 3.6 and Table 3.4). The herbivorous salp community ($m = -2.68$, PPMR ~ 7) is an exception (Figure 3.6 a). It supports the most abundant and productive fish community, yet it is a more stable system overall than the one dominated by herbivorous copepods and chaetognaths (Figure 3.6 b, c; Table 3.4). The salp community has the widest feeding kernel ($\sigma_z = 0.70$), which suggests a wider feeding kernel gives a more stable system without sacrificing the productivity of the fish community.

A lower, increasingly negative m -value results in a zooplankton community with a flatter abundance spectrum. In other words, increasing herbivory results in a higher abundance in the larger zooplankton size classes. For the fish community, a shallower zooplankton spectrum leads to a higher abundance in the smallest fish size classes. The overall average slope of the fish community spectrum is similar across the 6 plots (Figure 3.6). This suggests

Table 3.4 Fish community biomass (FB), fish to zooplankton biomass ratio (F:Z), fish community production to biomass ratio (P:B) and throughput (TP), and the variation in fish community biomass (coefficient of variation: CV) when the zooplankton community is defined by the feeding characteristics of different functional groups. The system has a stable steady state when $\lambda_{\max} < 0$, and an unstable, oscillating steady state when $\lambda_{\max} > 0$.

	FB	F:Z	P:B (Fish)	TP (Fish)	CV (Fish)	λ_{\max}
Salps & Doliodids	133.02	2.86	366.38	5402.88	1.11	0.25
Herb. Copepods	13.43	3.79	73.76	586.25	1.26	0.67
Chaetognaths	4.33	4.40	29.77	69.61	1.27	0.59
General	1.40	4.43	11.84	8.06	0.97	0.51
Flagellates	0.20	1.73	3.13	0.27	0.11	0.53
Carn. Copepods	0.13	2.15	2.42	0.11	0.01	0.20

the average slope of the fish community spectrum depends more on the feeding characteristics of the fish, over the dynamics of the zooplankton community.

The total average fish biomass increases with increasing phytoplankton abundance, across all 6 systems (Figure 3.7 a). The magnitude of the increase in fish biomass correlated with the F:Z and CV of the system (Table 3.4). More fish were associated with a higher F:Z, and lower CV. The general zooplankton community system had the highest fish to zooplankton biomass ratio (4.43) and had the largest increase in total fish abundance: an 800% increase in fish. In contrast, the herbivorous copepod and chaetognath systems had similar fish to zooplankton biomass ratios to the general community (4.40 and 3.78), but higher CV's (1.26 and 1.27). These systems' fish biomass increased by 340% and 410%, respectively. The flagellate system had the lowest fish to zooplankton biomass ratio (1.73), the second lowest CV (0.11) and the lowest increase in total fish biomass (170%).

Fish communities supported by herbivorous zooplankton communities were more resilient to fishing pressure, compared to fish supported by more carnivorous zooplankton (Figure 3.7 b). The salp system had a negligible decline in average fish biomass, and chaetognath, herbivorous copepod and general community systems declined by up to 1%, 2%, 5%, respectively, with increasing fishing pressure. The two systems with carnivorous zooplankton communities (flagellates and carnivorous copepods) had an almost identical relationship between total relative fish biomass and fishing pressure, with both losing up to 15% of their average unfished biomass.

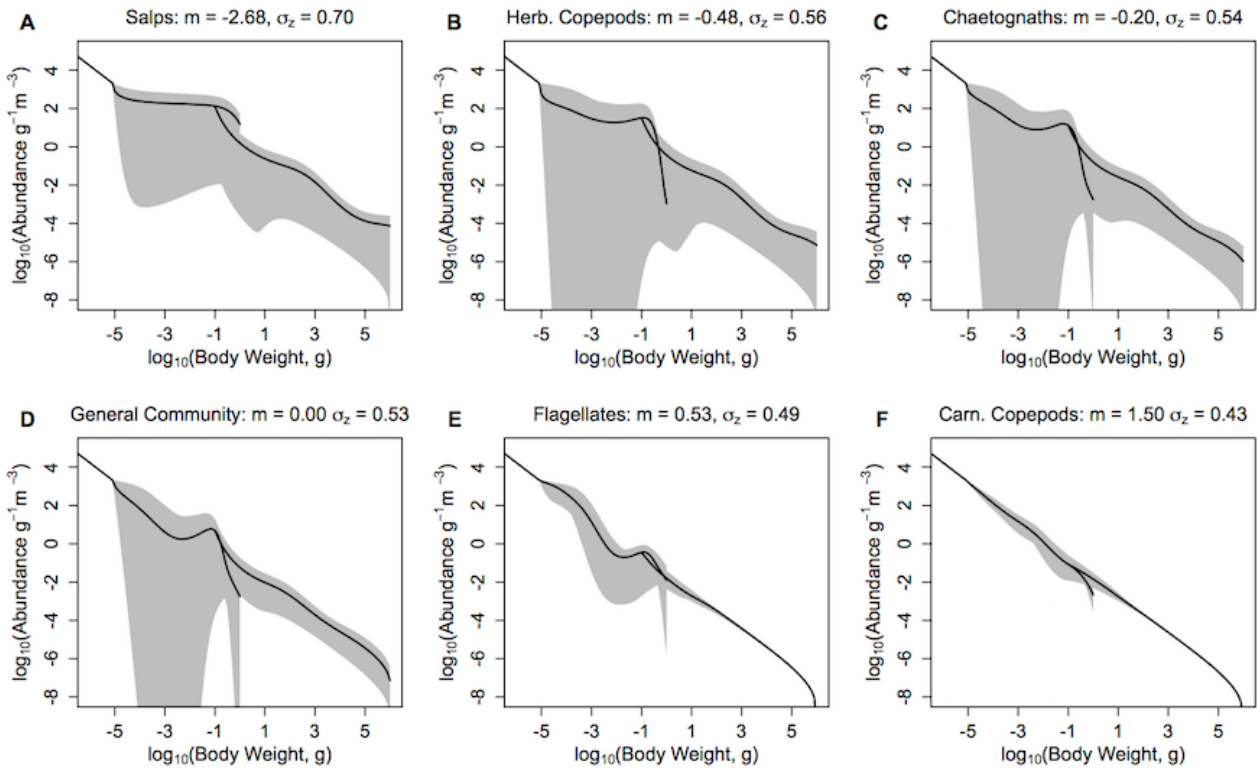


Figure 3.6 The zooplankton and fish community size-spectra when the zooplankton community is defined by the feeding characteristics of a single functional group (Fuchs and Franks 2010; Wirtz 2012). Here, m denotes the feeding mode of the zooplankton and σ_z the width of the feeding kernel. The solid lines denote the average abundance slope of the zooplankton and fish communities over 10 years. The shaded areas show the regions of the travelling wave solutions over 10 years if the steady state is unstable.

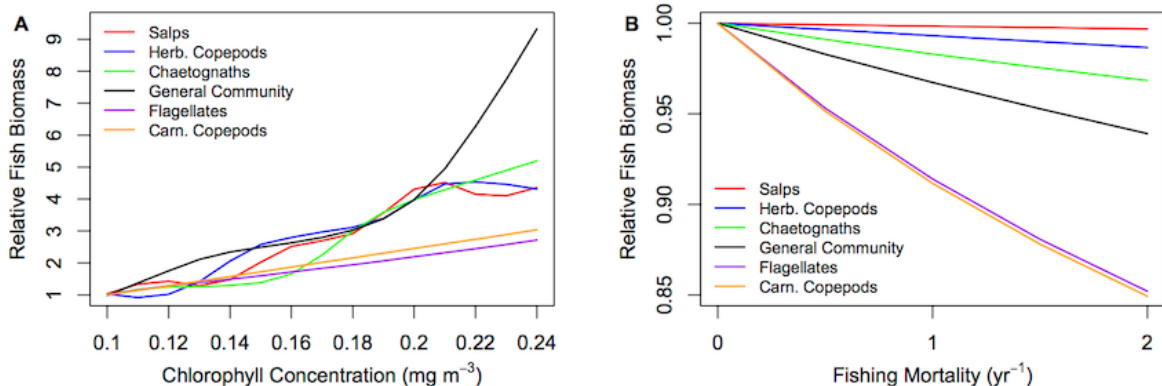


Figure 3.7 Relative fish biomass against (a) total phytoplankton abundance ($\text{g}^{-1}\text{m}^{-3}$) and (b) fishing mortality (yr^{-1}) for fish communities supported by a zooplankton community with the feeding characteristics of different functional groups. The relative fish biomass is calculated from the total fish biomass divided by the total fish biomass at a) the lowest phytoplankton abundance (0.1 mg m^{-3} chlorophyll a) and b) no fishing mortality (0 yr^{-1}).

3.5 Discussion

This study is the first qualitative assessment of how zooplankton feeding characteristics mediate the transfer of energy from phytoplankton to higher trophic levels with a dynamic size-spectrum model. Improving the realism of the zooplankton community with zooplankton-specific feeding parameters increased the transfer efficiency of the system and the total mean biomass of the fish community, but changed the steady state of the system from a stable linear spectrum, to a series of travelling waves of abundance from smaller to larger size classes (Table 3.3; Figure 3.3). The change in steady state came from updating the zooplankton community predator-prey mass ratio (PPMR) and feeding kernel width (σ_z). The general zooplankton community had a m -value of 0, which corresponds to a \log_{10} PPMR of between 3-5 across the size range of the zooplankton community, and σ_z of 0.75. This is in contrast to the fish community \log_{10} PPMR of 2, and feeding kernel width of 1. This observed change in the steady state agrees with the observed effects of increasing PPMR and decreasing σ_z for fish communities (Blanchard *et al.*, 2008; Law *et al.*, 2009; Datta *et al.*, 2011; Zhang *et al.*, 2013).

Our results suggest a trade-off mediated by the zooplankton community, between the stability of the overall system and the total biomass and productivity of the fish community. A zooplankton community with a more generalist, carnivorous feeding strategy – defined by a lower PPMR (larger, positive m) and a wider feeding kernel - stabilised the steady state of the system (Figure 3.5), but the fish community was less abundant and productive (Figure 3.4). In contrast, a zooplankton community characterised by specialised, herbivorous behavior – defined by a higher PPMR (larger, negative m) and a narrower feeding kernel - increased the total average biomass and productivity of the fish community (Figure 3.4), but destabilised the system steady state (Figure 3.5). Herbivorous and mixed communities ($m \leq 0$) with a narrower σ_z had a higher ratio of fish to zooplankton biomass (Figure 3.4 d,e), indicating a more efficient transfer of biomass from zooplankton to fish. This positive relationship between the zooplankton community PPMR and transfer efficiency corroborates with previous theoretical (Andersen *et al.*, 2009) and empirical work (Jennings *et al.*, 2002; Barnes *et al.*, 2010); a higher PPMR yields a higher transfer efficiency between trophic levels, and fewer trophic levels separating phytoplankton from fish.

Zooplankton communities with a higher PPMR and narrower σ_z had more variance in their abundance (Figure 3.5), which suggests that the abundance of zooplankton communities characterised by specialised herbivorous feeding behavior could exhibit more variation in

their abundance than carnivorous communities. A similar relationship for fish species was found by Blanchard (2008), who established a link between the variation in fisheries catch of certain species of fish with their PPMR and σ ; species with a higher PPMR and narrower feeding kernel had greater variability in their fishing catch through time. Jennings and Warr (2003) identified a link between environmental stability and a smaller ecosystem average PPMR, which in this context means increasing herbivory amongst zooplankton in unstable environments. Such a relationship has been observed in marine ecosystems; herbivorous zooplankton dominate in unstable coastal and upwelling regions, whereas more carnivorous zooplankton are abundant in the open ocean (Raymont, 1980).

The resilience of the fish community to fishing pressure increased, and ecosystems became more efficient in mediating energy from phytoplankton to fish, when zooplankton communities had a larger σ_z and higher PPMR characteristic of more herbivorous functional groups (Figure 3.7). The relationship between zooplankton community feeding characteristics, and the resilience of the fish community and ecosystem transfer efficiency, has potential implications for the marine environment under climate change. The world ocean's oligotrophic regions are expected to expand as a result of climate change (Sarmiento *et al.*, 2004; Polovina *et al.*, 2008; Doney *et al.*, 2012). Food chains in warmer, oligotrophic oceans are traditionally believed to be longer than other regions, as a result of the dominance of smaller phytoplankton (Morán *et al.*, 2010; Sprules and Munawar, 1986; Irwin *et al.*, 2006), which would result in lower rates of energy transfer from primary producers to higher trophic levels. Further, recent studies suggest possible climate-driven shifts in the dominance of certain zooplankton functional groups, such as salps or jellyfish (Atkinson *et al.*, 2004; Richardson *et al.*, 2009; Schofield *et al.*, 2010). Our results indicate that, everything else being equal, an increase in the dominance of carnivorous zooplankton groups could further decrease the transfer efficiency of expanding oligotrophic regions. Conversely, an increase in the abundance of herbivorous groups with a large PPMR, such as salps or herbivorous copepods, could decrease the number of trophic levels between phytoplankton and fish and thereby increase the transfer efficiency of these future oligotrophic regions.

Overall, increasing the zooplankton community PPMR had the greatest effect on increasing the total abundance, productivity and resilience of the fish community (Figure 3.4; Figure 3.7), and increasing σ_z had the greatest stabilising effect on the steady state of the system (Figure 3.5). Zooplankton have a higher average PPMR and smaller σ_z in comparison to average observed values for fish and this difference has enormous implications for

ecosystem transfer efficiency and stability (Barnes *et al.*, 2010). This means that zooplankton feeding characteristics – in particular PPMR and feeding kernel width – are a critical component to consider moving forward in how the transfer of energy from primary production to higher trophic levels is resolved in marine ecosystem models. This agrees with Jennings and Collingridge (2015), who suggest that a poor understanding of energy transfer in lower trophic levels is a potential cause for the order of magnitude discrepancy between model predictions and observed mesopelagic fish biomass over large spatial scales (Davison *et al.*, 2013; Irigoien *et al.*, 2014).

The large changes in fish biomass and productivity as a result of changes in the zooplankton community lead us to assess the implications of assuming a constant phytoplankton abundance spectrum within the model. In this study, we assume no feedbacks on the phytoplankton community from zooplankton (i.e. predation), however we know from empirical studies that the slope of the phytoplankton spectrum does change. The phytoplankton spectrum is shallower in eutrophic, upwelling systems – indicating a higher abundance of larger individuals such as diatoms - and steeper in oligotrophic systems where small-celled phytoplankton dominate (Sprules and Munawar, 1986; Irwin *et al.*, 2006). The effects of eutrophy or oligotrophy on higher trophic levels could be investigated by varying not only the intercept, but also the slope of the phytoplankton community and incorporating feedback from zooplankton predation.

Our model did not investigate how changes in the body composition of different zooplankton functional groups affects energy transfer from phytoplankton to fish. Gelatinous zooplankton have around one-tenth of the carbon content per unit of live mass compared to other groups (Kiørboe, 2013) and carbon content as a proportion of weight scales isometrically with increasing body size for carnivorous zooplankton (e.g., ctenophores and cnidarians), but decreases for filter feeders such as salps (Molina-Ramírez *et al.*, 2015). This would have implications for the nutritional value of different zooplankton groups for the fish community, and the fish community's resultant growth rates. Future work could investigate the effect zooplankton body composition might have on energy transfer, by varying the assimilation efficiency of the fish community for different zooplankton functional groups.

Looking forward, theoretical studies have shown that including more traits than just individual body size increases the stability of the size-spectrum (Datta *et al.*, 2011; Zhang *et al.*, 2013) and improves the realism of modelled predator-prey dynamics (Boukal, 2014). Recent developments in dynamic size-spectrum theory now allow multiple functional groups

and even species to be resolved within the community spectrum (Hartvig *et al.*, 2011; Maury, 2010; Scott *et al.*, 2014) and have been used to represent actual fish communities with increasing realism (e.g., Blanchard *et al.*, 2014; Dueri *et al.*, 2014; Spence *et al.*, 2016; Zhang *et al.*, 2016). The instabilities in our single-spectrum zooplankton community indicate that more complexity is needed if we are to represent realistic zooplankton communities within a dynamic size-spectrum framework. We envision the next steps toward this goal would involve a functional group approach, where the unique size-based characteristics of multiple size-based zooplankton communities are represented, and the model is calibrated and compared with real-world data. The growing literature on the size-based behavior of zooplankton functional groups – coupled with the recent theoretical developments in dynamic size-spectrum modelling – means size-spectrum models that realistically resolve both zooplankton and fish may now be within reach.

To conclude, in present size-spectrum model formulations focused on fish, small zooplankton are lumped together with phytoplankton in a background resource spectrum, and large zooplankton are represented as fish. The results of this study clearly demonstrate what we already know to be true: zooplankton are not fish, and nor are they phytoplankton. Current formulations that do not resolve the unique feeding characteristics of zooplankton are neglecting a significant factor in how energy is transferred from phytoplankton to fish. The results of this study motivate further work toward increasing the realism of zooplankton processes in size-spectrum models, and end-to-end marine ecosystem models more broadly.

3.6 Supplementary Information

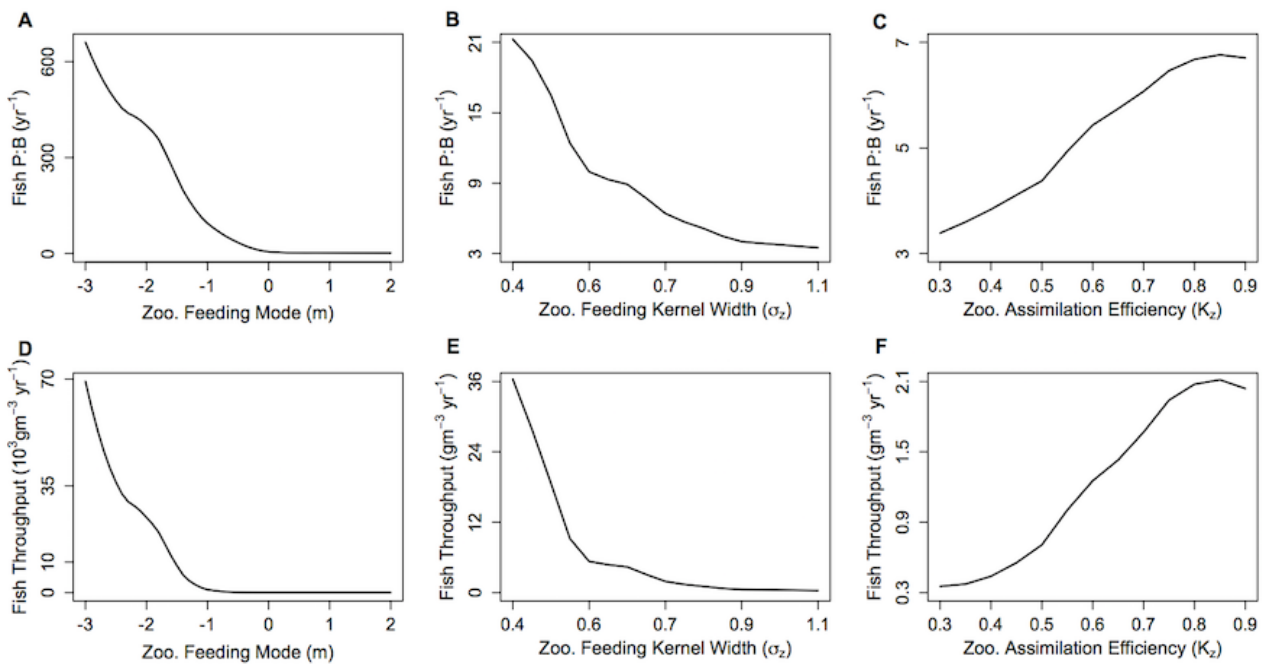


Figure S 3.1 a,b,c) The fish community production to biomass ratio (P:B) and d,e,f) throughput against zooplankton feeding mode (m), feeding kernel width (σ_Z) and assimilation efficiency (K_Z). In each plot, the other feeding parameters not specified are held constant at $m = 0$, $\sigma_Z = 0.75$ and $K_Z = 0.7$.

Chapter 4

Global patterns in zooplankton community composition: functional traits matter

4.1 Abstract

Zooplankton are the main energy pathway between phytoplankton and fish, and changes in the composition of the zooplankton have implications for how energy moves through marine food webs. Functional traits, such as body size and predator-prey mass ratio have been hypothesised to give rise to zooplankton community composition across global environmental gradients, because these traits determine the relative fitness of individual zooplankton under different environmental conditions. At the same time, the carbon content of different zooplankton groups varies from jellyfish (0.05%) to copepods (~12%), and this has implications for how efficiently energy is transferred through these groups to higher trophic levels. Here, we explore the role of body size, size-based feeding characteristics – including predator-prey mass ratio - and carbon content in structuring the zooplankton community across the global ocean. We develop a marine ecosystem model that represents these functional traits for nine major zooplankton functional groups (heterotrophic flagellates and ciliates, omnivorous and carnivorous copepods, chaetognaths, larvaceans, salps, euphausiids and jellyfish). The model is run globally, and the composition and total biomass of the zooplankton community emerges from the model, based on the relative fitness of the zooplankton groups under varying environmental conditions. Across the global ocean, the emergent patterns of abundance for the zooplankton groups and total zooplankton biomass broadly agreed with empirical distributions, and we identified clear changes in zooplankton community structure. Larvaceans, salps, carnivorous copepods and chaetognaths were most prevalent in the open ocean. Alternatively, euphausiids and jellyfish dominated in eutrophic regions and omnivorous copepods were prevalent everywhere. Our study demonstrates the significant role of body size, size-based feeding characteristics and carbon content for structuring the zooplankton community across the global ocean.

4.2 Introduction

Zooplankton are the lynchpin of the marine ecosystem, serving as the grazers of phytoplankton and bacteria, and prey of small fish (Mitra *et al.*, 2014). All marine phyla are represented in the zooplankton and this diversity is ubiquitous across the world, with most major groups present in every region of the world's oceans (O'Brien, 2005; Bucklin *et al.*, 2010). Despite their global presence, the composition of the zooplankton community is not constant, with groups dominating under different biotic and abiotic regimes depending on their relative fitness (Barton *et al.*, 2013). Variation in the zooplankton has implications for how efficiently energy moves through the marine food web from oligotrophic (low primary production) to eutrophic (high primary production) regions, with implications for ecosystem resilience, fisheries catch, and overall productivity (Friedland *et al.*, 2012; Jennings and Collingridge, 2015; Heneghan *et al.*, 2016; Dam and Baumman, 2017). Therefore, resolving the mechanisms that drive shifts in zooplankton community composition across environmental gradients is critical to understanding and predicting how marine ecosystems function.

The most common assumption with respect to zooplankton in current marine ecosystem modelling efforts is that the zooplankton community does not vary across time or space (Everett *et al.*, 2017). This is an understandable shortcoming – the zooplankton community exhibits tremendous taxonomic diversity, cannot be measured from space as phytoplankton can, and is difficult to measure *in situ*. An alternative to resolving taxonomic diversity is to model organisms based on functional traits, such as body size, body composition and feeding strategy, since these are factors that determine an organism's relative fitness (McGill *et al.*, 2006; Litchman *et al.*, 2013; Blanchard *et al.*, 2017; McConville *et al.*, 2017). In the past 10 years, the functional trait-based approach has been widely applied to explain the distribution of phytoplankton groups (e.g., Follows *et al.*, 2007; Edwards *et al.*, 2013), and there is a growing literature applying the approach to higher trophic levels (e.g., Fuchs and Franks, 2010; Blanchard *et al.*, 2014, Brun *et al.*, 2016).

Body size is a major determinant of the trophic position of zooplankton in the marine food web (Andersen *et al.*, 2016a) and the size-based feeding behaviour of different zooplankton groups structures the zooplankton community across oligotrophic and eutrophic systems (Mitra and Davis, 2010; Barton *et al.*, 2013). Zooplankton are the primary grazers of phytoplankton, which span up to nine orders of magnitude in body size – from picoplankton (0.2 - 2 µm equivalent spherical diameter, ESD; $10^{-14.5}$ – $10^{-11.5}$ g wet weight) to

microplankton ($>20 \mu\text{m}$ ESD; $>10^{-8.4}$ g wet weight). Moreover, the size structure of phytoplankton changes across environmental gradients (Agawin *et al.*, 2000; Brewin *et al.*, 2010; Barnes *et al.*, 2011). Phytoplankton communities in nutrient rich coastal and upwelling eutrophic systems have greater abundance and proportion of microplankton – a higher intercept and flatter abundance size-spectrum slope (Figure 4.1). In low nutrient oligotrophic systems, phytoplankton is less abundant and dominated by picoplankton ($<2 \mu\text{m}$ ESD), with little or no microplankton ($>20 \mu\text{m}$ ESD). In terms of the phytoplankton abundance spectrum, this means a lower intercept and a steeper slope (Figure 4.1). Changes in the size structure of the phytoplankton have implications for the structuring of the zooplankton community, which in turn affects how primary production is transported to higher trophic levels. This is because zooplankton exhibit vast diversity in their feeding behaviour, with observed predator-prey mass ratios (PPMRs) varying over 7 orders of magnitude across different functional groups, from ~ 10 for carnivorous copepods to $\sim 10^8$ for salps and larvaceans (Wirtz, 2012).

Different PMMRs mean that zooplankton do all not feed from the same prey size range. Therefore, depending on the size structure of the phytoplankton, certain zooplankton groups will have more prey than others in different regions. For instance, omnivorous copepods and euphausiids with large PMMRs ($10^3 - 10^7$) feed mostly from the microplankton (Sommer *et al.*, 2002; Henschke *et al.*, 2015). We hypothesise these groups would dominate in eutrophic regions where the phytoplankton community has a higher proportion of microplankton.

In contrast, picoplankton make up the bulk of the phytoplankton biomass in oligotrophic systems. These small phytoplankton mostly fall out of the prey size range of omnivorous copepods and euphausiids. Instead, omnivorous copepods and euphausiids would consume heterotrophic protists such as flagellates and ciliates that feed on the picoplankton. This would increase their trophic position to that of other carnivorous zooplankton such as chaetognaths and carnivorous copepods. Therefore, we hypothesise that these exclusively carnivorous groups will make up a higher proportion of the zooplankton community in oligotrophic systems. However, larvaceans and salps have very large PMMRs of $\sim 10^8$ (Diebel and Lee, 1992; Wirtz, 2012) and can directly access the picoplankton for food (Bone, 1997; Sutherland *et al.*, 2010), therefore we hypothesise that larvaceans and salps could make up a larger proportion of the zooplankton community in oligotrophic systems, where picoplankton is abundant.

Jellyfish are the largest zooplankton; they share the same size range as small fish but can reach up to 1 tonne in the case of the lion's mane jellyfish (Levinton, J., 2013). Their size and PPMR ~ 3 (Hansen *et al.*, 1997; Acuña *et al.*, 2011) mean that jellyfish are carnivores, competing with small fish to feed on smaller zooplankton and fish larvae. Their low carbon content and inflated body size mean that jellyfish face few predators – relative to fish of the same size - and can increase their biomass quickly in response to increases in prey (Pauly *et al.*, 2009; Acuña *et al.*, 2011). This suggests that jellyfish are more affected by changes in their prey than top-down control from predators (Pauly *et al.*, 2009). Therefore, we expect jellyfish to make up a larger proportion of the zooplankton community in eutrophic systems, where prey is more abundant.

A zooplankton community dominated by more gelatinous groups offers less nutritional value and growth potential for higher trophic levels. This means that resolving the carbon content of the different zooplankton is necessary to resolve the implications of changing zooplankton community composition for energy transfer from phytoplankton to fish. Moreover, the carbon content of different zooplankton groups affects their relative fitness under varying environmental conditions. Carbon is the primary structural component of zooplankton (Kiørboe, 2013), and critical physiological and competitive processes such as metabolism, search rate, and assimilation efficiency scale with carbon across zooplankton groups (Acuña *et al.*, 2011; Kiørboe, 2011; Kiørboe and Hirst, 2014; McConville *et al.*, 2017). This means that changes in carbon content affects the relative fitness of different zooplankton groups. For example, because respiration scales with carbon weight, jellyfish biomass, which is only 0.5% carbon, is metabolically cheaper to build and maintain than copepod biomass, which is 12% carbon (Kiørboe and Hirst, 2014). At the same time, because search rate also scales with carbon content across zooplankton groups (Kiørboe, 2011), a jellyfish of a certain wet weight has a lower search rate than a copepod of the same weight.

Resolving the carbon content, size-based feeding characteristics and body sizes of major zooplankton functional groups are critical to accurately resolving changes in zooplankton community composition, across varying environmental conditions. This idea is not entirely new; almost 25 years ago Hansen *et al.*, (1994) hypothesised that with knowledge of the size selectivity of different zooplankton groups, it would be possible to construct a simple size-based model of the pelagic food web. The extensive and growing literature on the size-dependency of zooplankton feeding strategies (e.g., Fuchs and Franks, 2010; Kiørboe, 2011; Wirtz, 2012), coupled with recent developments in functional size-based ecosystem modelling (Blanchard *et al.*, 2017) means that testing this hypothesis is now possible.

Here, we explore how body size, size-based feeding characteristics and carbon content affect the composition and total biomass of the zooplankton community globally. We developed a functional size-spectrum model that breaks the marine ecosystem into three components; phytoplankton, zooplankton and fish. The model resolves the size ranges, size-based feeding characteristics and carbon content of nine of the most abundant zooplankton functional groups: heterotrophic flagellates and ciliates, omnivorous and carnivorous copepods, larvaceans, euphausiids, salps, chaetognaths and jellyfish). Across the global ocean, the model is initialised with the same zooplankton community composition and community structure emerges, based on the traits of the different groups.

We separate our findings into two parts. First, we explore how the emergent zooplankton community composition changes across environmental gradients. We identified clear changes in the emergent zooplankton community across the global ocean, with salps, larvaceans, carnivorous copepods and chaetognaths most prevalent in the oligotrophic open ocean, omnivorous copepods prevalent everywhere, and euphausiids and jellyfish dominating in eutrophic waters. Second, we compared the emergent abundances of the zooplankton groups from the functional size-spectrum model with empirical distributions. These empirical distributions of different zooplankton groups were determined using generalised additive models (GAMs; Wood, 2017), based on *in situ* sampled abundance data and environmental variables. We found that the emergent distributions from the size-spectrum model broadly agreed with the empirical distributions calculated from the GAMs. Our study is the first to demonstrate how functional traits such as body size, size-based feeding behaviour and carbon content give rise to the zooplankton community across global environmental gradients, and is a step forward to improving our understanding of food web structure and ecosystem function across global environmental gradients.

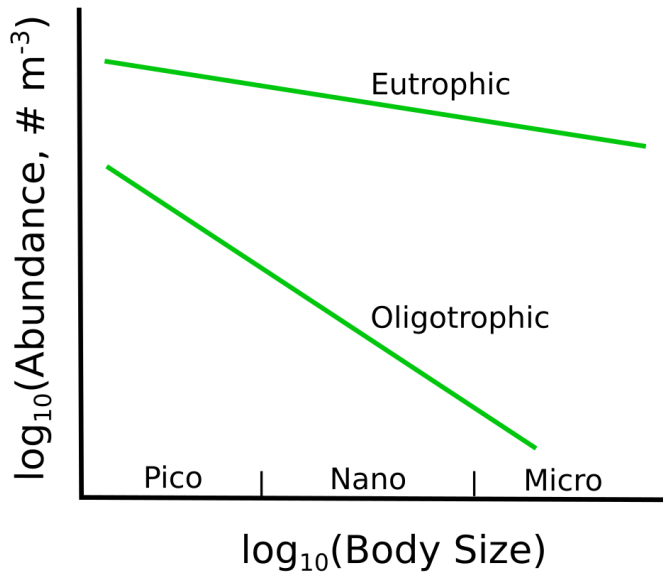


Figure 4.1 Change in phytoplankton community size structure across eutrophic (high chlorophyll) and oligotrophic (low chlorophyll systems).

4.3 Methods

We used the functional size-spectrum framework (Blanchard et al., 2017) to incorporate the body size ranges, size-based feeding characteristics and carbon content of nine of the most abundant zooplankton groups and three fish communities. Our model is run across the global ocean (broken into 5x5 degree grid squares) with annual average sea surface temperature and chlorophyll a concentration serving as environmental inputs. To test how well the theoretical size-spectrum model captures observed patterns of zooplankton abundance, we compare the emergent abundances for the different groups with empirical distributions. Empirical distributions of different zooplankton groups were determined using generalised additive models (GAMs), based on *in situ* data and environmental variables.

4.3.1 Overview of the size-spectrum model

We represented the marine size-spectrum as three communities: phytoplankton, zooplankton and fish. The zooplankton community consists of nine of the most abundant zooplankton groups, and the fish community was made up of a small, medium and large group (Figure 4.2; Table 4.1, 4.2, 4.3).

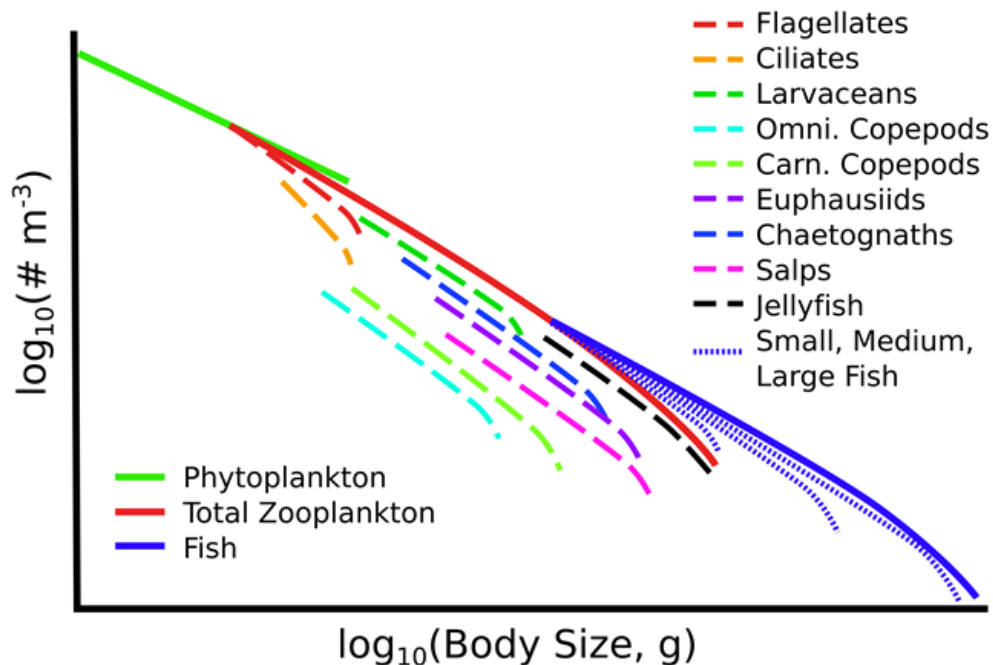


Figure 4.2 Conceptual illustration of the functional size-spectrum model.

In keeping with past size-spectrum models, the dynamics of the phytoplankton are not explicitly resolved in the model, with the phytoplankton size-spectrum serving as a static resource for zooplankton (Blanchard et al., 2009; Law et al., 2009; Guiet et al., 2016;

Heneghan et al., 2016). This is because the size structure of the phytoplankton community can be estimated directly from satellite chlorophyll a observations (Brewin et al., 2010; Barnes et al., 2011; Hirata et al., 2011). The abundances of the zooplankton and fish communities are driven by the size-dependent processes of growth and mortality, with the temporal dynamics of each functional group governed by separate second-order McKendrick-von Foerster equations,

$$\frac{\delta}{\delta t} N_i(w, t) = -\frac{\delta}{\delta w} (g_i(w, t)N_i(w, t)) - \mu_i(w, t)N_i(w, t) + \frac{1}{2} \frac{\partial^2}{\partial w^2} (f_i(w, t)N_i(w, t)).$$

The density of individuals in group i of weight w at time t per m^{-3} is given by $N_i(w, t)$ and their individual growth, mortality and diffusion rates are denoted by $g_i(w, t)$, $\mu_i(w, t)$ and $f_i(w, t)$, respectively. The diffusion term incorporates demographic variation in the growth rates of each community: individuals in the same functional group starting at the same weight grow differently over time (Datta et al., 2010).

From the perspective of a predator from group i , the feeding rate on prey group j depends on the density of suitable prey (g m^{-3}):

$$D_{ij}(w, t) = \int_{w_p}^w \phi_i(w, w') N_j(w', t) w' dw', \quad (\text{E7})$$

where $\phi_i(w, w')$ (E4, Table 4.1; all subsequent equations are also found in Table 4.1) is the probability a predator of size w would consumer an individual of size w' . The growth rate of a predator from group i , of size w at time t is fuelled by the consumption and conversion of prey biomass to new biomass (g yr^{-1}):

$$g_i(w, t) = \tau V_i(w) \sum_j GG_{ij} D_{ij}(w, t), \quad (\text{E9})$$

where $V_i(w)$ is the predator's search rate (E6), GG_{ij} is the growth conversion efficiency for predators from group i consuming prey from group j (E8) and τ is the effect of temperature on ingestion for group i (E3). Temperature effects are represented using the modified Arrhenius equation:

$$\tau = \exp \left(25.55 - \frac{0.63}{8.62 \times 10^{-5} K} \right), \quad (\text{E3})$$

where K is the temperature in Kelvin (Jennings et al., 2008; Blanchard et al., 2012; Woodworth-Jefcoats et al., 2015). For each 5x5 degree region, we obtained temporally and spatially averaged satellite sea surface temperature from MODIS-Aqua (accessed via the GIOVANNI portal: <https://giovanni.gsfc.nasa.gov/giovanni/>).

From the perspective of the prey, the total mortality from predation by the larger size classes $\mu_p(w, t)$ (yr^{-1}) is given by:

$$\mu_p(w, t) = \tau \sum_j \int_w^{\bar{W}_j} \phi_j(w', w) \theta(w', w) V_j(w') N_j(w', t) dw', \quad (\text{E11})$$

where \bar{W}_j is the maximum size of a predator from group j . Since individuals grow through time, an additional source of mortality from senescence was incorporated that increased with body size (yr^{-1}):

$$\mu_{S_i}(w, t) = \tau \delta \left(\frac{w}{W_{s_i}} \right)^\rho, \quad (\text{E12})$$

where W_{s_i} is the body size after which senescence mortality increases for an individual from group i . This senescence mortality term also acts as a closure term for the largest size classes, by preventing a build-up of large individuals who are not exposed to predation (Andersen *et al.*, 2016b). For an individual of size w , at time t , from group i , total mortality $\mu_i(w, t)$ (yr^{-1}) is given by summing predation and senescence mortality (yr^{-1}):

$$\mu_i(w, t) = \mu_p(w, t) + \mu_S(w, t). \quad (\text{E13})$$

4.3.2 Parameterising the static phytoplankton abundance spectrum

We split the global ocean into 5x5 degree regions. For each region, the slope a , intercept b and maximum size of the static phytoplankton spectrum were derived from temporally and spatially averaged satellite chlorophyll a obtained from MODIS-Aqua (accessed via the GIOVANNI portal: <https://giovanni.gsfc.nasa.gov/giovanni/>), using the synoptic model developed by Brewin *et al.*, (2010). The Brewin model gives an estimate of the percentage contribution of 3 phytoplankton size classes - pico ($0.2\text{-}2 \mu\text{m ESD}$), nano ($2\text{-}20 \mu\text{m ESD}$) and micro ($>20 \mu\text{m ESD}$) – to the total chlorophyll a concentration (mg m^{-3}). Pico-phytoplankton comprise ~60% of the biomass in oligotrophic waters, declining to around 10% in eutrophic waters as micro-phytoplankton increase from <5% in oligotrophic waters to ~45% in eutrophic waters, and nano-phytoplankton increase marginally from 30% in oligotrophic to 45% in eutrophic waters (Figure 4.3 a, b, c).

The contribution of micro phytoplankton, and the phytoplankton community's maximum size increases with chlorophyll a concentration (Brewin *et al.*, 2010; Hirata *et al.*, 2011; Barnes *et al.*, 2011). We incorporated this relationship by linearly increasing the maximum size of

the micro group from 21 - 60 μm ESD, depending on the percentage contribution of the micro group to total chlorophyll a. We used 60 μm as the maximum possible ESD for the phytoplankton following Barnes et al.'s (2011) finding that 90% of phytoplankton fall below 55-65 μm across polar, tropical and upwelling environments. Total chlorophyll a concentration for each of the 3 size classes was converted to grams wet weight (assuming 1 g chlorophyll a = 50 g C; Zhou *et al.*, 2010, and 1 g C = 10 g wet weight; Hansen *et al.*, 1994, Boudreau & Dickie, 1992, Woodworth-Jefcoats *et al.*, 2013) and the three size ranges were also converted from ESD to grams wet weight (assuming 1 cm^{-3} = 1 g wet weight; Boudreau & Dickie, 1992).

Total biomass in each of the size ranges was then spread uniformly across each size range (Sheldon *et al.*, 1972; Blanchard *et al.*, 2009; Woodworth-Jefcoats *et al.*, 2013; Barange *et al.*, 2014) before being converted to numerical abundance. Finally, slope and intercept were determined by calculating the line of best fit through the log-transformed phytoplankton abundances, from the smallest to the largest size class. Our phytoplankton slope estimates for the global ocean ranged from -1.1 to -0.8 (Figure 4.3 d), which is within the range reported by previous empirical studies (Moreno-Ostos *et al.*, 2015).

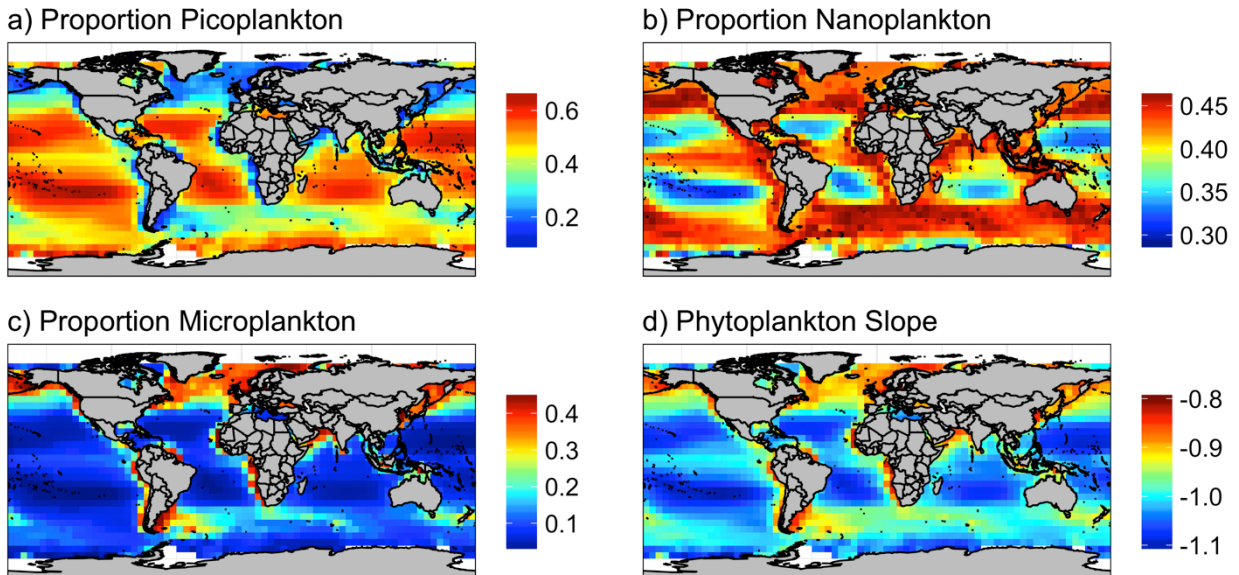


Figure 4.3 Global maps of the phytoplankton community. Proportion of phytoplankton that is a) picoplankton ($< 2\mu\text{m}$ ESD), b) nanoplankton ($2\mu\text{m}-20\mu\text{m}$ ESD), c) microplankton ($> 20\mu\text{m}$ ESD), and d) the slope distribution of the phytoplankton abundance spectrum.

Table 4.1 Model equations with their units and in-text reference numbers.

Description	Equation	Units	Equation Number
Phytoplankton spectrum	$N_p(w, t) = aw^b$	# m ⁻³	E1
Lower boundary condition for group i	$N_i(w_i, t) = P_i \sum_{j \neq i} N_j(w_i, t)$	# m ⁻³	E2
Temperature effect for group i	$\tau = \exp \left(25.55 - \frac{0.63}{8.62 \times 10^{-5} K} \right)$	-	E3
<u>Feeding, Growth and Diffusion:</u>			
Size selection for group i	$\phi_i(w, w') = \exp \left[-(ln(\beta_i(w)w'/w))^2 / 2\sigma_i^2 \right] / (\sigma_i \sqrt{2\pi})$	-	E4
Feeding kernel width parameter for group i	$\sigma_i = 0.05 \log_{10}(\bar{\beta}_i) + 0.33$		E5
Search rate for group i	$V_i(w) = C_i \gamma_i w^{\alpha_i}$	m ³ yr ⁻¹	E6
Density of suitable prey from group j for group i	$D_{ij}(w, t) = \int_{w_p}^w \phi_i(w, w') N_j(w', t) w' dw'$	g m ⁻³	E7
Gross Growth Efficiency for predator of group i eating prey of group j	$GG_{ij} = 0.25 \frac{C_j}{C_i}$	-	E8
Individual growth rate for group i	$g_i(w, t) = \tau V_i(w) \sum_j GG_{ij} D_{ij}(w, t)$	g yr ⁻¹	E9
Individual diffusion term for group i	$f_i(w, t) = \gamma_i w^{\alpha_i} \sum_j (\tau_G GG_{ij})^2 \int_{w_p}^w (w')^2 \phi_i(w, w') N_j(w', t) dw'$	g ² yr ⁻¹	E10
<u>Mortality:</u>			
Individual predation rate	$\mu_p(w, t) = \tau \sum_j \int_w^{\bar{W}_j} \phi_j(w', w) V_j(w') N_j(w', t) dw'$	yr ⁻¹	E11
Intrinsic mortality	$\mu_S(w, t) = \tau \delta \left(\frac{w}{W_{S_i}} \right)^\rho$	yr ⁻¹	E12
Total Mortality	$\mu_i(w, t) = \mu_p(w, t) + \mu_S(w, t)$	yr ⁻¹	E13

4.3.3 Incorporating functional traits

The zooplankton groups and the fish community were defined by size range, predator-prey mass ratio (PPMR), feeding kernel width, and carbon-wet weight ratio (Table 4.2; Figure 4.4).

4.3.3.1 PPMR and diet

Across zooplankton taxa, the predator-prey mass ratio (PPMR) increases with predator size, due to the non-isometric scaling of feeding-related apparatus with body size (Pearre, 1980; Wirtz, 2012). We used the mechanistic formulation from Wirtz (2012) to calculate the PPMR range for each zooplankton group. Wirtz (2012) links PPMR to a quantitative measure of the feeding mode: raptorial, active feeding is linked to a lower PPMR because predators eat prey closer to their own size. By contrast, passive, suspension feeding yields a higher

PPMR. The PPMR for the fish communities were held constant at 100 across their entire size ranges as is common (Peters, 1983; Jennings et al., 2001; Andersen et al., 2016b).

The body sizes and relatively high PPMRs of salps, larvaceans and omnivorous copepods means that these groups feed exclusively on phytoplankton, heterotrophic flagellate and ciliate communities. Euphausiids also have high a PPMR range, but not as large as salps and larvaceans, which means that their largest size classes also access smaller copepods, larvaceans and euphausiids, consistent with their diet in the oceans (Schmidt and Atkinson, 2016). The low PPMR ranges of carnivorous copepods, chaetognaths and jellyfish, coupled with their larger body size means that these groups are almost totally carnivorous, we further restricted their diets so that they do not feed on phytoplankton at all, which is consistent with most current understandings (Terazaki, 2000; Purcell and Arai, 2001).

4.3.3.2 Prey size selection

The range of available prey sizes for an individual predator of body size w from group i is defined by a log-normal feeding kernel, centred on the predator's predator-prey mass ratio (PPMR; $\beta_i(w)$) and a standard deviation (σ_i) given by the kernel width parameter for that predator's group:

$$\phi_i(w, w') = \exp \left[- \left(\ln \left(\frac{\beta_i(w)w'}{w} \right) \right)^2 / 2\sigma_i^2 \right] / (\sigma_i \sqrt{2\pi}). \quad (\text{E4})$$

A wider feeding kernel means a predator can feed from a larger size range of prey. For zooplankton, feeding kernel width is positively correlated with PPMR (Hansen et al., 1994; Fuchs and Franks, 2010; Kiørboe, 2016); filter feeders such as larvaceans or salps with a large average PPMR feed over a wider size range than carnivorous copepods or heterotopic flagellates. We used the empirical model developed by Fuchs and Franks (2010) to link the feeding kernel width of each zooplankton group (σ_i), to that group's average PPMR ($\bar{\beta}_i$):

$$\sigma_i = 0.05 \log_{10}(\bar{\beta}_i) + 0.33 \quad (\text{E5})$$

The feeding kernel width for the fish communities were held constant at 1.3 (Andersen et al., 2016b).

4.3.3.3 Search rate

The search rate of individual zooplankton scales with body carbon, across seven functional groups (including heterotrophic flagellates and ciliates, copepods and jellyfish) and 12 orders of magnitude in body size (Kiørboe, 2011). This means that, per unit of wet weight,

more gelatinous groups will have a lower search rate, compared to more carbon dense functional groups. Carbon content is incorporated into the search rate equation $V_i(w)$ as a multiplier. For an individual of group i , with carbon content C_i of wet weight body size w , the search rate ($\text{m}^{-3} \text{ yr}^{-1}$) is:

$$V_i(w) = C_i \gamma_i w^{\alpha_i}, \quad (\text{E6})$$

where γ_i is the search rate coefficient ($\text{g C}^{-1} \text{ m}^{-3} \text{ yr}^{-1}$) and α_i is the exponent of search. The search rate coefficient γ_i and exponent α_i are different for the zooplankton and fish communities (Kiørboe, 2011, Andersen *et al.*, 2016b; see Table 4.3).

4.3.3.4 Growth conversion efficiency and carbon content

Straile (1997) found that gross growth conversion efficiency (GGE) – as a measure of prey carbon converted to predator carbon – was fixed at around 0.25 across a large range of zooplankton taxa. This agrees with the hypothesis that prey groups with a comparatively higher carbon content and energy density contribute more to predator wet-weight growth in comparison to lower carbon groups such as jellyfish (Spitz *et al.*, 2010; Kiørboe, 2013; Mitra *et al.*, 2014). In terms of wet weight, the GGE of a group i predator on a group j prey is

$$GG_{ij} = 0.25 \left(\frac{C_j}{C_i} \right), \quad (\text{E8})$$

where C_j and C_i are the carbon-wet weight ratios of group j and i , respectively.

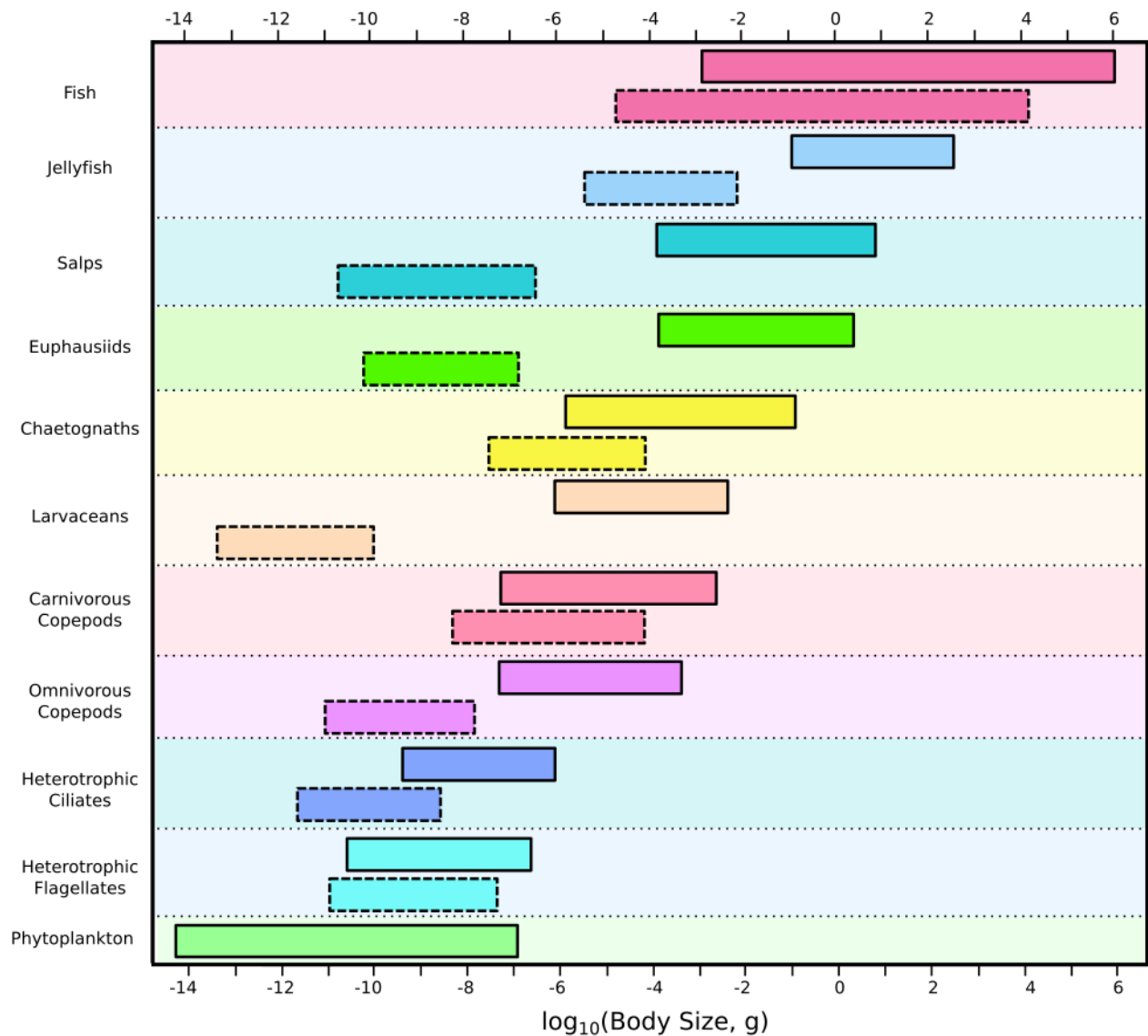


Figure 4.4 Overview of the size ranges of the model's functional groups (solid boxes), and their prey size ranges (dashed boxes).

Table 4.2 Parameter values for the nine zooplankton and three fish groups.

Group	Min. Size, w_i			Max Size, \bar{W}_i			$\log_{10}\text{PPMR}$ range, $\beta_i(w)$	Feeding Kernel Width, σ_i	Carbon - Wet Weight Ratio, C_i
	Length	ESD	$\log_{10}(g)^*$	Length	ESD	$\log_{10}(g)^*$			
Hetero. Flagellates	-	3 μm^a	-10.7 ^a	-	70 μm^a	-6.8 ^a	0.2 – 0.7 ²	0.36 ^{3^a}	0.15 ⁴
Hetero. Ciliates	-	10 μm^b	-9.3 ^b	-	100 μm^b	-6.3 ^a	2.5 – 2.9 ²	0.47 ^{3^a}	0.15 ⁴
Larvaceans	80 μm^c	100 μm^c	-6.3 ^c	3 mm ^c	2 mm ^c	-2.3 ^c	6.8 – 7.8 ⁷	0.7 ^{3^a}	0.01 ⁹
Omni. Cop.	-	60 μm^d	-7.5 ^d	2.8 mm ^e	0.9 mm ^e	-3.5 ^e	3.6 – 4.6 ²	0.57 ^{3^a}	0.12 ⁹
Carn. Cop.	-	60 μm^d	-7.5 ^d	6 mm ^e	1.8 mm ^e	-2.5 ^e	0.8 – 1.9 ²	0.4 ^{3^a}	0.12 ⁹
Euphausiids	-	0.6 mm ^f	-4.2 ^f	6 cm ^g	1.5 cm ^g	0.3 ^g	6.6 – 7.8 ^{3,15}	0.70 ^{3^a}	0.12 ⁹
Chaetognaths	1 mm ^h	150 μm^h	-5.9 ^h	4 cm ^h	6 mm ^h	-0.9 ^h	1.9 – 3.4 ¹⁶	0.46 ^{3^a}	0.04 ⁹
Salps	0.5 mm ⁱ	0.5 mm ⁱ	-4.3 ⁱ	1.9 cm ⁱ	1.6 cm ⁱ	0.6 ⁱ	6.8 – 8.5 ²	0.7 ^{3^a}	0.01 ⁹
Jellyfish	-	1 mm ^j	-3 ^j	-	15 cm ^j	2.6 ^j	2.7 – 4.7 ¹	0.52 ^{3^a}	0.005 ⁹
Small Fish	-	1 mm ^k	-3 ^k	-	6 cm	2	2 ²¹	1.3 ²²	0.10 ²³
Medium Fish	-	1 mm ^k	-3 ^k	-	27 cm	4	2 ²¹	1.3 ²²	0.10 ²³
Large Fish	-	1 mm ^k	-3 ^k	-	125 cm ^k	6 ^k	2 ²¹	1.3 ²²	0.10 ²³

* g wet weight calculated from ESD, assuming 1 gram = 1 cm³.

^a Feeding kernel widths were calculated with the empirical equation derived in (3), using mean $\log_{10}(\text{PPMR})$ for this group.

Size range source notations: ^a: From Table 3 in (1), ^b: From figure 1 in (5), ^c: Minimum and maximum larvacean trunk lengths taken from (6) and (8) respectively, and converted to ESD and wet weight using equation derived in (7), ^d: Carbon mass obtained from supplementary material in (10), converted to wet weight and ESD using carbon: wet weight ratio from (9) ^e: Maximum omnivorous and carnivorous copepod lengths taken from (11) and converted to ESD and then wet weight using equation derived in (12), ^f: Euphausiid embryo ESD from figure 2 in (13), ^g: Maximum length taken from supplementary material in (3) and converted to ESD and wet weight using equation from (14), ^h: ESD from supplementary material in (3), derived using head width: body length ratio from (16) ⁱ: Minimum and maximum salp length taken from (17) and converted to ESD and wet weight using equation derived in (18), ^j: Taken from supplementary material in (19), ^k: Maximum fish community size taken from (20).

1. Hansen et al. (1997), 2. Wirtz (2012), 3. Fuchs and Franks (2010), 4. Menden-Deuer and Lessard (2000), 5. Taylor (1978), 6. López-Urrutia (2004), 7. Deibel (1998), 8. Hopcroft et al. (1998), 9. Kiørboe (2013), 10. Kiørboe & Hirst (2014), 11. Benedetti et al. (2016), 12. Azevedo and Dias (2012), 13. Kawaguchi et al. (2011), 14. Meyer and Teschke (2016), 15. Schmidt and Atkinson (2016), 16. Pearre (1982), 17. Henschke et al. (2016), 18. Heron (1988), 19. Acuña et al. (2011), 20. Heneghan et al. (2016), 21. Kerr and Dickie (2001), 22. Andersen et al., (2016b), 23. Pauly and Christensen (1995).

Table 4.3 Model parameter values.

Symbol	Definition	Value	Unit	Source
γ	Coefficient of search rate	$\gamma_Z = 8750$	$\text{g C}^{-\alpha}\text{m}^{-3}\text{yr}^{-1}$	1
		$\gamma_F = 6400$		2
α	Exponent of search rate	$\alpha_Z = 1$	-	1
		$\alpha_F = 0.8$		2
W_S	Body size at which senescence mortality begins	$0.01\bar{W}$	g	5,6
δ	Coefficient of senescence mortality	0.05	$\text{g}^{-\rho}\text{yr}^{-1}$	5,6
ρ	Exponent of senescence mortality	0.3	-	5,6
P	Relative abundance of smallest size class	Flagellates = 1 Ciliates = 0.5 Larvaceans = 0.3 Omni. Copepods = 0.3 Carn. Copepods = 0.7 Euphausiids = 0.7 Chaetognaths = 0.3 Salps = 0.1 Jellyfish = 0.2 Fish = 1	-	See 4.3.5.1

Z, zooplankton; F, fish.

1. Kiørboe, 2011, 2. Peters 1983, 3. Jennings et al., 2008, 4. Blanchard et al., 2012, 5. Hall et al., 2006, 6. Heneghan et al., 2016.

4.3.4 Testing the size-spectrum model

To assess the size-spectrum model, we used generalised additive models (GAMs, Wood et al. 2007), which modelled the relationship between *in situ* sample data, and environmental variables and sampling equipment. GAMs were used to model the relationship between sampled abundances for each zooplankton group (excluding flagellates and ciliates), and chlorophyll *a*, sea surface temperature, bathymetry, time of year, and the sample equipment (gear type and mesh size). We used GAMs because they make few assumptions about the relationship between explanatory and predictor variables, and they are an increasingly popular choice for extrapolating patchy sample data using environmental variables (Drexler and Ainsworth, 2013; Rutherford et al., 2015). The “mgcv” package (version 1.8-15) in the R program (R Development Core Team, 2016) was used to build the GAMs.

Using GAMs, instead of simply the raw data, added complexity to the model validation that was unavoidable. Zooplankton observations were collected using a range of mesh sizes and sampling gears, from over a dozen cruises since 1958, and different sampling equipment and methods can lead to very different samples (Everett et al., 2017). We could control for the effect of gear and mesh type on sampled abundance by including them as explanatory

variables in the GAMs. Further, the relationship between zooplankton abundance and environmental factors, such as sea surface temperature, are not static across time or space. For example, zooplankton experience blooms following seasonal phytoplankton blooms and busts, which are characteristic in temperate and polar waters (Mann and Lazier, 2006). This means that the sampled zooplankton abundance in any given location would be different depending on the time of year. What is more, the magnitude of the change in abundance across the year is larger in colder regions with greater seasonal cycles compared to more stable tropical locations. This makes it difficult to compare the emergent abundances from the theoretical model – which does not incorporate seasonality – with *in situ* data taken at different times across the year. Although GAMs added complexity, they allowed us to control for these factors and wrangle the data into a form that we could use for model validation (Everett *et al.*, 2017). Indeed, we believe the empirical abundance and biomass fields we developed here could be useful for assessing and initialising current and future zooplankton models.

For each group, we calculated the predicted annual mean empirical abundance by averaging over the predicted abundances for all twelve months, and all gear and mesh factor levels. Empirical annual abundance maps and emergent abundance maps from the size-spectrum model were then compared using Pearson's correlation coefficient.

4.3.4.1 Data sources and handling

Samples of the abundance of different zooplankton groups in the top 200 m of the water column from 1958 to the present were obtained from the COPEPOD (O'Brien, 2005; <https://www.st.nmfs.noaa.gov/copepod/>) and IMOS (<http://imos.org.au/>) databases. Each observation contained information on location and time, sampled abundance (# m⁻³), species or taxonomic group, and the gear type and mesh size used to obtain the sample. To ensure a consistent data quality, we only included data that was originally recorded in # m⁻³, or # per haul with the total # m⁻³ for the haul recorded. To incorporate seasonality uniformly across the globe, we standardised the time of year for all observations from the southern hemisphere to the corresponding month in the northern hemisphere. For example, an observation taken in January (southern hemisphere summer, northern hemisphere winter) in the southern hemisphere was treated as an observation taken in July in the northern hemisphere (northern hemisphere summer).

Monthly local sea surface temperature, chlorophyll a concentration and bathymetry were obtained for each zooplankton sample. Since zooplankton data extended back to 1958, we

used mean monthly climatologies for sea surface temperature and chlorophyll a from 2002 – 2016, obtained from MODIS-Aqua 4km measurements, accessed via the GIOVANNI portal (<https://giovanni.gsfc.nasa.gov/giovanni/>). Bathymetry data was obtained from GEBCO (<https://www.gebco.net/>).

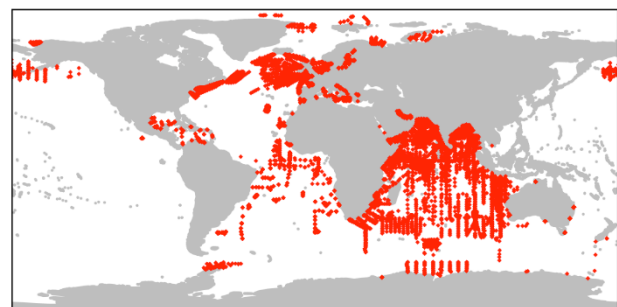
For each zooplankton group, recorded abundances from the same sample that were separated by species were summed to obtain the total group abundance for that sample (Figure 4.5). For copepods, a similar process was followed but only after the dataset was split into carnivorous and non-carnivorous (omnivorous) groups using diet information from the literature (Wickstead, 1961; Davis, 1984; Huys and Boxshall, 1991; Boxshall and Halsey, 2004; Rakhesh *et al.*, 2008). In total, we had thousands of aggregated samples for each zooplankton functional group - between 2,707 for salps (Figure 4.5 f) and 21,203 for omnivorous copepods (Figure 4.5 b).

For all groups, but especially for salps (Figure 4.5 f) and larvaceans (Figure 4.5 a), we did not have complete latitudinal coverage in our data, so we restricted our predictions to latitudes that contained 85% of the data (larvaceans: $\pm 38^\circ$, omnivorous copepods: $\pm 48^\circ$, carnivorous copepods: $\pm 43^\circ$, chaetognaths: $\pm 50^\circ$, euphausiids: $\pm 42^\circ$, salps: $\pm 38^\circ$, jellyfish: $\pm 40^\circ$).

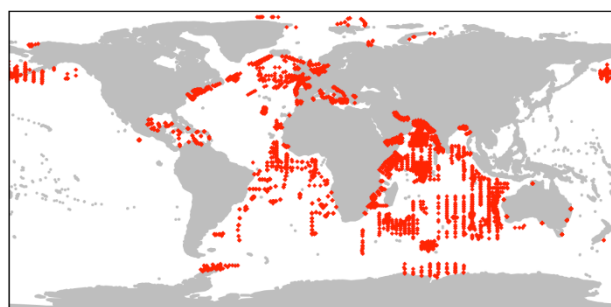
a) Larvaceans (n = 2735)



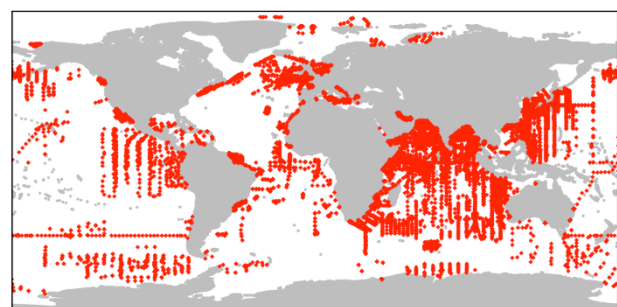
b) Omnivorous Copepods (n = 21203)



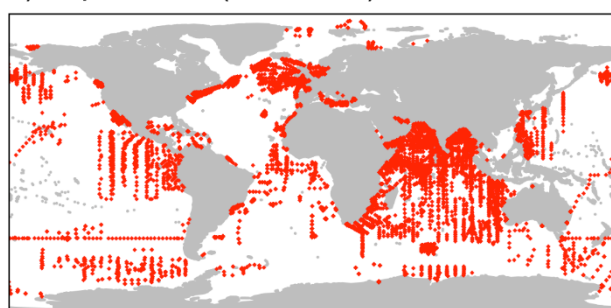
c) Carnivorous Copepods (n = 9695)



d) Chaetognaths (n = 19607)



e) Euphausiids (n = 16956)



f) Salps (n = 2707)



g) Jellyfish (n = 17293)

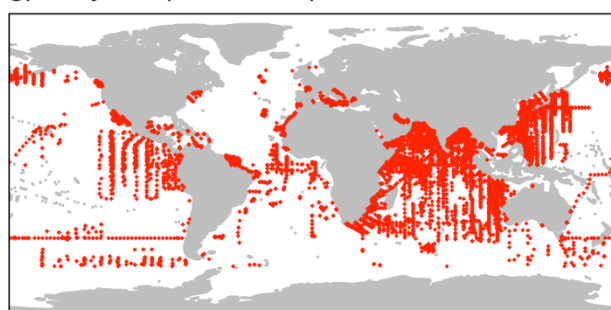


Figure 4.5 Data locations for a) Larvaceans, b) Omnivorous Copepods, c) Carnivorous Copepods, d) Chaetognaths, e) Euphausiids, f) Salps and g) Jellyfish. Number of datapoints after aggregating samples by functional group and sample given in parentheses.

4.3.4.2 Statistical modelling

We built seven GAMs, one for each of the zooplankton groups (excluding flagellates and ciliates), with the response variable being abundance. After viewing residual plots, we log-transformed the response for each zooplankton group (abundance) and chlorophyll *a* – to improve assumptions of homogeneity of variance and normality. We incorporated sample gear type and mesh size by treating unique combinations of these variables as discrete factor levels. Chlorophyll *a* and bathymetry (depth) were fitted using thin plate regression splines with five degrees of freedom.

The seasonal cycle of zooplankton changes with latitude, with greater seasonality toward the poles. However, as latitude and temperature is strongly correlated ($r = -0.92$, $p < 0.001$), we included a term to assess how the seasonal cycle changed with temperature rather than with latitude

To include this variable relationship between abundance and both temperature and day of year, we included a tensor smooth term with both predictors. This produces a surface of abundance in relation to temperature and day of year.

We checked our environmental variables for collinearity using Pearson's correlation coefficient (r). The maximum correlation was between $\log_{10}(\text{chlorophyll } a)$ and depth ($r = 0.5$; Supplementary Information Table S 4.1). This is below the threshold of $|r| = 0.7$ suggested by Dormann et al. (2013), above which collinearity between predictor variables can cause substantial distortions in model predictions. The best combination of the predictors for each zooplankton group was determined by the model which yielded the minimum Akaike Information Criterion and largest deviance explained (see Supplementary Table S 4.3 for details of variables combinations, AIC and deviance explained).

4.3.5 Numerical implementation

4.3.5.1 Boundary conditions for the theoretical model

For each zooplankton group, the abundance of the smallest size class at time t , $N_i(w_i, t)$, was fixed with respect to the total abundance of the other groups in that size class:

$$N_i(w_i, t) = P_i \sum_{j \neq i} N_j(w_i, t), \quad (\text{E2})$$

where P_i is the relative abundance of group i in size class w_i , with respect to the total abundance of the other groups. We used taxa-level abundance data sampled in the upper 200m ocean layer from the COPEPOD database (<https://www.st.nfms.noaa.gov/copepod>), to calibrate P so that the emergent composition of the model's zooplankton community above 100 μm ESD ($10^{-6.4}$ g wet weight) averaged across all grid squares, was approximately equal to the average observed composition from the COPEPOD samples. We used 100 μm ESD as a cut off because it was the smallest recorded mesh size used to obtain samples in the COPEPOD data, across all the zooplankton groups considered here.

COPEPOD did not have data for heterotrophic flagellates or ciliates. Therefore, for heterotrophic flagellates, we fixed the smallest size class abundance to be equal to abundance of the phytoplankton community in the same size class. For heterotrophic ciliates, the abundance of their smallest size class was fixed at half the abundance of heterotrophic flagellates in the same size class. The smallest size class abundance for the total fish community was fixed at the total zooplankton abundance in that size class, and divided equally among the three fish groups.

4.3.5.2 Running the theoretical model

Dynamics of the zooplankton and fish groups are modelled with separate second order McKendrick-von Foerster equations, which we solve numerically in the R program using a second order semi-implicit upwind finite difference scheme (see Appendix 1 for derivation; Press *et al.*, 2007). For numerical implementation we discretised the zooplankton and fish community size ranges into equal 0.1 \log_{10} size intervals. The model is initialised with the same zooplankton community, then integrated forward through time for 1000 years, with a half weekly time step. We chose these values to discretise the weight and time intervals to ensure convergence in our numerical implementation, in keeping with past studies (Blanchard *et al.*, 2009; Heneghan *et al.*, 2016).

After approximately 200 years of integration, abundances of the different zooplankton groups settle into their own oscillating cycles. Overall, these cycles repeat themselves, however under certain environmental conditions abundances of the different groups showed some small-scale variation through time. This small-scale variation was a result of the different zooplankton groups interacting through time, and was not caused by numerical instability (the small-scale variation did not change across multiple model runs with the same inputs). We found the characteristics of the model output were not significantly affected by

these variations after the first 400 years of the simulation. However, to ensure our results were not influenced by this variation, results were calculated by averaging over the last 500 years of the 1000 year simulation.

4.4 Results

4.4.1 Size-spectrum model predictions

4.4.1.1 Zooplankton biomass

Except for heterotrophic ciliates and larvaceans, the emergent biomass of the zooplankton functional groups predicted from the functional size-spectrum model all increased with chlorophyll a concentration (Figure 4.6, 4.7): more primary production means there is more food for all functional groups. Heterotrophic ciliates and larvacean biomass also increased with chlorophyll a up to around 0.5 mg m^{-3} (-0.3 on \log_{10} scale, Figure 4.6 b, c; 4.7 b, c), but declined as chlorophyll a increased passed this level. Heterotrophic ciliates and larvaceans prey on picoplankton ($< 2 \mu\text{m ESD}$), which makes up a large proportion of the phytoplankton community in the open ocean, but less than 20% in high chlorophyll coastal regions. This means that these groups have limited scope to balance increasing predation pressure from more abundant predators in these regions, compared to other zooplankton groups such as omnivorous copepods and euphausiids, which feed on the larger phytoplankton that dominate in coastal regions.

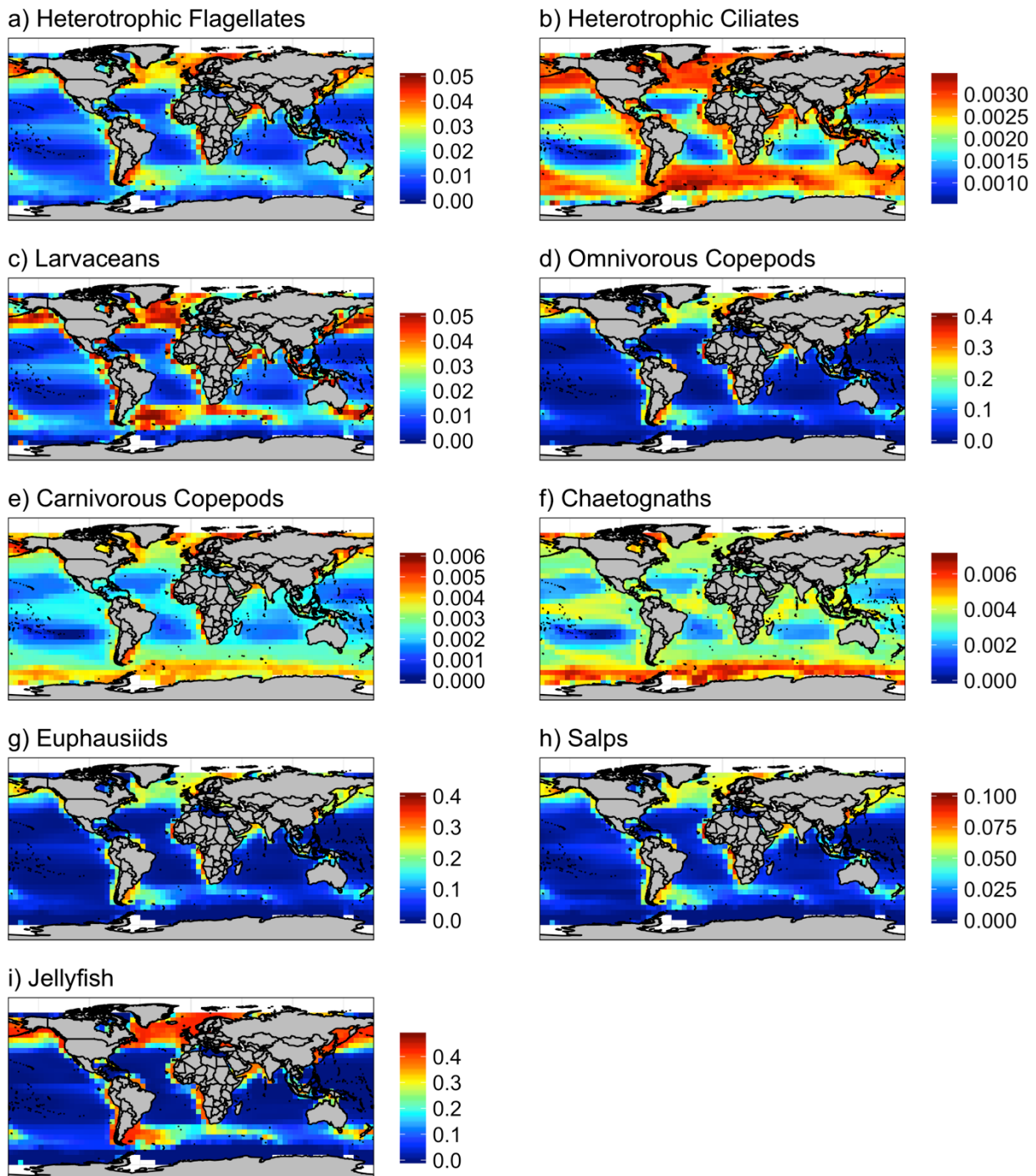


Figure 4.6 Annual average wet weight biomass from the size-spectrum model (g m^{-3}) for a) Heterotrophic Flagellates, b) Heterotrophic Flagellates, c) Larvaceans, d) Omnivorous Copepods, e) Carnivorous Copepods, f) Chaetognaths, g) Euphausiids, h) Salps and i) Jellyfish.

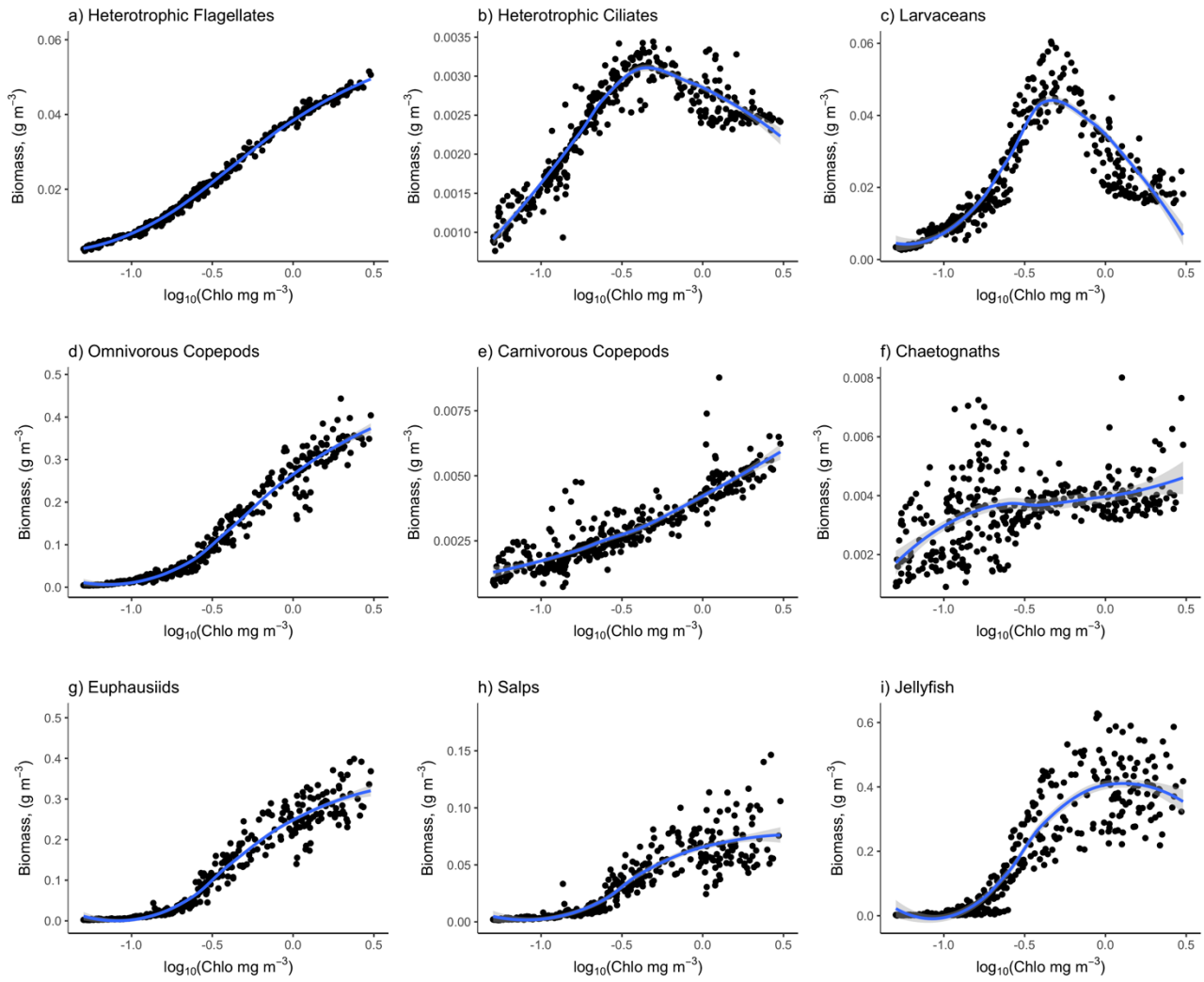


Figure 4.7 Plots of wet weight biomass g m^{-3} against chlorophyll a for a) Heterotrophic Flagellates, b) Heterotrophic Ciliates, c) Larvaceans, d) Omnivorous Copepods, e) Carnivorous Copepods, f) Chaetognaths, g) Euphausiids, h) Salps and i) Jellyfish.

4.4.1.2 Zooplankton community composition

Across the global ocean, the emergent composition of the zooplankton was not uniform (Figure 4.8, 4.9). The combined biomass of heterotrophic flagellates and ciliates was around 10% of the biomass of phytoplankton, from about 11% in the oligotrophic open ocean to 6% in eutrophic regions.

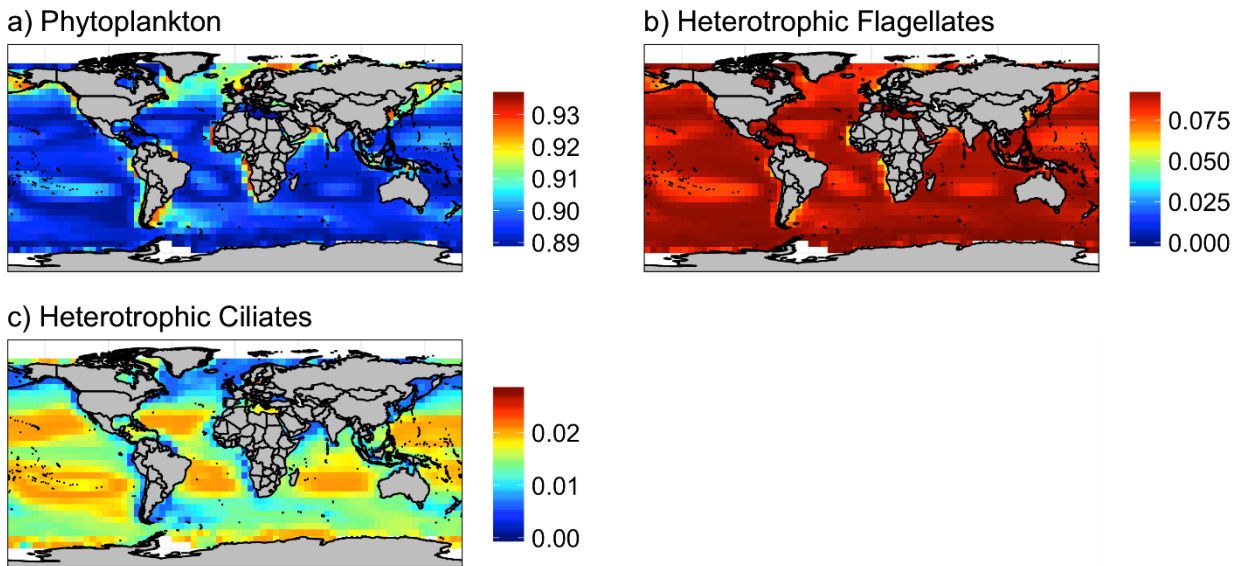


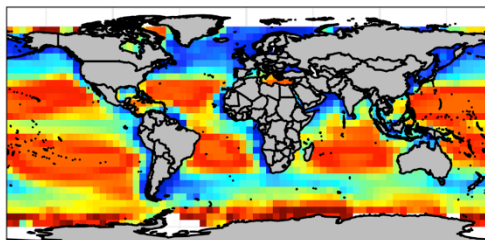
Figure 4.8 Relative biomass (wet weight composition) of the micro-plankton community, from the size-spectrum model. Proportion of total wet weight from a) Phytoplankton, b) Heterotrophic Flagellates, c) Heterotrophic Ciliates.

Omnivorous copepods were a prominent component of the macro zooplankton community (excluding flagellates and ciliates) across all regions, making up around 20-30% of the macro zooplankton biomass in the open ocean and coastal areas (Figure 4.9 b). Euphausiids increased with increasing phytoplankton biomass (chlorophyll a), comprising 15% of macro zooplankton biomass in the oligotrophic gyres, increasing to 30% in eutrophic regions (Figure 4.9 e). Jellyfish also increased with increasing primary production, comprising up to 45% of macro zooplankton wet weight biomass in eutrophic regions, declining to 10-20% in other areas (Figure 4.9 g).

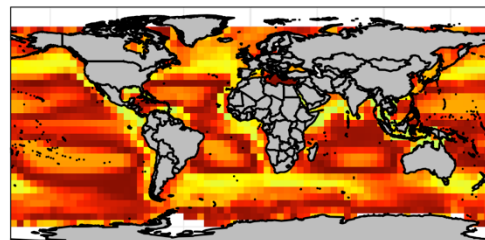
In contrast, larvaceans had an inverse relationship with primary production, making up 20% of macro zooplankton biomass in the oligotrophic gyres, declining to ~15% in other parts of the open ocean, then to <5% in coastal areas with the greatest phytoplankton biomass (Figure 4.9 a). Salps demonstrated a similar pattern over a smaller range: 13% in the oligotrophic gyres decreasing to 7% in other open ocean and coastal regions (Figure 4.9 f).

Carnivorous copepods and chaetognaths were most prominent in the oligotrophic gyres, respectively making up to 8% and 12% of the macro zooplankton biomass in those regions, declining to less than 1% in eutrophic coastal and upwelling regions (Figure 4.9 c, d).

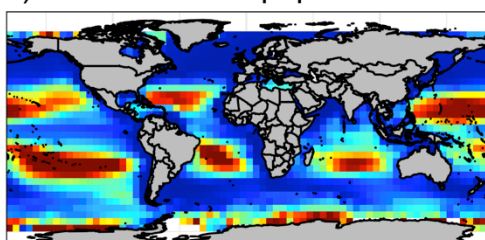
a) Larvaceans



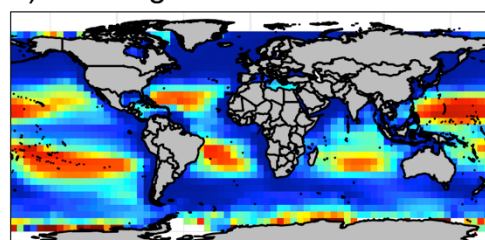
b) Omnivorous Copepods



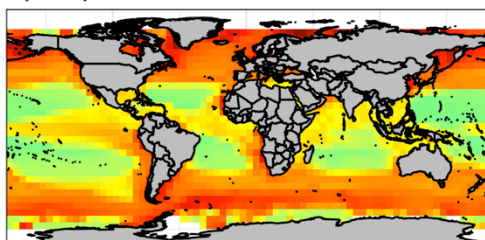
c) Carnivorous Copepods



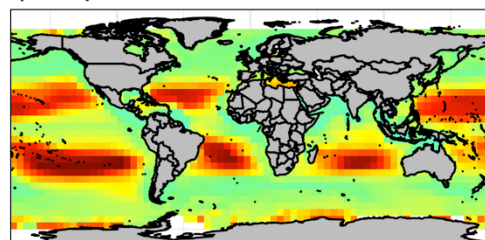
d) Chaetognaths



e) Euphausiids



f) Salps



g) Jellyfish

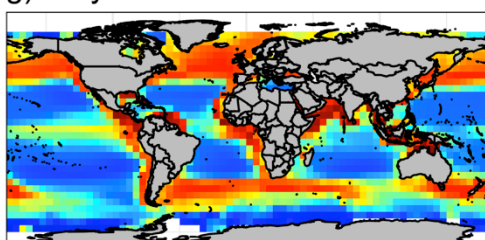


Figure 4.9 Relative biomass (wet weight composition) of the macro zooplankton community (excluding flagellates and ciliates), from the size-spectrum model. Proportion of total zooplankton wet weight (excluding flagellates and ciliates) from a) Larvaceans, b) Omnivorous Copepods, c) Carnivorous Copepods, d) Chaetognaths, e) Euphausiids, f) Salps and g) Jellyfish.

4.4.2 Size-spectrum model assessment

The final set of predictors used in the generalised additive models (GAMs) for the different zooplankton groups were the gear and mesh factor, the interaction term between sea surface temperature (SST) and day of the year, depth and $\log_{10}(\text{chlorophyll a})$ (Supplementary Information Table S 4.2). The models explained between 35.4% (salps) to 60.9% (omnivorous copepods) of the deviance, with a median value of 46.1%. Model skill tests for each group are in Supplementary Information Table S 4.3, and plots of the model terms are in Supplementary Information Figures S 4.2 - S 4.8.

Except for carnivorous copepods, the emergent zooplankton distributions from the functional size-spectrum model broadly agreed with the empirical distributions. For all zooplankton groups, except for carnivorous copepods, the annual average empirical abundances from the GAMs (Figure 4.10 a, d, j, m, p, s) showed a positive relationship between chlorophyll a concentration and abundance, with the highest abundances for all groups found in eutrophic regions (maps of annual average chlorophyll a and sea surface temperature in Supplementary Information Figure S 4.1). Carnivorous copepods, chaetognaths and salps had a noticeable relationship with temperature, with some of their empirical highest abundances found along the equator (Figure 4.10 g, m, p). The empirical abundance of carnivorous copepods seemed to be driven primarily by temperature, with the highest empirical abundances in water about 20°C (Figure 4.10 g). From the size-spectrum model, all zooplankton groups showed increasing abundance with increasing chlorophyll a concentration (Figure 4.10 b, e, h, k, n, q, t). For all groups, the lowest abundances were in the oligotrophic gyres and the highest in eutrophic regions. In other words, increasing phytoplankton biomass leads to an increase in abundance for all groups, irrespective of their feeding characteristics.

Excluding carnivorous copepods, correlations between the model and the GAM distributions ranged from 0.41 for chaetognaths to 0.89 for euphausiids (Figure 4.10 c, f, l, o, r, u). Carnivorous copepods had a weak, negative correlation of $r = -0.24$ between empirical and theoretical abundances (Figure 4.10 i). The poor correlation for carnivorous copepods can be explained by the different relationships between temperature and abundance in the empirical and size-spectrum model. Empirical abundances for carnivorous copepods are primarily driven by temperature, with chlorophyll a (phytoplankton biomass) serving at best as a secondary driver (Supplementary Figure S 4.4). In contrast, the size-spectrum model does show some of the highest carnivorous copepods abundances in eutrophic high temperature regions around the equator, however chlorophyll a concentration

(phytoplankton biomass) is still the main driver of abundance for this group. However, the absolute abundance of carnivorous copepods changed the least of all groups from oligotrophic to eutrophic waters in the theoretical model – increasing by only 3-fold (half an order of magnitude), compared to at least 10-fold (1 order of magnitude) for the other groups.

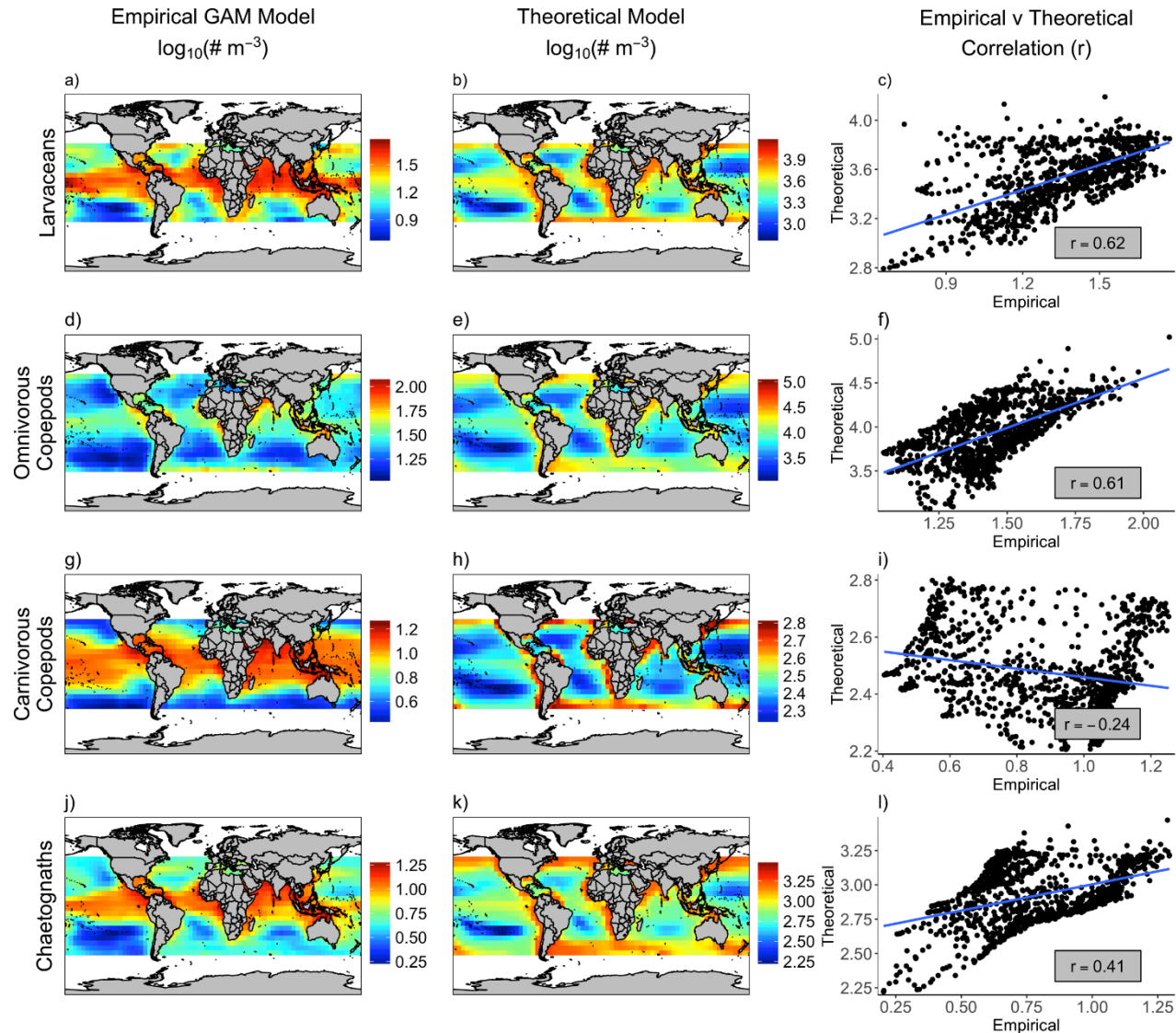


Figure 4.10 Assessing emergent abundance distributions from the size-spectrum model. The empirical abundance distributions from the generalised additive models (GAMs) (left column, $\log_{10}(\# \text{ m}^{-3})$), the emergent zooplankton distributions from the size-spectrum model (centre column, $\log_{10}(\# \text{ m}^{-3})$, and Pearson's correlation plots between the two a) Larvaceans, b) Omnivorous Copepods, c) Carnivorous Copepods and d) Chaetognaths.

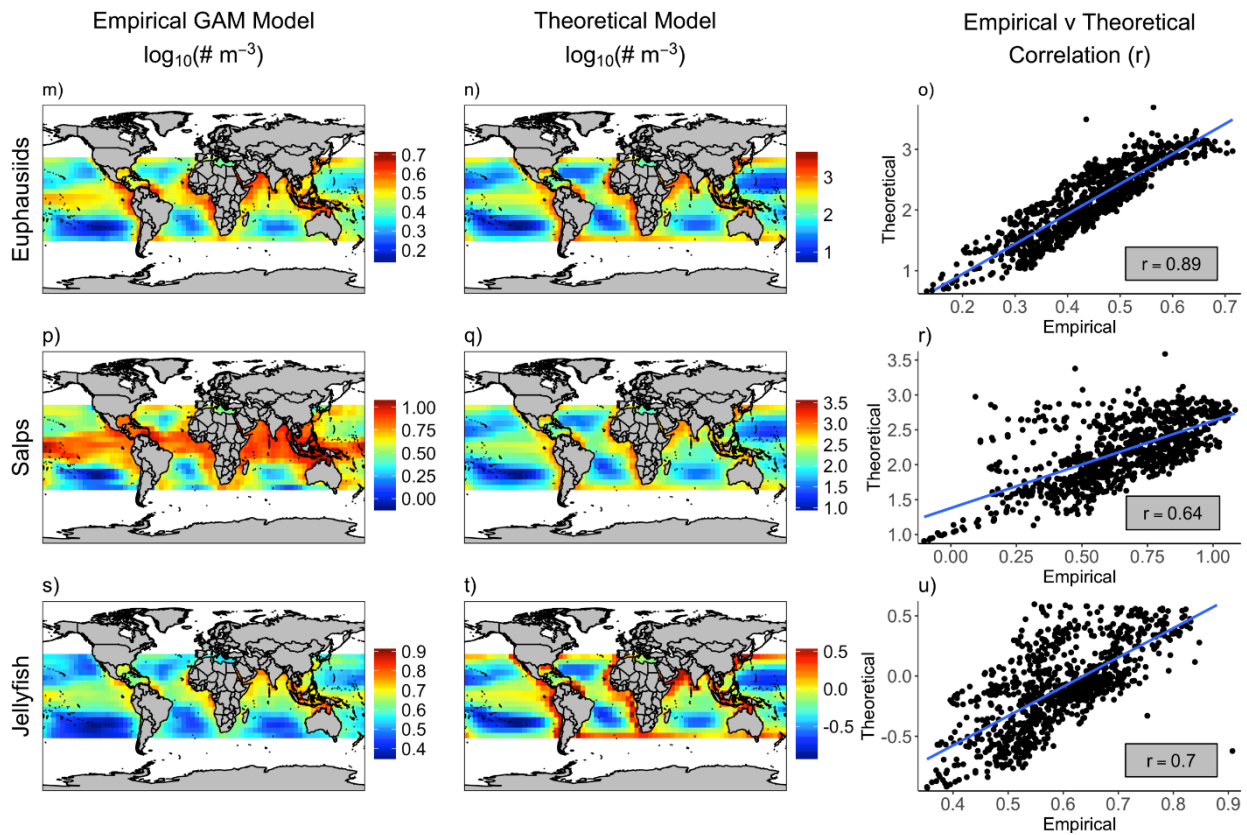


Figure 4.10 (continued) Assessing emergent abundance distributions from the size-spectrum model. The empirical abundance distributions from the generalised additive models (GAMs) (left column, $\log_{10}(\# \text{ m}^{-3})$), the emergent zooplankton distributions from the size spectrum model (centre column, $\log_{10}(\# \text{ m}^{-3})$), and Pearson's correlation plots between the two a) Euphausiids, b) Salps, c) Jellyfish.

4.5 Discussion

The challenge of resolving the zooplankton in ecosystem models lies in their diversity of species, life histories and ecological strategies (Litchman *et al.*, 2013). A significant advantage of the trait-based approach is that community structure can emerge based on the functional traits of the community, and environmental conditions. Our results demonstrate the importance of functional traits to explain global patterns in zooplankton community composition. With only the body size ranges, size-based feeding traits and carbon content of nine zooplankton functional groups, it was possible to resolve emergent changes in the zooplankton community across the global ocean that agreed well with observation and theory. This is an important result; resolving the mechanisms that give rise to the zooplankton community across environmental gradients is critical to better understanding overall ecosystem function, particularly the resilience and productivity of higher trophic levels across environmental gradients (Mitra *et al.*, 2010, 2014; Irigoein *et al.*, 2014; Jennings and Collingridge, 2015; Steinberg and Landry, 2017).

As we hypothesised in the introduction, the composition of the zooplankton was primarily driven by the size structure of their prey. The phytoplankton community is mostly picoplankton ($< 2 \mu\text{m}$ ESD) in the oligotrophic open ocean (Figure 4.3 a). In response, heterotrophic flagellates and ciliates were most prevalent in oligotrophic waters. Similarly, carnivorous copepods and chaetognaths – both carnivorous groups – were most prominent in oligotrophic regions. Their prevalence in low chlorophyll a regions agrees with the hypothesis that stable, oligotrophic environments favour longer food chains with a smaller average PPMR (Lalli and Parsons, 1995; Sommer *et al.*, 2002; Jennings and Warr, 2003). Eutrophic regions are hypothesised to favour short food chains, where large phytoplankton are consumed directly by crustaceans such as copepods and euphausiids, who are then consumed by planktivorous fish. We found that euphausiids – the largest omnivorous crustacean group – were most dominant in eutrophic waters, which agrees with the hypothesis of short food chains in eutrophic waters, however omnivorous copepods were ubiquitous across the global ocean. Kiørboe (2010) hypothesised that the success of pelagic copepods could be accounted for by their body shape, feeding style and their ability to find mating partners, our model indicates the success of omnivorous copepods could also be partly explained by their body size and PPMR: over their size range, omnivorous copepods have an ideal prey size of $4 \mu\text{m}$ to $22 \mu\text{m}$ ($10^{-10.1} - 10^{-8.1} \text{ g}$), which covers the size range of the nanoplankton ($2 \mu\text{m} - 20 \mu\text{m}$). The nanoplankton are a significant proportion of the phytoplankton community across the global ocean (Figure 4.3 b) and do not vary as much

as pico or micro-plankton. This means that omnivorous copepods face less variation in the relative quantity of their prey, compared to other zooplankton groups.

Jellyfish, which do not feed on phytoplankton, also increased in eutrophic coastal and open ocean regions (Figure 4.9 g). This is similar to the patterns in gelatinous zooplankton biomass found by Lucas *et al.*, (2014) and Schnedler-Meyer *et al.*, (2016). Owing to their low carbon content, jellyfish are usually considered to represent a “trophic dead-end”, in contrast to planktivorous fish which are an important prey source for higher trophic levels (Robinson *et al.*, 2014). Jellyfish and planktivorous fish share similar body size and prey size ranges (Figure 4.4), our model could be used to explore the trophic interplay between jellyfish and planktivorous fish, and how they compete across oligotrophic and eutrophic waters. There is evidence that human-induced stresses such as eutrophication promote increases jellyfish blooms, although whether increases in jellyfish are driven by human pressures or are part of a larger natural cycle is still strongly debated (Richardson *et al.*, 2009; Condon *et al.*, 2013; Gibbons and Richardson, 2013; Lucas *et al.*, 2014). Our model could be used to explore whether increasing fishing pressure across oligotrophic and eutrophic waters leads to a more jellyfish-dominated ecosystem.

The presence of salps and larvaceans in low chlorophyll *a* areas challenges the idea that average PPMR decreases and the trophic level of larger organisms increases with decreasing primary productivity. Larvaceans and salps have the largest PPMRs of the zooplankton functional groups, as a result, these two groups were most prevalent in oligotrophic waters. What is more, their large body sizes mean that they fall within the prey size range for planktivorous fish (< 100 gm; Figure 4.4). The “larvacean shunt” has been hypothesised as an energy pathway from the dominant pico-phytoplankton in oligotrophic waters, to planktivorous fish (Diebel and Lee, 1992; Bone, 1997). Our results here support this hypothesis; the prevalence of larvaceans – and salps – in oligotrophic waters, coupled with their large body sizes, indicates that they would be an important food source for planktivorous fish in these waters, and so represent a direct pathway from picoplankton to higher trophic levels.

Our theoretical model was able to capture broad-scale empirical patterns of abundance for six of the seven largest zooplankton groups. Chlorophyll *a* concentration – a measure of primary production – was the primary driver of abundance in the theoretical model. More primary production means more food for omnivores, which, in turn, means more food for carnivores. However, the relationship between chlorophyll *a* and abundance and biomass

varied across the zooplankton groups in the theoretical model, which is what gave rise to the changing composition of the zooplankton community. Simpler models have also captured this relationship between primary production and consumer abundance (e.g., Jennings *et al.*, 2008; Strömberg *et al.*, 2009; Ward *et al.*, 2012) however ours is the first to capture changes in the composition of the zooplankton with increasing primary production.

The poor correlation between the modelled and empirical abundance of carnivorous copepods (Figure 4.10 i) probably highlights the necessarily crude way we incorporated temperature effects in the theoretical model. The empirical abundance distribution of carnivorous copepods was related more to sea surface temperature, over chlorophyll a (in contrast with all our other statistical models), and our model has only a rudimentary implementation of temperature dependence that is the same for all zooplankton groups (Figure 4.10 g-i). We used the same temperature effect for all groups because the zooplankton and fish in our model are resolved by feeding traits at the functional group level, and it is unclear how temperature will affect organisms at this level. There is information available on temperature scaling for copepods as a group (Hansen *et al.*, 1997; Forster *et al.*, 2011; Kiørboe and Hirst, 2014) or by species (e.g., Lee *et al.*, 2003; Holste and Peck, 2006; Rhyne *et al.*, 2009), but to our knowledge there are no studies that evaluate temperature effects by omnivorous and carnivorous groups.

The deviance explained for the fitted GAMs varied from 35.4% for salps, to 60.9% for omnivorous copepods, which is within the range reported by other studies that use statistical models to link environmental variables with sample data (Drexler *et al.*, 2013; Lucas *et al.*, 2014; Brun *et al.*, 2016). The theoretical model uses sea surface temperature and chlorophyll a concentration as environmental inputs, so we only used those environmental variables (and depth) when fitting the GAMs. However, other environmental variables such as euphotic depth and dissolved oxygen have been linked with the distribution of zooplankton (Lucas *et al.*, 2014). Looking forward, incorporating other variables could increase the predictive power of the statistical models developed here, and allow more accurate predictions of the distribution of different zooplankton functional groups across the global ocean.

By using satellite sea surface temperature and chlorophyll a concentration as environmental inputs, our model represents the sunlit surface waters of the global ocean (0-200m), but does not resolve the vertical distribution of the zooplankton and fish. Diel vertical migration (DVM) of macro zooplankton (>0.2 mm ESD) and nekton to epipelagic waters (> 200 m

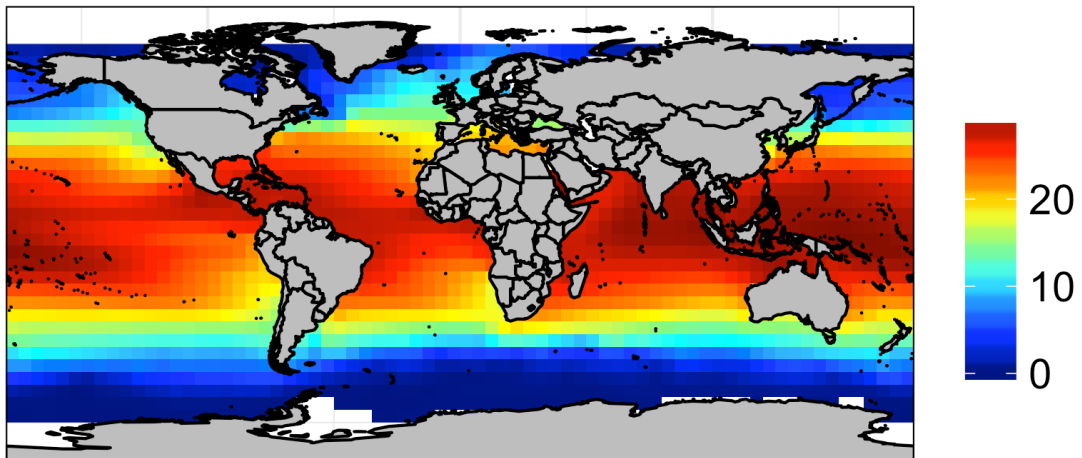
depth) during the night and deeper waters during the day is ubiquitous across practically every taxonomic group in all the world's oceans (Hays, 2003; Bianchi *et al.*, 2013). The central cue for the length of time away from the surface waters is believed to be day length, with migrating individuals staying away from surface waters for longer in areas with longer days (Haren and Compton, 2013) to minimise predation risk. However, similar to temperature effects, we did not resolve DVM in the model because the patterns of movement in and out of the surface waters vary considerably between and within species (Richards *et al.*, 1996), and it is difficult to do more than guess the proportion of time individuals in different functional groups and body sizes that would stay away from surface waters and out of the spatial domain of the model.

Future work could address these issues by allowing the community structure across depth and environmental gradients to emerge based on randomly assigned physiological traits, following the example of Follows *et al.*, (2007), who developed this approach for phytoplankton. For example, temperature response, extent of DVM and feeding traits such as PPMR could be represented as a continuum, where different combinations are randomly assigned and community structure emerges from the functional size-spectrum model.

The theoretical model we developed here demonstrates the importance of body size, size-based feeding behaviour and carbon content to explain global patterns in the abundance and composition of the zooplankton community. Our results demonstrate that the composition of the zooplankton is not static across environmental gradients, and resolving this diversity is possible with functional traits. Looking forward, our model could be used to investigate how changes in the zooplankton community affects the global carbon cycle (Steinberg and Landry, 2017), and energy pathways from phytoplankton to fish across oligotrophic and eutrophic waters.

4.6 Supplementary Information

a) Sea Surface Temperature



a) $\log_{10}(\text{Chlorophyll mg m}^{-3})$

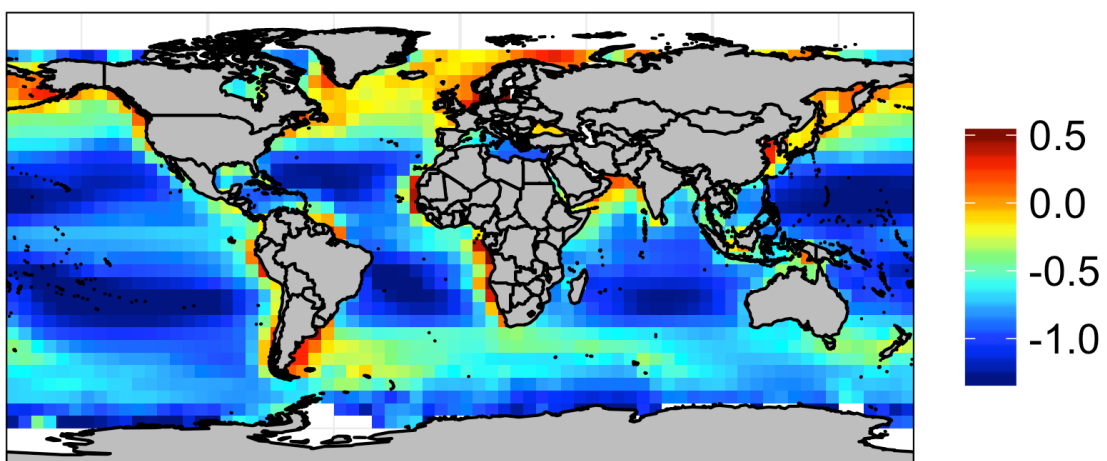


Figure S 4.1 Annual average a) sea surface temperature (SST) and b) $\log_{10}(\text{Chlorophyll a mg m}^{-3})$, aggregated to 5 degree latitude by 5 degree longitude grid squares. These fields are used as environmental inputs to drive the size-spectrum model. For both SST and $\log_{10}(\text{Chlorophyll a mg m}^{-3})$, we obtained the annual average for each grid square by averaging over the monthly climatologies obtained from MODIS-Aqua, standardised for the number of months in which satellite observations were taken.

4.6.1 Empirical abundance distributions (GAMs)

The abundances of all zooplankton groups increased with chlorophyll *a* (Figures S 4.2-S 4.8, subplot b). However, the abundances of larvaceans, euphausiids and salps decline slightly at very high chlorophyll *a* levels (Figures S 4.2, S 4.6, S 4.7, subplot b). For all groups, the relationship between abundance and depth was the weakest of all the environmental predictors and was not constant across the groups: larvaceans increased with increasing depth (Figure S 4.2, c), whilst omnivorous copepods, chaetognaths, salps and jellyfish decreased (Figures S 4.3, S 4.5, S 4.7, S 4.8, subplot c). Euphausiids increased with increasing depth to 1000 – 2000 metres, before declining (Figure S 4.6, subplot c) and the highest abundances of carnivorous copepods was around 3000m (Figure S 4.4 subplot c). The weak relationship could be due to the collinearity between chlorophyll *a* concentration and depth ($r = 0.5$; Table S 4.1).

The greatest seasonal effect for the abundances of all zooplankton groups was in low temperature waters (Figures S 4.2-S 4.8, subplot a), however the relationship was not the same across the groups. Omnivorous copepods, carnivorous copepods, chaetognaths and euphausiids had peaks in their abundance in low temperature waters in the middle of the year (northern hemisphere summer). In contrast, larvaceans, salps and jellyfish had the opposite relationship, with the highest abundances in low temperature waters occurring outside of the northern hemisphere summer. Across the year, the highest abundances for omnivorous copepods and euphausiids were predicted to be in low temperature water. In contrast, the average abundances across the year increased with increasing temperature for larvaceans, carnivorous copepods, salps and jellyfish.

Table S 4.1 Pearson correlation coefficient between environmental predictor variables used for empirical abundance GAMs of larvaceans, omnivorous copepods, carnivorous copepods, chaetognaths, salps, krill and jellyfish.

	SST	$\log_{10}(\text{Chlorophyll } a)$	Depth	Day of year
SST	1	-0.216	-0.068	0.044
$\log_{10}(\text{Chlorophyll } a)$	-0.216	1	-0.5	0.01
Depth	-0.068	-0.5	1	-0.08
Day of year	0.044	0.01	-0.08	1

Table S 4.2 Summary of final GAMs for the seven zooplankton functional groups, with Akaike information criterion (AIC) and deviance explained.

Response $\log_{10}(\# \text{ m}^{-3} + 1)$	Predictors	AIC	Deviance Explained (%)
Larvaceans	GM + f(SST, day of year) + Depth + $\log_{10}(\text{chlo})$	4374	39.3 %
Omnivorous Copepods	GM + f(SST, day of year) + Depth + $\log_{10}(\text{chlo})$	50316	60.9 %
Carnivorous Copepods	GM + f(SST, day of year) + Depth + $\log_{10}(\text{chlo})$	15378	56.8 %
Chaetognaths	GM + f(SST, day of year) + Depth + $\log_{10}(\text{chlo})$	18252	46.1 %
Euphausiids	GM + f(SST, day of year) + Depth + $\log_{10}(\text{chlo})$	27484	50 %
Salps	GM + f(SST, day of year) + Depth + $\log_{10}(\text{chlo})$	3989	35.4 %
Jellyfish	GM + f(SST, day of year) + Depth + $\log_{10}(\text{chlo})$	14881	41.7 %

Table S 4.3 Skill of empirical GAMs with different predictor combinations. Model skill given in terms of Akaike Information Criterion (AIC) and deviance explained. Best models for each group are highlighted in yellow.

Response $\log_{10}(\# \text{ m}^{-3} + 1)$	Predictors	AIC	Deviance Explained
Larvaceans	-	5625	0 %
	Gear-Mesh factor (GM)	5093	19.4 %
	f(SST, day of year)	4820	26.8 %
	$\log_{10}(\text{chlo})$	5421	7.7 %
	Depth	5555	2.9 %
	GM + f(SST, day of year)	4496	36.1 %
	GM + Depth	4817	27.1 %
	GM + $\log_{10}(\text{chlo})$	4736	29.3 %
	GM + f(SST, day of year) + Depth	4484	36.6 %
	GM + f(SST, day of year) + $\log_{10}(\text{chlo})$	4400	38.5 %
	GM + f(SST, day of year) + Depth + $\log_{10}(\text{chlo})$	4374	39.3 %
Omnivorous Copepods	-	71995	0 %
	Gear-Mesh factor (GM)	67931	17.5 %
	f(SST, day of year)	56996	50.8 %
	$\log_{10}(\text{chlo})$	64290	22.2 %
	Depth	67593	18.7 %
	GM + f(SST, day of year)	55206	54.9 %
	GM + Depth	56181	52.7 %
	GM + $\log_{10}(\text{chlo})$	53176	55.1 %
	GM + f(SST, day of year) + Depth	53924	57.6 %
	GM + f(SST, day of year) + $\log_{10}(\text{chlo})$	50712	60.3 %
	GM + f(SST, day of year) + Depth + $\log_{10}(\text{chlo})$	50316	60.9 %

Carnivorous Copepods	-	23879	0 %
	Gear-Mesh factor (GM)	22722	11.5 %
	f(SST, day of year)	18900	40.5 %
	$\log_{10}(\text{chlo})$	23191	0.05 %
	Depth	23498	4 %
	GM + f(SST, day of year)	16129	55.4 %
	GM + Depth	18770	41.3 %
	GM + $\log_{10}(\text{chlo})$	18260	41.2 %
	GM + f(SST, day of year) + Depth	16015	56 %
	GM + f(SST, day of year) + $\log_{10}(\text{chlo})$	15489	56.3 %
	GM + f(SST, day of year) + Depth + $\log_{10}(\text{chlo})$	15378	56.8 %
Chaetognaths	-	31172	0 %
	Gear-Mesh factor (GM)	29382	8.9 %
	f(SST, day of year)	22932	34.8 %
	$\log_{10}(\text{chlo})$	29272	2.4 %
	Depth	30764	2.1 %
	GM + f(SST, day of year)	20768	41.8 %
	GM + Depth	22135	37.5 %
	GM + $\log_{10}(\text{chlo})$	21353	36.2 %
	GM + f(SST, day of year) + Depth	20070	43.8 %
	GM + f(SST, day of year) + $\log_{10}(\text{chlo})$	18335	45.8 %
	GM + f(SST, day of year) + Depth + $\log_{10}(\text{chlo})$	18252	46.1 %
Euphausiids	-	39644	0 %
	Gear-Mesh factor (GM)	38546	7 %
	f(SST, day of year)	30301	42.9 %
	$\log_{10}(\text{chlo})$	36450	12.2 %
	Depth	38054	9 %
	GM + f(SST, day of year)	29399	46 %
	GM + Depth	30006	43.9 %
	GM + $\log_{10}(\text{chlo})$	28649	46 %
	GM + f(SST, day of year) + Depth	28979	47.3 %
	GM + f(SST, day of year) + $\log_{10}(\text{chlo})$	27620	49.4 %
	GM + f(SST, day of year) + Depth + $\log_{10}(\text{chlo})$	27484	50 %
Salps	-	5062	0 %
	Gear-Mesh factor (GM)	4483	21 %
	f(SST, day of year)	4513	19.6 %
	$\log_{10}(\text{chlo})$	4964	4 %
	Depth	5046	1 %
	GM + f(SST, day of year)	4096	32.4 %
	GM + Depth	4511	20 %
	GM + $\log_{10}(\text{chlo})$	4423	22.6 %
	GM + f(SST, day of year) + Depth	4069	33.3 %

Salps (continued)	GM + f(SST, day of year) + $\log_{10}(\text{chlo})$	3991	35.2 %
	GM + f(SST, day of year) + Depth + $\log_{10}(\text{chlo})$	3989	35.4 %
Jellyfish	-	24104	0 %
	Gear-Mesh factor (GM)	23546	3.4 %
	f(SST, day of year)	16101	37.3 %
	$\log_{10}(\text{chlo})$	23602	2.3 %
	Depth	23430	3.9 %
	GM + f(SST, day of year)	15461	39.8 %
	GM + Depth	15880	38.2 %
	GM + $\log_{10}(\text{chlo})$	15760	38.5 %
	GM + f(SST, day of year) + Depth	15229	40.6 %
	GM + f(SST, day of year) + $\log_{10}(\text{chlo})$	14884	41.7 %
	GM + f(SST, day of year) + Depth + $\log_{10}(\text{chlo})$	14881	41.7 %

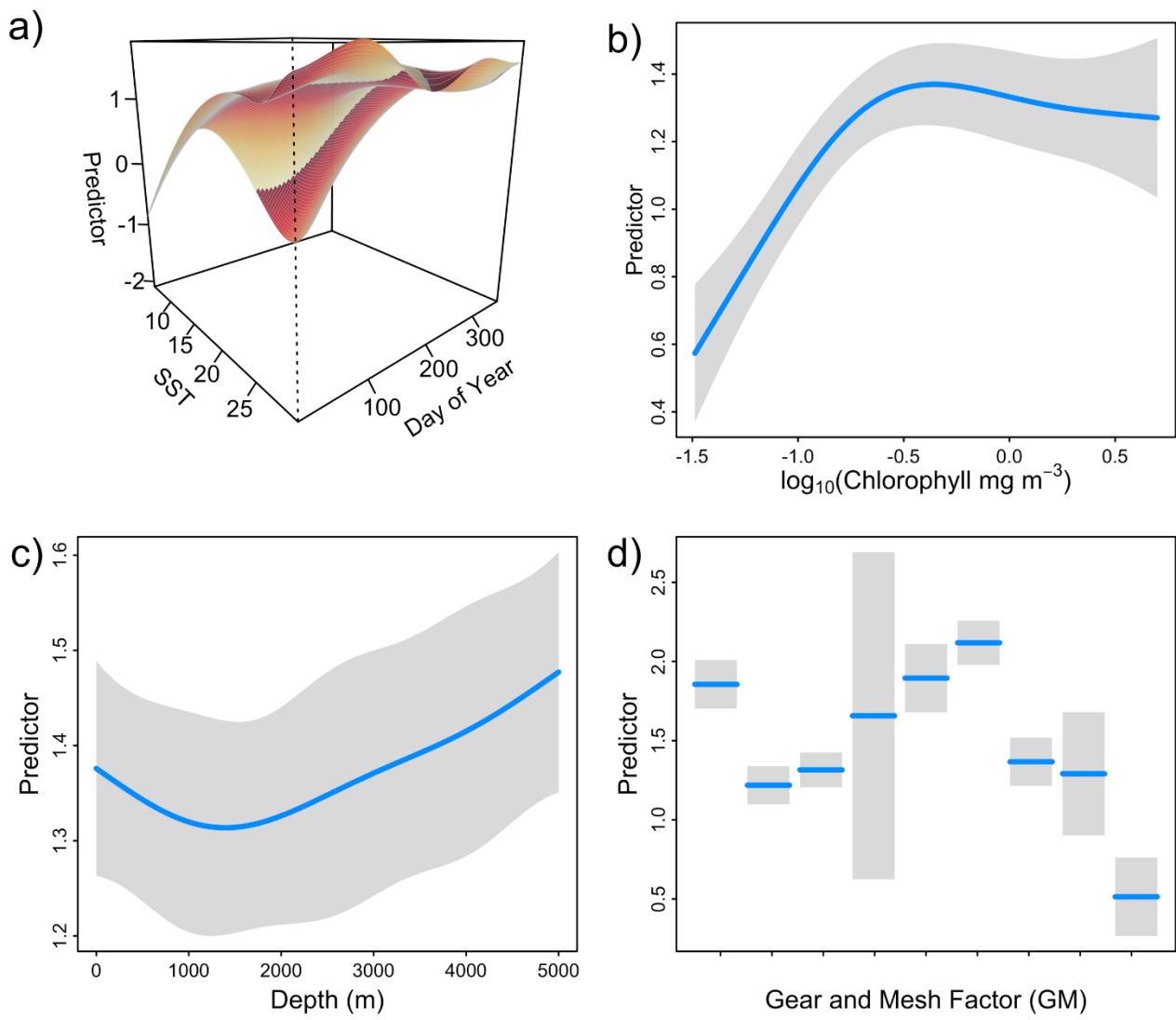


Figure S 4.2 Best model fit for larvaceans: a) Fitted interaction surface between sea surface temperature (SST) and day of year, standardised to the northern hemisphere, and partial residuals from the main effect of b) $\log_{10}(\text{Chlorophyll } a)$, c) Depth and d) the Gear and Mesh factor levels. For b, c and d) the main effect for each predictor is given by the blue line, with the 95% confidence intervals given by the shaded areas.

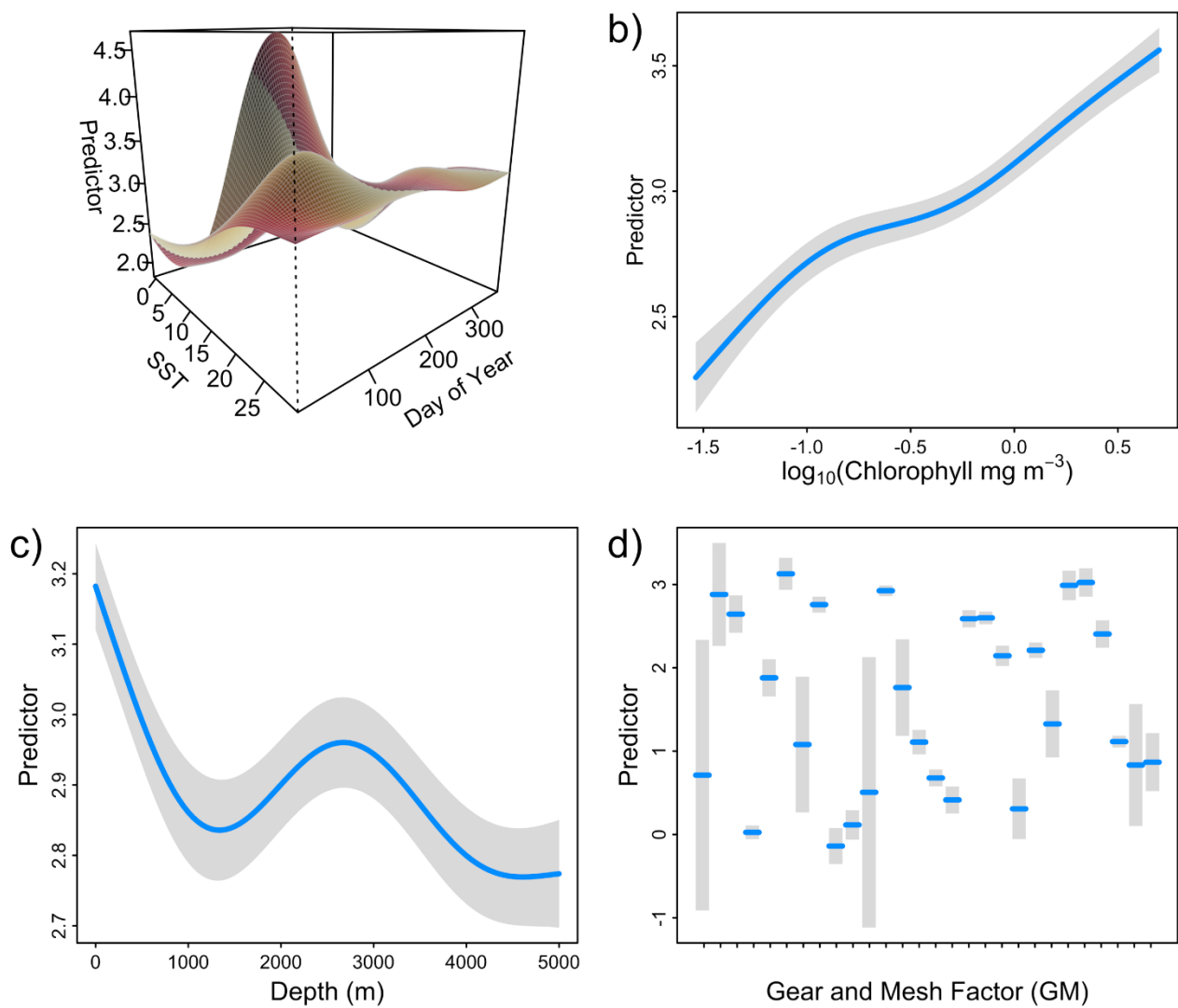


Figure S 4.3 Best model fit for omnivorous copepods: a) Fitted interaction surface between sea surface temperature (SST) and day of year, standardised to the northern hemisphere, and partial residuals from the main effect of b) $\log_{10}(\text{Chlorophyll } a)$, c) Depth and d) the Gear and Mesh factor levels. For b, c and d) the main effect for each predictor is given by the blue line, with the 95% confidence intervals given by the shaded areas.

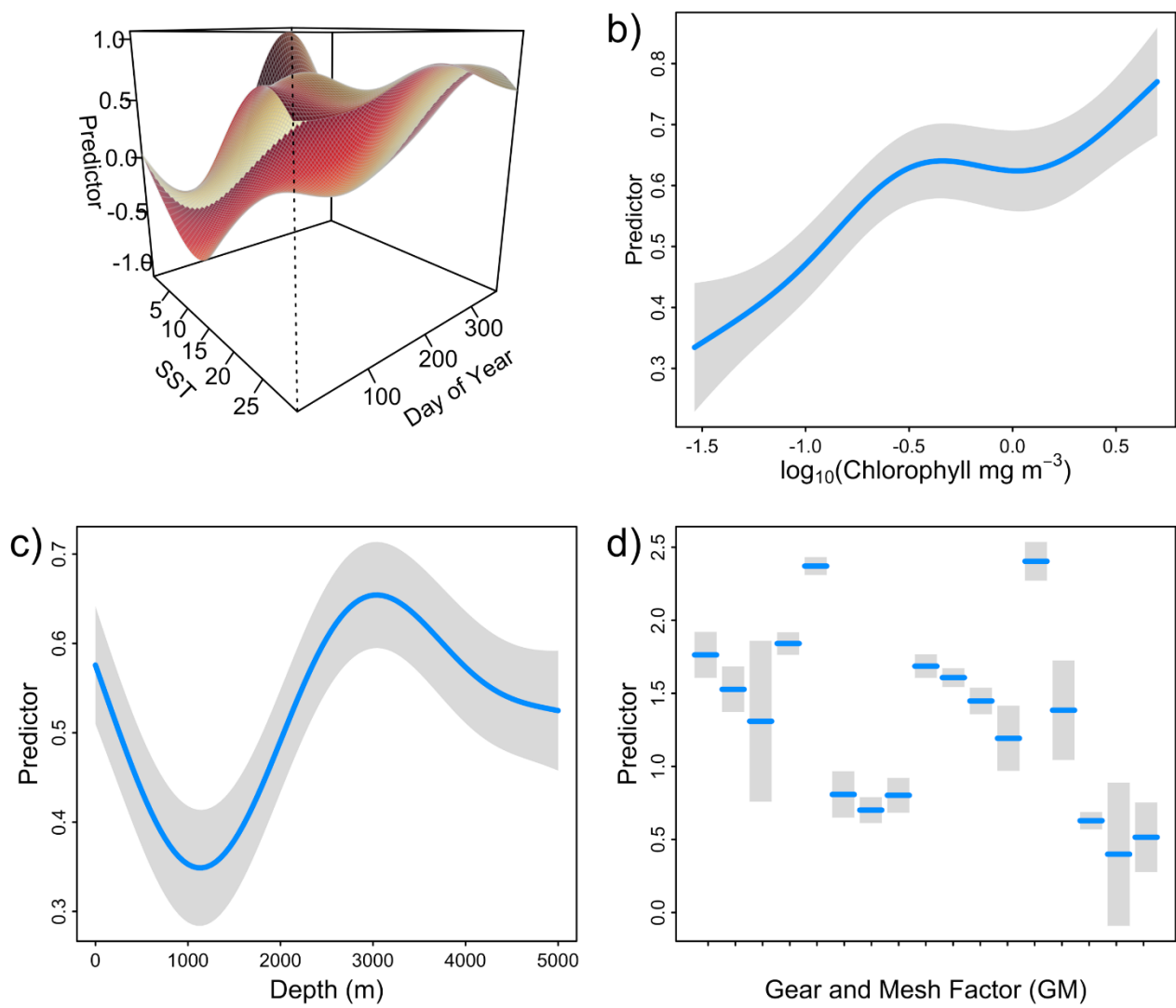


Figure S 4.4 Best model fit for carnivorous copepods: a) Fitted interaction surface between sea surface temperature (SST) and day of year, standardised to the northern hemisphere, and partial residuals from the main effect of b) $\log_{10}(\text{Chlorophyll } \text{a})$, c) Depth and d) the Gear and Mesh factor levels. For b, c and d) the main effect for each predictor is given by the blue line, with the 95% confidence intervals given by the shaded areas.

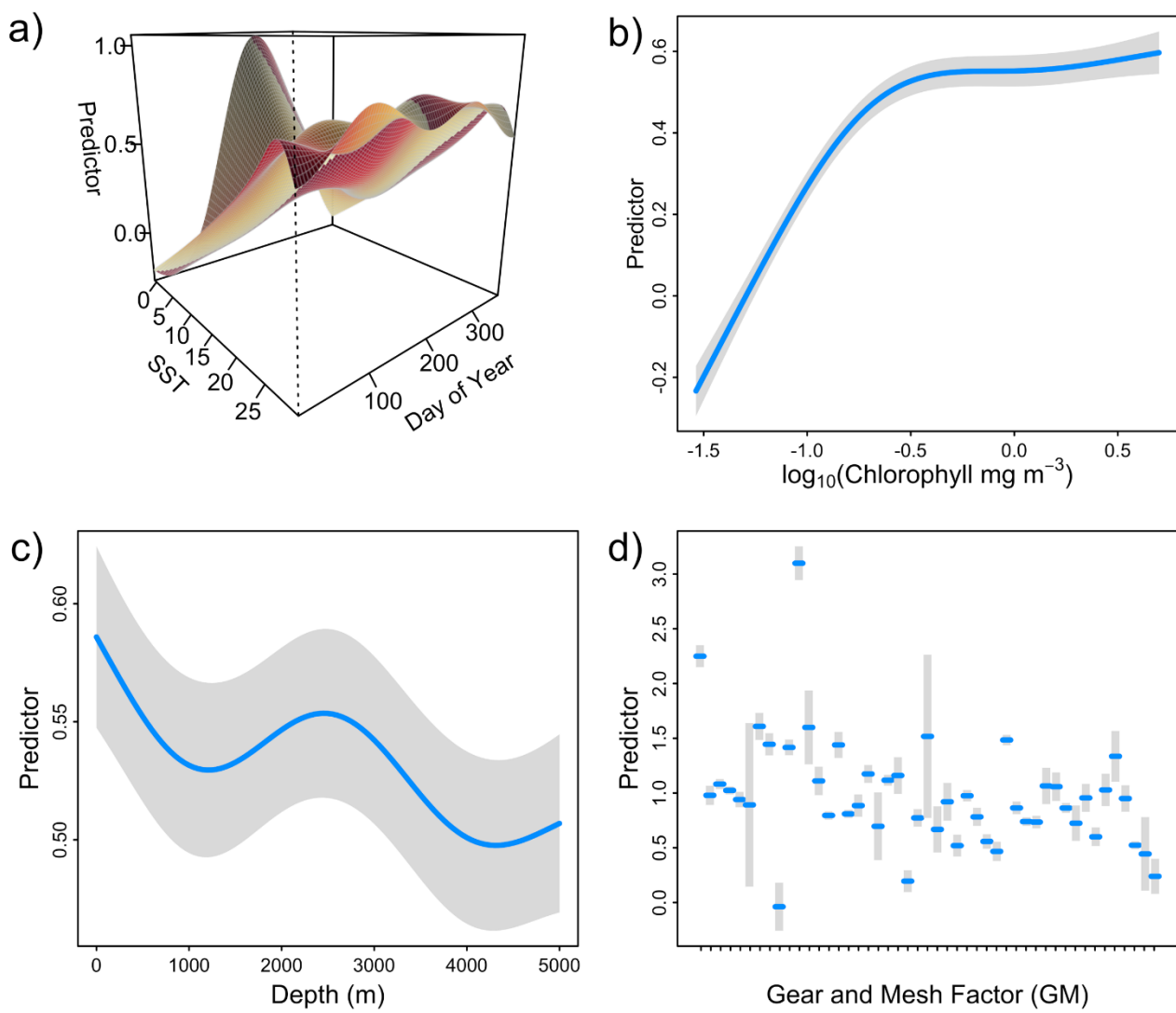


Figure S 4.5 Best model fit for chaetognaths: a) Fitted interaction surface between sea surface temperature (SST) and day of year, standardised to the northern hemisphere, and partial residuals from the main effect of b) $\log_{10}(\text{Chlorophyll a})$, c) Depth and d) the Gear and Mesh factor levels. For b, c and d) the main effect for each predictor is given by the blue line, with the 95% confidence intervals given by the shaded areas.

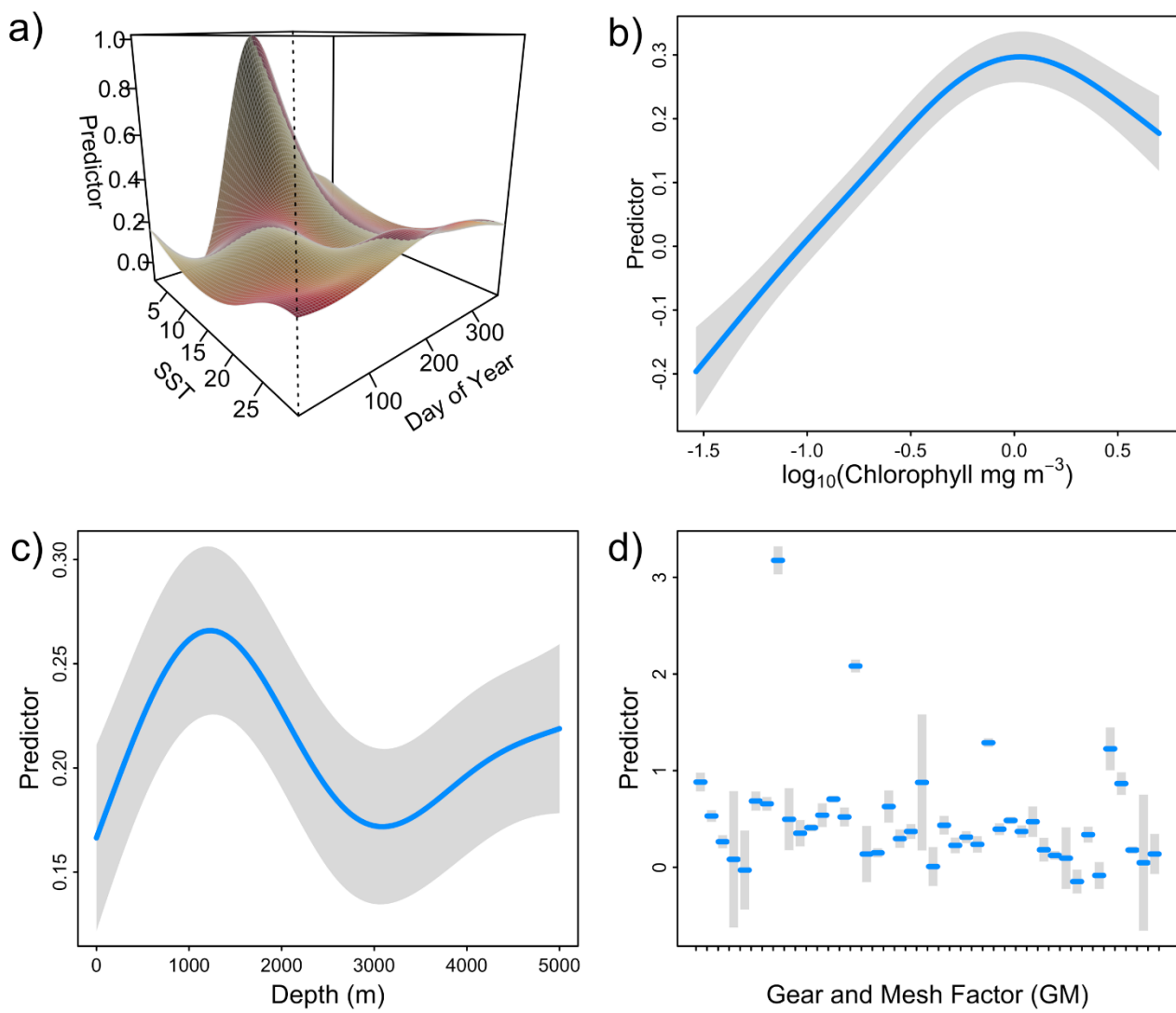


Figure S 4.6 Best model fit for euphausiids: a) Fitted interaction surface between sea surface temperature (SST) and day of year, standardised to the northern hemisphere, and partial residuals from the main effect of b) $\log_{10}(\text{Chlorophyll a})$, c) Depth and d) the Gear and Mesh factor levels. For b, c and d) the main effect for each predictor is given by the blue line, with the 95% confidence intervals given by the shaded areas.

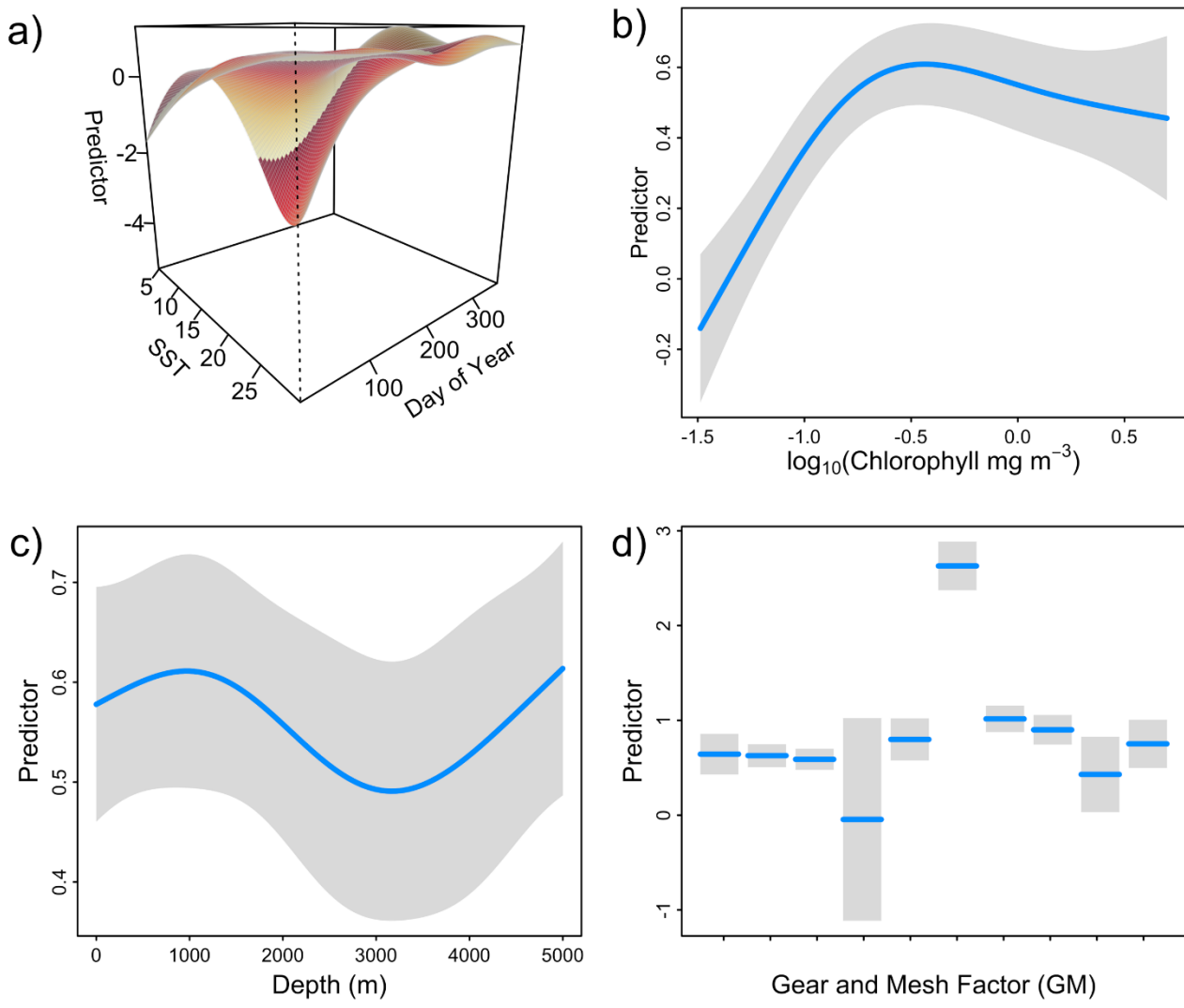


Figure S 4.7 Best model fit for salps: a) Fitted interaction surface between sea surface temperature (SST) and day of year, standardised to the northern hemisphere, and partial residuals from the main effect of b) log10(Chlorophyll a), c) Depth and d) the Gear and Mesh factor levels. For b, c and d) the main effect for each predictor is given by the blue line, with the 95% confidence intervals given by the shaded areas.

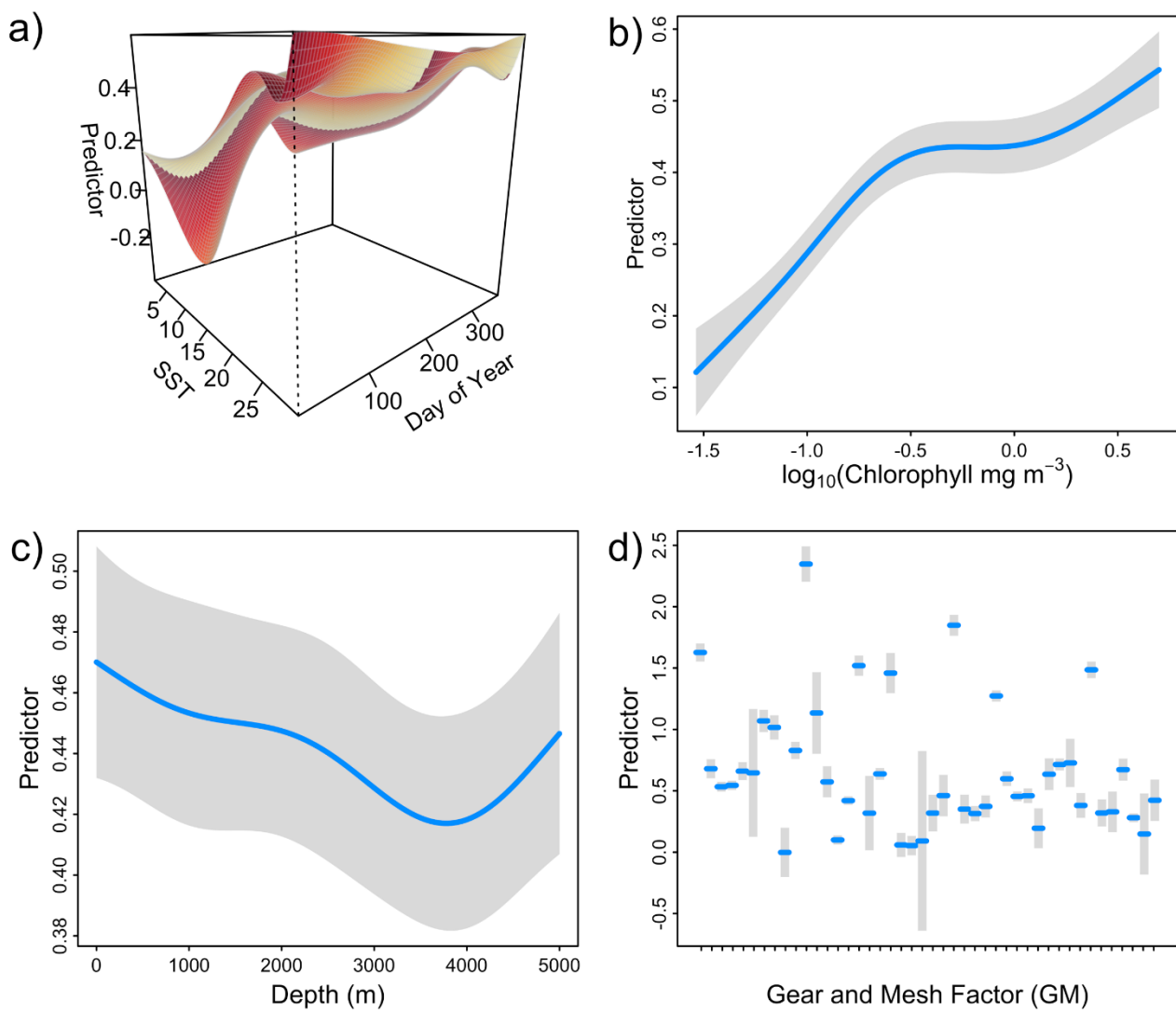


Figure S 4.8 Best model fit for jellyfish: a) Fitted interaction surface between sea surface temperature (SST) and day of year, standardised to the northern hemisphere, and partial residuals from the main effect of b) $\log_{10}(\text{Chlorophyll a})$, c) Depth and d) the Gear and Mesh factor levels. For b, c and d) the main effect for each predictor is given by the blue line, with the 95% confidence intervals given by the shaded areas.

Chapter 5

Zooplankton composition across oligotrophic and eutrophic waters mediates transfer efficiency from phytoplankton to fish

5.1 Abstract

The transfer of energy from phytoplankton to fish in marine systems depends on the abundance and structure of the zooplankton community. However, despite the body of theoretical and experimental work demonstrating how zooplankton community structure shifts from oligotrophic to eutrophic waters, most models assume that zooplankton composition is unchanging. Here, we use a functional size-spectrum model to explore how changes in zooplankton community composition from oligotrophic to eutrophic waters affects energy pathways and transfer efficiency from phytoplankton to fish. The model resolves the body sizes, carbon content and feeding characteristics of nine of the most abundant zooplankton groups (heterotrophic flagellates and ciliates, larvaceans, omnivorous and carnivorous copepods, chaetognaths, euphausiids, salps and jellyfish). Across environmental gradients, the zooplankton community emerges based on changes in the size structure of the phytoplankton, and the size-based feeding characteristics of the nine functional groups. Heterotrophic flagellates and ciliates, salps, larvaceans, carnivorous copepods and chaetognaths were more prevalent in oligotrophic waters, euphausiids and jellyfish dominated the zooplankton in eutrophic waters, and omnivorous copepods were prevalent everywhere. From oligotrophic to eutrophic waters, shifts in the size structure of the phytoplankton and composition of the zooplankton resulted decreases in the trophic levels of all zooplankton groups - except chaetognaths - and planktivorous fish. Moreover, we observed a three-fold increase in the ratio of fish to phytoplankton biomass from oligotrophic to eutrophic waters, which was driven by changes in how energy moved through the zooplankton community. In oligotrophic systems where phytoplankton communities are dominated by picoplankton (< 2 μm equivalent spherical diameter - ESD), over 50% of phytoplankton consumption was from heterotrophic flagellates and ciliates (protists). These are then consumed by crustaceans (copepods and euphausiids), which are finally consumed by planktivorous fish. In contrast, in eutrophic waters, over 85% of phytoplankton consumption was directly from crustaceans, cutting out the extra protist step. In oligotrophic

waters, salps and larvaceans partially offset the extra protist step, by providing a direct pathway from picoplankton to fish. Without salps and larvaceans, total fish biomass was up to 50% lower in oligotrophic waters, and 17% lower across the global ocean. Our results demonstrate how changes in the zooplankton drive shifts in ecosystem transfer efficiency, and the critical role of salps larvaceans as an alternative energy pathway from phytoplankton to fish in the oligotrophic open ocean.

5.2 Introduction

As the intermediate trophic level between phytoplankton and fish, zooplankton play a critical role as the main energy pathway linking lower and higher trophic levels (Kiørboe, 2008). Despite their importance, the processes that give rise to zooplankton community structure across environmental gradients are poorly resolved in current marine ecosystem models (Rose, 2010; Mitra *et al.*, 2014). Commonly, zooplankton community structure and their feeding behaviour is assumed to not change across environmental gradients or time (Everett *et al.*, 2017). However, zooplankton are extremely diverse taxonomically and physiologically, with all major phyla present (Bucklin *et al.*, 2010), and assorted feeding strategies, from passive suspension feeding to active ambush and carnivory (Kiørboe, 2011). Zooplankton range over 14 orders of magnitude in body size, from single-cell protists ($\sim 1 \mu\text{m}$, 10 pg; Hansen *et al.*, 1997), to jellyfish (10s of kg; Acuña *et al.*, 2011; Levinton, 2013).

Energy transfer through food webs is dependent upon the relative size of predator and prey (Jennings and Mackinson, 2003), known as the predator-prey mass ratio (PPMR). The larger the predator relative to its prey, the more efficiently energy is passed from lower to higher trophic levels. Zooplankton have enormous variation in PPMR from ~ 10 for carnivorous copepods to $\sim 10^8$ for salps and larvaceans (Bone, 1997; Wirtz, 2012). What is more, this diversity in size and feeding behaviour is not static, with different groups prevailing under different environmental conditions, based on their relative fitness (Barton *et al.*, 2013). Given the enormous diversity of zooplankton, and their vastly different feeding strategies, this means that energy pathways through the zooplankton from phytoplankton to fish are not static, but change across environmental gradients. It follows that accounting for the mechanisms that gave rise to zooplankton community structure is very important to understand how energy moves through marine systems under different environmental conditions.

Ultimately the productivity of the marine ecosystem is constrained by primary production (Pauly and Christensen, 1995; Chassot *et al.*, 2010; Friedland *et al.*, 2012; Stock *et al.*, 2017), however, as Ryther identified almost 50 years ago, primary production alone cannot explain the productivity of higher trophic levels across oligotrophic and eutrophic waters (Ryther, 1969). Ryther hypothesised that this is because marine food chains are more efficient in eutrophic systems compared to oligotrophic with fewer trophic steps between phytoplankton and fish (Ryther, 1969). This is believed to be primarily driven by changes in the size structure of the phytoplankton (Stibor *et al.*, 2004; Stock *et al.*, 2008; Barnes *et al.*, 2011; Marañón, 2015): from oligotrophic to eutrophic waters, the median cell size of the phytoplankton community increases (Brewin *et al.*, 2010; Barnes *et al.*, 2010; Hirata *et al.*, 2011), as the community size structure shifts from one dominated by picoplankton ($< 2 \mu\text{m}$ ESD) to larger nano ($2 \mu\text{m} - 20 \mu\text{m}$ equivalent spherical diameter - ESD) and microplankton ($> 20 \mu\text{m}$ ESD). As a result, the availability of food for zooplankton groups with different body sizes and PPMRs will change as the phytoplankton community shifts across oligotrophic and eutrophic waters.

Generally, picoplankton cannot be directly consumed by larger crustaceans such as copepods and euphausiids (crustaceans), which are nutritious food for planktivorous fish (Lalli and Parsons, 1995; Sommer and Stibor, 2002; Stibor *et al.*, 2004). This is why it is hypothesised that in oligotrophic systems where picoplankton dominate the phytoplankton, crustaceans would consume heterotrophic protists (e.g., flagellates and ciliates) that feed on the smaller phytoplankton and fall within the prey size range of crustaceans (Ryther, 1969; Stoecker and Capuzzo, 1990; Boyce *et al.*, 2015). This adds an additional trophic step in the food chain, leading to less available energy for fish (Figure 5.1 a). In eutrophic waters, crustaceans directly consume the larger phytoplankton that are abundant, resulting in a shorter, more efficient phytoplankton-crustacean-fish energy pathway (Figure 5.1 b; Lalli and Parsons, 1995; Stibor *et al.*, 2004).

This idea of changes in phytoplankton size structure leading to a more efficient eutrophic food chain is complicated by salps and larvaceans. These groups broadly cover the same size range as omnivorous copepods and euphausiids, but they can directly access picoplankton for food, circumventing the longer pathway through flagellates and ciliates in oligotrophic waters (Figure 5.1 a; Bone, 1998). These groups have been hypothesised to provide a more efficient direct transfer of energy from phytoplankton to fish in oligotrophic systems, in contrast to the longer phytoplankton-protist-crustacean-fish pathway (Diebel and Lee, 1992; Mosseau *et al.*, 1998; Jaspers *et al.*, 2009). However, these groups have a lower

carbon content compared to protists and crustacean zooplankton (Taylor, 1978; Menden-Deuer and Lessard, 2000; Kiørboe, 2013). Prey with a comparatively higher carbon content and energy density can support more predator production, compared to more gelatinous zooplankton groups (Sommer *et al.*, 2002; Robinson *et al.*, 2014). This means that the efficiency of the salp and larvaceans pathway from picoplankton to planktivorous fish in oligotrophic waters, may be offset by their low carbon content and nutritional quality.

Despite the extensive empirical and theoretical work identifying the pivotal role of zooplankton in the marine ecosystem, current global ecosystem models have a very simple zooplankton formulation (usually with only one or two groups) and none represent the functional complexity of the zooplankton (Everett *et al.*, 2017). The assumption implicit in models neglecting the diversity of the zooplankton is that it does not significantly affect ecosystem function. However, recent work has shown that the productivity of higher trophic levels is sensitive to the transfer efficiency of lower trophic levels (Mitra *et al.*, 2014; Jennings and Collingridge, 2015). In a simple size-structured model resolving phytoplankton, zooplankton and fish, Stock *et al.*, (2008) found that the size structure of the marine ecosystem is sensitive to the gross growth efficiency of the zooplankton. Heneghan *et al.*, (2016) demonstrated that the productivity of fish, and their resilience to fishing pressure, is strongly affected by changes in the size-based feeding behaviour of the zooplankton. Moreover, Irigoien *et al.*, (2015) hypothesised that their finding that global fish biomass could be an order of magnitude higher than previously thought could be partly because current models poorly resolve factors influencing transfer efficiency in the zooplankton. It follows that current formulations which do not resolve the dynamics of the zooplankton are neglecting a critical component of how the marine ecosystem functions.

Using functional traits, such as body size, feeding behaviour, and carbon content has been proposed as a way forward to improving the representation of the zooplankton in ecosystem models (Litchman *et al.*, 2013; Heneghan *et al.*, 2016; McConville *et al.*, 2017). This is because functional traits determine individual organisms' relative fitness in a given environment. Body size is a major functional trait, dictating the pace of physiological processes and the trophic position of individual zooplankton in the marine food web (Andersen *et al.*, 2016a). Size-based feeding behaviour, such as PPMR and the prey size range (feeding kernel width), have also been identified as traits which structure the zooplankton community across environmental gradients (Sommer and Stibor, 2002; Stibor *et al.*, 2004; Wirtz, 2012; Boyce *et al.*, 2015). This is because the size structure of the phytoplankton changes from being dominated by picoplankton (< 2 µm ESD) to larger nano

(2 μm - 20 μm ESD) and micro plankton (> 20 μm ESD) from oligotrophic to eutrophic waters (Brewin *et al.*, 2010; Barnes *et al.*, 2010; Hirata *et al.*, 2011). This means that the availability of food for zooplankton with different body sizes and PPMRs will change with shifts in phytoplankton community size structure across oligotrophic and eutrophic waters. For example, salps and larvaceans consume organisms 6-8 orders of magnitude smaller than themselves (Deibel, 1998; Wirtz 2012), allowing them to access the picoplankton for food. This means that, in oligotrophic areas where picoplankton is abundant, salps and larvaceans will have comparatively more food than groups such as omnivorous copepods and euphausiids, which cannot directly access the picoplankton for food (Sommer and Stibor, 2002; Stibor *et al.*, 2004; Wirtz, 2012). Finally, carbon is the major structural component of zooplankton (Kiørboe, 2013; McConville *et al.*, 2017), and the carbon content of different zooplankton groups affects their relative fitness by influencing their growth rates (McConville *et al.*, 2017) and how efficiently they mediate energy from phytoplankton to higher trophic levels (Robinson *et al.*, 2014).

Here, we use a functional size-spectrum model which breaks the marine ecosystem into three components: phytoplankton, zooplankton and fish. The model resolves nine major zooplankton functional groups (heterotrophic flagellates and ciliates, larvaceans, omnivorous and carnivorous copepods, chaetognaths, euphausiids, salps and jellyfish) based on their body size ranges, size-based feeding characteristics (including PPMR) and carbon content. Across the global ocean, the composition, body sizes and total biomass of the zooplankton community emerges from the model under different chlorophyll a and temperature conditions that change the size structure of the phytoplankton community and are transferred through the feeding characteristics of the nine zooplankton groups. We use the model to assess how energy pathways from phytoplankton to fish change with increasing primary production, by looking at the diets of the zooplankton groups, and planktivorous fish (< 100 g) across oligotrophic (which we define as areas where chlorophyll a < 0.1 mg m⁻³) to eutrophic (which we define as areas where chlorophyll a > 1 mg m⁻³) waters, and the resulting changes in the trophic levels of these functional groups. We then evaluate how changes in the composition and diets of the zooplankton affects the transfer efficiency (using biomass ratio as a proxy) from phytoplankton to fish. We hypothesise that 1) there will be more trophic steps through the zooplankton in oligotrophic than eutrophic waters and 2) this will lead to a less efficient energy transfer from phytoplankton to fish, with less fish per unit phytoplankton in oligotrophic waters. Finally, we explore the role of larvaceans in supporting

fish biomass in oligotrophic waters, by considering the change in total fish biomass across oligotrophic and eutrophic waters when these groups are removed from the model.

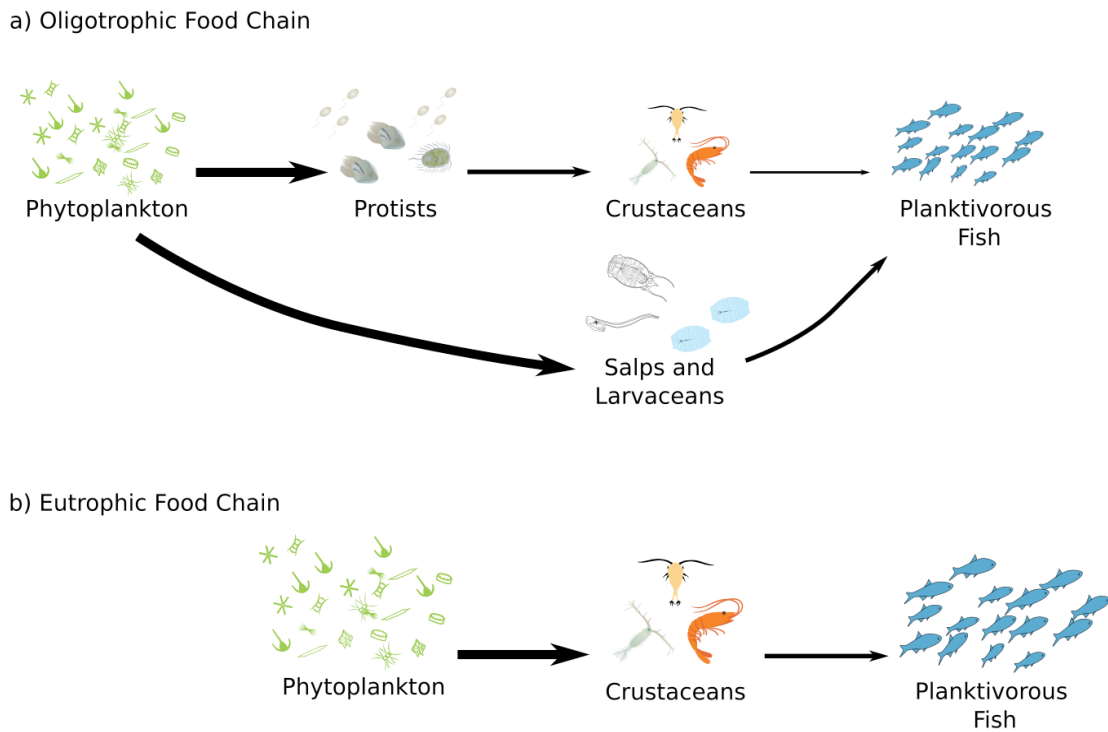


Figure 5.1 Hypothesised food chains in a) oligotrophic versus b) eutrophic systems. Width of arrows shows the magnitude of energy transfer between steps in the food chain.

5.3 Methods

5.3.1 The zooplankton-resolved functional size-spectrum model

The zooplankton-resolved functional size-spectrum model (full model equations and parameters given in Supplementary Information Table S 5.1, 5.2 and 5.3) represents the pelagic ecosystem as three size-structured communities: phytoplankton, zooplankton and fish. The dynamics of the phytoplankton community are not represented in the model, with the phytoplankton community serving as a static resource for zooplankton. The abundances of the zooplankton and fish communities are driven by the size-dependent processes of growth and mortality using the second order McKendrick-von Foerster partial differential equation

$$\frac{\delta}{\delta t} N_i(w, t) = -\frac{\delta}{\delta w} (g_i(w, t)N_i(w, t)) - \mu_i(w, t)N_i(w, t) + \frac{1}{2} \frac{\partial^2}{\partial w^2} (f_i(w, t)N_i(w, t)).$$

The density of individuals in group i of weight w at time t per m^{-3} is given by $N_i(w, t)$ and their individual growth, mortality and diffusion rates are denoted by $g_i(w, t)$ (g yr^{-1}), $\mu_i(w, t)$ (g yr^{-1}) and $f_i(w, t)$ ($\text{g}^2 \text{yr}^{-1}$), respectively (see Supplementary Information Table S 5.1 for equations).

The slope a , intercept b and maximum size $w_{p_{max}}$ of the static phytoplankton community is driven by chlorophyll a , using the synoptic model developed by Brewin *et al.*, (2010). Brewin's model estimates the percentage contribution of pico ($0.2\text{-}2 \mu\text{m ESD}$), nano ($2\text{-}20 \mu\text{m ESD}$) and micro ($>20 \mu\text{m ESD}$) phytoplankton to the total chlorophyll a concentration. Chlorophyll a is converted to grams wet weight (assuming $1 \text{ g chlorophyll } a = 50 \text{ g C}$; Zhou *et al.*, 2010, and $1 \text{ g carbon} = 10 \text{ g wet weight}$; Hansen *et al.*, 1994, Boudreau & Dickie, 1992, Woodworth-Jefcoats *et al.*, 2013) and the total biomass in each of the three size ranges is spread uniformly across the size classes in the size range (Sheldon *et al.*, 1972; Blanchard *et al.*, 2009; Woodworth-Jefcoats *et al.*, 2013; Barange *et al.*, 2014) and converted to abundance ($N_p(w)$, $\# \text{ m}^{-3}$). Finally, slope and intercept are calculated with the line of best fit through the log-transformed phytoplankton abundances. We allowed the maximum size of the phytoplankton community to increase linearly from $21\text{-}60 \mu\text{m ESD}$, depending on the contribution of the microplankton group to total chlorophyll a . We used $60 \mu\text{m}$ as the maximum possible ESD of the phytoplankton community following Barnes *et al.*'s (2011) finding that 90% of phytoplankton cells fall below $55\text{-}65 \mu\text{m ESD}$ in 12 sites covering polar, tropical and upwelling environments.

With increasing chlorophyll a concentration, the total biomass of the phytoplankton community increases, and the phytoplankton size-spectrum has a higher intercept, flatter slope and a larger maximum size. In other words, in oligotrophic waters there is less phytoplankton and the phytoplankton community is dominated by picoplankton whereas in eutrophic areas there is more phytoplankton and the average size of the phytoplankton increases, as microplankton become more prevalent. Our phytoplankton slope estimates for the global ocean ranged from -1.1 in oligotrophic to -0.8 in the most eutrophic regions, which is within the range reported by previous empirical studies (Moreno-Ostos *et al.*, 2015).

The zooplankton community consists of nine functional groups (heterotrophic flagellates and ciliates, larvaceans, omnivorous and carnivorous copepods, chaetognaths, euphausiids, salps and jellyfish), and the fish community is broken into three size-based communities (small $< 100 \text{ g}$, medium $100 \text{ g} - 10,000 \text{ g}$ and large $>10,000 \text{ g}$). Each functional group is defined by its size range, size-based feeding characteristics (predator-prey mass ratio –

PPMR - and feeding kernel width) and carbon content (see Supplementary Information Table S 5.2).

The carbon content of the different groups is included to represent nutritional quality, so that the quality of prey affects how much new wet weight biomass a predator can build. This was to allow prey groups with a comparatively higher carbon content and energy density (e.g., crustaceans) to contribute more to predator wet-weight growth in comparison to lower carbon groups (e.g., jellyfish and larvaceans, Spitz *et al.*, 2010; Kiørboe, 2013; Mitra *et al.*, 2014). The growth conversion efficiency of predators of group i consuming prey from group j is

$$GG_{ij} = 0.25 \frac{C_j}{C_i},$$

where C_j and C_i are the carbon-wet weight ratios of group j and i , respectively. Kiørboe (2011) found that the search rate of individual zooplankton scales with body carbon, across seven functional groups (including flagellates ciliates, copepods and jellyfish) and 12 orders of magnitude in body size. This means that, per unit of wet weight, more gelatinous groups will have a lower search rate, compared to more carbon dense functional groups. Carbon content is incorporated into the search rate equation $V_i(w)$ as a multiplier. For an individual of group i , with carbon content C_i of wet weight body size w , the search rate ($\text{m}^{-3} \text{ yr}^{-1}$) is:

$$V_i(w) = C_i \gamma_i w^{\alpha_i},$$

where γ_i is the search rate coefficient ($\text{g C}^{-1} \text{ m}^{-3} \text{ yr}^{-1}$) and α_i is the exponent of search. The search rate coefficient γ_i and exponent α_i are held constant across the different zooplankton groups (Kiørboe, 2011; see Supplementary Information Table S 5.3).

Temperature effects are also included as a multiplier on the feeding and mortality rates of zooplankton and fish, using the modified Arrhenius function from the metabolic theory of ecology (Brown *et al.*, 2004):

$$\tau = \exp \left(25.55 - \frac{0.63}{8.62 \times 10^{-5} K} \right),$$

where K is the temperature in Kelvin (Jennings *et al.*, 2008; Blanchard *et al.*, 2012; Woodworth-Jefcoats *et al.*, 2013).

From the perspective of the predator from group i of body size w , the quantity of food available to fuel new growth $D_i(w, t)$ is given by the total biomass of suitable prey (g m^{-3}):

$$D_i(w, t) = V_i(w) \sum_j \int_{w_{\min_j}}^w \theta(w, w') N_j(w', t) w' dw',$$

where w_{\min_j} is the minimum size of group j . $N_j(w', t)$ is the number of individuals from group j of body size w' and $\theta(w, w')$ is the prey feeding kernel, which gives the probability a predator of size w eats a prey of size w' . The prey feeding kernel is a log-normal probability density function centred on the ideal prey size, determined by the predator's PPMR, body size, with a standard deviation giving the breadth of prey sizes the predator can eat. In the zooplankton, the width of the feeding kernel increases with increasing PPMR (Hansen *et al.*, 1994; Fuchs and Franks, 2010; Kiørboe, 2016). So larvaceans, with a $\log_{10}(\text{PPMR})$ of ~ 8 consume a wider range of prey than heterotrophic flagellates, with a $\log_{10}(\text{PPMR})$ of ~ 1 . The growth rate (g yr^{-1}) of an individual group i , of size w at time t is fuelled by the consumption and conversion of prey biomass to new biomass:

$$g_i(w, t) = \tau \sum_j G G_{ij} D_{ij}(w, t),$$

From the prey's perspective, total mortality from predation is given by the sum of the predation pressure from all larger size classes (yr^{-1}):

$$\mu_p(w, t) = \tau \sum_j \int_w^{\bar{W}_i} \theta(w', w) V_i(w') N_i(w', t) dw',$$

where \bar{W}_i is the maximum size of a predator from group i . Since individuals grow through time, an additional source of mortality from senescence was incorporated that increased with body size (yr^{-1}):

$$\mu_{S_i}(w, t) = \tau \delta \left(\frac{w}{W_{S_i}} \right)^\rho,$$

where W_{S_i} is the body size after which senescence mortality increases for an individual from group i . This senescence mortality term also acts as a closure term for the largest size classes, by preventing a build-up of very large individuals who are not exposed to predation (Andersen *et al.*, 2016b). For an individual of size w , at time t , from group i , total mortality $\mu_i(w, t)$ is given by the sum of predation and senescence mortality (yr^{-1}):

$$\mu_i(w, t) = \mu_p(w, t) + \mu_S(w, t).$$

The functional size-spectrum model is forced with annual mean sea surface temperature and chlorophyll a , obtained from MODIS-Aqua (accessed via the GIOVANNI portal: <https://giovanni.gsfc.nasa.gov/giovanni/>). For each chlorophyll a and temperature

combination, the model is run for 1000 years on a half-weekly time step. The model has a burn-in period of 500 years, with the results presented here obtained by calculating the mean over the last 500 years of the simulation in each grid square.

5.3.2 Diets and trophic levels

To explore changes in the energy pathways from phytoplankton to fish across oligotrophic to eutrophic waters, we derived the mean diets of the 9 zooplankton functional groups and planktivorous fish (< 100gm). The proportion of the diet of group i , that comes from group j is:

$$PD_{ij} = \frac{C_{ij}}{\sum_j C_{ij}},$$

where C_{ij} is the total biomass from group j consumed by group i (g yr^{-1}):

$$C_{ij} = \int_{w_{\min_i}}^{\bar{W}_i} N_i(w) V_i(w) \int_{w_{\min_j}}^{\bar{W}_j} \theta(w, w') N_j(w') w' dw' dw,$$

where $N_j(w')$ is the mean number of individuals of group j who have a body mass of w' , over the final 500 years of the simulation. We used PD_{ij} to calculate the average trophic level of the different groups using the trophic position equation from Pauly and Palomares (2005). Phytoplankton, at the base of the food web, are given a trophic level of 1, and the mean trophic level of group i (TL_i) is given by solving:

$$TL_i = 1 + \sum_j TL_j \times PD_{ij}.$$

Except for phytoplankton, the trophic level of the different groups changes with their diet, so for each simulation we used the Gauss-Jacobi iteration method to solve TL_i for each i (Sauer, 2012).

5.3.3 Ecosystem efficiency

Across oligotrophic and eutrophic waters, we evaluated the efficiency of the emergent energy pathways through the zooplankton by considering the ratio of total fish to phytoplankton biomass (FPBR). Ecological efficiency is usually measured as the ratio of predator-prey productivity (Brown *et al.*, 2004), but we used the FPBR because the model does not resolve the dynamics of production and mortality in the phytoplankton community. Predator-prey biomass ratios have been used in previous empirical studies as a proxy for transfer efficiency (Yvon-Durocher *et al.*, 2011; Ye *et al.*, 2013; Heneghan *et al.*, 2016) and Garcíá-Comas *et al.* (2016) found empirically that predator-prey biomass ratios are strongly

correlated with predator-prey productivity. The interpretation of the FPBR is intuitive: the higher the FPBR, the more fish biomass per unit of phytoplankton biomass, which implies a higher transfer efficiency from phytoplankton to fish.

5.4 Results

5.4.1 The emergent plankton community

Size classes in the phytoplankton community were set and are not emergent from the model, but help drive changes in the zooplankton community. Pico-phytoplankton comprise ~60% of the biomass in oligotrophic waters, declining to around 10% in eutrophic waters as micro-phytoplankton increase from <5% in oligotrophic waters to ~45% in eutrophic waters, and nano-phytoplankton increase marginally from 30% in oligotrophic to 45% in eutrophic waters (Figure 5.2 a).

From oligotrophic (which we define as areas where chlorophyll *a* < 0.1 mg m⁻³) to eutrophic (which we define as areas where chlorophyll *a* > 1 mg m⁻³) waters, there were distinct changes in the emergent composition of the zooplankton community (Figure 5.2 a, b). In the microplankton, heterotrophic flagellates and ciliates constituted ~10% of the biomass in oligotrophic regions, decreasing to around 5% in eutrophic regions, with phytoplankton making up the remaining bulk of the biomass across all chlorophyll *a* levels (Figure 5.2 a). In the seven meso- and macro zooplankton groups (Figure 5.2 b), omnivorous copepods and euphausiids were a significant component of the zooplankton in all regions, comprising 25% and 10% respectively of the macro zooplankton biomass in oligotrophic waters, increasing to around 25% and 30% in eutrophic waters. In contrast, salps, larvaceans, carnivorous copepods and chaetognaths were most prevalent in oligotrophic waters, with larvaceans making up about 20% of the biomass in low chlorophyll *a* waters, declining to around 1% in eutrophic waters. Similarly, carnivorous copepods and chaetognaths each made up just under 10% of the biomass in oligotrophic waters, declining to less than 1% in eutrophic waters. Salps comprised about 10% of the biomass in oligotrophic waters, declining marginally to around 7% in eutrophic waters. Jellyfish were the only group that did not increase or decrease monotonically with chlorophyll *a*, with the proportion of macro zooplankton biomass from the jellyfish increasing from 5% in oligotrophic waters, to about 35% in waters with 1 mg m⁻³ chlorophyll *a* (0 on log₁₀ scale), and declining to about 25% as chlorophyll *a* increased past this level.

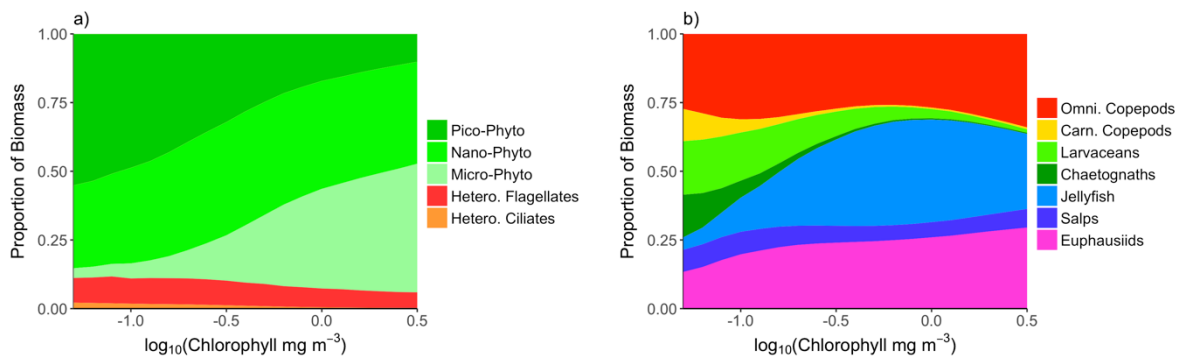


Figure 5.2 Plots of the proportion of the total biomass of a) phytoplankton, comprising pico ($<2 \mu\text{m}$), nano (2-20 μm) and micro ($>20 \mu\text{m}$) size classes), heterotrophic flagellates and ciliates, and b) zooplankton, comprising omnivorous copepods, carnivorous copepods, larvaceans, chaetognaths, jellyfish, salps and euphausiids. To clarify the trend with chlorophyll *a*, over temperature, we used a spline smoother with 5 degrees of freedom.

5.4.2 Who is eating phytoplankton?

We considered how the consumption of phytoplankton shifts to different zooplankton groups across oligotrophic and eutrophic waters (Figure 5.3). In oligotrophic waters, heterotrophic flagellates and ciliates are responsible for over 50% of phytoplankton consumption, and larvaceans between 5-10%. As chlorophyll *a* increases, the share of consumption from these groups declines as more phytoplankton consumption goes directly to omnivorous copepods and euphausiids. These two groups are responsible for just 30% of consumption in oligotrophic waters, increasing to over 85% in eutrophic waters. The remaining 15% of phytoplankton consumption in eutrophic waters is from heterotrophic flagellates and salps. Salps are a minor consumer of phytoplankton, responsible for about 3% of consumption across oligotrophic and eutrophic waters.

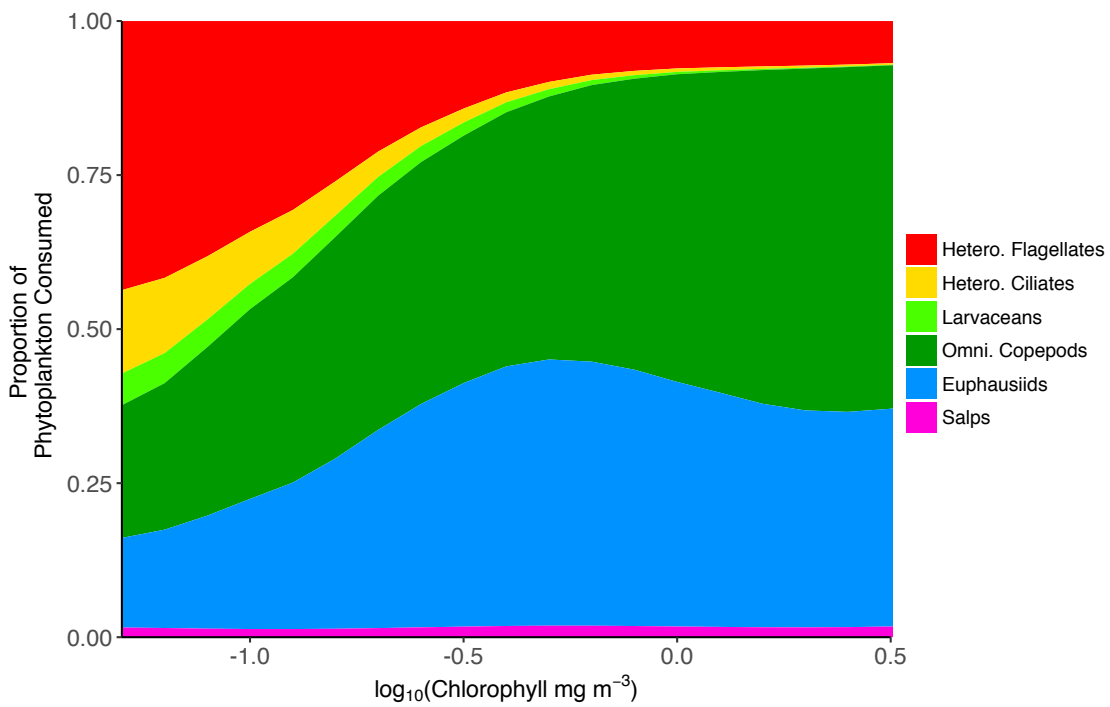


Figure 5.3 Proportion of total phytoplankton consumed by various zooplankton groups, versus chlorophyll *a*. To clarify the trend with chlorophyll *a*, over temperature, we used a spline smoother with 5 degrees of freedom.

5.4.3 Emergent diets and trophic levels

Except for larvaceans, the six omnivorous groups (heterotrophic flagellates and ciliates, omnivorous copepods, larvaceans, euphausiids and salps) were more carnivorous in oligotrophic waters (Figure 5.4 a, c, g, i, k). For heterotrophic ciliates, omnivorous copepods, euphausiids and salps, up to 20% of their diet consisted of mostly heterotrophic flagellates and ciliates in oligotrophic waters, with this proportion declining in eutrophic waters to around 5% for heterotrophic ciliates, around 1% for the other groups (Figure 5.4 a, c, g, i, k). Heterotrophic flagellates were the most carnivorous zooplankton group – with over 20% of their diet consisting of heterotrophic flagellates and ciliates in oligotrophic waters, declining to about 10% in eutrophic waters (Figure 5.4 a). In contrast, across oligotrophic and eutrophic waters, the diet of the larvaceans was over 99% phytoplankton (Figure 5.4 e). Changes in diet are reflected in how the emergent trophic levels of the omnivorous groups change with increasing chlorophyll *a* (Figure 5.4 b, d, f, h, j, l). The trophic levels of omnivorous copepods, euphausiids and salps declined from around 2.2 in oligotrophic

waters, to 2 in eutrophic waters (Figure 5.4 h, j, k). The most carnivorous of the omnivorous groups, heterotrophic flagellates and ciliates, declined from 2.3 and 2.2 respectively, to around 2.1 in eutrophic waters (Figure 5.4 b, d). In contrast, the trophic level of the

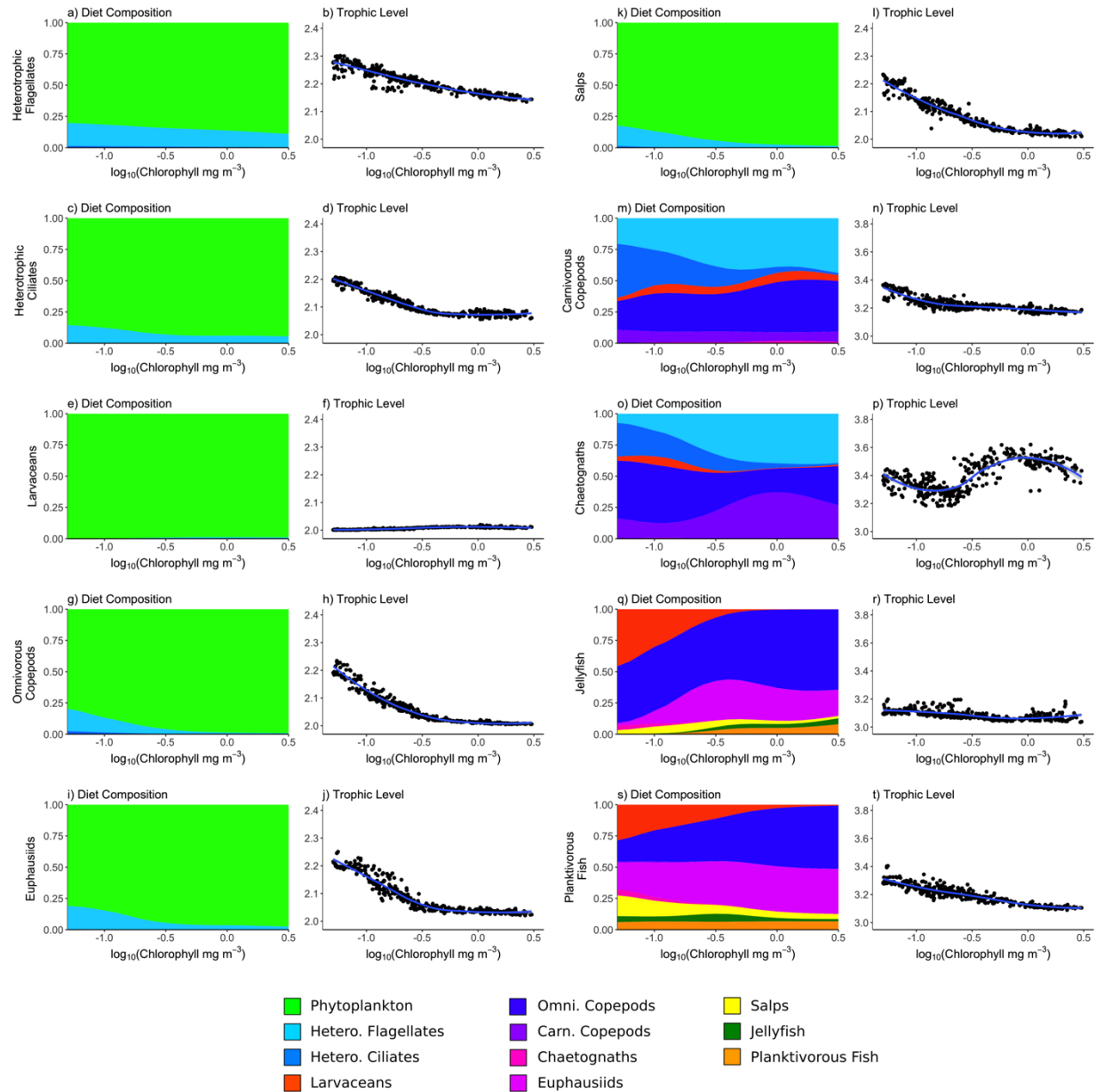


Figure 5.4 Diet composition and resulting trophic levels across chlorophyll a for heterotrophic flagellates (a, b), heterotrophic ciliates, (c, d), larvaceans (e, f), omnivorous copepods (g, h), euphausiids (i, j), salps (k, l), carnivorous copepods (m, n), chaetognaths (o, p), jellyfish (q, r) and planktivorous fish (s, t). To highlight the trend with chlorophyll a, rather than temperature, we used a spline smoother with 5 degrees of freedom.

larvaceans – whose diet is over 99% phytoplankton across oligotrophic and eutrophic waters – remained around 2 across oligotrophic and eutrophic waters (Figure 5.4 f).

Around 50% of the diets of carnivorous copepods and chaetognaths consisted of heterotrophic flagellates and ciliates, with the other 50-60% split between the other zooplankton groups (Figure 5.4 m, o). Heterotrophic flagellates and ciliates were around 40% and 10% of the diets in oligotrophic waters for both carnivorous copepods and chaetognaths, but as chlorophyll a increased the proportion taken by heterotrophic ciliates declined to less than 1% and heterotrophic flagellates increased to about 50%. For carnivorous copepods, 40% of their diet was omnivorous copepods across oligotrophic and eutrophic waters, with the remaining 10-20% from larvaceans, carnivorous copepods and euphausiids (Figure 5.4 m). With increasing chlorophyll, the diets of chaetognaths shifted from 10% carnivorous copepods, 30% omnivorous copepods and 10% larvaceans, to 30% carnivorous copepods, 20% omnivorous copepods and less than 1% from larvaceans (Figure 5.4 o). For these groups, the change in trophic level from oligotrophic to eutrophic waters was not as large as it was for the larger omnivorous groups. The trophic level of carnivorous copepods decreased from 3.4 to 3.2 with increasing chlorophyll a (Figure 5.4 n). For chaetognaths their trophic level varied around 3.4, but did not decrease with increasing chlorophyll a (Figure 5.4 p).

Jellyfish and planktivorous fish have similar diets, reflecting the overlap in their body sizes and prey size ranges (Figure 5.4 q, s), with salps and larvaceans making up a large proportion of their diets in oligotrophic waters, shifting to omnivorous copepods and euphausiids in eutrophic waters. However, although similar, the diets of these two groups are not identical. Larvaceans make up 45% of the diet of jellyfish in oligotrophic waters (Figure 5.4 q), but only 30% of the diet of planktivorous fish (Figure 5.4 s). Salps comprise 15% of the diet of planktivorous fish in oligotrophic waters, declining to around 5% in eutrophic waters, but only make up to 5% of the diet of jellyfish across oligotrophic and eutrophic waters. Omnivorous copepods are only 15% of the diet of planktivorous fish in oligotrophic waters (Figure 5.4 s), but 50% for jellyfish (Figure 5.4 q). These differences in diet are reflected in the change in trophic level of these groups with increasing chlorophyll a (Figure 5.4 r, t). Jellyfish have a maximum trophic level of around 3.2 in oligotrophic waters, declining to around 3.05 in eutrophic waters (Figure 5.4 r). In contrast, the maximum trophic level of planktivorous fish is 3.35 in oligotrophic waters, declining to around 3.1 in eutrophic waters (Figure 5.4 t). The lower trophic level for jellyfish in oligotrophic waters would be

because larvaceans comprise almost 50% of their diet, compared to around 30% for planktivorous fish.

5.4.4 The emergent food web in oligotrophic versus eutrophic waters

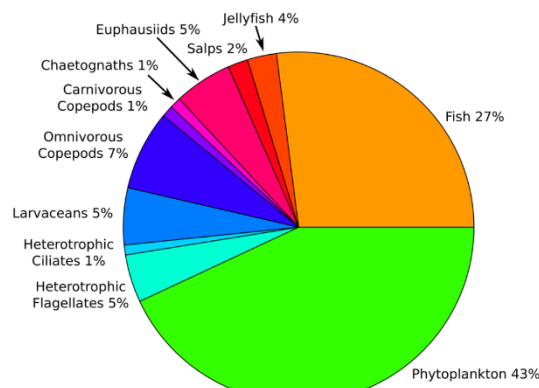
When considered side-by-side, clear differences can be seen in the composition and structure of oligotrophic and eutrophic food webs (Figure 5.5). In particular, the ratio of phytoplankton to higher trophic level biomass shifts, with phytoplankton comprising 43% of the biomass in the oligotrophic system (Figure 5.5 a), but only 21% in eutrophic system (Figure 5.5 b). This means that, per unit of phytoplankton biomass, there is approximately three times as much higher trophic level biomass in eutrophic compared to oligotrophic waters.

Changes in the composition of the community across oligotrophic and eutrophic waters are driven by changes in the structure of the food web. The food chain is more diverse, connected and longer in oligotrophic versus eutrophic waters, primarily due to more carnivory in the zooplankton, with an increase in the prevalence and importance of groups such as carnivorous heterotrophic flagellates and ciliates, carnivorous copepods and chaetognaths. Heterotrophic flagellates and ciliates comprise only 6% of the biomass in oligotrophic waters (Figure 5.5 a), yet they are responsible for over 50% of phytoplankton consumption in the oligotrophic food web (Figure 5.5 c). The energy from the phytoplankton consumed by heterotrophic flagellates and ciliates is then passed through to larger zooplankton groups, in particular omnivorous copepods and euphausiids, which are then consumed by planktivorous fish (Figure 5.5 c). Larvaceans are also an important part of the oligotrophic food web, comprising about 6% of the total biomass and 10% of phytoplankton consumption (Figure 5.5 c). However, in contrast to heterotrophic flagellates and ciliates, larvaceans are a direct pathway for energy transfer from phytoplankton to fish (Figure 5.5 c).

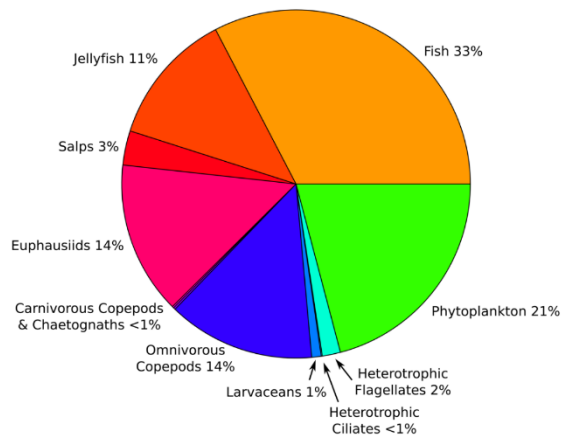
The eutrophic food web is simpler than oligotrophic food web, with over 90% of phytoplankton consumption going directly to omnivorous copepods and euphausiids, which collectively comprise 28% of the community biomass (Figure 5.5 b) and make up around 90% of the diet of planktivorous fish in eutrophic waters (Figure 5.5 d). This change in how energy moves through the zooplankton from oligotrophic to eutrophic waters, is reflected in the change in trophic level of planktivorous fish from around 3.35 in oligotrophic waters to 3.1 in eutrophic waters (Figure 5.5 c, d), meaning there is around an extra one quarter step in the food chain from phytoplankton to fish in oligotrophic versus eutrophic waters. As

expected, the shorter food chain in eutrophic waters is more efficient at transferring energy from phytoplankton to fish, leading to almost a three-fold increase in the ratio of fish to phytoplankton biomass from around 0.5 in oligotrophic waters, to approximately 1.5 in eutrophic waters (Figure 5.6).

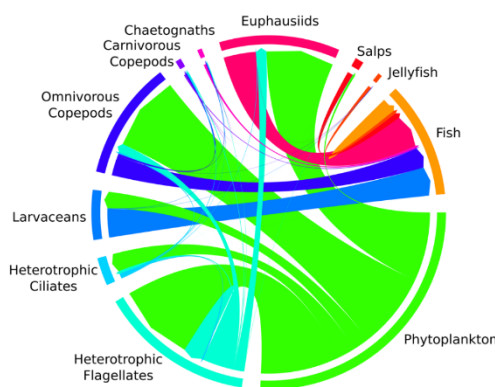
a) Oligotrophic Biomass Composition (Chlorophyll a < 0.1 mg m⁻³)



b) Eutrophic Biomass Composition (Chlorophyll a > 1 mg m⁻³)



c) Oligotrophic Food Web (Chlorophyll a < 0.1 mg m⁻³)



d) Eutrophic Food Web (Chlorophyll a > 1 mg m⁻³)

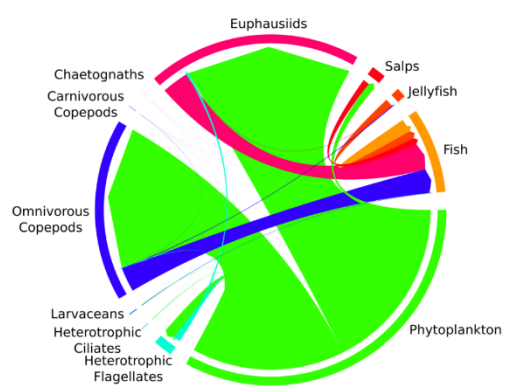


Figure 5.5 The average emergent community composition and food web for oligotrophic (a, c) and eutrophic (b, d) waters. The food web diagrams (c, d) show the flow of biomass from predation between the different groups, with the width of the arrows proportional to the biomass flow (g yr⁻¹).

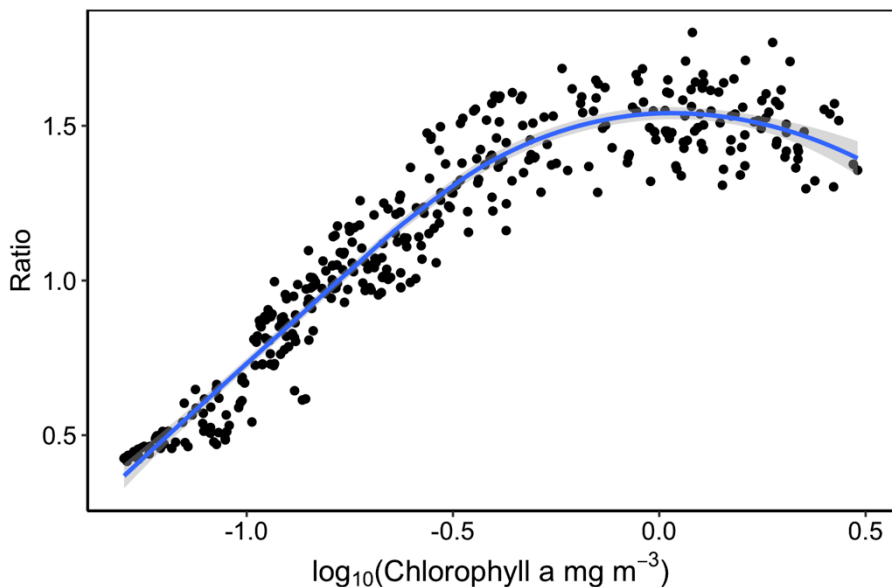


Figure 5.6 Fish-Phytoplankton Biomass Ratio against chlorophyll a.

5.4.5 The role of salps and larvaceans as an energy pathway from phytoplankton to fish

To evaluate the importance of salps and larvaceans as an energy pathway from phytoplankton to fish, we compared the total fish biomass from the model run without them, with total fish biomass from the standard model run that included them. Salps and larvaceans make up about 35% of the zooplankton community (Figure 5.2 b) and comprise almost 50% of the diet of planktivorous fish in oligotrophic waters (Figure 5.4 s). This proportion declines to around 5% in eutrophic waters, as they are replaced in the diet of planktivorous fish by omnivorous copepods and euphausiids. Salps and larvaceans have a lower carbon content compared to crustaceans: 1% of their total wet weight is carbon, compared to 12% for copepods and euphausiids (Kiørboe, 2013). The higher proportion of salps and larvaceans in the diet of planktivorous fish in oligotrophic waters is reflected in the carbon content of the diet of planktivorous fish, which increases from around 0.07 in oligotrophic waters, to 0.11 in eutrophic waters as euphausiids and omnivorous copepods increase (Figure 5.7).

Despite their lower carbon content, when salps and larvaceans are excluded from the model there is a noticeable change in total fish biomass. Oligotrophic waters are affected much more than eutrophic regions, with declines of over 40% in fish biomass when salps and larvaceans are excluded, whereas there is no significant change in fish biomass in eutrophic waters (Figure 5.8). Overall, when salps and larvaceans are included there is 17% more fish globally (Figure 5.8).

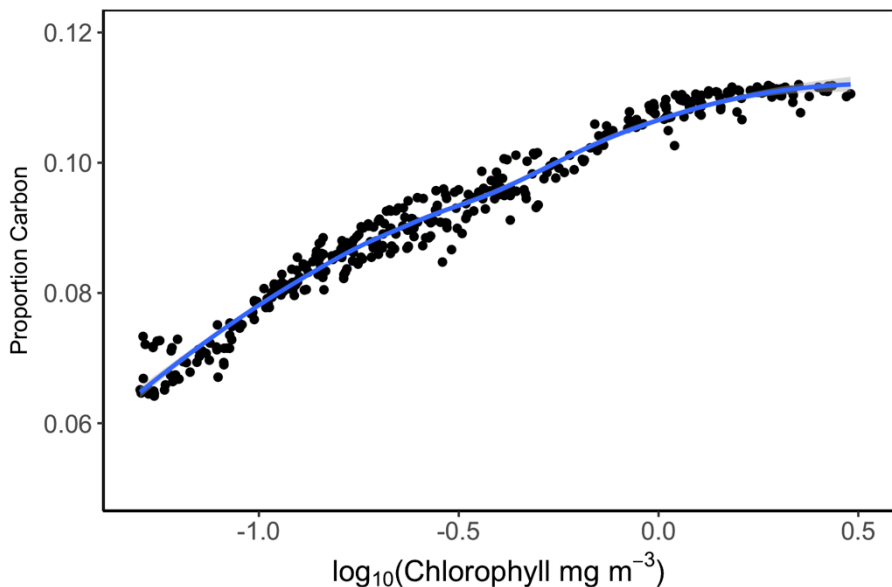


Figure 5.7 Proportion of ingested wet weight by planktivorous fish that is carbon, against chlorophyll a.

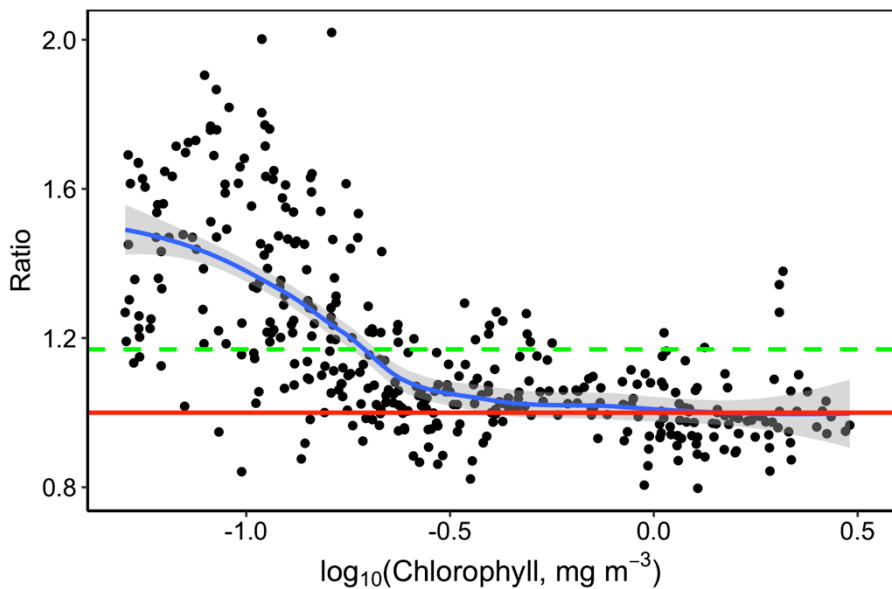


Figure 5.8 Ratio of total fish biomass when zooplankton community includes salps and larvaceans, over total fish biomass when salps and larvaceans are removed from the model, against chlorophyll a. The red line shows where the ratio is 1, the green dashed line is the global average ratio.

5.5 Discussion

Our results support the hypotheses that 1) there will be more trophic steps from phytoplankton to fish in oligotrophic (which we define as areas where chlorophyll *a* < 0.1 mg m⁻³) over eutrophic (which we define as areas where chlorophyll *a* > 1 mg m⁻³) waters, and 2) this will lead to a less efficient energy transfer from phytoplankton to fish, with less fish per unit phytoplankton in oligotrophic waters. Changes in phytoplankton size structure and zooplankton community composition (Figure 5.2) result in almost an extra one third of a trophic step between phytoplankton and planktivorous fish in oligotrophic waters, with the trophic level of planktivorous fish increasing from 3.1 in eutrophic to 3.35 in oligotrophic waters (Figure 5.4 t). In oligotrophic systems where phytoplankton is dominated by picoplankton (Figure 5.2 a), over half of the phytoplankton is consumed by heterotrophic flagellates and ciliates (protist), which are then consumed by crustaceans – omnivorous copepods and euphausiids – (Figure 5.3), which are finally consumed by planktivorous fish (Figure 5.4; Figure 5.5). In contrast, in eutrophic systems where larger microplankton dominate the phytoplankton community, crustaceans consume almost 90% of the phytoplankton directly. As a result, transfer efficiency increases with primary production, with a three-fold increase in the ratio of fish to phytoplankton biomass (Figure 5.6) from oligotrophic (fish-phytoplankton biomass ratio: 0.5) to eutrophic waters (fish-phytoplankton biomass ratio: 1.5). However, our model shows that salps and larvaceans partially offset the decrease in transfer efficiency in oligotrophic waters (Figure 5.8). These groups – with their large body sizes and high predator-prey mass ratios (Supplementary Information Table S 5.2) – are a direct pathway from phytoplankton to planktivorous fish in oligotrophic waters (Figure 5.5 c). However, salps and larvaceans have a lower carbon content compared to crustaceans, which is reflected in the lower carbon content in the diet of planktivorous fish in oligotrophic waters (Figure 5.7). This means they are a less nutritious food source for planktivorous fish. Nevertheless, without salps and larvaceans, total fish biomass is over 40% lower in oligotrophic waters, and 17% lower across the global ocean (Figure 5.8).

Recent studies have suggested that zooplankton amplify climate-driven changes in the phytoplankton, with total zooplankton biomass predicted to vary 10-100% more than phytoplankton in response to climate change (Chust *et al.*, 2014; Stock *et al.*, 2014; Woodworth-Jefcoats *et al.*, 2016). Our results suggest that trophic amplification under climate change could also occur in the fish community. Changes in zooplankton community composition, in response to changes in the phytoplankton, mean that a one unit change in phytoplankton biomass does not necessarily lead to a proportional change in fish biomass

(Figure 5.6). In regions where chlorophyll *a* is greater than 0.5 mg m^{-3} (-0.3 on \log_{10} scale), the ratio of fish to phytoplankton biomass varies around 1.5, which means that any change in fish biomass will be roughly proportional to the change in phytoplankton biomass. However, in regions where the chlorophyll *a* concentration is less than 0.5 mg m^{-3} , the ratio of fish to phytoplankton biomass declines with declining chlorophyll *a*, meaning that any decrease in phytoplankton in these regions will lead to a greater decline in fish biomass. Chust *et al.*, (2014) suggested something similar for zooplankton, where under climate change any decline in phytoplankton biomass in the oligotrophic open ocean led to proportionally larger declines in the zooplankton, whereas in eutrophic areas, the decline in the zooplankton was less than the phytoplankton. Given that regions where average chlorophyll *a* concentration is lower than 0.5 mg m^{-3} comprise a majority of the world's oceans (Supplementary Information Figure S 5.1 b), our results suggest that the dominant response across most the world's oceans to climate-induced declines in the phytoplankton will be negative trophic amplification in the biomass of fish.

Compared to other zooplankton groups, the role of the salps and larvaceans is overlooked and understudied (Henschke *et al.*, 2016), with these groups often lumped with jellyfish as "gelatinous zooplankton". However, owing to their very large predator-prey mass ratios, salps and larvaceans can directly access picoplankton for food (Wirtz, 2012; Supplementary Information Table S 5.2). As a result, these groups emerge from the model as most prevalent in the oligotrophic open ocean, comprising up to 30% of the zooplankton biomass in these regions (Figure 5.2 b). In oligotrophic waters, they make up to 50% of the diet of planktivorous fish, therefore serving a critical role by partially offsetting the decline in ecosystem transfer efficiency by providing a short, efficient pathway from the dominant pico-dominated phytoplankton to planktivorous fish.

Cardona *et al.*, (2012) found that gelatinous zooplankton such as salps make up a large proportion of the diet of large apex predator fish such as tuna and swordfish. This means that the strong presence of salps and larvaceans in oligotrophic waters could be part of the reason why some of the world's largest tuna fisheries are supported in oligotrophic regions (WBPP, 2015) and one of the mechanisms behind Irigoien *et al.*'s (2014) discovery that the global biomass of fish is up to 10 times higher than previously thought. Irigoien *et al.*, (2014) speculated that one of the reasons for their finding was because the transfer efficiency of the oligotrophic open ocean was higher than previously thought, even rivalling eutrophic systems. Our results indicate one possible mechanism behind Irigoien *et al.*'s (2014) findings is the prevalence of salps and larvaceans in the oligotrophic open ocean, efficiently

shunting energy from picoplankton to higher trophic levels and supporting up to half of the total fish biomass. Looking forward, given the ocean's oligotrophic regions are expanding under climate change (Sarmiento *et al.*, 2004; Hays, 2005; Polovina *et al.*, 2008; Acevedo-Trejos *et al.*, 2014; Stock *et al.*, 2014), our results indicate that salps and larvaceans will become a larger component of global zooplankton community, and serve an increasingly important role for energy transfer in less productive future seas.

We included the effect of predator and prey carbon content as a multiplier on gross growth conversion efficiency, which means that prey groups with a higher carbon content contribute more to predator growth, and predators with a low carbon content can grow faster per unit of ingested food (McConville *et al.*, 2017). However this was balanced in the model by how we parameterised predator search rate to scale with carbon content. This was following Kiørboe's (2011) study, who found that search rate scales the same way with carbon weight across 7 different zooplankton functional groups and 12 orders of magnitude in individual carbon weight. We used Kiørboe's (2011) results to parameterise the search rate of the zooplankton groups in the model to scale with their carbon content. This means that predators with a lower carbon content generally grow more per unit of ingested food, however because search rate scales with carbon, this is offset by their lower search rate, which in turn leads to a lower ingestion rate.

Zooplankton with lower carbon content grow faster than more high carbon groups (McConville *et al.*, 2017). Acuña *et al.*, (2011) found that jellyfish clearance rate had the same scaling with wet weight as crustacean zooplankton such as euphausiids and copepods, this conflicts with Kiørboe's (2011) study and means that, per unit carbon, jellyfish have a higher search rate than crustacean zooplankton. Moreover, salps and larvaceans, two of the more gelatinous zooplankton groups, have reported growth rates that are much higher than more carbon rich copepods (Hopcroft and Roff, 1995; Hopcroft *et al.*, 1998; Jaspers *et al.*, 2009). It follows that our model is underestimating the comparatively fast growth rates of more gelatinous groups. This means that we could be underestimating the proportion of the zooplankton made up of salps and larvaceans in oligotrophic waters, and jellyfish in eutrophic waters. By not explicitly incorporating the higher growth rates of the gelatinous groups, we could be underestimating how much fish biomass is supported by salps and larvaceans in oligotrophic areas. On the other hand, if jellyfish are more abundant in eutrophic areas, our model could be overestimating fish productivity in eutrophic regions, by giving them a diet that is more carbon dense than it would be if jellyfish were more dominant.

The model does not incorporate the dynamics of the phytoplankton, instead representing the community as a continually renewable resource for zooplankton, not affected by predation. Because of this, our model could be overestimating the degree of herbivory of groups such as omnivorous copepods and euphausiids in oligotrophic regions, by providing them with a food source of large phytoplankton that is unaffected by predation pressure. No predation feedbacks in the phytoplankton mean that omnivorous groups with an overlap in their phytoplankton prey size ranges are not competing for a limited resource. However, this would not qualitatively change our results, but everything else being equal it does mean that our estimates of the decline in transfer efficiency from eutrophic to oligotrophic waters could be conservative, because we would be underestimating the role of carnivorous groups such as chaetognaths and carnivorous copepods, which do not feed from the phytoplankton community. The processes of nutrient uptake, growth and mortality are strongly size-structured in the phytoplankton, and these size-based relationships have been used to resolve the dynamics of the phytoplankton over large spatial scales (Follows *et al.*, 2007; Fuchs and Franks, 2010; Ward *et al.*, 2012, 2014; Cuesta *et al.*, 2017). An important next step to improving the model presented here would be to incorporate the size-dependent dynamics of the phytoplankton.

Our model only considers how changes in the zooplankton affects energy transfer from phytoplankton to fish, however we know that higher trophic levels are supported by other energy pathways. In shelf regions, a significant part of the phytoplankton sinks to the bottom, where they are consumed by benthic organisms, who are in turn consumed by demersal fish. This benthic energy pathway has implications for the stability, productivity and composition of higher trophic levels (Blanchard *et al.*, 2009; 2011, van Denderen *et al.*, 2018). Similarly, in the open ocean, stocks of tuna and other large fish are supported by mesopelagic fish (Longhurst and Pauly, 1987; Battaglia *et al.*, 2013; Olafsdottir *et al.*, 2016), which feed on zooplankton and detritus from the epi-pelagic zone (Irigoién *et al.*, 2014). Both benthic and mesopelagic pathways are strongly size-structured and have been resolved in functional size-spectrum models (Blanchard *et al.*, 2009, 2011; Maury, 2010). It follows that – along with representing the dynamics of the phytoplankton – it would be possible to integrate these pathways with what has been presented here into a functional size-spectrum model that resolves the major energy pathways from phytoplankton to fish in the global ocean (Blanchard *et al.*, 2017).

The ideas we have considered here are not new (Ryther, 1969; Boyce *et al.*, 2015; Heneghan *et al.*, 2016; Blanchard *et al.*, 2017), but to our knowledge this is the first time

they have been implemented in a trait-based ecosystem model. Despite the pivotal role that zooplankton play in food webs, current global ecosystem models do not represent the functional complexity of the zooplankton (Everett *et al.*, 2017). Here, we used the functional size-spectrum framework to incorporate the extensive experimental work elucidating the size-based feeding characteristics of the zooplankton community. Our application demonstrates the importance of the size structure of the phytoplankton community, and the size-based feeding characteristics of the zooplankton in mediating energy transfer up the marine food chain across the global ocean.

5.6 Supplementary Information

Table S 5.1 Model equations with their units

Description	Equation	Units
Phytoplankton spectrum	$N_p(w, t) = aw^b$	# m ⁻³
Lower boundary condition for group i	$N_i(w_i, t) = P_i \sum_{j \neq i} N_j(w_i, t)$	# m ⁻³
Temperature effect for group i	$\tau = \exp \left(25.55 - \frac{0.63}{8.62 \times 10^{-5} K} \right)$	-
<u>Feeding, Growth and Diffusion:</u>		
Size selection for group i	$\phi_i(w, w') = \exp \left[-\left(\ln(\beta_i(w)w'/w) \right)^2 / 2\sigma_i^2 \right] / (\sigma_i \sqrt{2\pi})$	-
Feeding kernel width parameter for group i	$\sigma_i = 0.05 \log_{10}(\bar{\beta}_i) + 0.33$	-
Search rate for group i	$V_i(w) = C_i \gamma_i w^{\alpha_i}$	m ³ yr ⁻¹
Density of suitable prey from group j for group i	$D_{ij}(w, t) = \int_{w_p}^w \phi_i(w, w') \theta(w, w') N_j(w', t) w' dw'$	g m ⁻³
Gross Growth Efficiency for predator of group i eating prey of group j	$GG_{ij} = 0.25 \frac{C_j}{C_i}$	-
Individual growth rate for group i	$g_i(w, t) = \tau V_i(w) \sum_j GG_{ij} D_{ij}(w, t)$	g yr ⁻¹
Individual diffusion term for group i	$f_i(w, t) = \gamma_i w^{\alpha_i} \sum_j (\tau_G GG_j)^2 \int_{w_p}^w (w')^2 \phi_i(w, w') \theta(w) N_j(w', t) dw'$	g ² yr ⁻¹
<u>Mortality:</u>		
Individual predation rate	$\mu_p(w, t) = \tau \sum_j \int_w^{\bar{W}_j} \phi_j(w', w) \theta(w') V_j(w') N_j(w', t) dw'$	yr ⁻¹
Intrinsic mortality	$\mu_s(w, t) = \tau \delta \left(\frac{w}{W_{s_i}} \right)^\rho$	yr ⁻¹
Total Mortality	$\mu_i(w, t) = \mu_p(w, t) + \mu_s(w, t)$	yr ⁻¹
<u>Diets and Trophic Levels:</u>		
Total biomass from group j consumed by group i	$C_{ij} = \int_{w_{\min_i}}^{\bar{W}_i} N_i(w) V_i(w) \int_{w_{\min_j}}^{\bar{W}_j} \theta(w, w') N_j(w') w' dw' dw$	g yr ⁻¹
Proportion of the diet of group i , that comes from group j	$PD_{ij} = \frac{C_{ij}}{\sum_j C_{ij}}$	-
Trophic level of group i	$TL_i = 1 + \sum_j TL_j \times PD_{ij}$	-

Table S 5.2 Parameter values for the nine zooplankton and three fish groups.

Group	Min. Size, w_i			Max Size, \bar{W}_i			$\log_{10}\text{PPMR}$ range, $\beta_i(w)$	Feeding Kernel Width, σ_i	Carbon - Wet Weight Ratio, C_i
	length	ESD	$\log_{10}(g)^*$	length	ESD	$\log_{10}(g)^*$			
Hetero. Flagellates	-	3 μm^a	-10.7 ^a	-	70 μm^a	-6.8 ^a	0.2 – 0.7 ²	0.36 ^{3^a}	0.15 ⁴
Hetero. Ciliates	-	10 μm^b	-9.3 ^b	-	100 μm^b	-6.3 ^a	2.5 – 2.9 ²	0.47 ^{3^a}	0.15 ⁴
Larvaceans	80 μm^c	100 μm^c	-6.3 ^c	3 mm ^c	2 mm ^c	-2.3 ^c	6.8 – 7.8 ⁷	0.7 ^{3^a}	0.01 ⁹
Omni. Cop.	-	60 μm^d	-7.5 ^d	2.8 mm ^e	0.9 mm ^e	-3.5 ^e	3.6 – 4.6 ²	0.57 ^{3^a}	0.12 ⁹
Carn. Cop.	-	60 μm^d	-7.5 ^d	6 mm ^e	1.8 mm ^e	-2.5 ^e	0.8 – 1.9 ²	0.4 ^{3^a}	0.12 ⁹
Euphausiids	-	0.6 mm ^f	-4.2 ^f	6 cm ^g	1.5 cm ^g	0.3 ^g	6.6 – 7.8 ^{3,15}	0.70 ^{3^a}	0.12 ⁹
Chaetognaths	1 mm ^h	150 μm^h	-5.9 ^h	4 cm ^h	6 mm ^h	-0.9 ^h	1.9 – 3.4 ¹⁶	0.46 ^{3^a}	0.04 ⁹
Salps	0.5 mm ⁱ	0.5 mm ⁱ	-4.3 ⁱ	1.9 cm ⁱ	1.6 cm ⁱ	0.6 ⁱ	6.8 – 8.5 ²	0.7 ^{3^a}	0.01 ⁹
Jellyfish	-	1 mm ^j	-3 ^j	-	15 cm ^j	2.6 ^j	2.7 – 4.7 ¹	0.52 ^{3^a}	0.005 ⁹
Small Fish	-	1 mm ^k	-3 ^k	-	6 cm	2	2 ²¹	1.3 ²²	0.10 ²³
Medium Fish	-	1 mm ^k	-3 ^k	-	27 cm	4	2 ²¹	1.3 ²²	0.10 ²³
Large Fish	-	1 mm ^k	-3 ^k	-	125 cm ^k	6 ^k	2 ²¹	1.3 ²²	0.10 ²³

* g wet weight calculated from ESD, assuming 1 gram = 1 cm³.

^a Feeding kernel widths were calculated with the empirical equation derived in (3), using mean $\log_{10}(\text{PPMR})$ for this group.

Size range source notations: ^a: From Table 3 in (1), ^b: From figure 1 in (5), ^c: Minimum and maximum larvacean trunk lengths taken from (6) and (8) respectively, and converted to ESD and wet weight using equation derived in (7), ^d: Carbon mass obtained from supplementary material in (10), converted to wet weight and ESD using carbon: wet weight ratio from (9) ^e: Maximum omnivorous and carnivorous copepod lengths taken from (11) and converted to ESD and then wet weight using equation derived in (12), ^f: Euphausiid embryo ESD from figure 2 in (13), ^g: Maximum length taken from supplementary material in (3) and converted to ESD and wet weight using equation from (14), ^h: ESD from supplementary material in (3), derived using head width: body length ratio from (16) ⁱ: Minimum and maximum salp length taken from (17) and converted to ESD and wet weight using equation derived in (18), ^j: Taken from supplementary material in (19), ^k: Maximum fish community size taken from (20).

1. Hansen et al. (1997), 2. Wirtz (2012), 3. Fuchs and Franks (2010), 4. Menden-Deuer and Lessard (2000), 5. Taylor (1978), 6. López-Urrutia (2004), 7. Deibel (1998), 8. Hopcroft et al. (1998), 9. Kiørboe (2013), 10. Kiørboe & Hirst (2014), 11. Benedetti et al. (2016), 12. de Azevedo and Dias (2012), 13. Kawaguchi et al. (2011), 14. Meyer and Teschke (2016), 15. Schmidt and Atkinson (2016), 16. Pearre (1982), 17. Henschke et al. (2016), 18. Heron (1988), 19. Acuña et al. (2011), 20. Heneghan et al. (2016), 21. Kerr and Dickie (2001), 22. Andersen et al., (2016b), 23. Pauly and Christensen (1995).

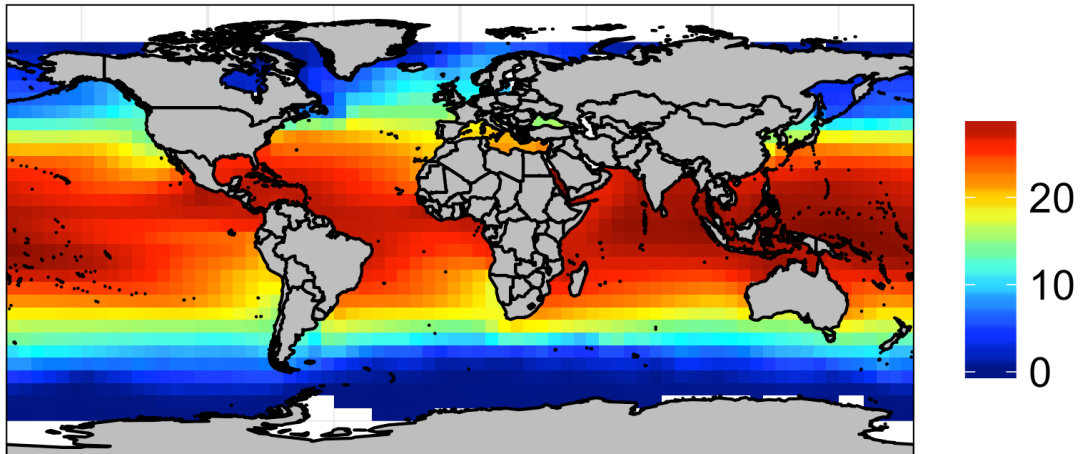
Table S 5.3 Other model parameter values.

Symbol	Definition	Value	Unit	Source
γ	Coefficient of search rate	$\gamma_Z = 8750$	$\text{g C}^{-\alpha}\text{m}^{-3}\text{yr}^{-1}$	1
		$\gamma_F = 6400$	$\text{g C}^{-\alpha}\text{m}^{-3}\text{yr}^{-1}$	2
α	Exponent of search rate	$\alpha_Z = 1$	-	1
		$\alpha_F = 0.8$	-	2
W_S	Body size at which senescence mortality begins	$0.01\bar{W}$	g	5,6
δ	Coefficient of senescence mortality	0.05	$\text{g}^{-\rho}\text{yr}^{-1}$	5,6
ρ	Exponent of senescence mortality	0.3	-	5,6
P	Relative abundance of smallest size class	Flagellates = 1 Ciliates = 0.5 Larvaceans = 0.3 Omni. Copepods = 0.3 Carn. Copepods = 0.7 Euphausiids = 0.7 Chaetognaths = 0.3 Salps = 0.1 Jellyfish = 0.2 Fish = 1	-	-

Z, zooplankton; F, fish.

1. Kiørboe, 2011, 2. Peters 1983, 3. Jennings *et al.*, 2008, 4. Blanchard *et al.*, 2012, 5. Hall *et al.*, 2006, 6. Heneghan *et al.*, 2016.

a) Sea Surface Temperature



a) $\log_{10}(\text{Chlorophyll } \text{mg m}^{-3})$

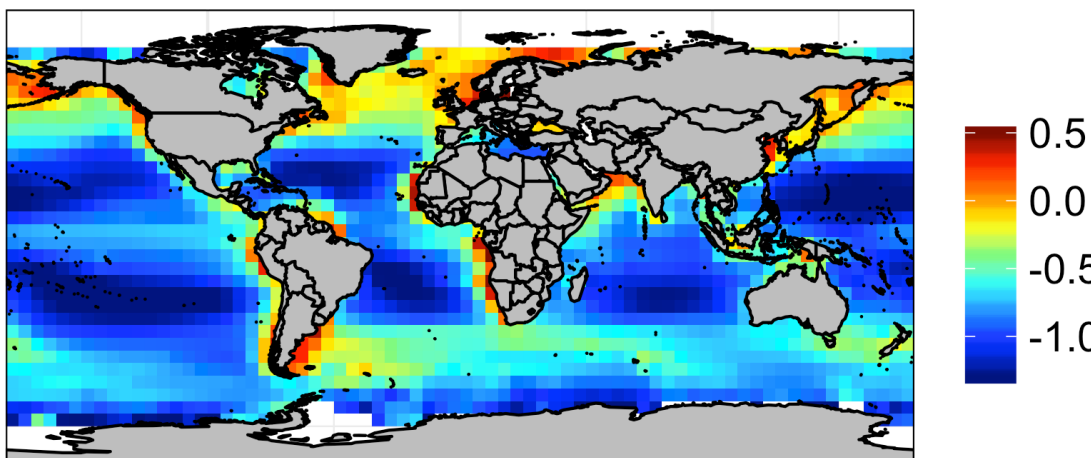


Figure S 5.1 Annual average a) sea surface temperature (SST) and b) $\log_{10}(\text{Chlorophyll } \text{a mg m}^{-3})$, aggregated to 5 degree latitude by 5 degree longitude grid squares. These fields are used as environmental inputs to drive the size-spectrum model. For both SST and $\log_{10}(\text{Chlorophyll } \text{a mg m}^{-3})$, we obtained the annual average for each grid square by averaging over the monthly climatologies obtained from MODIS-Aqua, standardised for the number of months in which satellite observations were taken.

Chapter 6

Concluding Discussion

In this thesis, I have drawn on recent developments in the integration of functional traits in size-spectrum modelling, and the extensive literature on zooplankton physiology, to explore how functional traits give rise to the global zooplankton community, and what this means for how energy moves from phytoplankton to fish across oligotrophic and eutrophic waters. This work has important implications for ecosystem modelling, and our understanding of the role of zooplankton in a changing ocean. In this Chapter, I discuss these implications, highlight future areas of research and finish by identifying some of the limitations of the approach.

6.1 Integrating zooplankton using functional traits

Zooplankton are a complex, ubiquitous group of organisms, serving a critical role in the marine ecosystem as the main pathway of energy transfer from phytoplankton to higher trophic levels (Kiørboe, 2008). However, the complexity of the zooplankton is a subset of the greater complexity of the entire marine ecosystem, from bacteria to whales. The need to understand and predict how entire marine ecosystems function, and their response to external pressures such as climate change and fishing, is critical given our large and growing dependence on their services (Sumaila *et al.*, 2012; Merino *et al.*, 2013; UN DESA, 2015; FAO, 2016), and their contribution to maintaining life on Earth (Field *et al.*, 1998).

This thesis demonstrates the power of the functional size-spectrum framework for resolving the zooplankton in marine ecosystem models. With only the body size ranges, size-based feeding behaviour and carbon content of nine of the most abundant zooplankton functional groups, we could evaluate the response of the marine ecosystem to changes in zooplankton feeding traits (Chapter 3), resolve the emergent structure of the zooplankton community across the global ocean (Chapter 4), and explore the implications for how energy moves from phytoplankton to fish in oligotrophic and eutrophic waters (Chapter 5). These are important results: despite their importance and complexity, zooplankton are typically sidelined within ecosystem studies (Mitra *et al.*, 2014; Everett *et al.*, 2017), with the entire community often represented as one or two amorphous boxes. Our results demonstrate that the trait-based approach is a promising avenue for resolving the dynamics of the zooplankton in marine ecosystem models.

In Chapter 2, we explored the current state of size-spectrum modelling, which has been successfully used to resolve the dynamics of the pelagic size-selective marine consumers spanning sizes of macro zooplankton to large fish (Benoît and Rochet, 2004; Law *et al.*, 2009; Blanchard *et al.*, 2014) and to allow the inclusion of functional groups that behave differently such as the benthic detritivores (Blanchard *et al.*, 2009, 2012), the depth-structured groups in open ocean (Maury, 2012) and recently dynamics of phytoplankton (Law *et al.*, 2016). Although we identified that the vision of representing the whole ecosystem from “bacteria to whales” (Sheldon *et al.*, 1972) has been largely realised, this has been in a rather piecemeal way, and representing whole ecosystems in functional size-spectrum modelling is still an open problem. In other words, despite the advances in resolving the phytoplankton (Law *et al.*, 2016; Cuesta *et al.*, 2017), fish (Maury, 2012; Scott *et al.*, 2014; Andersen *et al.*, 2016b) and even zooplankton on their own (Zhou *et al.*, 2009, 2010), there is limited cross-fertilisation between plankton-focused and higher trophic level functional

size-spectrum models. Our work developing a zooplankton-resolved functional size spectrum model demonstrates that the recent developments in functional size-spectrum modelling, coupled with the extensive literature exploring zooplankton functional traits, means that resolving the zooplankton missing link between plankton-focused and higher trophic level models is achievable.

6.2 Higher trophic levels are sensitive to zooplankton feeding behaviour

How zooplankton are parameterised is one of the most critical components of ecosystem models. Mitra *et al.*, (2014) demonstrated that in a modelled plankton food web, trophic dynamics were sensitive to small changes in parameterisation of zooplankton feeding rates. Similarly, Fuchs and Franks (2010) found that zooplankton with high predator-prey mass ratios (PPMR) which ate a narrow size range (feeding kernel) of prey gave rise to a flatter plankton abundance size spectra (relatively more large organisms), in comparison to zooplankton with small PPMRs and a larger feeding kernel, which led to a steeper plankton size spectra. Moving beyond the plankton, Jennings and Collingridge (2015) demonstrated that the productivity and total biomass of the global fish community was highly sensitive to how energy moved through the lower planktonic trophic levels – from phytoplankton to zooplankton. In Chapter 3, we developed the first functional size-spectrum model which resolved the unique feeding characteristics of the zooplankton, and assessing implications for the resilience, stability and productivity of the fish community. We demonstrated that the resilience and productivity of the fish community, and the stability of the entire system, is highly sensitive to the feeding characteristics of the zooplankton. Zooplankton communities with low PPMRs – such as carnivorous copepods (PPMR ~ 10; Wirtz, 2012) - and wider feeding kernels, stabilised the steady state of the system, but the fish community was less productive, and not as resilient to increasing fishing pressure. In contrast, zooplankton with high PPMRs – such as salps (PPMR ~ 10^8 ; Wirtz, 2012) - and narrower feeding kernels, had more variation in abundance through time, but supported a fish community that had over 100 times more biomass (compared to carnivorous copepods), and was very resilient to increasing fishing pressure. In other words, there is a positive relationship between zooplankton PPMR and ecosystem transfer efficiency, which agrees with previous theoretical (Andersen *et al.*, 2009) and empirical work (Jennings *et al.*, 2002; Barnes *et al.*, 2010). However, higher PPMRs and narrower feeding kernels lead to more variation in the biomass of zooplankton and fish communities through time, which corroborates with theoretical results from previous size-spectrums studies (Law *et al.*, 2009; Datta *et al.*, 2011; Plank and Law, 2012; Zhang *et al.*, 2013), and empirical findings for fish (Blanchard 2008).

6.3 Functional traits explain global patterns in zooplankton community composition

The most common assumption with respect to zooplankton in ecosystem models is that the community structure does not change spatially or temporally (Everett *et al.*, 2017). However, the zooplankton community is not homogenous across environmental gradients, with different groups dominating depending on their relative fitness (Hansen *et al.*, 1994; Barton *et al.*, 2013). Our results in Chapter 3 indicate that this variation in the zooplankton has implications for ecosystem efficiency and productivity, and current model formulations that do not resolve the feeding behaviour of the zooplankton are neglecting a vital ecosystem component.

The challenge of resolving the zooplankton lies in their significant diversity of life histories, and ecological strategies (Litchman *et al.*, 2013). A major advantage of using functional traits is that it allows community structure to emerge based on functional traits and the environment (Bruggemann and Kooijman, 2007; Litchman and Klausmeier, 2008; Litchman *et al.*, 2013). This approach has been successfully demonstrated by Follows *et al.*, (2007) for phytoplankton, and later by Ward *et al.*, (2012, 2014), who showed that size-based processes of nutrient uptake and growth give rise to global patterns in the size structure of the global plankton community. Recently, van Denderen *et al.*, (2018) explained global patterns in marine predatory fish by changes in energy pathways from coastal regions to the open ocean.

In Chapter 4, we developed the first functional size-spectrum model of the marine ecosystem that used body size ranges, size-based feeding characteristics and the carbon content as the governing traits of nine major zooplankton functional groups (heterotrophic flagellates and ciliates, larvaceans, omnivorous and carnivorous copepods, chaetognaths, euphausiids, salps and jellyfish). Across the global ocean, the zooplankton community emerged in response to changes in the size structure of the phytoplankton, and the size-based feeding characteristics and body size ranges of the nine zooplankton groups. We identified clear shifts in the zooplankton community from oligotrophic to eutrophic waters: heterotrophic flagellates and ciliates, larvaceans, carnivorous copepods, chaetognaths and salps were more abundant in oligotrophic waters, omnivorous copepods were prevalent everywhere and euphausiids and jellyfish dominated in eutrophic waters.

To assess how well the emergent patterns of abundance from the functional size-spectrum model represented the actual abundance distributions of the zooplankton functional groups

(excluding heterotrophic flagellates and ciliates), we used *in situ* abundance data from the COPEPOD and IMOS databases. To do this, we had to wrangle the data into a form that was comparable with the output from the model (Everett *et al.*, 2017). We used generalised additive models (GAMs; Wood, 2017), to interpolate the sample data for the different zooplankton groups using environmental variables (sea surface temperature, chlorophyll a concentration and bathymetry), to incorporate the effects of seasonality, and to factor in the dozens of sampling gears and mesh sizes from dozens of cruises over the last 50 years. Except for carnivorous copepods, the emergent distributions of abundance for the different zooplankton from the size-spectrum model broadly agreed with the empirical distributions.

Interpolating zooplankton sample data using environmental variables has been used to create global maps of total zooplankton biomass (Moriarty and O'Brien, 2013), copepod functional traits (Brun *et al.*, 2016) and the abundances of different gelatinous zooplankton groups (Lucas *et al.*, 2014). These statistical models are very useful for constraining and validating ecosystem model estimates (Everett *et al.*, 2017). To that end, we intend to make the statistical models we developed in Chapter 3 publicly available for validation and constraining current and future zooplankton models.

To our knowledge, no global ocean or Earth-system models for carbon cycling currently includes more than two zooplankton groups. However, different zooplankton functional groups have varying body sizes, carbon content and physiology, all of which impact their contribution to carbon cycling (Steinberg and Landry, 2017). For instance, larvaceans are the second most abundant zooplankton group, and shed gelatinous houses every 6 hours. This shedding is a major contributor to marine snow and carbon export to the deep ocean, rivalling the contribution of copepods in the open ocean (Jaspers *et al.*, 2009). Further, salps have large, fast-sinking faecal pellets that contribute disproportionately to carbon flux compared with other zooplankton, providing up to 10-fold more carbon transfer to the seafloor (Fischer *et al.*, 1988). By resolving nine major zooplankton functional groups, their size-based feeding behaviour and their emergent distributions across the global ocean, our model could be extended to refine estimates of carbon export to the deep ocean. Better understanding of the role of zooplankton in the global carbon budget may prove critical in determining whether we achieve the Paris agreement target of < 2°C warming (UN FCCC, 2016).

6.4 Implications for higher trophic levels

The productivity of the fish community ultimately depends on primary production (Pauly and Christensen, 1995; Chassot *et al.*, 2010; Friedland *et al.*, 2012; Stock *et al.*, 2017). However,

it has long been established that primary production alone cannot explain global patterns in higher trophic level productivity across oligotrophic and eutrophic waters (Ryther, 1969). The main hypothesis to explain this is that oligotrophic food webs are less efficient at mediating primary production to higher trophic levels, compared to eutrophic food webs. This is believed to be driven by changes in the size structure of the phytoplankton, which in turn leads to shifts in zooplankton community structure from oligotrophic to eutrophic waters (Stibor *et al.*, 2004; Stock *et al.*, 2008; Barnes *et al.*, 2011; Marañón, 2015). In Chapter 5, we tested these hypotheses using the zooplankton-resolved functional size-spectrum model. We found that from oligotrophic to eutrophic waters, changes in the size structure of the phytoplankton and in the composition of the zooplankton community led to shifts in how energy moved from phytoplankton to fish. In oligotrophic waters, the phytoplankton community is dominated by picoplankton, and over half of the phytoplankton consumption is by heterotrophic flagellates and ciliates (protists), which are then consumed by larger zooplankton - mainly omnivorous copepods and euphausiids (crustaceans) – which are finally consumed by carnivorous zooplankton (chaetognaths, carnivorous copepods and jellyfish) and planktivorous fish. In contrast, in eutrophic waters, large crustaceans directly accessed the more prevalent nano- and micro-phytoplankton for food, cutting out the extra protist step. As a result, the trophic level of planktivorous fish decreased from 3.35 in oligotrophic to 3.1 in eutrophic waters, which means there was an extra one quarter of a trophic step separating phytoplankton and fish in oligotrophic regions. This lead to a shift in the ratio of fish to phytoplankton biomass, with eutrophic waters supporting 1.5 units of fish biomass per unit of phytoplankton, declining to around 0.5 in oligotrophic waters.

Salps and larvaceans, with their large predator-prey mass ratios (PPMRs), are able to directly access picoplankton for food, and these groups were most abundant in oligotrophic waters, comprising about 435% of the zooplankton biomass in low chlorophyll areas. Salps and larvaceans broadly cover the same body size ranges as copepods and euphausiids, and comprised about 50% of the diet of planktivorous fish in oligotrophic regions. These groups were a direct pathway from picoplankton to planktivorous fish in oligotrophic waters, circumventing the longer picoplankton-protist-crustacean-planktivorous fish pathway. Without these groups, total fish biomass was up to 50% lower in oligotrophic waters, with little change in eutrophic waters, and 17% lower across the global ocean.

The role of protists as an intermediate link between picoplankton and larger zooplankton in oligotrophic waters has long been hypothesised (Ryther, 1969; Lalli and Parsons, 1995) and observed (Sommer and Stibor, 2002; Stibor *et al.*, 2004). However, the role of salps and

larvaceans as a direct pathway from picoplankton to planktivorous fish has not been included alongside protists in theoretical studies of how food web structure changes from eutrophic to oligotrophic waters. Instead these groups are lumped together with other large herbivorous zooplankton. This thesis is the first time the unique roles of protists, salps and larvaceans have been explored together in an ecosystem model. Our finding that salps and larvaceans almost double the total biomass of fish in oligotrophic waters highlights the important role these groups play as an alternate energy pathway from picoplankton to fish. This is a significant result, and highlights the need to include these groups in global ecosystem models.

One of the major reasons salps and larvaceans have been underappreciated is their gelatinous body types, which break down quickly and are difficult to identify in stomach content analysis (Henschke *et al.*, 2016), however Cardona *et al.*, (2012) found that gelatinous zooplankton such as salps make up a large proportion of the diet of large apex predator fish such as tuna and swordfish. This means that the strong presence of salps and larvaceans in oligotrophic waters could be part of the reason why some of the world's largest tuna fisheries are supported in oligotrophic regions (WBPP, 2015) and one of the mechanisms behind Irigoien *et al.*'s (2014) discovery that the global biomass of fish is up to 10 times higher than previously thought. What is more, the ocean's oligotrophic regions are expected to expand under climate change (Sarmiento *et al.*, 2004; Hays, 2005; Polovina *et al.*, 2008; Acevedo-Trejos *et al.*, 2014; Stock *et al.*, 2014), which means that salps and larvaceans will become a larger component of the global zooplankton community, and serve an increasingly important role for energy transfer in future, less productive seas.

Our results suggest that changes in the composition of the zooplankton, in response to shifts in phytoplankton community structure, mean that a one unit change in phytoplankton biomass does not necessarily lead to a proportional change in fish biomass. This is corroborated by recent studies which have found that zooplankton amplify changes in the phytoplankton under climate change (Stock *et al.*, 2014; Woodworth-Jefcoats *et al.*, 2016), especially in oligotrophic waters (Chust *et al.*, 2014). In regions where chlorophyll *a* is greater than 0.5 mg m^{-3} (-0.3 on \log_{10} scale), the ratio of fish to phytoplankton biomass varies around 1.5, which means that any change in fish biomass will be roughly proportional to the change in phytoplankton biomass. However, in regions where the chlorophyll *a* concentration is less than 0.5 mg m^{-3} , the ratio of fish to phytoplankton biomass declines with declining chlorophyll *a*, meaning that any decrease in phytoplankton in these regions will lead to a greater decline in fish biomass. This means that anticipated declines in

phytoplankton biomass under climate change will lead to non-linear changes in fish biomass from oligotrophic to eutrophic waters. This agrees with Barange *et al.*, (2014), who found that countries with fisheries in oligotrophic waters at low/mid latitudes, would see their fisheries worse off under climate change, compared to other nations. Amplification of declining phytoplankton biomass, due to changes in the zooplankton, would be a devastating outcome for smaller Pacific Island nations surrounded by oligotrophic waters, where fisheries constitute 5-25% of GDP (Sumaila *et al.*, 2016).

Our zooplankton-resolved functional size-spectrum model could help refine global estimates of fish biomass and its distribution, which would allow better forecasts of future fisheries and inform global food security. Estimates of fish biomass are contingent upon model choice, since different models include contrasting assumptions about top-down and bottom-up processes, the role of different functional groups and the parameterisation of processes such as growth and mortality (Tittensor *et al.*, 2018). In response to this, there have been studies comparing the output of different ecosystem models, and their responses to external pressures such as fishing and climate change (Fulton and Smith, 2004; Travers *et al.*, 2004; Jones *et al.*, 2013; Jones and Cheung, 2014; Woodworth-Jefcoats *et al.*, 2015). More recently, the Fisheries and Marine Ecosystem Model Intercomparison Project (Fish-MIP) has been established to analyse the output of over a dozen ecosystem models to assess climate and fisheries impacts on marine ecosystems, and highlight areas of uncertainty associated with different model structures and assumptions (Tittensor *et al.*, 2018). Given that our model is the first functional size-spectrum model to resolve the emergent zooplankton community, whilst resolving phytoplankton community size structure and the dynamics of the fish community, we believe it would be an important contribution to the Fish-MIP project, by permitting a more detailed study of how sensitive total fish biomass and fisheries output is to the dynamics of lower trophic levels.

Fishing causes perturbations in the upper trophic levels of marine ecosystems, however trophic cascades can mean that fishing has implications beyond trophic levels directly targeted (Frank *et al.*, 2005; Andersen and Pedersen, 2010; Steneck, 2012). By resolving the size-based feeding interactions between fish and the zooplankton, our model could be used to explore the effects of fishing on zooplankton community structure, and possible feedbacks from zooplankton, to the fish community. Further, we could investigate how different fishing methods could influence carbon export via the zooplankton. This could inform future fishing practices: in land-based agriculture carbon credits are earned for

changing farming practices to promote carbon sequestration. Future fishing methods which increase carbon sequestration by the zooplankton could be identified and promoted.

There is evidence that human-induced stresses such as overfishing, eutrophication and climate change are promoting increases in jellyfish, although whether the mechanisms behind increasing jellyfish blooms are human-induced or part of a natural cycle is strongly debated (Richardson *et al.*, 2009; Condon *et al.*, 2013; Gibbons and Richardson, 2013; Lucas *et al.*, 2014). Planktivorous fish and jellyfish share similar body size ranges and prey, however jellyfish are usually considered to represent a “trophic dead-end”, in contrast with planktivorous fish which are an important prey source for piscivorous fish, seabirds and mammals (Robinson *et al.*, 2014). Planktivorous fish are a target for commercial and recreational fishers in most regions, whereas jellyfish are only targeted in relatively few areas such as the seas around China and South East Asia (Angel *et al.*, 2014; Robinson *et al.*, 2014). Our model resolves the trophic interplay between planktivorous fish and jellyfish, by resolving the significant overlap in the composition of their diets from oligotrophic to eutrophic waters. Looking forward, our model could be used to explore how increasing harvesting pressure on fish across oligotrophic and eutrophic waters could lead to shifts from an ecosystem where fish are the top predator, to a less desirable gelatinous apex predator state. We could also explore the efficacy of proposed management strategies such as fishing jellyfish populations to reduce their numbers (Purcell *et al.*, 2007; Boero, 2013; Gibbons *et al.*, 2016).

6.5 Limitations of approach

In this thesis, we were able resolve the composition of the zooplankton community and their role in the marine ecosystem across global environmental gradients, using a handful of functional traits. Our focus here was improving the dynamics of the zooplankton in a global-scale model, however there are several limitations to our approach, and the model we constructed, which must be addressed.

The focus of current functional size-spectrum models is on fish, with the dynamics of the plankton either ignored or poorly resolved. This was a major motivation for the work presented in this thesis. The importance of zooplankton in the marine ecosystem is well established, and the recent theoretical developments in functional size-spectrum modelling, coupled with the extensive empirical work exploring their functional traits means that improving their representation is achievable. To that end, we have made significant advances incorporating the role of the zooplankton. However, poor plankton resolution also includes the phytoplankton, the dynamics of which we did not resolve. Instead, we held the

phytoplankton community spectrum static, with the slope, intercept and maximum size determined by the synoptic model developed by Brewin *et al.*, (2010), which divides total chlorophyll *a* into pico, nano and micro plankton size classes.

Without incorporating feedback from predation, omnivorous zooplankton groups in the model effectively have a constantly renewing phytoplankton resource, no matter how much predation pressure is exerted on the phytoplankton community. No predation feedbacks in the phytoplankton mean that omnivorous groups with an overlap in their phytoplankton prey size ranges are not competing for a limited resource. This gives omnivorous groups an advantage over carnivorous groups such as carnivorous copepods, chaetognaths and jellyfish, which are unable to access the phytoplankton for food. As a result, our model could be underestimating the role of carnivorous groups such as carnivorous copepods, chaetognaths and jellyfish. However, we do not believe that this would not change our finding that oligotrophic systems are less efficient than eutrophic systems. In fact, if the role of carnivorous groups is underestimated in oligotrophic waters, it would probably mean our estimates of the decline in transfer efficiency from eutrophic to oligotrophic waters are conservative. Recent size-based models of the phytoplankton take advantage of the size-structured processes of nutrient uptake, growth and mortality to resolve the structure and dynamics of the phytoplankton community over large spatial scales (Follows *et al.*, 2007; Fuchs and Franks, 2010; Ward *et al.*, 2012, 2014; Cuesta *et al.*, 2018). Future work could involve coupling the innovations of current phytoplankton size-based models, with the model presented here, using the functional size-spectrum framework.

We included the effect of predator and prey carbon content on growth gross efficiency as a multiplier on the ingestion rate, which means that prey groups with a higher carbon content contribute more to predator growth, and predators with a low carbon content can grow faster per unit of ingested food (McConville *et al.*, 2017). However this was balanced in the model by how we parameterised predator search rate to scale with carbon content. This was following Kiørboe's (2011) study, who found that search rate scales the same way with carbon weight across 7 different functional groups – including jellyfish - and 12 orders of magnitude in individual carbon weight. Our parameterisation means that predators with a lower carbon content generally grow more per unit of ingested food, however because search rate scales with carbon, this is offset by their lower search rate, which leads to a lower ingestion rate.

McConville *et al.*, (2017) found that growth rates in the zooplankton were inversely rated to carbon content; zooplankton with lower carbon content grow faster than more high carbon

groups, and Acuña *et al.*, (2011) found that jellyfish clearance rate had the same scaling with wet weight as crustacean zooplankton such as euphausiids and copepods. This conflicts with Kiørboe's (2011) study and means that, per unit carbon, jellyfish have a higher search rate than crustacean zooplankton. Moreover, salps and larvaceans, two of the more gelatinous zooplankton groups, have reported growth rates that are much higher than more carbon rich copepods (Hopcroft and Roff, 1995; Hopcroft *et al.*, 1998; Jaspers *et al.*, 2009). It follows that our model is underestimating the comparatively fast growth rates of more gelatinous groups. This means that we could be underestimating the proportion of the zooplankton made up of salps and larvaceans in oligotrophic waters, and jellyfish in eutrophic waters. By not explicitly incorporating the higher growth rates of salps and larvaceans, we could be underestimating how much fish biomass is supported by the salps and larvaceans in oligotrophic areas. On the other hand, if jellyfish are more abundant in eutrophic areas, our model could be overestimating fish productivity in eutrophic regions, by giving them a diet that is more carbon dense than it would be if higher growth rates meant that jellyfish were a larger component of the zooplankton in eutrophic regions.

The model was driven using annual average chlorophyll a concentration and sea surface temperature, aggregated to 5 x 5 degree grid squares. This allowed us to demonstrate how macro-trends in environmental conditions, coupled with size-based functional traits, drive the global structure of the zooplankton community. The main driver of the abundance and composition of the zooplankton community was changes in the size structure of the phytoplankton community, which was controlled by annual average chlorophyll a concentration. However, the time-scale of growth and mortality in the phytoplankton is daily, not yearly. What is more, seasonal cycles of boom and bust in the phytoplankton is a major driver of variation of zooplankton productivity (Falkowski *et al.*, 1988; Atkinson, 1996), which we smoothed over by using a yearly temporal resolution. A recent functional size-spectrum study found that seasonal variations in the size structure of the plankton did not affect the average community size-spectrum (Datta and Blanchard, 2016). However, that study was focused on fish. Future study, investigating how seasonal processes affect zooplankton community structure at the global scale, would be worth considering.

The effects of sea surface temperature were incorporated in the model as a multiplier on growth and mortality terms, held constant across all functional groups. The poor correlation between the modelled and empirical abundance of carnivorous copepods in Chapter 4 highlights the important role of temperature in explaining the distribution of this group, which our model was not able to resolve. We used the same temperature scaling for all groups

because, despite the range of studies elucidating temperature scaling for different zooplankton species and groups (e.g., Hansen *et al.*, 1997; Forster *et al.*, 2011; Kiørboe and Hirst, 2014), the model's functional groups are resolved by body size, feeding behaviour and carbon content, and it is unclear how temperature affects organisms grouped at this level. Future work could address this by relaxing the definition of the functional groups, letting them emerge across environmental gradients within the functional size-spectrum framework, based on randomly assigned physiological traits. This would be similar to Follows *et al.*, (2007), who used this approach to derive the global composition of the phytoplankton community. Similarly, Andersen *et al.*, (2015a), suggested this approach could be applied to resolve a continuum of trophic strategies in unicellular plankton, between pure phototrophy (phytoplankton) and phagotrophy (unicellular zooplankton). For the heterotrophic zooplankton considered in this thesis, temperature scaling, PPMR and body size range could be defined as continuums, where various randomly assigned combinations of these functional traits compete with one another, until a global community structure emerges from the functional size-spectrum model. An approach like this could also be used to resolve other continuous functional traits which we did not include in this thesis, such as offspring size and extent of diel vertical migration, both of which have been established as important functional traits governing the distribution and role of zooplankton in the marine ecosystem (Hays, 2003; Bianchi *et al.*, 2013; Litchman *et al.*, 2013; Brun *et al.*, 2016).

Our model follows the current common practice of assuming plankton communities can be cleanly divided into autotrophs and heterotrophs. However, there is growing evidence that the line between producers and consumers is unclear, with a growing number of plankton taxa identified which can both photosynthesise and consume living prey (Stoecker, 1998; Mitra *et al.*, 2016). The role of mixotrophic plankton in marine food webs is unclear (Stocker *et al.*, 2017), however modelling studies suggest that this group could increase transfer efficiency and carbon flux in the marine ecosystem (Mitra and Flynn, 2010; Mitra *et al.*, 2014; Ward and Follows, 2015). Further work is required to investigate their role in the marine ecosystem, and the processes that give rise to their distribution across the global ocean.

6.6 Final remarks

There is a growing recognition amongst modellers of the need to develop ecosystem models which couple the dynamics of higher and lower trophic levels (Fulton, 2010; Rose *et al.*, 2010; Mitra *et al.*, 2014). The functional size-spectrum framework has emerged as a flexible framework to do this, with the potential to address many of the limitations discussed in Section 6.5. In this thesis, we have demonstrated the power of the functional size-spectrum

framework to resolve the dynamics of the zooplankton across the global ocean. The model we developed is the first functional size-spectrum model to resolve key size-based traits of important zooplankton functional groups, and is a step toward the goal of resolving the dynamics of the entire ecosystem, from bacteria to whales, within a single modelling framework.

“With more knowledge about the size selectivity of the various functional groups of the zooplankton and about their actual occurrence in a given pelagic environment, it should be possible to construct a reliable yet simple size-based model of the pelagic food web for that particular situation.”

Benni Hansen et al., (1994)

References

- Abe, Y., Natsuike, M., Matsuno, K., Terui, T., Yamaguchi, A., and Imai, I. (2013). Variation in assimilation efficiencies of dominant *Neocalanus* and *Eucalanus* copepods in the subarctic Pacific: Consequences for population structure models. *Journal of Experimental Marine Biology and Ecology* 449, 321–329.
- Acevedo-Trejos, E., Brandt, G., Steinacher, M., and Merico, A. (2014). A glimpse into the future composition of marine phytoplankton communities. *Frontiers in Marine Science* 1, 1–12.
- Acuña, J.L., López-Urrutia, A., and Colin, S. (2011). Faking Giants: The Evolution of High Prey Clearance Rates in Jellyfishes. *Science* 333, 1627–1629.
- Agawin, N. S. R., Duarte, C. M., and Agustí, S. (2000). Nutrient and temperature control of the contribution of picoplankton to phytoplankton biomass and production. *Limnology and Oceanography* 45, 591–600.
- Andersen, K. H., Aksnes, D. L., Berge, T., Fiksen, O. (2015a). Modelling emergent trophic strategies in plankton. *Journal of Plankton Research*, 37, 862-868.
- Andersen, K. H., Berge, T., Gonçalves, R. J., Hartvig, M., Heuschele, J., Hylander, S., et al., (2016a). Characteristic sizes of life in the oceans, from bacteria to whales. *Annual Review of Marine Science* 8, 1–25.
- Andersen, K. H., and Beyer, J. E. (2006). Asymptotic Size Determines Species Abundance in the Marine Size-spectrum. *American Naturalist* 168, 54–61.
- Andersen, K. H. and Beyer, J. E. (2015b). Size structure, not metabolic scaling rules, determines fisheries reference points. *Fish and Fisheries* 16, 1–22.
- Andersen, K. H., Beyer, J. E., and Lundberg, P. (2009). Trophic and individual efficiencies of size-structured communities. *Proceedings of the Royal Society B: Biological Sciences* 276, 109–114.
- Andersen, K. H., Jacobsen, N. S., Life, O., Resources, A., Castle, C., Security, G. F., et al. (2016b). The theoretical foundations for size-spectrum models of fish communities. *Canadian Journal of Fisheries and Aquatic Sciences* 588, 1–47.
- Andersen, K. H., and Pedersen, M. (2010). Damped trophic cascades driven by fishing in model marine ecosystems. *Proceedings of the Royal Society B: Biological Sciences* 277, 795–802.

- Angel, D. L., Edelist, D., and Freeman, S. (2016). Local perspectives on regional challenges: jellyfish proliferation and fish stock management along the Israeli Mediterranean coast. *Regional Environmental Change* 16, 315–323.
- Atkinson, A., Shreeve, R. S., Pakhomov, E. A., Priddle, J., Blight, S. P., and Ward, P. (1996). Zooplankton response to a phytoplankton bloom near South Georgia, Antarctica. *Marine Ecology Progress Series* 144, 195–210.
- Atkinson, A., Siegel, V., Pakhomov, E. A., and Rothery, P. (2004). Long-term decline in krill stock and increase in salps within the Southern Ocean. *Nature* 432, 100–103.
- Azevedo, F. de., Dias, J.D., De, Louizi and Braghin, L. (2012). Length – weight regressions of the microcrustacean species from a tropical floodplain. *Acta Limnologica Brasiliensis* 24, 1–11.
- Baird, M. E., and Suthers, I. M. (2007). A size-resolved pelagic ecosystem model. *Ecological Modelling* 3, 185–203.
- Banas, N. S. (2011). Adding complex trophic interactions to a size-spectral plankton model: Emergent diversity patterns and limits on predictability. *Ecological Modelling* 222, 2663–2675.
- Barange, M., Merino, G., Blanchard, J. L., Scholtens, J., Harle, J., Allison, E. H., et al. (2014). Impacts of climate change on marine ecosystem production in societies dependent on fisheries. *Nature Climate Change* 4, 211–216.
- Barnes, C., Bethea, D. M., Brodeur, R. D., Spitz, J., Ridoux, V., Pusineri, C., et al. (2008). Predator and Prey body size in marine food webs. *Ecology* 89, 81.
- Barnes, C., Irigoien, X., De Oliveira, J. A. A., Maxwell, D., and Jennings, S. (2011). Predicting marine phytoplankton community size structure from empirical relationships with remotely sensed variables. *Journal of Plankton Research* 33, 13–24.
- Barnes, C., Maxwell, D., Reuman, D. C., and Jennings, S. (2010). Global patterns in predator-prey size relationships reveal size dependency of trophic transfer efficiency. *Ecology* 91, 222–232.
- Barton, A. D., Pershing, A. J., Litchman, E., Record, N. R., Edwards, K. F., Finkel, Z. V., et al. (2013). The biogeography of marine plankton traits. *Ecology Letters*, 16, 522–534.
- Battaglia, P., Andaloro, F., Consoli, P., Esposito, V., Malara, D., Musolino, S., et al. (2013). Feeding habits of the Atlantic bluefin tuna, *Thunnus thynnus* (L . 1758), in the central Mediterranean Sea (Strait of Messina). *Helgoland Marine Research*. 67, 97–107.
- Benedetti, F., Gasparini, S., and Ayata, S. (2016). Identifying copepod functional groups from species functional traits. *Journal of Plankton Research*. 38, 159–166.

- Benoît, E., and Rochet, M.-J. (2004). A continuous model of biomass size-spectra governed by predation and the effects of fishing on them. *Journal of Theoretical Biology* 226, 9–21.
- Bianchi, D., Stock, C., Galbraith, E.D., and Sarmiento, J.L. (2013). Diel vertical migration: ecological controls and impacts on the biological pump in a one-dimensional ocean model. *Global Biogeochemical Cycles* 27, 478–491.
- Blanchard, J.L. (2008). “The dynamics of size-structured ecosystems.” [PhD dissertation]. [York (UK)]: University of York.
- Blanchard, J. L., Andersen, K. H., Scott, F., Hintzen, N. T., Piet, G., and Jennings, S. (2014). Evaluating targets and trade-offs among fisheries and conservation objectives using a multispecies size-spectrum model. *Journal of Applied Ecology* 51, 612–622.
- Blanchard, J. L., Dulvy, N. K., Jennings, S., Ellis, J. R., Pinnegar, J. K., Tidd, A., et al. (2005). Do climate and fishing influence size-based indicators of Celtic Sea fish community structure? *ICES Journal of Marine Science* 62, 405–411.
- Blanchard, J.L., Heneghan, R.F., Everett, J.D., Trebilco, R. and Richardson, A.J. (2017). From Bacteria to Whales: Using Functional Size Spectra to Model Marine Ecosystems. *Trends in Ecology and Evolution*. 32, 174–186.
- Blanchard, J. L., Jennings, S., Holmes, R., Harle, J., Merino, G., Allen, J. I., et al. (2012). Potential consequences of climate change for primary production and fish production in large marine ecosystems. *Philosophical Transactions of the Royal Society B: Biological Sciences* 367, 2979–2989.
- Blanchard, J. L., Jennings, S., Law, R., Castle, M. D., McCloghrie, P., Rochet, M. J., et al. (2009). How does abundance scale with body size in coupled size-structured food webs? *Journal of Animal Ecology* 78, 270–280.
- Blanchard, J. L., Law, R., Castle, M. D., and Jennings, S. (2011). Coupled energy pathways and the resilience of size-structured food webs. *Theoretical Ecology* 4, 289–300.
- Bone, Q. (1997). *The biology of pelagic tunicates*. Oxford: Oxford University Press.
- Boudreau, P.R., and Dickie, L.M. (1992). Biomass spectra of aquatic ecosystems in relation to fisheries yield. *Canadian Journal of Fisheries and Aquatic Sciences* 49, 1528–1538.
- Boukal, D. S. (2014). Trait- and size-based descriptions of trophic links in freshwater food webs: Current status and perspectives. *Journal of Limnology* 73, 171–185.
- Boyce, D.G., Frank, K.T., and Leggett, W.C. (2015). From mice to elephants: Overturning the “one size fits all” paradigm in marine plankton food chains. *Ecology Letters* 18, 504–515.

- Boxshall, G.A. and Halsey, S.H. (2004). *An Introduction to Copepod Diversity*. London: The Ray Society.
- Brewin, R.J.W., Sathyendranath, S., Hirata, T., Lavender, S.J., Barciela, R., and Hardman-Mountford, N.J. (2010). A three-component model of phytoplankton size class for the Atlantic Ocean. *Ecological Modelling* 221, 1472–1483.
- Brierley, A. S., and Kingsford, M. J. (2009). Impacts of Climate Change on Marine Organisms and Ecosystems. *Current Biology* 19, R602–R614.
- Brierley, A.S. (2014). Diel vertical migration. *Current Biology* 24, R1074–R1076.
- Brose, U., Blanchard, J.L., Eklöf, A., Galiana, N., Hartvig, M., Hirt, M.R., et al. (2016). Predicting the consequences of species loss using size-structured biodiversity approaches. *Biological Reviews* 92, 684–697.
- Brown, J. H., Gillooly, J. F., Allen, A. P., Savage, V. M., and West, G. B. (2004). Toward a metabolic theory of ecology. *Ecology* 85, 1771–1789.
- Bruggeman, J., and Kooijman, S. A. L. M. (2007). A biodiversity-inspired approach to aquatic ecosystem modelling. *Limnology and Oceanography* 52, 1533–1544.
- Brun, P., Payne, M.R., and Kiørboe, T. (2016) Trait biogeography of marine copepods – an analysis across scales. *Ecology Letters* 19, 1403–1413.
- Bucklin, A., Nishida, S., Shnack-Schiel, S., Wiebe, P.H., Lindsay, D., Machida, R.J., et al. “A Census of Zooplankton of the Global Ocean”. *Life in the World’s Oceans: Diversity, Distribution, and Abundance*. 1st ed. Blackwell Publishing, 2010. 247 – 265.
- Canales, T. M., Law, R., and Blanchard, J. L. (2015). Shifts in plankton size spectra modulate growth and coexistence of anchovy and sardine in upwelling systems. *Canadian Journal of Fisheries and Aquatic Sciences* 73, 611–621.
- Cardona, L., de Quevedo, I. Á., Borrell, A., and Aguilar, A. (2012). Massive consumption of gelatinous plankton by mediterranean apex predators. *PLoS ONE* 7, e31329.
- Carlotti, F., and Poggiale, J. C. (2010). Towards methodological approaches to implement the zooplankton component in “end to end” food web models. *Progress in Oceanography* 84, 20–38.
- Carozza, D. A., Bianchi, D., and Galbraith, E. (2016). The ecological module of BOATS-1.0: a bioenergetically-constrained model of marine upper trophic levels suitable for studies of fisheries and ocean biogeochemistry. *Geosciences Model Development* 8, 10145–10197.
- Castle, M.D., Blanchard, J. L., and Jennings, S. (2011). Predicted Effects of Behavioural Movement and Passive Transport on Individual Growth and Community Size Structure in Marine Ecosystems. *Advances in Ecological Research* 45, 41–66.

- Cermeño, P. and Figueiras, F.G. (2008). Species richness and cell-size distribution: Size structure of phytoplankton communities. *Marine Ecology Progress Series* 357, 79–85.
- Chang, C. W., Miki, T., Shah, F. K., Kao, S. J., Wu, J. T., Sastri, A. R., et al. (2014). Linking secondary structure of individual size distribution with nonlinear size-trophic level relationship in food webs. *Ecology*, 95, 897–909.
- Chassot, E., Bonhommeau, S., Dulvy, N.K., Mélin, F., Watson, R., Gascuel, D., et al. (2010). Global marine primary production constrains fisheries catches. *Ecology Letters* 13, 495-505.
- Cheung, W. W. L., Lam, V. W. Y., Sarmiento, J. L., Kearney, K., Watson, R., and Pauly, D. (2009). Projecting global marine biodiversity impacts under climate change scenarios. *Fish and Fisheries* 10, 235–251.
- Chust, G., Allen, J. I., Bopp, L., and Schrum, C. (2014). Biomass changes and trophic amplification of plankton in a warmer ocean. *Global Change Biology* 2010, 2124–2139.
- Condon, R. H., Duarte, C. M., Pitt, K. A., Robinson, K. L., Lucas, C. H., Sutherland, K. R., et al. (2013). Recurrent jellyfish blooms are a consequence of global oscillations. *Proceedings of the National Academy of Sciences* 110, 1000–1005.
- Cuesta, J.A., Delius, G.W., and Law, R. (2018). Sheldon spectrum and the plankton paradox: two sides of the same coin—a trait-based plankton size-spectrum model. *Journal of Mathematical Biology* 76, 67-96.
- Datta, S. and Blanchard, J. L. (2016). The effects of seasonal processes on size-spectrum dynamics. *Canadian Journal of Fisheries and Aquatic Sciences* 73, 598–610.
- Datta, S., Delius, G. W., and Law, R. (2010). A jump-growth model for predator-prey dynamics: Derivation and application to marine ecosystems. *Bulletin of Mathematical Biology* 72, 1361–1382.
- Datta, S., Delius, G. W., Law, R., and Plank, M. J. (2011). A stability analysis of the power-law steady state of marine size-spectra. *Journal of Mathematical Biology* 63, 779–799.
- Dam, H and Baumman, H. “Climate Change, Zooplankton and Fisheries”. *Climate Change Impacts on Fisheries and Aquaculture: A Global Analysis*. 1st ed. John Wiley and Sons, 2017. 851-874.
- Davis, C.S. (1984). Predatory Control of Copepod Seasonal Cycles on Georges Bank. *Marine Biology* 82, 31-40.
- Davison, P. C., Checkley, D. M., Koslow, J. A., and Barlow, J. (2013). Carbon export mediated by mesopelagic fishes in the northeast Pacific Ocean. *Progress in Oceanography* 116, 14–30.
- De Roos, A. M., Persson, L. (2013). *Population and community ecology of ontogenetic*

- development*, Princeton, NJ: Princeton University Press.
- De Roos, A. M., Schellekens, T., Van Kooten, T., Van De Wolfshaar, K., Claessen, D., and Persson, L. (2008). Simplifying a physiologically structured population model to a stage-structured biomass model. *Theoretical Population Biology* 73, 47–62.
- Diebel, D. and Lee, S.H. (1992). Retention efficiency of submicron particles by the pharyngeal filter of the pelagic tunicate *Oiopleura vanhoeffeni*. *Marine Ecology Progress Series* 81, 25-30.
- Doney, S. C., Ruckelshaus, M., Duffet, J. E., Barry, J. P., Chan, F., English, C. A., et al. (2002). Climate Change Impacts on Marine Ecosystems. *Estuaries* 25, 149–164.
- Dormann, C.F., Elith, J., Bacher, S., Buchmann, C., Carl, G., Carré, G., et al. (2012). Collinearity: a review of methods to deal with it and a simulation study evaluating their performance. *Ecography* 36, 27-46.
- Drexler, M. and Ainsworth, C.H. (2013). Generalised Additive Models Used to Predict Species Abundance in the Gulf of Mexico: An Ecosystem Modelling Tool. *PLoS One* 8, 1–7.
- Dueri, S., Bopp, L., and Maury, O. (2014). Projecting the impacts of climate change on skipjack tuna abundance and spatial distribution. *Global Change Biology* 20, 742–753.
- Dueri, S. and Maury, O. (2012) Modelling the effect of marine protected areas on the population of skipjack tuna in the Indian Ocean. *Aquatic Living Resources*, 26, 171-178.
- Duplisea, D. E., Jennings, S., Warr, K. J., and Dinmore, T. A. (2002). A size-based model of the impacts of bottom trawling on benthic community structure. *Canadian Journal of Fisheries and Aquatic Sciences* 59, 1785–1795.
- Edwards, K.F., Litchman, E. & Klausmeier, C.A. (2013). Functional traits explain phytoplankton community structure and seasonal dynamics in a marine ecosystem. *Ecology Letters* 16, 56–63.
- Elton, C.S. (1927). *Animal Ecology*, New York, NY: The MacMillan Company.
- Everett, J.D., Baird, M.E., Buchanan, P., Bulman, C., Davies, C., Downie, R., et al. (2017). Modelling What We Sample and Sampling What We Model: Challenges for Zooplankton Model Assessment. *Frontiers in Marine Science* 4, 1–19.
- Falkowski, P. G., Barber, R. T., and Smetacek, V. (1998). Biogeochemical controls and feedbacks on ocean primary production. *Science* 281, 200–206.
- FAO. (2016). *The State of World Fisheries and Aquaculture 2016. Contributing to food security and nutrition for all*. Rome.

- Field, C. B., Behrenfeld, M. J., Randerson, J. T., and Falkowski, P. (1998). Primary production of the biosphere: Integrating terrestrial and oceanic components. *Science* 281, 237–240.
- Fischer, C., Fütterer, D., Gersonde, R., Honjo, S., Ostermann, D., and Wefer, G. (1988). Seasonal variability of particle flux in the Weddell Sea and its relation to ice-cover. *Nature* 335, 426-428.
- Frank, K. T., Petrie, B., Choi, J. S., and Leggett, W. C. (2005). Ecology: Trophic cascades in a formerly cod-dominated ecosystem. *Science* 308, 1621–1623.
- Friedland, K. D., Stock, C., Drinkwater, K. F., Link, J. S., Leaf, R. T., Shank, B. V., et al. (2012). Pathways between Primary Production and Fisheries Yields of Large Marine Ecosystems. *PLoS One* 7, e28945.
- Follows, M.J., Dutkiewicz, S., Grant, S., and Chisholm, S. (2007). Emergent biogeography of microbial communities in a model ocean. *Science* 315, 1843–6.
- Forster, J., Hirst, A.G. and Woodward, G. (2011). Growth and Development Rates Have Different Thermal Responses. *The American Naturalist* 178, 668-678.
- Fuchs, H. L., and Franks, P. J. S. (2010). Plankton community properties determined by nutrients and size-selective feeding. *Marine Ecology Progress Series* 413, 1–15.
- Fulton, E. A., and Smith, A. D. M. (2004). Lessons learnt from a comparison of three ecosystem models for Port Phillip Bay, Australia. *African Journal of Marine Science* 26, 219–243.
- Fulton, E. A. (2010). Approaches to end-to-end ecosystem models. *Journal of Marine Systems* 81, 171–183.
- Fung, T., Farnsworth, K. D., Reid, D. G., and Rossberg, A. G. (2015). Impact of biodiversity loss on production in complex marine food webs mitigated by prey-release. *Nature Communications* 6, 6657.
- García-Comas, C., Chang, C., Ye, L., Sastri, A.R., Lee, Y., Gong, G., et al. (2014). Mesozooplankton size structure in response to environmental conditions in the East China Sea: How much does size spectra theory fit empirical data of a dynamic coastal area? *Progress in Oceanography* 121, 141–157.
- Gibbons, M. J., Boero, F., and Brotz, L. (2016). We should not assume that fishing jellyfish will solve our jellyfish problem. *ICES Journal of Marine Science* 73, 1012–1018.
- Gibbons, M. J., and Richardson, A. J. (2013). Beyond the jellyfish joyride and global oscillations: Advancing jellyfish research. *Journal of Plankton Research* 35, 929–938.
- Gillooly, J. F., Charnov, E. L., and West, G. B. (2002). Effects of size and temperature on developmental time. *Nature* 417, 70–73.

- Goldman, J. C., and Dennett, M. R. (1990). Dynamics of prey selection by an omnivorous flagellate. *Marine Ecology Progress Series* 59, 183–194.
- Gorsky, G., Dallot, S., Sardou, J., Fenaux, R., Carré, C., Palazzoli, I. (1988). C and N composition of some northwestern Mediterranean zooplankton and micronekton species. *Journal of Experimental Marine Biology and Ecology* 124, 133–144.
- Guillet, J., Aumont, O., Poggiale, J.-C., and Maury, O. (2016b). Effects of lower trophic level biomass and water temperature on fish communities: A modelling study. *Progress in Oceanography* 146, 22–37.
- Guillet, J., Poggiale, J.-C., and Maury, O. (2016a). Modelling the community size-spectrum: recent developments and new directions. *Ecological Modelling* 337, 4–14.
- Hall, S. J., Collie, J. S., Duplisea, D. E., Jennings, S., Bravington, M., and Link, J. (2006). A length-based multispecies model for evaluating community responses to fishing. *Canadian Journal of Fisheries and Aquatic Sciences* 63, 1344–1359.
- Hansen, B., Bjørnsen, P. K., and Hansen, P. J. (1994). The size ratio between planktonic predators and their prey. *Limnology and Oceanography* 39, 395–403.
- Hansen, P.J. Bjørnsen, P. K., and Hansen, P. J. (1997). Zooplankton grazing and growth: Scaling within the 2-2,000- μm body size range. *Limnology and Oceanography* 42, 687–704.
- Haren, H. van, and Compton, T.J. (2013). Diel vertical migration in deep sea plankton is finely tuned to latitudinal and seasonal day length. *PLoS One* 8, e64435.
- Harfoot, M. B. J., Newbold, T., Tittensor, D.P., Emmott, S., Hutton, J., Lyutsarev, V., et al. (2014). Emergent Global Patterns of Ecosystem Structure and Function from a Mechanistic General Ecosystem Model. *PLoS Biology* 12, e1001841.
- Hartvig, M., Andersen, K. H., and Beyer, J. E. (2011). Food web framework for size-structured populations. *Journal of Theoretical Biology* 272, 113–122.
- Hartvig, M. and Andersen, K. H. (2013). Coexistence of structured populations with size-based prey selection. *Theoretical Population Biology* 89, 24–33.
- Havens, K. E., and Beaver, J. R. (2013). Zooplankton to phytoplankton biomass ratios in shallow Florida lakes: An evaluation of seasonality and hypotheses about factors controlling variability. *Hydrobiologia* 703, 177–187.
- Hays, G.C. (2003). A review of the adaptive significance and ecosystem consequences of zooplankton diel vertical migrations. *Hydrobiologia* 503, 163–170.
- Hays, G. C., Richardson, A. J., and Robinson, C. (2005). Climate change and marine plankton. *Trends in Ecology and Evolution* 20, 337-344.

- Heath, M. R. (1995). Size-spectrum dynamics and the planktonic ecosystem of Loch Linnhe. *ICES Journal of Marine Science* 52, 627–642.
- Henschke, N., Everett, J. D., Richardson, A. J., and Suthers, I. M. (2016). Rethinking the Role of Salps in the Ocean. *Trends in Ecology and Evolution* 31, 720-733.
- Heneghan, R.F., Everett, J.D., Blanchard, J.L., Richardson, A.J. (2016). Zooplankton Are Not Fish: Improving Zooplankton Realism in Size-Spectrum Models Mediates Energy Transfer in Food Webs. *Frontiers in Marine Science* 3, 1–15.
- Henschke, N., Everett, J.D., Richardson, A.J., and Suthers, I.M. (2016). Rethinking the role of salps in the ocean. *Trends in Ecology and Evolution* 31, 720-733.
- Heron, A.C. (1988). Length-weight relation in the salp *Thalia democratica* and potential of salps as a source of food. *Marine Ecology Progress Series* 42, 125–132
- Hirata, T., Hardman-Mountford, N.J., Brewin, R.J.W., Aiken, J., Barlow, R., Suzuki, K., et al. (2011). Synoptic relationships between surface Chlorophyll- a and diagnostic pigments specific to phytoplankton functional types. *Biogeosciences* 8, 311-327.
- Hoegh-Guldberg, O., and Bruno, J. F. (2010). The impact of climate change on the world's marine ecosystems. *Science* 328, 1523–1528.
- Holste, L. and Peck, M.A. (2006). The effects of temperature and salinity on egg production and hatching success of Baltic *Acartia tonsa* (Copepoda: Calanoida): a laboratory investigation. *Marine Biology* 148, 1061-1070.
- Hopcroft, R.R., Roff, J.C. and Bouman, H.A. (1998). Zooplankton growth rates: the larvaceans Appendicularia, Fritallaria and Oikopleura in trophic waters. *Journal of Plankton Research*. 20, 539-555.
- Houle, J. E., de Castro, F., Cronin, M. A., Farnsworth, K. D., Gosch, M., and Reid, D. G. (2016). Effects of seal predation on a modelled marine fish community and consequences for a commercial fishery. *Journal of Applied Ecology* 53, 54–63.
- Hua, E., Zhang, Z., Warwick, R. M., Deng, K., Lin, K., Wang, R., et al. (2013). Pattern of benthic biomass size spectra from shallow waters in the East China Seas. *Marine Biology* 160, 1723–1736.
- Huys, R. and Boxshall, G.A. (1991). *Copepod Evolution*. London: The Ray Society.
- IPCC, (2014). “Summary for Policymakers.” *Climate Change 2014: Mitigation of Climate Change. Contribution of Working Group III to the Fifth Assessment Report of the Intergovernmental Panel on Climate Change*. Cambridge University Press, Cambridge, United Kingdom and New York, NY, USA.

- Irigoién, X., Klevjer, T. A., Røstad, A., Martinez, U., Boyra, G., Acuña, J. L., et al. (2014). Large mesopelagic fishes biomass and trophic efficiency in the open ocean. *Nature Communications* 5, 3271.
- Irwin, A. J., Finkel, Z. V., Schofield, O. M. E., and Falkowski, P. G. (2006). Scaling-up from nutrient physiology to the size-structure of phytoplankton communities. *Journal of Plankton Research* 28, 459–471.
- Jacobsen, N. S., Burgess, M. G., and Andersen, K. H. (2016). Efficiency of fisheries is increasing at the ecosystem level. *Fish and Fisheries*, 18, 199–211.
- Jacobsen, N. S., Essington, T. E., and Andersen, K. H. (2015). Comparing model predictions for ecosystem-based management. *Canadian Journal of Fisheries and Aquatic Sciences* 73, 666–676.
- Jacobsen, N. S., Gislason, H., and Andersen, K. H. (2014). The consequences of balanced harvesting of fish communities. *Proceedings of the Royal Society B: Biological Sciences* 281, 20132701.
- Jaspers, C., Nielsen, T. G., Carstensen, J., Hopcroft, R. R., and Møller, E. F. (2009). Metazooplankton distribution across the Southern Indian Ocean with emphasis on the role of Larvaceans. *Journal of Plankton Research* 31, 525–540.
- Jennings, S., and Blanchard, J. L. (2004). Fish abundance with no fishing: Predictions based on macroecological theory. *Journal of Animal Ecology* 73, 632–642.
- Jennings, S., and Collingridge, K. (2015). Predicting Consumer Biomass, Size-Structure, Production, Catch Potential, Responses to Fishing and Associated Uncertainties in the World's Marine Ecosystems. *PLoS One* 10, e0133794.
- Jennings, S. and Mackinson, S. (2003). Abundance-body mass relationships in size-structured food webs. *Ecology Letters* 6, 971–974.
- Jennings, S., Pinnegar, J. K., Polunin, N. V. C., and Boon, T. W. (2001). Weak cross-species relationships between body size and trophic level belie powerful size-based trophic structuring in fish communities. *Journal of Animal Ecology* 70, 934–944.
- Jennings, S., Warr, K. J., and Mackinson, S. (2002). Use of size-based production and stable isotope analyses to predict trophic transfer efficiencies and predator-prey body mass ratios in food webs. *Marine Ecology Progress Series* 240, 11–20.
- Jennings, S., Mélin, F., Blanchard, J. L., Forster, R. M., Dulvy, N. K., and Wilson R. W. (2008). Global-scale predictions of community and ecosystem properties from simple ecological theory. *Proceedings of the Royal Society B: Biological Sciences* 275, 1375–1383.

- Jennings, S., and Warr, K. J. (2003). Smaller predator-prey body size ratios in longer food chains. *Proceedings of the Royal Society B: Biological Sciences* 270, 1413–1417.
- Jennings, S. and Wilson, R.W. (2009). Fishing impacts on the marine inorganic carbon cycle. *Journal of Applied Ecology* 46, 976–982.
- Jones, M. C., and Cheung, W. W. L. (2015). Multi-model ensemble projections of climate change effects on global marine biodiversity. *ICES Journal of Marine Science* 72, 741–752.
- Jones, M. C., Dye, S. R., Pinnegar, J. K., Warren, R., and Cheung, W. W. L. (2013). Applying distribution model projections for an uncertain future: The case of the Pacific oyster in UK waters. *Aquatic Conservation: Marine and Freshwater Ecosystems* 23, 710–722.
- Kawaguchi, S., Kurihara, H., King, R., Hale, L., Berli, T., Robinson, J. P., et al. (2011). Will krill fare well under Southern Ocean acidification? *Biology Letters* 7, 288–291.
- Kelly-Gerrey, B. A., Martin, A. P., Bett, B. J., Anderson, T. R., Kaariainen, J. I., Main, C. E., et al. (2014). Benthic biomass size spectra in shelf and deep-sea sediments. *Biogeosciences* 11, 6401–6416.
- Kerr, S. R. (1974). Theory of size distribution in ecological communities. *Journal of the Fisheries Research Board of Canada* 31, 1859–1862.
- Kerr, S.R and Dickie, L.M. (2008). *The Biomass Spectrum: A Predator-Prey Theory of Aquatic Production*. New York: Columbia University Press.
- Kleiber, M. (1932). Body size and metabolism. *Hilgardia* 6, 315–351.
- Kiørboe, T. (2008). *A Mechanistic Approach to Plankton Ecology*. Princeton, NJ: Princeton University Press.
- Kiørboe, T. (2010). What makes pelagic copepods so successful? *Journal of Plankton Research* 33, 677–685.
- Kiørboe, T. (2011). How zooplankton feed: Mechanisms, traits and trade-offs. *Biological Reviews* 86, 311–339.
- Kiørboe, T. (2013). Zooplankton body composition. *Limnology and Oceanography* 58, 1843–1850.
- Kiørboe T (2016). Foraging mode and prey size spectra of suspension-feeding copepods and other zooplankton. *Marine Ecology Progress Series* 558, 15-20.
- Kiørboe, T., and Hirst, A. G. (2014). Shifts in mass scaling of respiration, feeding, and growth rates across life-form transitions in marine pelagic organisms. *The American Naturalist* 183, E118-30.

- Lalli, C., and Parseon, T. (1997). *Biological Oceanography An Introduction 2nd Edition.* Oxford: Elsevier.
- Landry, M. R. (1981). Switching between herbivory and carnivory by the planktonic marine copepod *Calanus pacificus*. *Marine Biology* 65, 77–82.
- Landry, M. R., Hassett, R. P., Fagerness, V., Downs, J., and Lorenzen, C. J. (1984). Effect of food acclimation on assimilation efficiency of *Calanus pacificus*. *Limnology and Oceanography* 29, 361–364.
- Lassalle, G., Lobry, J., Le Loc'h, F., Mackinson, S., Sanchez, F., Tomczak, M. T., et al. (2013). Ecosystem status and functioning: searching for rules of thumb using an intersite comparison of food web models of Northeast Atlantic continental shelves. *ICES Journal of Marine Science* 70, 135–149.
- Law, R., Plank, M. J., James, A., and Blanchard, J. L. (2009). Size-spectra dynamics from stochastic predation and growth of individuals. *Ecology* 90, 802–811.
- Law, R., Plank, M. J., and Kolding, J. (2016). Balanced exploitation and coexistence of interacting, size-structured, fish species. *Fish and Fisheries* 17, 281–302.
- Leadbeater, B and Green J.C. (2000). *The flagellates: unity, diversity and evolution.* London: CRC Press.
- Lee, H., Ban, S., Ikeda, T. and Matsuishi, T. (2003). Effect of temperature on development, growth and reproduction in the marine copepod *Pseudocalanus newmani* at satiating food condition. *Journal of Plankton Research* 25, 261-271.
- Lefort, S., Aumont, O., Bopp, L., Arsouze, T., Gehlen, M., and Maury, O. (2015). Spatial and body-size dependent response of marine pelagic communities to projected global climate change. *Global Change Biology* 21, 154–164.
- Le Mézo, P., Lefort, S., Séférian, R., Aumont, O., Maury, O., Murtugudde, R., et al. (2016). Natural variability of marine ecosystems inferred from a coupled climate to ecosystem simulation. *Journal of Marine Systems* 153, 55–66.
- Le Quéré, C., Buitenhuis, E.T., Moriarty, R., Alvain, S., Aumont, O., Bopp, L., et al. (2016). Role of zooplankton dynamics for Southern Ocean phytoplankton biomass and global biogeochemical cycles. *Biogeosciences* 13, 4111–4133.
- Levinton, J.S. (2013). *Marine Biology: Function, Biodiversity, Ecology.* 4th ed, Oxford: Oxford University Press.
- Ling, S. D., Scheibling, R. E., Rassweiler, A., Johnson, C. R., Shears, N., Connell, S. D., et al. (2014). Global regime shift dynamics of catastrophic sea urchin overgrazing. *Philosophical Transactions of the Royal Society B: Biological Sciences* 370, 20130269.

- Litchman, E. and Klausmeier, C. A. (2008). Trait-based community ecology of phytoplankton. *Annual Review of Ecology, Evolution and Systematics* 39, 615–639.
- Litchman, E., Ohman, M.D., and Kiørboe, T. (2013). Trait-based approaches to zooplankton communities. *Journal of Plankton Research* 35, 473–484.
- Longhurst, A.R., and Pauly, D. (1987). *Ecology of Tropical Oceans*. London: Academic Press Inc.
- López-Urrutia, A., Acuña, J. L., Irigoien, X., and Harris, R. (2003). Food limitation and growth in temperate epipelagic appendicularians (Tunicata). *Marine Ecology Progress Series* 252, 143–157.
- López-Urrutia, A., Harris, R.P., and Smith, T. (2004). Predation by calanoid copepods on the appendicularian *Oikopleura*. *Limnology and Oceanography* 49, 303–307.
- López-Urrutia, A., San Martin, E., Harris, R.P., and Irigoien, X. (2006). Scaling the metabolic balance of the oceans. *Proceedings of the National Academy of Sciences* 103, 8739–8744.
- Lucas, C.H., Jones, D.O.B., Hollyhead, C.J., Condon, R.H., Duarte, C.M., Graham, W.M., et al. (2014). Gelatinous zooplankton biomass in the global oceans: geographic variation and environmental drivers. *Global Ecology and Biogeography* 23, 701-714.
- Mack, H.R., Conroy, J.D., Blocksom, K.A., Stein, R.A., and Ludsin, S.A. (2012). A comparative analysis of zooplankton field collection and sample enumeration methods. *Limnology and Oceanography* 10, 41-53.
- Mann, K.H. and Lazier, J.R.N. (2006). *Dynamics of Marine Ecosystems: Biological-Physical Interactions in the Oceans*. Oxford: Oxford University Press.
- Macpherson, E., Gordoa, A., and García-Rubies, A. (2002). Biomass Size Spectra in Littoral Fishes in Protected and Unprotected Areas in the NW Mediterranean. *Estuarine, Coastal and Shelf Science* 55, 777–788.
- Marañón, E. (2015). Cell Size as a Key Determinant of Phytoplankton Metabolism and Community Structure. *Annual Review of Marine Science* 7, 241–264.
- Maury, O. (2010). An overview of APECOSM, a spatialized mass balanced “Apex Predators ECOSystem Model” to study physiologically structured tuna population dynamics in their ecosystem. *Progress in Oceanography* 84, 113–117.
- Maury, O., Faugeras, B., Shin, Y. -J., Poggiale, J. -C. C, Ari, T. Ben, and Marsac, F. (2007a). Modelling environmental effects on the size-structured energy flow through marine ecosystems. Part 1: The model. *Progress in Oceanography* 74, 479–499.
- Maury, O., Faugeras, B., Shin, Y.-J., Poggiale, J. -C. C, Ari, T. Ben, and Marsac, F. (2007b). Modelling environmental effects on the size-structured energy flow through marine

- ecosystems. Part 2: Simulations. *Progress in Oceanography* 74, 500–514.
- Maury, O. and Poggiale, J. -C. C. (2013). From individuals to populations to communities: A dynamic energy budget model of marine ecosystem size-spectrum including life history diversity. *Journal of Theoretical Biology* 324, 52–71.
- McGill, B.J., Enquist, B.J., Weiher, E., and Westoby, M. (2006). Rebuilding community ecology from functional traits. *Trends in Ecology and Evolution* 21, 178-185.
- Menden-Deuer, S. and Lessard, E.J. (2000). Carbon to volume relationships for dinoflagellates, diatoms, and other protist plankton. *Limnology and Oceanography* 45, 569–579
- Merino, G., Barange, M., Blanchard, J. L., Harle, J., Holmes, R., Allen, I., et al. (2012). Can marine fisheries and aquaculture meet fish demand from a growing human population in a changing climate? *Global Environmental Change* 22, 795–806.
- Meyer, B. and Teschke, M. “Physiology of Euphausia superba”. *Biology and Ecology of Antarctic Krill*. 1st ed, Springer International Publishing, 2016. 145-175.
- Mitra, A., and Davis, C. (2010) Defining the ‘to’ in end-to-end models. *Progress in Oceanography* 84, 39-42.
- Mitra, A. and Flynn, K. J. (2010). Modelling mixotrophy in harmful algal blooms: more or less the sum of the parts? *Journal of Marine Systems* 83, 158 – 169.
- Mitra, A., Castellani, C., Gentleman, W.C., Jónasdóttir, S.H., Flynn, K.J., Bode, A., et al. (2014). Bridging the gap between marine biogeochemical and fisheries sciences; configuring the zooplankton link. *Progress in Oceanography* 129, 176–199.
- Moloney, C. L. and Field, J. G. (1989). General allometric equations for rates of nutrient uptake, ingestion, and respiration in plankton organisms. *Limnology and Oceanography* 34, 1290–1299.
- Montagnes, D. J. S., and Fenton, A. (2012). Prey-abundance affects zooplankton assimilation efficiency and the outcome of biogeochemical models. *Ecological Modelling* 243, 1–7.
- Morán, X. A. G., López-Urrutia, Á., Calvo-Díaz, A., and Li, W. K. W. (2010). Increasing importance of small phytoplankton in a warmer ocean. *Global Change Biology* 16, 1137–1144.
- Moreno-Ostos, E., Blanco, J.M., Agustí, S., Lubián, L.M., Rodríguez, V., Palomino, R.L., et al. (2015). Phytoplankton biovolume is independent from the slope of the size-spectrum in the oligotrophic Atlantic Ocean. *Journal of Marine Systems* 152, 42–50
- Moriarty, R. (2009). “The role of macro-zooplankton in the global carbon cycle.” [PhD dissertation]. [Norwich (UK)]: University of East Anglia.

- Moriarty, R., and O'Brien, T. D. (2013). Distribution of mesozooplankton biomass in the global ocean. *Earth System Science Data* 5, 45–55.
- Mousseau, L., Fortier, L., and Legendre, L. (1998). Annual production of fish larvae and their prey in relation to size-fractionated primary production (Scotian Shelf, NW Atlantic). *ICES Journal of Marine Science*. 55, 44–57.
- Mulder, C. (2010). Soil fertility controls the size-specific distribution of eukaryotes. *Annals of the New York Academy of Sciences* 1195, E74-81.
- Mullaney, T. J. and Suthers, I. M. (2013). Entrainment and retention of the coastal larval fish assemblage by a short-lived, submesoscale, frontal eddy of the East Australian Current. *Limnology and Oceanography* 58, 1546–1556.
- Naito, Y., Costa, D. P., Adachi, T., Robinson, P. W., Fowler, M., and Takahashi, A. (2013). Unravelling the mysteries of a mesopelagic diet: a large apex predator specialises on small prey. *Functional Ecology* 27, 710–717.
- Nash, K. L., Graham, N. A. J., Wilson, S. K., and Bellwood, D. R. (2013). Cross-scale Habitat Structure Drives Fish Body Size Distributions on Coral Reefs. *Ecosystems* 16, 478–490.
- O'Brien, T., 2005. Copepod: a global plankton database. U.S. Dep. Commerce, NOAA Tech. Memo. NMFS-F/SPO-73, 136.
- Ohman, M.D. and Romagnan, J.-B. (2016). Nonlinear effects of body size and optical attenuation on Diel Vertical Migration by zooplankton. *Limnology and Oceanography*. 61, 765–770.
- Olafsdottir, D., Mackenzie, B. R., and Chosson-p, V. (2016). Dietary Evidence of Mesopelagic and Pelagic Foraging by Atlantic Bluefin Tuna (*Thunnus thynnus* L.) during Autumn Migrations to the Iceland Basin. *Frontiers in Marine Science* 3, 1–23.
- Pauly, D., Graham, W., Libralato, S., Morissette, L., and Deng Palomares, M.L. (2009). Jellyfish in ecosystems, online databases, and ecosystem models. *Hydrobiologia* 616, 66-85.
- Pauly, D. and Christensen, V. (1995). Primary production required to sustain global fisheries. *Nature* 374, 255–2.
- Pauly, D. & Palomares, M. (2005). Fishing down the marine food web: it is far more pervasive than we thought. *Bulletin of Marine Science* 76, 197–211.
- Pearre, S. (1980). Feeding by chaetognatha: the relation of prey size to predator size in several species. *Marine Ecology Progress Series* 3, 125–134.
- Pearre, S. (1982). Feeding by Chaetognatha : Aspects of Inter- and Intra-Specific Predation. *Marine Ecology Progress Series* 7, 33–45.

- Pearre, S. (2003). Eat and run? The hunger\satiation hypothesis in vertical migration : history, evidence and consequences. *Biological Reviews of the Cambridge Philosophical Society* 78, 1–79.
- Peters, R.H. (1983). *The Ecological Implications of Body Size*. Cambridge: Cambridge University Press.
- Plagányi, É.E. (2007). *Models for an ecosystem approach to fisheries*. FAO Fisheries Technical Paper. No. 477. Rome, FAO.
- Plank, M.J. and Law, R. (2012). Ecological drivers of stability and instability in marine ecosystems. *Theoretical Ecology* 5, 465–480.
- Plank, M. J., Kolding, J., Law, R., Gerritsen, H. D., and Reid, D. (2016). Balanced harvesting can emerge from fishing decisions by individual fishers in a small-scale fishery. *Fish and Fisheries*, 18, 212-225.
- Polovina, J. J., Howell, E. A., and Abecassis, M. (2008). Ocean's least productive waters are expanding. *Geophysical Research Letters* 35, 2–6.
- Pope, J. G., Rice, J. C., Daan, N., Jennings, S., and Gislason, H. (2006). Modelling an exploited marine fish community with 15 parameters - results from a simple size-based model. *ICES Journal of Marine Science* 63, 1029–1044.
- Press, W.H., Teukolsky, S.A., Vetterling, W.T., Flannery, B.P. (2007). *Numerical Recipes: The Art of Scientific Computing, Third Edition*. New York: Cambridge University Press.
- Purves, D. (2013) Ecosystems: Time to model all life on Earth. *Nature* 493, 7–9.
- Purcell J.E, and Arai M.N. (2001) Interactions of pelagic cnidarians and ctenophores with fish: a review. *Hydrobiologia* 451, 27–44.
- Purcell, J. E., Uye, S. I., and Lo, W. T. (2007). Anthropogenic causes of jellyfish blooms and their direct consequences for humans: A review. *Marine Ecology Progress Series* 350, 153–174.
- R Development Core Team. 2016. R: a Language and Environment for Statistical Computing. R Foundation for Statistical Computing, Vienna, Austria. ISBN 3-900051-07-0, <http://www.R-project.org>.
- Rakhesh, A.V., Raman, A.V., Kalavati, C., Subramanain, B.R., Sharma, V.S., Sunitha Babu, E., et al. (2008) Zooplankton community structure across an eddy-generated upwelling band close to a tropical bay-mangrove ecosystem. *Marine Biology* 154, 953-972.
- Raymont, J.E.G. (2014). *Plankton and Productivity in the Oceans: Volume 1: Phytoplankton*. London: Pergamon Press

- Richardson, A. J., Bakun, A., Hays, G. C., and Gibbons, M. J. (2009). The jellyfish joyride: causes, consequences and management responses to a more gelatinous future. *Trends in Ecology and Evolution* 24, 312–322.
- Reuman, D. C., Gislason, H., Barnes, C., Melin, F., and Jennings, S. (2014). The marine diversity spectrum. *Journal of Animal Ecology* 83, 963–979.
- Reuman, D. C., Mulder, C., Banašek-Richter, C., Cattin Blandenier, M., Breure, A. M., Den Hollander, H., et al. (2009). Allometry of Body Size and Abundance in 166 Food Webs. *Advances in Ecological Research*, 41, 1–44.
- Reuman, D. C., Mulder, C., Raffaelli, D., and Cohen, J. E. (2008). Three allometric relations of population density to body mass: Theoretical integration and empirical tests in 149 food webs. *Ecology Letters* 11, 1216–1228.
- Rhyne, A.L.. Ohs, C.L. and Stenn, E. (2009). Effects of temperature on reproduction and survival of the calanoid copepod *Pseudodiaptomus pelagicus*. *Aquaculture*, 292, 53-59.
- Richardson, S.A., Possingham, H.P. and Noye, J. (1996). Diel vertical migration: modelling light-mediated mechanisms. *Journal of Plankton Research* 18, 2199-2222.
- Robinson, K., Ruzicka, J., Decker, M. B., Brodeur, R., Hernandez, F., Quiñones, J., et al. (2014). Jellyfish, Forage Fish, and the World's Major Fisheries. *Oceanography* 27, 104–115.
- Rodríguez, J., Tintoré, J., Allen, J. T., Blanco, J. M., Gomis, D., Reul, A., et al. (2001). Mesoscale vertical motion and the size structure of phytoplankton in the ocean. *Nature* 410, 360–363.
- Rogers, A., Blanchard, J. L., and Mumby, P. J. (2014). Vulnerability of coral reef fisheries to a loss of structural complexity. *Current Biology* 24, 1000–1005.
- Rose, K.A., Allen, J.I., Artioli, Y., Barange, M., Blackford, J., Carlotti, F., et al. (2011). End-To-End Models for the Analysis of Marine Ecosystems: Challenges, Issues and Next Steps. *Marine and Coastal Fisheries: Dynamics, Management, and Ecosystem Science* 2, 115-130.
- Rousseaux, C. S., and Gregg, W. W. (2015). Recent decadal trends in global phytoplankton composition. *Global Biogeochemical Cycles* 29, 1674–1688.
- Rutherford, L.A., Simpson, S.D., Jennings, S., Johnson, M.P., Blanchard, J.L., Schön, P., et al. (2015). Future fish distributions constrained by depth in warming seas. *Nature Climate Change*. 5, 569–573.
- Ryther J.H. (1969). Photosynthesis and fish production in the sea. *Science* 166, 72-76

- Sailley, S.E., Polimene, L., Mitra, A., Atkinson, A. and Allen, J. Icarus. (2015). Impact of zooplankton food selectivity on plankton dynamics and nutrient cycling. *Journal of Plankton Research* 37, 519-529.
- Saiz, E., and Kiørboe, T. (1995). Predatory and suspension feeding of the copepod *Acartia tonsa* in turbulent environments. *Marine Ecology Progress Series* 122, 147–158.
- San Martin, E., Harris, R. P., and Irigoien, X. (2006). Latitudinal variation in plankton size spectra in the Atlantic Ocean. *Deep Sea Research. Part II, Topical Studies in Oceanography* 53, 1560–1572.
- Sarmiento, J. L., Slater, R., Barber, R., Bopp, L., Doney, S. C., Hirst, A. C., et al. (2004). Response of ocean ecosystems to climate warming. *Global Biogeochemical Cycles* 18, GB3003.
- Sauer, T. (2012). *Numerical Analysis*. 2nd ed, Boston: Pearson Education.
- Schmidt, K and Atkinson, A. "Feeding And Food Processing Antarctic Krill (*Euphausia Superba Dana*)". *Biology And Ecology Of The Antarctic Krill*. 1st ed. Springer International Publishing, 2016. 175-224.
- Schnedler-Meyer, N. A., Mariani, P., and Kiørboe, T. (2016). The global susceptibility of coastal forage fish to competition by large jellyfish. *Proceedings of the Royal Society B: Biological Sciences* 283, 20161931.
- Schofield, O., Ducklow, H. W., Martinson, D. G., Meredith, M. P., Moline, M. a., and Fraser, W. R. (2010). How Do Polar Marine Ecosystems Respond to Rapid Climate Change? *Science*, 328, 1520–1523.
- Schwinghamer, P. (1988). Influence of pollution along a natural gradient and in a mesocosm experiment on biomass-size spectra of benthic communities . *Marine Ecology Progress Series* 46, 199–206.
- Scott, F., Blanchard, J. L., and Andersen, K. H. (2014). mizer: an R package for multispecies, trait-based and community size-spectrum ecological modelling. *Methods in Ecology and Evolution* 5, 1121–1125.
- Sheldon, R. W., Evelen, T. P. T., and Parsons, T. R. (1967). On the Occurrence and Formation of Small Particles in Seawater. *Limnology and Oceanography* 7, 367–375.
- Sheldon, R. W., Prakash, A., and Sutcliffe Jr., W.H. (1972). The size distribution of particles in the ocean. *Limnology and Oceanography* 17, 327–340.
- Sheldon, R. W., Sutcliffe, W. H., and Paranjape, M. A. (1977). Structure of pelagic food chain and relationship between plankton and fish production. *Journal of the Fisheries Research Board of Canada* 34, 2344–2353.
- Shin, Y. J., and Cury, P. (2004). Using an individual-based model of fish assemblages to

- study the response of size spectra to changes in fishing. *Canadian Journal of Fisheries and Aquatic Sciences* 61, 414–431.
- Silvert, W., and Platt, T. (1978). Energy flux in the pelagic ecosystem: A time-dependent equation. *Limnology and Oceanography* 23, 813–816.
- Sommer, U., and Stibor, H. (2002). Copepoda - Cladocera - Tunicata: The role of three major mesozooplankton groups in pelagic food webs. *Ecological Research* 17, 161–174.
- Spence, M. A., Blackwell, P. G., and Blanchard, J. L. (2016). Parameter uncertainty of a dynamic multi-species size-spectrum model. *Canadian Journal of Fisheries and Aquatic Sciences* 9, 1–9.
- Spitz, J., Mourocq, E., Schoen, V., and Ridoux, V. (2010). Proximate composition and energy content of forage species from the Bay of Biscay: high-or low-quality food? *ICES Journal of Marine Science* 67, 909–915.
- Sprules, W.G. and Barth, L.E. (2015). Surfing the biomass size-spectrum: some remarks on history, theory, and application. *Canadian Journal of Fisheries and Aquatic Sciences* 73, 477–495.
- Sprules, W. G., Brandt, S. B., Stewart, D. J., Munawar, M., Jin, E. H., and Love, J. (1991). Biomass Size-spectrum of the Lake-Michigan Pelagic Food Web. *Canadian Journal of Fisheries and Aquatic Sciences* 48, 105–115.
- Sprules, W. G., and Munawar, M. (1986). Plankton Size-spectra in Relation to Ecosystem Productivity, Size, and Perturbation. *Canadian Journal of Fisheries and Aquatic Sciences* 43, 1789–1794.
- Steinberg, D. K., and Landry, M.R. (2017). Zooplankton and the Ocean Carbon Cycle. *Annual Review of Marine Science*. 9, 413–444.
- Steneck, R. S. (2012). Apex predators and trophic cascades in large marine ecosystems: Learning from serendipity. *Proceedings of the National Academy of Sciences* 109, 7953–7954.
- Stibor, H., Vadstein, O., Diehl, S., Gelzleichter, A., Hansen, T., Hantsche, F., et al. (2004). Copepods act as a switch between alternative trophic cascades in marine pelagic food webs. *Ecology Letters* 7, 321–328.
- Stock, C.A., J.P. Dunne, and J.G. John. (2014). Drivers of trophic amplification of ocean productivity trends in a changing climate. *Biogeosciences* 11, 7125-7135.
- Stock, C. A., Powell, T. M., and Levin, S. A. (2008). Bottom-up and top-down forcing in a simple size-structured plankton dynamics model. *Journal of Marine Systems* 74, 134–152.

- Stoecker, D. K., Hansen, P. J., Caron, D. A., and Mitra, A. (2017). Mixotrophy in the Marine Plankton. *Annual Review of Marine Science* 9, 311–335.
- Straile, D. (1997). Gross growth efficiencies of protozoan and metazoan zooplankton and their dependence on food concentration, predator-prey weight ratio, and taxonomic group. *Limnology and Oceanography* 42, 1375–138.
- Strömberg, K.H.P., Smith, T.J., Allen, J.I., Pitois, S., and O'Brien, T.D. (2009). Estimation of global zooplankton biomass from satellite ocean colour. *Journal of Marine Systems* 78, 18–27.
- Sumaila, U. R., Cheung, W., Dyck, A., Gueye, K., Huang, L., Lam, V., et al. (2012). Benefits of rebuilding global marine fisheries outweigh costs. *PLoS ONE* 7, e40542.
- Sutherland, K.R., Madin, L.P. and Stocker, R. (2010). Filtration of submicrometer particles by pelagic tunicates. *Proceedings of the National Academy of Science*, 107, 15129–15134.
- Taylor, W.D. (1978). Maximum growth rate, size and commonness in a community of bactivorous ciliates. *Oecologia* 36, 263–272.
- Terazaki, M. “Feeding of Carnivorous Zooplankton, Chaetognaths in the Pacific”. *Dynamics and Characterization of marine Organic Matter*. 1st ed. TERRAPUB, 2000. 257-276.
- Thorpe, R. B., Le Quesne, W. J. F., Luxford, F., Collie, J. S., and Jennings, S. (2015). Evaluation and management implications of uncertainty in a multispecies size-structured model of population and community responses to fishing. *Methods in Ecology and Evolution* 6, 49–58.
- Tittensor, D. P., Eddy, T.D., Lotze, H.K., Galbraith, E.D., Cheung, W., Barange, M., et al. (2018). A protocol for the intercomparison of marine fishery and ecosystem models: Fish-MIP v1.0. *Geoscientific Model Development* 11, 1421–1442.
- Travers, M., Shin, Y. J., Jennings, S., and Cury, P. (2007). Towards end-to-end models for investigating the effects of climate and fishing in marine ecosystems. *Progress in Oceanography* 75, 751–770.
- Travers, M., Shin, Y. J., Jennings, S., Machu, E., Huggett, J. A., Field, J. G., and Cury, P. M. (2009). Two-way coupling versus one-way forcing of plankton and fish models to predict ecosystem changes in the Benguela. *Ecological Modelling* 220, 3089–3099.
- Trebilco, R., Baum, J.K., Salomon, A.K., and Dulvy, N.K. (2013). Ecosystem ecology: Size-based constraints on the pyramids of life. *Trends in Ecology and Evolution* 28, 423–431.
- Turnbull, M. S., George, P. B. L., and Lindo, Z. (2014). Weighing in: Size spectra as a standard tool in soil community analyses. *Soil Biology and Biochemistry*, 68, 366–372.

- UN DESA. (2015). *World Population Prospects: The 2015 Revision, Key Findings and Advance Tables*. Working Paper No. ESA/P/WP.241.
- UN FCCC. (2015). *Paris Agreement. Conference of the Parties on Its Twenty-First Session, (December)*, 32.
- van Denderen, P. D., Lindegren, M., MacKenzie, B. R., Watson, R. A., and Andersen, K. H. (2018). Global patterns in marine predatory fish. *Nature Ecology and Evolution* 2, 65-70.
- Violle, C., Navas, M. L., Vile, D., Kazakou, E., Fortunel, C., Hummel, I., and Garnier, E. (2007). Let the concept of trait be functional! *Oikos* 116, 882–892.
- Ward, B. A., Dutkiewicz, S., and Follows, M. J. (2014). Modelling spatial and temporal patterns in size-structured marine plankton communities: Top-down and bottom-up controls. *Journal of Plankton Research* 36, 31–47.
- Ward, B. A., Dutkiewicz, S., Jahn, O., and Follows, M. J. (2012). A size-structured food web model for the global ocean. *Limnology and Oceanography* 57, 1877–1891.
- Warren, C. P., Pascual, M., Lafferty, K. D., and Kuris, A. M. (2010). The inverse niche model for food webs with parasites. *Theoretical Ecology* 3, 285–294.
- Ward, B. A., and Follows, M. J. (2016). Marine mixotrophy increases trophic transfer efficiency, mean organism size, and vertical carbon flux. *Proceedings of the National Academy of Sciences* 113, 2958–2963.
- Watson, J. R., Stock, C. A., and Sarmiento, J. L. (2014). Exploring the role of movement in determining the global distribution of marine biomass using a coupled hydrodynamic – Size-based ecosystem model. *Progress in Oceanography* 138, 521–532.
- WBPP. (2015). *Tuna Fisheries*. Pacific Possible: World Bank Group.
- Webb, T. J., Dulvy, N. K., Jennings, S., and Polunin, N. V. C. (2011). The birds and the seas: Body size reconciles differences in the abundance-occupancy relationship across marine and terrestrial vertebrates. *Oikos* 120, 537–549.
- West, G. B., Brown, J. H., and Enquist, B. J. (1997). A general model for the origin of allometric scaling laws in biology. *Science* 276, 122–126.
- Wickstead, J.H. (1961). Food and Feeding in Pelagic Copepods. *Proceedings of the Zoological Society of London* 139, 545-555.
- Wilson, R. W., Millero, F. J., Taylor, J. R., Walsh, P. J., Christensen, V., Jennings, S., et al. (2009). Contribution of fish to the marine inorganic carbon cycle. *Science* 323, 359–362.
- Wilson, W. H., Trran, G. A., Schroeder, D., Cox, M., Oke, J., and Malin, G. (2002) Isolation of viruses responsible for the demise of an *Emiliania huxleyi* bloom in the English

- Channel. *Journal of the Marine Biology Association of the United Kingdom* 82, 369–377.
- Wirtz, K. W. (2012). Who is eating whom? Morphology and feeding type determine the size relation between planktonic predators and their ideal prey. *Marine Ecology Progress Series* 445, 1–12.
- Wirtz, K. W. (2014). A biomechanical and optimality-based derivation of prey-size dependencies in planktonic prey selection and ingestion rates. *Marine Ecology Progress Series* 507, 81–94.
- Wood, S.N. (2017). *Generalised Additive Models: An Introduction with R*, 2nd edn. Boca Raton: Chapman and Hall
- Woodward, G., Ebenman, B., Emmerson, M., Montoya, J. M., Olesen, J. M., Valido, A., et al. (2005). Body size in ecological networks. *Trends in Ecology and Evolution* 20, 402–409.
- Woodworth-Jefcoats, P. A., Polovina, J. J., Dunne, J. P., and Blanchard, J. L. (2013). Ecosystem size structure response to 21st century climate projection: Large fish abundance decreases in the central North Pacific and increases in the California Current. *Global Change Biology* 19, 724–733.
- Woodworth-Jefcoats, P. A., Polovina, J. J., Howell, E. A., Blanchard, J. L. (2015). Two takes on the ecosystem impacts of climate change and fishing: Comparing a size-based and a species-based ecosystem model in the central North Pacific. *Progress in Oceanography* 138, 533–545.
- Woodworth-Jefcoats, P. A., Polovina, J. J., and Drazen, J. C. (2017). Climate change is projected to reduce carrying capacity and redistribute species richness in North Pacific pelagic marine ecosystems. *Global Change Biology* 23, 1000–1008.
- Ye L., Chang, C.Y., García-Comas, C., Gong, G.C., and Hsieh, C.H. (2013). Increasing zooplankton size diversity enhances the strength of top-down control on phytoplankton through diet niche partitioning. *Journal of Animal Ecology* 82, 1052–1061.
- Yvon-Durocher, G., Montoya, J. M., Trimmer, M., and Woodward, G. (2011). Warming alters the size-spectrum and shifts the distribution of biomass in freshwater ecosystems. *Global Change Biology* 17, 1681–1694.
- Zhang, L., Andersen, K. H., Dieckmann, U., and Bränström, A. (2015). Four types of interference competition and their impacts on the ecology and evolution of size-structured populations and communities. *Journal of Theoretical Biology* 380, 280–290.

- Zhang, C., Chen, Y., and Ren, Y. (2015). Assessing uncertainty of a multispecies size-spectrum model resulting from process and observation errors. *ICES Journal of Marine Science* 72, 2223–2233.
- Zhang, C., Chen, Y., and Ren, Y. (2016). An evaluation of implementing long-term MSY in ecosystem-based fisheries management: Incorporating trophic interaction, bycatch and uncertainty. *Fisheries Research* 174, 179–189.
- Zhang, L., Hartvig, M., Knudsen, K., and Andersen, K. H. (2014). Size-based predictions of food web patterns. *Theoretical Ecology* 7, 23–33.
- Zhang, L., Thygesen, U. H., Knudsen, K., and Andersen, K. H. (2013). Trait diversity promotes stability of community dynamics. *Theoretical Ecology* 6, 57–69.
- Zhou, M. (2006). What determines the slope of a plankton biomass spectrum? *Journal of Plankton Research* 28, 437–448.
- Zhou, M., Carlotti, F., and Zhu, Y. (2010). A size-spectrum zooplankton closure model for ecosystem modelling. *Journal of Plankton Research* 32, 1147–1165.
- Zhou, M., and Huntley, M. E. (1997). Population dynamics theory of plankton based on biomass spectra. *Marine Ecology Progress Series* 159, 61–73.
- Zhou, M., Tande, K. S., Zhu, Y., and Basedow, S. (2009). Productivity, trophic levels and size spectra of zooplankton in northern Norwegian shelf regions. *Deep-Sea Research Part II: Topical Studies in Oceanography* 56, 1934–1944.

Appendix 1

Numerical Implementation of Second Order McKendrick-von Foerster Equation

In \log_{10} weight space, the McKendrick-von Foerster with diffusion (MvF-D) has the form:

$$\frac{\partial N(x, t)}{\partial t} = -\frac{\partial}{\partial x} g(x, t)N(x, t) - u(x, t)N(x, t) + \frac{1}{2} \left(\frac{\partial^2}{\partial x^2} f(x, t)N(x, t) \right), \quad (1)$$

where $N(x, t)$ represents the abundance of individuals of body size 10^x at time t , and their individual growth, mortality and diffusion rates are denoted by $g(x, t)$, $u(x, t)$ and $f(x, t)$, respectively. We solve equation 1 using the semi-implicit upward finite difference scheme (Press *et al.*, 2007), explicit in body size and implicit in time. Breaking the total time into k equal intervals: $\Delta t = t_{j+1} - t_j$, ($j \in [1, k - 1]$) and the body size range into n equal $0.1 \log_{10}$ size intervals: $\Delta x = x_{i+1} - x_i = 0.1$, ($i \in [1, n - 1]$), equation 1 is discretised:

$$\frac{N_i^{j+1} - N_i^j}{\Delta t} = -\frac{g_i^j N_i^{j+1} - g_{i-1}^j N_{i-1}^{j+1}}{\Delta x} - \mu_i^j N_i^{j+1} + \frac{1}{2} \left(\frac{f_{i+1}^j N_{i+1}^{j+1} - 2f_i^j N_i^{j+1} + f_{i-1}^j N_{i-1}^{j+1}}{\Delta x^2} \right). \quad (2)$$

Rearranging (2), for $i = 2: (n - 1)$:

$$N_i^{j+1} = \frac{N_i^j + N_{i-1}^{j+1} \frac{\Delta t}{\Delta x} \left(g_{i-1}^j + \frac{f_{i-1}^j}{2\Delta x} \right) + \left(\frac{\Delta t}{2\Delta x^2} f_{i+1}^j \right) N_{i+1}^{j+1*}}{1 + \Delta t \mu_i^j + \frac{\Delta t}{\Delta x} \left(g_i^j + \frac{f_i^j}{\Delta x} \right)}, \quad (3)$$

where N_{i+1}^{j+1*} is found beforehand by solving the first order McKendrick-von Foerster equation

$$\frac{\partial N(x, t)}{\partial t} = -\frac{\partial}{\partial x} g(x, t)N(x, t) - u(x, t)N(x, t). \quad (4)$$

using the semi-implicit upward finite difference scheme:

$$\frac{N_{i+1}^{j+1*} - N_{i+1}^j}{\Delta t} = - \frac{g_{i+1}^j N_{i+1}^{j+1*} - g_i^j N_i^{j+1}}{\Delta x} - \mu_{i+1}^j N_{i+1}^{j+1*}$$

$$N_i^{j+1*} = \frac{N_i^j + N_{i-1}^{j+1} \frac{\Delta t}{\Delta x} g_{i-1}^j}{1 + \Delta t \mu_i^j + \frac{\Delta t}{\Delta x} g_i^j}. \quad (5)$$

For $i = n$, we cannot use the MvF-D, so we also use the first order McKendrick-von Foerster: $N_i^{j+1} = N_i^{j+1*}$.